

# **A comparative analysis of CoA biosynthesis in selected organisms: a metabolite study**

by

René Goosen

*Dissertation presented for the degree*  
*Doctorate of Science in Biochemistry at the University*  
*of Stellenbosch*

The crest of the University of Stellenbosch is centered behind the text. It features a shield with various symbols, topped by a crown and flanked by two figures. Below the shield is a banner with the Latin motto "Pacta conseruant cultus recti".

Supervisor: Prof E. Strauss  
Co-supervisor: Prof. J. L. Snoep

Faculty of Science

March 2016

## **Declaration**

By submitting this dissertation electronically, I declare that the entirety of the work contained therein is my own, original work, that I am the authorship owner thereof (unless to the extent explicitly otherwise stated) and that I have not previously in its entirety or in part submitted it for obtaining any qualification.

March 2016

## Abstract

This study investigated the biochemical regulation of CoA production because it is an essential pathway that presents an important target for antimicrobial drug discovery studies. Currently, the specific life-sustaining functions of CoA are not clearly defined and a better understanding of the regulation of the CoA biosynthesis pathway would aid in the understanding of the relevance of maintaining specific CoA levels for survival. Regulation of CoA production was investigated on two levels. First, it was determined if production is up-regulated under conditions predicted to be associated with increased demand in *S. aureus*. Second, regulation of production of CoA by the salvage pathway in *E. coli* was investigated. In *S. aureus* it was found that CoA production is up-regulated under conditions of oxidative stress by an as yet unidentified mechanism. This led to an investigation of the regulation in the CoA biosynthesis pathway to understand how production is controlled. At present, the regulation of CoA production is thought to occur at a single, rate-limiting step identified as the first enzyme in the pathway, pantothenate kinase (PanK). Failure of inhibition of PanK to result in growth inhibition suggested that a re-evaluation of this premise is required. To this end, a systems analysis approach was taken in this study to elucidate the control of CoA production by the salvage pathway. Previously, a lack of analytical tools to measure the intermediates of CoA biosynthesis hampered investigations into regulation of the pathway and a holistic study has not been performed to elucidate the control profile. Consequently a method was also developed for the quantification of all the intermediates of the CoA salvage pathway based on derivatization with a fluorescent thiol probe and HPLC analysis. This method allowed for time course analysis of the reconstituted pathway to be performed to provide a holistic interpretation of CoA production. A kinetic model of the pathway was constructed from rate equations parameterized with a combination of experimentally determined values and values reported in the literature. Time course profiles were used to validate the model for subsequent control analyses. Both time course profiles and predictions made by the model indicated that PanK is unlikely to control the rate of CoA production under most conditions, and that it is in fact dephospho-CoA kinase (DPCK), the last enzyme in the pathway, that controls the rate under physiological conditions. This implies that DPCK is the best target for inhibition of the CoA biosynthetic pathway because it is far more likely to be in control of the rate of CoA production under physiological conditions. This finding is significant to antimicrobial drug development efforts because it suggests that the target focus should be shifted from PanK to DPCK. Therefore the findings of this study represent a major shift in our current understanding of the regulation of the rate of CoA production. It also highlights the importance of conducting a detailed systems analysis when studying metabolic pathways from both regulatory and drug development perspectives.

## Opsomming

Hierdie studie het die biochemiese regulering van KoA produksie ondersoek, want dit is 'n noodsaaklike padweg wat 'n belangrike teiken bied vir studies vir die ontdekking van antimikrobiese middels. Die spesifieke lewensonderhoudende funksies van KoA word tans nie duidelik gedefinieer nie en 'n beter begrip van die regulering van die KoA biosintese padweg sal help om die rol van die handhawing van spesifieke KoA vlakke vir oorlewing te verstaan. Regulering van KoA produksie word ondersoek op twee vlakke. Eerstens, word daar vasgestel of die produksie vermeerder word onder toestande waar 'n verhoogde aanvraag na KoA voorspel word in *S. aureus*. Tweedens, word die regulering van die produksie van KoA deur die herwinningspadweg in *E. Coli*, ondersoek. In *S. aureus* is bevind dat KoA produksie wel vermeerder onder toestande van oksidatiewe stres deur 'n onbekende meganisme. Dit het gelei tot 'n ondersoek van die regulasie in die KoA biosintese pad om te verstaan hoe die produksie beheer word. Tans word dit verstaan dat die regulering van KoA produksie plaasvind by 'n enkele, koers-bepalende stap, algemeen aanvaar as die eerste ensiem in die pad, pantotenaatkinase (PanK). Die mislukking van die inhibisie van PanK om groei te inhibeer, stel voor dat 'n herevaluering van hierdie uitgangspunt vereis word. Vir hierdie doel is 'n stelselontleding benadering gevolg wat in hierdie studie lig werp op die beheer van KoA produksie in die KoA-herwinningspadweg. Voorheen, was daar 'n gebrek aan analitiese gereedskap om die intermediate van die KoA biosintese padweg te meet. Dit het die uitvoer van 'n holistiese studie van die regulering van die padweg belemmer. Gevolglik is daar in hierdie studie 'n metode ontwikkel vir die kwantifisering van al die intermediate van die KoA herwinningspadweg, gebaseer op derivatisasie van die intermediate en hoë-prestasie vloeistof chromatografie analise. Hierdie metode het toegelaat vir tydsverlooptoetsing van die padweg wat uitgevoer moet word om 'n holistiese interpretasie van KoA produksie lewer. A kinetiese model van die padweg is opgebou uit snelheidsvergelings wat geparameteriseer is met 'n kombinasie van eksperimenteel bepaalde waardes en waardes wat in die literatuur gerapporteer is. Gevolglik is tydsverloop profiele gebruik om die model vir beheer ontledings te bekragtig. Beide tydsverloop profiele en voorspellings deur die model het aangedui dat dit onwaarskynlik is vir PanK om die koers van KoA produksie onder die meeste omstandighede te beheer, en dat dit in werklikheid dephospho-KoA kinase (DPCK) is, die laaste ensiem in die pad, wat die produksie beheer onder fisiologiese toestande. Dit impliseer dat DPCK die beste teiken is vir die inhibisie van KoA biosintese, want dit is meer geneig om in beheer te wees van die koers van KoA produksie onder fisiologiese toestande. Hierdie bevinding is betekenisvol vir studies vir die ontwikkeling van antimikrobiese middels, want dit dui daarop dat die teiken fokus moet verskuif van PanK na DPCK. Dus verteenwoordig die bevindinge van hierdie studie 'n

groot verskuiwing in die huidige begrip van die regulering van KoA produksie. Dit beklemtoon ook die belangrikheid van die uitvoer van 'n omvattende stelselontledingsstudie van metaboliese padweë wat ondersoek word vir die ontwikkeling van antimikrobiese middels.

## Acknowledgements

- Prof. Erick Strauss, my supervisor, thank you for guidance and support.
- Prof. Jacky Snoep, my co-supervisor, performed the physical implementation of rate equations in Mathematica for the construction of kinetic models in this study. Thank you for your valuable input and guidance.
- Prof. Michael Lalk, my host at the University of Greifswald, Germany, where the studies on *S. aureus* USA 300 was performed. Thank you for your valuable input and guidance.
- Kirsten Dörries and Philip Gierok thank you for training, guidance and support in the culture of *S. aureus* and MS-analyses.
- Helba Bredell, our lab manager, thank you for practical support and ensuring that materials were available when requested.
- Strauss group members, past and present, thank you for support and inspiring conversations.
- Melissa Opperman, my partner, thank you for unwavering moral support especially on weekend- and midnight HPLC escapades.
- My parents and extended family, thank you for all of your support and interest in every step of my studies. It took a village.
- For financial assistance, I thank the following organizations:
  - NRF-DAAD
  - Ernst and Ethel Eriksen Trust
  - Stellenbosch University

# Table of Contents

## Chapter 1: Introduction to CoA biosynthesis

1.1 Introduction .....	15
1.2 The importance of CoA .....	16
1.3 The supply of CoA: CoA biosynthesis .....	17
1.3.1 Biosynthesis of pantothenate .....	18
1.3.2 Transport of pantothenate and pantetheine .....	19
1.3.3 The CoA biosynthesis pathway .....	21
1.3.4 Pantothenate kinase .....	21
1.3.4.1 Type I PanK .....	23
1.3.4.2 Type II PanK .....	25
1.3.4.2 Type III PanK .....	28
1.3.5 Phosphopantothenoylcysteine synthetase .....	29
1.3.6 Phosphopantothenoylcysteine decarboxylase .....	32
1.3.7 Phosphopantetheine adenylyltransferase .....	32
1.3.8 Dephospho-CoA kinase .....	33
1.3.8.1 A conformational change of DPCK .....	34
1.3.8.2 Relaxed substrate specificity of <i>EcDPCK</i> .....	36
1.4 The demand for CoA .....	37
1.4.1 CoA degradation .....	37
1.4.2 Synthesis of acyl carrier proteins .....	38
1.4.3 Acyl-CoA synthesis .....	39
1.4.4 CoA as redox buffer .....	42
1.5 Problem statement .....	44
1.5.1 Objective 1: Determine if CoA contributes to the oxidative stress resistance of the <i>S. aureus</i> USA300 strain .....	45
1.5.2 Objective 2: Develop a method for the quantification of all the intermediates of the CoA salvage pathway .....	45
1.5.3 Objective 3: Systems analysis of the CoA salvage pathway in <i>E. coli</i> .....	45

1.6 References.....	47
---------------------	----

## **Chapter 2: CoA and oxidative stress resistance in *Staphylococcus aureus***

2.1 Introduction .....	60
2.1.1 The role of CoA and BSH in <i>S. aureus</i> .....	61
2.1.2 Regulation of CoA production under oxidative stress .....	62
2.1.3 Objective of this study .....	63
2.2 Results and discussion .....	65
2.2.1 Cultivation and stress of <i>S. aureus</i> USA 300.....	65
2.2.2 Harvest and metabolite extraction of <i>S. aureus</i> .....	66
2.2.3 Analysis of <i>S. aureus</i> extracts .....	67
2.2.3.1 Adenylate energy charge .....	67
2.2.3.2 The impact of stress on levels of intracellular CoA and its precursors .....	70
2.3 Conclusion .....	75
2.4 Experimental procedures .....	77
2.4.1 <i>S. aureus</i> strains and growth conditions.....	77
2.4.2 Cell harvest and quenching of metabolism .....	77
2.4.3 Extraction of intracellular metabolites.....	78
2.4.4 Analysis and quantification of metabolites .....	78
2.4.5 LC-MS data analysis .....	79
2.5 References.....	80

## **Chapter 3: Measuring CoA salvage intermediates**

3.1 Introduction .....	83
3.2 Methods currently available for measuring CoA and its precursors .....	84
3.2.1 Spectrophoto- and spectrofluorometric methods .....	84
3.2.2 Chromatographic methods .....	86
3.2.3 Pre-column derivatization and chromatographic analysis .....	87
3.2.3.1 Halides.....	87

3.2.3.1.1 Ammonium 7-Fluorobenzo-2-oxa1,3-diazole-4-sulfonate .....	87
3.2.3.1.2 Monobromobimane .....	88
3.2.3.2 N-substituted maleimides .....	89
3.2.3.2.1 N-6[4-(6-dimethylamino-2-benzofuranyl)phenyl]-maleimide.....	89
3.2.3.2.2 7-Diethylamino-3-(4-maleimidophenyl)-4-methylcoumarin.....	90
3.3 Objective of this study .....	90
3.4 Results and Discussion .....	92
3.4.1 CPM derivatization of CoA and its thiol precursors.....	92
3.4.1.1 Reactivity of CPM.....	92
3.4.1.2 Specificity of CPM .....	92
3.4.1.3 Stability of CPM derivatives .....	93
3.4.2 Sample preparation for derivatization and analysis of CoA and its thiol precursors ....	93
3.4.3 Resolving the analytes of interest.....	94
3.4.4 Quantification strategy.....	97
3.4.4.1 Standardizing the concentrations of the external standards.....	99
3.4.4.2 Preparing calibration curves of analyte standards .....	99
3.4.5 Method validation .....	101
3.4.6 Measuring intermediates of CoA salvage in <i>E. coli</i> and <i>S. aureus</i> .....	102
3.4.7 Application of the method for time course analysis of CoA salvage biosynthesis.....	106
3.5 Conclusion .....	108
3.6 Experimental procedures .....	109
3.6.1 Overexpression and purification of CoA salvage pathway proteins.....	109
3.6.2 CoA salvage reactions, quenching and sample treatment .....	109
3.6.3 Standardization of standards.....	110
3.6.4 Calibration curves of analyte standards.....	110
3.6.5 Extraction and derivatization of CoA salvage intermediates in <i>E. coli</i> and <i>S. aureus</i>	111
3.6.6 HPLC analysis of CPM-derivatized CoA salvage intermediates .....	111
3.7 References.....	113

## Chapter 4: Systems analysis of the regulation of the CoA salvage pathway in *E. coli*

4.1 Introduction .....	118
4.1.1 Regulation of <i>E. coli</i> pantothenate kinase activity .....	119
4.1.2 Regulation of <i>E. coli</i> phosphopantetheine adenylyltransferase activity .....	120
4.1.3 Regulation of <i>E. coli</i> dephospho-coenzyme A kinase activity .....	121
4.1.4 Observations on the regulation of CoA production in vivo .....	121
4.1.5 Shortcomings of currently accepted view of the regulation of CoA production .....	123
4.1.6 Requirements for a systems analysis of CoA production .....	125
4.1.6.1 Modelling the reaction components of the system .....	125
4.1.6.2 Linking components for a model of the pathway .....	127
4.1.7 Objective of this study .....	128
4.2 Results and Discussion .....	129
4.2.1 <i>EcPanK</i> kinetics .....	129
4.2.1.1 Literature survey of the kinetic parameters and mechanistic properties of <i>EcPanK</i> .....	129
4.2.1.2 Proposed <i>EcPanK</i> kinetic mechanism and rate equation .....	130
4.2.1.3 Kinetic studies of <i>EcPanK</i> to determine its kinetic parameters .....	133
4.2.1.5 Confirming the $V_M$ for <i>EcPanK</i> under model conditions .....	137
4.2.1.5 Validation of <i>EcPanK</i> rate equation .....	141
4.2.2 <i>EcPPAT</i> kinetics .....	142
4.2.2.1 Literature survey of the kinetic parameters of <i>EcPPAT</i> .....	142
4.2.2.2 <i>EcPPAT</i> mechanism and proposed rate equation .....	142
4.2.2.3 Kinetic parameters of <i>EcPPAT</i> included in the rate equation .....	143
4.2.2.4 Validation of the <i>EcPPAT</i> rate equation .....	145
4.2.3 <i>EcDPCK</i> kinetics .....	146
4.2.3.1 Overview of the current knowledge of the properties of <i>EcDPCK</i> .....	146
4.2.3.2 Proposed rate equation for <i>EcDPCK</i> .....	148
4.2.3.3 Kinetic parameters of <i>EcDPCK</i> included in the rate equation .....	148
4.2.4 In vitro reconstitution of the CoA salvage pathway and validation of the model .....	149

4.2.4.1 Reactions with equivalent amounts of <i>EcPanK</i> , <i>EcPPAT</i> and <i>EcDPCK</i> .....	149
4.2.4.2 Reduced <i>EcPanK</i> concentrations in reconstitution of the CoA salvage pathway ...	152
4.2.4.3 Reconstitution of the CoA salvage pathway with physiological ratios of the enzymes .....	153
4.2.4.4 Validation of the CoA salvage pathway model.....	155
4.2.5 Applying the model to evaluate the contribution of PanK to the control of the rate of CoA synthesis.....	155
4.3 Conclusion .....	158
4.4 Experimental procedures .....	159
4.4.1 Materials and methods .....	159
4.4.2 Expression and purification of <i>EcPanK</i> , <i>EcPPAT</i> and <i>EcDPCK</i> .....	159
4.4.2.1 Expression conditions .....	159
4.4.2.1 Purification conditions .....	160
4.4.2.2 Protein determinations .....	160
4.4.3 Spectrophotometric activity assays .....	161
4.4.3.1 <i>EcPanK</i> activity assays .....	161
4.4.3.2 <i>EcDPCK</i> activity assays .....	162
4.4.4 Single enzyme progress curves .....	162
4.4.4.5 <i>EcPanK</i> progress curves.....	162
4.4.4.6 <i>EcPPAT</i> progress curves .....	162
4.4.4.6 <i>EcDPCK</i> progress curves.....	163
4.4.6 Reconstituted pathway time courses.....	163
4.4.6.1 Equivalent amounts of enzymes.....	163
4.4.6.2 Reduced <i>EcPanK</i> concentrations.....	164
4.4.6.3 Physiological enzyme ratios .....	164
4.4.7 Measuring PanSH, PPanSH, DePCoA and CoA.....	164
4.4.8 Computational methods .....	165
4.5 References.....	166

## Chapter 5: Conclusion

5.1 Overview of achievements .....	169
5.2 Future work .....	171
5.2.1 Regulation of CoA by a redox switch mechanism .....	171
5.2.2. The relevance of CoA regulation in other metabolic pathways .....	171
5.2.3 Extending time course analysis of the CoA salvage pathway to other species .....	171
5.2.1 Optimization of the kinetic model of the CoA salvage pathway in <i>E. coli</i> .....	172
5.3 Final remarks .....	172

## Appendix

A. Derivation of the PanK rate equation .....	173
---	-----

## List of Abbreviations

4-DPS	4,4-Dithiopyridine
ACP	Acyl carrier proteins
ACS	Acyl-CoA synthetase
ADC	Aspartate 1-decarboxylase
ADP	Adenosine 5'-diphosphate
AEC	Adenylate energy charge
ALDH	Aldehyde dehydrogenase
AMP	Adenosine 5'-monophosphate
AMPPNP	Adenylyl-imidodiphosphate
ASKHA	sugar kinase/heat-shock protein 70/actin 1.3.4.2
ATP	Adenosine 5'-triphosphate
BME	$\beta$ -mercaptoethanol
BSA	Bovine serum albumin
BSH	Bacillithiol
<i>Ca</i>	<i>Corynebacterium ammoniagenes</i>
CDNB	1-Chloro-2,4-dinitrobenzene
CFeSP	Corrinoid iron-sulfure protein
CoA	Coenzyme A
CoADR	CoA disulfide reductase
CoASy	CoA synthase
CODH	Carbon monoxide dehydrogenase
CPM	7-Diethylamino-3-(4-maleimidophenyl)-4-methylcoumarin
CSA	Camphorsulfonic acid
DBPM	N-6[4-(6-dimethylamino-2-benzofuranyl)phenyl]-maleimide
dcw	Dry cell weight
DePCoA	3'-Dephospho-CoA
DPCK	Dephospho-CoA kinase
DTBA	Dithiobutylamine
DTNB	5,5'-Dithio-bis-(2-nitrobenzoic acid)
DTT	Dithiothreitol
<i>Ec</i>	<i>E. coli</i>
EDTA	Ethylenediaminetetraacetic acid
ENPP	Ectonucleotide pyrophosphatase
FAS	Fatty acid synthase

GSH	Glutathione
GST	Glutathione S-transferase
ho-Pan	Homopantothenamides
HPLC	High performance liquid chromatography
HTS	High throughput screening
ICH	International Conference on Harmonization
IMAC	immobilized metal affinity chromatography
ITC	Isothermal titration calorimetry
KPHMT	Ketopantoate hydroxymethyltransferase
KPR	Ketopantoate reductase
LB	Luria Bertani
LC-ESI-MS	Liquid chromatography electrospray ionization mass spectrometry
LC-MS	Liquid chromatography mass spectrometry
LDH	Lactate dehydrogenase
LMW	Low molecular weight
LOD	Limit of detection
LOQ	Limits of quantification
mBBr	Monobromobimane
MCA	Metabolic control analysis
MCAT	Malonyl-CoA:acyl carrier protein transacylase
MeCN	Acetonitrile
Methylene-THF	Methylene tetrahydrofolate
MIC	Minimum inhibitory concentration
MRSA	Methicillin-resistant <i>S. aureus</i>
<i>Mt</i>	<i>Mycobacterium tuberculosis</i>
N5-Pan	<i>N</i> -pentyl pantothenamide
N7-Pan	<i>N</i> -heptyl pantothenamide
NaBH <sub>4</sub>	Sodium borohydride
NaCl	Sodium chloride
NAD <sup>+</sup>	Nicotinamide adenine dinucleotide
NADH	Nicotinamide adenine dinucleotide (reduced)
NADPH	Nicotinamide adenine dinucleotide
NaOH	Sodium hydroxide
NBIA	Neurodegeneration with brain iron accumulation
NiSO <sub>4</sub>	Nickel sulfate
OD <sub>500</sub>	Optical density at 500 nm

ODE	Ordinary differential equation
$P$	Partition coefficient
PanK	Pantothenate kinase
PanSH	Pantetheine
PEP	Phosphoenolpyruvate
PFOR	Pyruvate:ferredoxin oxidoreductase
PK	Pyruvate kinase
PK/LDH	Pyruvate kinase and lactate dehydrogenase
PKAN	PanK associated neurodegeneration
PPan $\Delta$ SH	4'-phospho- <i>N</i> -(1-mercaptomethyl-cyclopropyl)-pantothenamide
PPanSH	4'-Phosphopantetheine
PPAT	Phosphopantetheine adenylyltransferase
PPC	4'-Phosphopantothenoylcysteine
PPCDC	Phosphopantothenoylcysteine decarboxylase
PPCS	Phosphopantothenoylcysteine synthetase
PP <sub>i</sub>	Pyrophosphate
PS	Pantothenate synthetase
ROPT	Reversibly oxidized protein thiol
Rt	Retention time
<i>Sa</i>	<i>S. aureus</i>
SAM	S-adenosyl methionine
SBD-F	Ammonium 7-fluorobenzo-2-oxa1,3-diazole-4-sulfonate
TCA	Trichloroacetic acid
TCEP	Tris(2-carboxyethyl) phosphine
<i>Tm</i>	<i>Thermatoga maritima</i>
TPP	Thiamine pyrophosphate
TSB	Tryptic soy broth
$V_M$	Maximal rate
<i>wt</i>	Wild type
$\alpha$ -KGDH	$\alpha$ -ketoglutarate dehydrogenase
$k_{cat}$	Turnover number
$K_d$	Dissociation constant
$K_{eq}$	Equilibrium constant
$K_i$	Inhibition constant
$K_M$	Michaelis constant
$K_M^{app}$	Apparent Michaelis constant

# Chapter 1

## Introduction to CoA biosynthesis

---

### 1.1 Introduction

Drug resistance of pathogenic organisms have become alarmingly common globally as stressed in the 2014 World Health Organization report titled *Antimicrobial Resistance: Global Report on Surveillance*.<sup>1</sup> Therein it is reported that numerous infections that could previously be controlled with antibiotics have now become insensitive to treatment, even with combination therapies. Prominent examples of pathogens where multidrug-resistance have become prevalent include *Mycobacterium tuberculosis* (tuberculosis), *Plasmodium falciparum* (malaria) and *Staphylococcus aureus* (hospital- and community-associated infections). It is clear that there is a critical need for the development of antimicrobial compounds with novel modes of action.

Biochemical pathways leading up to the production of the cofactor coenzyme A (CoA) has been identified as a viable target for the development of antimicrobial compounds. Successful inhibition of CoA production would constitute a novel mode of action as there are currently no therapeutic compounds that target CoA production. The following attributes of CoA and CoA biosynthesis make it a suitable drug target: First, CoA is required for energy metabolism and is essential to the survival of all organisms. Second, with the exception of a few intracellular parasites, all organisms are required to synthesize CoA *de novo* because all indications are that they cannot import it from the extracellular environment. Third, current knowledge suggests that there are sufficient differences between prokaryotes and eukaryotes in regards to some of the key enzymes involved in the biosynthesis of CoA to allow for selective inhibition of the one in the presence of the other.<sup>2</sup>

Taken together, these factors serve as a strong motivation for the study of CoA biosynthesis as drug target. Furthermore, deficiencies in CoA production are responsible for the diseased phenotype in PanK associated neurodegeneration (PKAN disease), a type of neurodegeneration linked with brain iron accumulation (NBIA) in humans. The CoA biosynthesis pathway stands central to research in both these fields. In this chapter, we

present a detailed review of all the components of CoA production and specifically highlight their relevance to the abovementioned fields of study.

## 1.2 The importance of CoA

CoA is a versatile cofactor that is involved in a myriad of metabolic reactions. The reason for its popularity as cofactor is because it—and the CoA-derived phosphopantetheine tether found on various carrier proteins—carries a host of metabolically active chemical groups. The various processes that depend on CoA are summarized in Figure 1.1 but it is probably best known as the carrier of metabolites containing carboxylic acid groups. It functions as acyl carrier from glycolysis to the Krebs-cycle but also for the transfer of acetyl groups among various other small and macromolecules. It shuttles a host of other groups required in metabolism such as short and long carbon chain acids and amino acids.

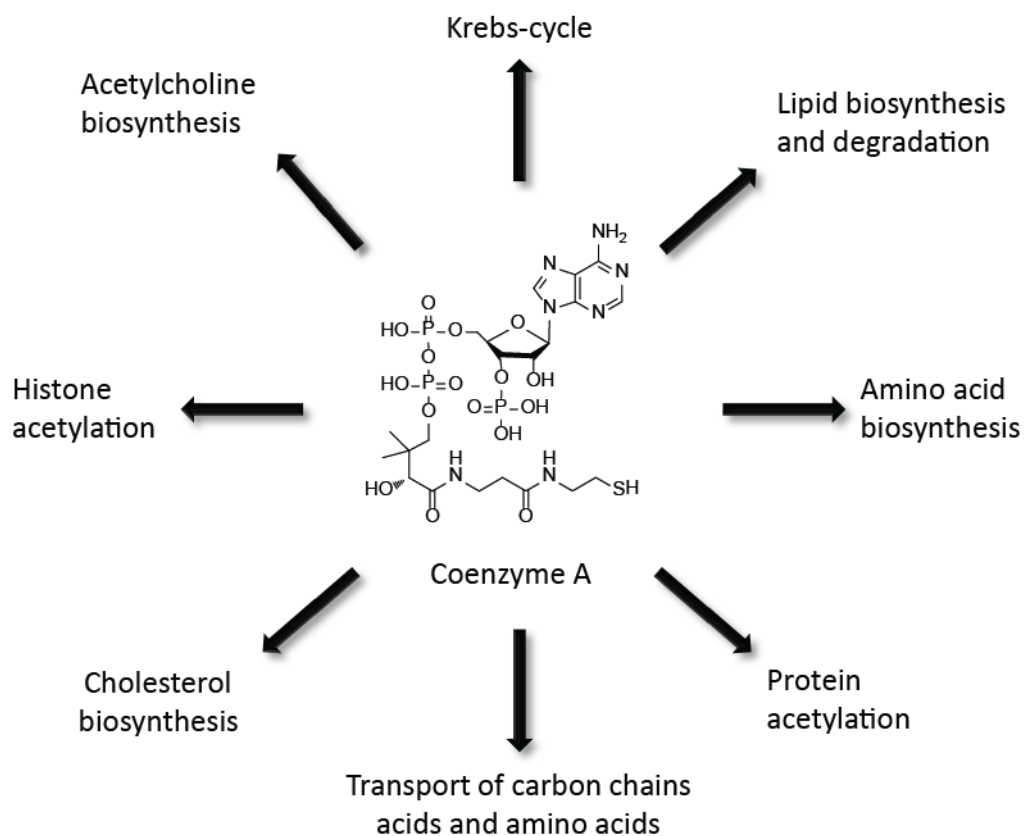


*Figure 1.1: Diversity of CoA dependent processes.* CoA is a well-known role player in processes related to energy metabolism such as the Krebs cycle and lipid biosynthesis and degradation. The recent discovery of its role in post-translational protein modification by acetylation adds to the diversity of processes that have been discovered that require CoA.

CoA's power as a diverse metabolite carrier lies in its terminal thiol group and the unique chemistry and reactivity of thiols and thioesters in comparison to the biochemical properties

of other functional groups. The multitude of CoA thioesters that we are familiar with such as acetyl-CoA, succinyl-CoA, malonyl-CoA, butyryl-CoA etc.,<sup>3</sup> are good electrophiles toward heteroatom nucleophiles such as amines and alcohols, but also carbon nucleophiles such as enolates. Therefore acyl transfer from CoA thioesters to these groups readily occur because of favourable kinetic and thermodynamic driving forces. In spite of this reactivity profile where groups are readily received, carried and transferred, thioesters are no more susceptible to hydrolysis than oxoesters, making CoA the ideal carrier of acyl groups in an aqueous environment.<sup>4,5</sup>

CoA and its thioester derivatives feature in diverse metabolic pathways such as the biosynthesis and degradation of lipids as well as the biosynthesis of amino acids, cholesterol and the neurotransmitter acetylcholine. Beyond its role in metabolic pathways acetyl-CoA has also emerged as a kinetic regulator of metabolic pathways by direct post-translational regulation of enzyme activity by protein acetylation.<sup>6</sup> Furthermore, acetyl-CoA is involved in modulation of the epigenome by histone acetylation to regulate gene expression.<sup>7</sup>

The requirement of CoA and CoA thioesters for the survival of all organisms is undebatable. The biochemistry of CoA biosynthesis is highly conserved but significant differences in the sequence and structure of microbial and human biosynthetic enzymes indicate that selective inhibition would be possible. In the following sections we discuss the biosynthesis of CoA and its relevance as a drug target.

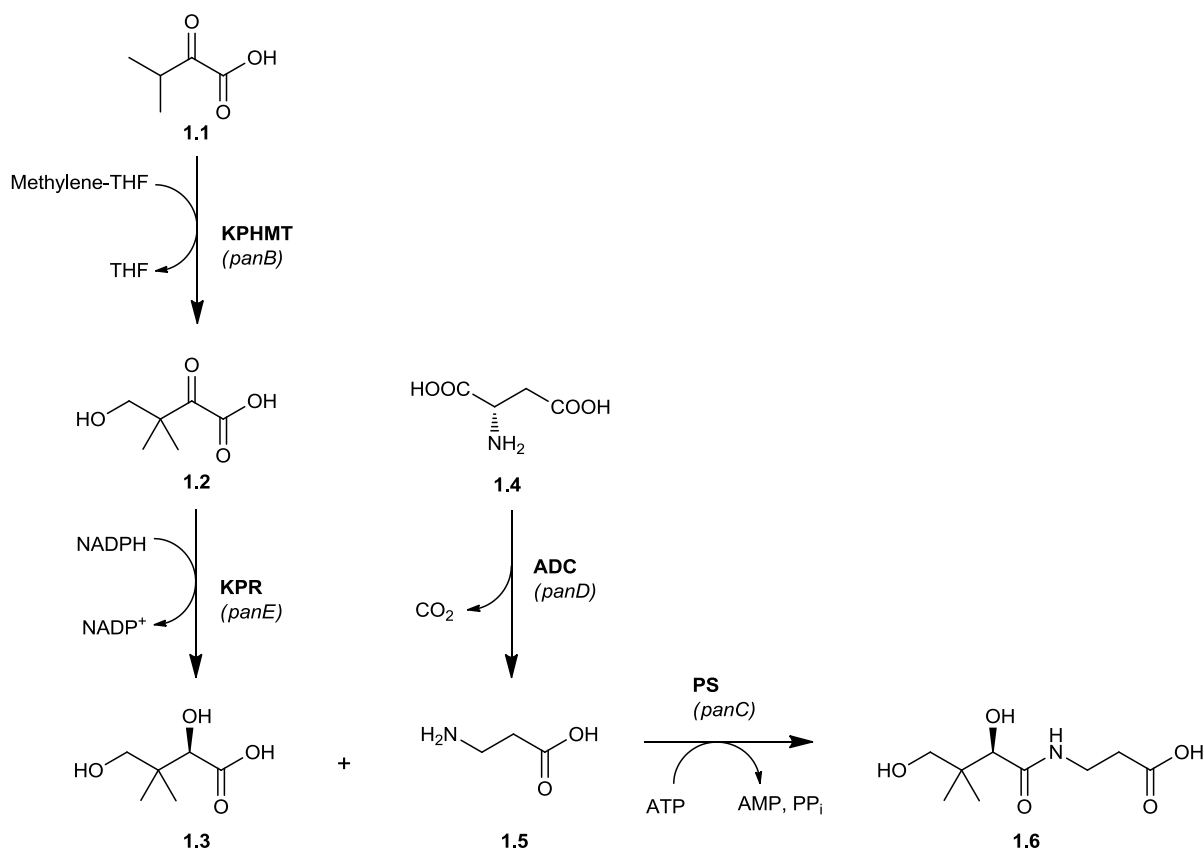
### **1.3 The supply of CoA: CoA biosynthesis**

CoA can be synthesized from two substrates, pantothenate or pantetheine. Pantothenate is the common precursor of CoA in all organisms and has to be taken up from the extracellular environment or synthesized *de novo*.<sup>8</sup> It is transformed to CoA by the universal five-step pathway first formulated by Brown *et al.*<sup>9</sup> Pantetheine (PanSH) is also acquired from the extracellular environment but it is formed as a product in the degradation of CoA and holo-carrier proteins. Consequently, its transformation to CoA by three of the enzymes found in the five-step pathway is referred to as the CoA salvage pathway. Not all organisms are able to make use of this pathway to salvage CoA as outlined in detail in the following sections. Next, the origins and transport of pantothenate is discussed and evaluated it as a target point for the inhibition of CoA production.

### 1.3.1 Biosynthesis of pantothenate

Pantothenate (**1.6**, Scheme 1.1) is a ubiquitous vitamin classified as a B-complex vitamin, specifically vitamin B<sub>5</sub>. Its structure consists of a  $\beta$ -alanine moiety and pantoic acid, bound together with an amide linkage.<sup>10</sup> Plants, fungi and most bacteria are capable of synthesizing pantothenate *de novo* and often produce more than is required to fulfil the requirement for CoA production. It is reported that *E. coli* produces 15 times more pantothenate than it needs and secretes the excess into the environment.<sup>11</sup> The needs of organisms that lack the capacity to produce pantothenate are met by this oversupply and availability in the environment. The general steps for the synthesis of pantothenate are shown in Scheme 1.1. Maas *et al.* showed that pantothenate (**1.6**) is formed by the ATP dependent coupling of pantoic acid (**1.3**) and  $\beta$ -alanine (**1.5**) and AMP and pyrophosphate are formed as side products.<sup>12,13</sup> Pantoic acid is produced from ketoisovaleric acid (**1.1**) by the action of ketopantoate hydroxymethyltransferase (KPHMT). This reaction is dependent on N<sup>6</sup>,N<sup>10</sup>-methylene tetrahydrofolate (Methylene-THF) as a cofactor as it provides the source of the hydroxymethyl group. The reduction of ketopantoic acid (**1.2**) to pantoic acid is facilitated by ketopantoate reductase (KPR) in an NADPH dependent manner. Pantothenate synthetase (PS) then catalyzes the coupling of pantoic acid with  $\beta$ -alanine by utilizing ATP to activate the carboxylate of pantoic acid. During activation a transient acyl-adenylylate forms that is subsequently attacked by the amine of  $\beta$ -alanine. The source of  $\beta$ -alanine depends on the organism. In *E. coli* and most bacteria, aspartate 1-decarboxylase (ADC) produces  $\beta$ -alanine by the pyruvoyl dependent decarboxylation of aspartic acid (**1.4**).<sup>14</sup> In yeast it is produced from the degradation of spermine and spermidine while in other organisms it can be produced by the degradation of uracil.<sup>15</sup>

In humans, the pantothenate biosynthesis pathway is absent and therefore it is a vitamin that must be acquired from the diet and the gut microbiome. Consequently the pantothenate biosynthesis pathway present in numerous bacteria and fungi presents an attractive target for the selective inhibition of CoA production in these organisms. However, pantothenate uptake mechanisms that are present in many microorganisms render the pantothenate biosynthesis pathway nonessential in these cases. In spite of this, studies have demonstrated the viability of targeting this pathway. Impaired survival and pathogenesis was reported for *panC* and *panD* knock-out strains of *M. tuberculosis* in immunocompetent and immunocompromised mice.<sup>16,17,15</sup> Currently, PS is receiving attention as a target for inhibition because it is the last enzyme in the pantothenate synthesis pathway and has been shown to be essential in pantothenate producing organisms under conditions where the environmental availability of pantothenate is limited.<sup>18,19</sup>



**Scheme 1.1: Pantothenate synthesis.** Pantothenate (**1.6**) is produced from pantoic acid (**1.3**) and β-alanine (**1.5**) by pantothenate synthetase (**PS**). Pantoic acid is synthesized in two steps from ketoisovaleric acid (**1.1**). First ketopantoate hydroxymethyltransferase (**KPHMT**) transfers a hydroxymethyl group from methylene-THF to form ketopantoic acid (**1.2**) which is then reduced to pantoic acid (**1.3**) by ketopantoate reductase (**KPR**). In *E. coli* β-alanine (**1.5**) is produced by aspartate 1-decarboxylase (**ADC**) that decarboxylates aspartic acid (**1.4**).

### 1.3.2 Transport of pantothenate and pantetheine

Most organisms are able to actively import pantothenate from their immediate environment regardless of their ability to produce it *de novo*.<sup>20</sup> *E. coli* achieves this with the well characterized pantothenate permease (*panF* gene product) transport system.<sup>21,22</sup> This system consists of a unidirectional sodium-based symporter that is very specific for pantothenate with a maximum transport rate of 1.6 pmol/min per 10<sup>8</sup> cells.<sup>22,23</sup> The transport rate is not regulated by intracellular CoA concentration and overexpression of the protein increases the transport rate 10-fold.<sup>21</sup> The higher rate of pantothenate import leads to an increase in the intracellular concentration of pantothenate. However, CoA levels are not affected which suggests that pantothenate transport does not contribute to the regulation of CoA biosynthesis. *panF* mutants are still able to excrete pantothenate in the absence of pantothenate permease but this occurs via an as-yet unidentified pantothenate efflux

system.<sup>22</sup> In *S. cerevisiae*, a high-affinity proton-coupled symporter (*FEN2* gene product) that bears no similarity to the *E. coli* transporter facilitates pantothenate import.<sup>24,25</sup> Higher organisms typically make use of a sodium-dependent multivitamin transporter for pantothenate import along with biotin and lipoate import.<sup>26,27</sup> Human erythrocytes are normally impermeable to pantothenate but infection with the malaria parasite *P. falciparum* leads to the formation of new permeation pathways in the cell membrane, allowing pantothenate to enter the cell and reach the parasite.<sup>28</sup> The parasite then imports pantothenate by a low-affinity proton-coupled transporter that bears little resemblance to the mammalian transport system indicating the possibility that selective inhibition of uptake could be achieved.<sup>29</sup>

*E. coli* can reportedly utilize PanSH for CoA synthesis and the phosphorylated version, 4'-phosphopantetheine (PPanSH), can be exported but not reimported.<sup>30</sup> No transporter for PanSH or PPanSH has been identified, but considering the amphipathic nature of the PanSH molecule it probably enters the cell through a diffusion based mechanism. This is supported by recent studies that have shown that a large variety of pantothenamide compounds analogous to pantothenate are freely taken up by *E. coli*.<sup>31,32</sup> PanSH has been shown to support the growth of various bacteria in the absence of pantothenate, regardless of its ability to produce it.<sup>33</sup> Furthermore, a study revealed that when the second and third steps required for the conversion of pantothenate to CoA are inactivated by using an arabinose-regulated expression system, cell growth is sustained on media containing pantetheine, the disulfide of PanSH.<sup>34</sup> Taken together, these findings indicate that the CoA requirements for growth can be met by the effective utilization of PanSH when pantothenate is absent or if cells are unable to utilize it. Therefore, although the differences between bacterial and human import of pantothenate suggests that selective inhibition of either system would be possible, microorganisms that are able to utilize PanSH would still be able to import it for rescue by means of the CoA salvage pathway.

A recent study showed that extracellular CoA levels influence intracellular CoA levels in mammalian cells. This occurs by degradation of CoA to PPanSH by ectonucleotide pyrophosphatases (ENPPs) in serum. Surprisingly, PPanSH is then taken up by the cells by passive diffusion and converted back to CoA in the intracellular environment. This finding has major implications for PKAN disease where symptoms are caused by CoA deficiencies. Treatment with CoA has successfully alleviated symptoms due to extracellular degradation to PPanSH, diffusion to the intracellular environment and conversion to CoA.<sup>35</sup> This necessitates re-evaluation of the role that PanK plays in the regulation of intracellular CoA levels, at least in organisms where diffusion of PPanSH has been observed (such as

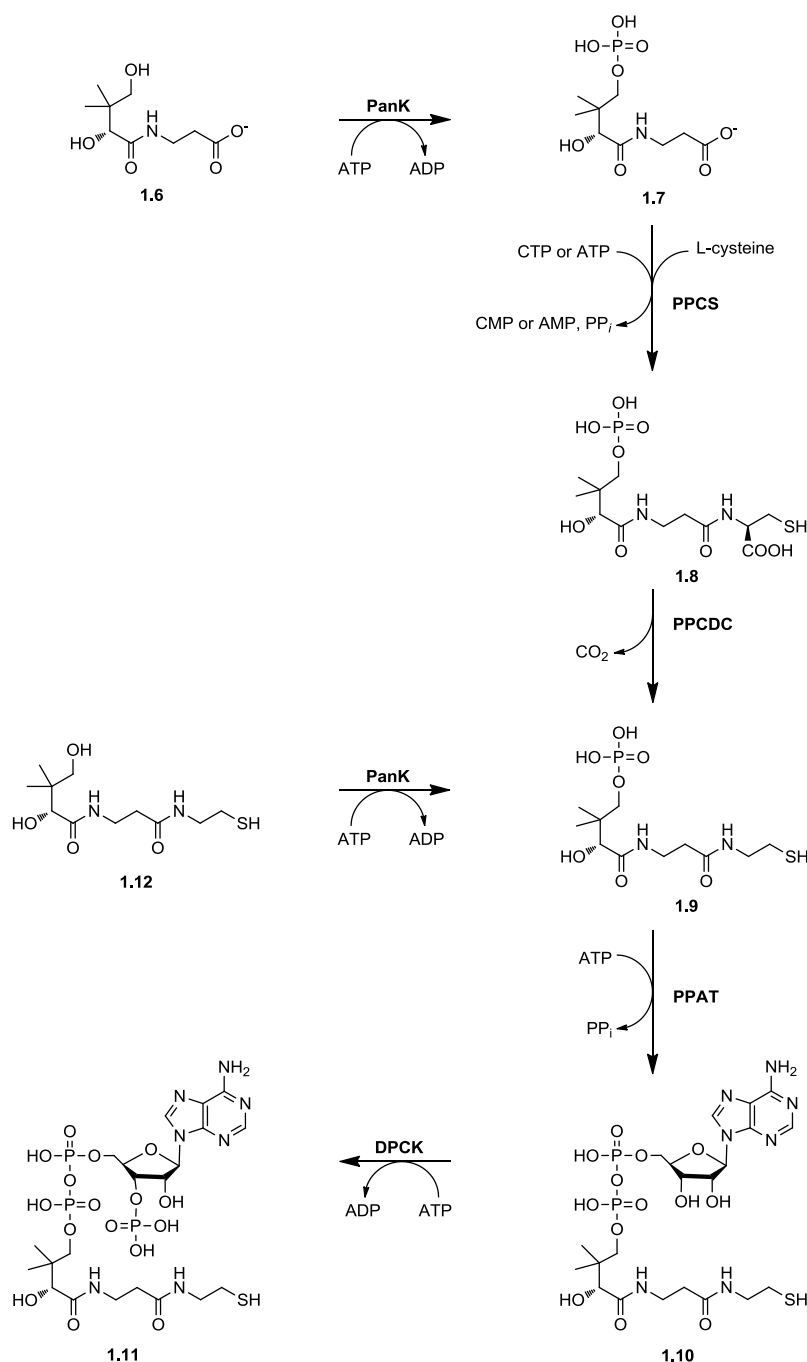
humans, mice and fruit flies). A similar passive import of PPanSH has not been observed in bacteria.

### 1.3.3 The CoA biosynthesis pathway

Following pantothenate biosynthesis or uptake, it is transformed to CoA by a universal five step pathway (Scheme 1.2) catalysed by four enzymes, several variants of which have been cloned and characterized. Pantothenate (**1.6**) is first phosphorylated by pantothenate kinase (PanK) to 4'-phosphopantothenate.<sup>36</sup> Condensation of 4'-phosphopantothenate (**1.7**) with cysteine then occurs in a reaction catalysed by phosphopantothenoylcysteine synthetase (PPCS) to yield phosphopantothenoylcysteine (**1.8**). The third step involves the decarboxylation of the cysteine moiety by phosphopantothenoylcysteine decarboxylase (PPCDC) to yield PPanSH, **1.9**. In the penultimate step, phosphopantetheine adenylyltransferase (PPAT) transfers an adenylyl group from ATP to PPanSH to form dephospho-CoA (DePCoA, **1.10**). Finally, DePCoA is phosphorylated by dephospho-CoA kinase (DPCK) to form CoA (**1.11**). Alternatively, CoA can also be synthesized via the salvage pathway mentioned earlier. Here PanSH (**1.12**) is phosphorylated by a PanK variant (three PanK types exist, as explained below) that accepts analogues of pantothenate. The resulting PPanSH is then converted to CoA by PPAT and DPCK. All five enzymes in the CoA biosynthesis pathway are potential targets for the development of selective inhibitors because CoA is an essential cofactor and *de novo* synthesis is required by nearly all organisms. The enzymes that comprise the CoA salvage pathway have received more attention in drug development efforts because PPCS and PPCDC can be bypassed in organisms with a PanK that allows for operation of the salvage pathway. In the following subsections, the general characteristics and suitability of each of these enzymes as drug target will be discussed.

### 1.3.4 Pantothenate kinase

This enzyme is the product of *coaA* or *coaX* genes and catalyses the first and committed step of the CoA biosynthesis pathway by phosphorylating pantothenate, usually using ATP as phosphoryl donor. PanK is the best-studied enzyme of the pathway and the PanKs from various organisms have been expressed and purified including examples from bacteria, fungi, plants and mammals.<sup>11</sup> PanK has received special attention in drug development studies due to its apparent central role in the control of CoA biosynthesis. PanKs can be grouped into three distinct types with a common catalytic function but diverse catalytic and inhibition properties.<sup>37</sup> Previously they were grouped along phylogenetic lines and defined as



**Scheme 1.2: CoA biosynthesis.** In the first step of the universal five step pathway pantothenate (**1.6**) is phosphorylated by pantothenate kinase (**PanK**) to 4'-phosphopantothenate (**1.7**). Phosphopantothenoylcysteine synthetase (**PPCS**) then catalyses the condensation of 4'-phosphopantothenate (**1.7**) with cysteine to yield phosphopantothenoylcysteine (**1.8**) followed by a decarboxylation reaction catalysed by phosphopantothenoylcysteine decarboxylase (**PPCDC**) to form 4'-phosphopantetheine (**1.9**). Phosphopantetheine adenyltransferase (**PPAT**) subsequently adenylates 4'-phosphopantetheine (**1.9**) to form dephospho-CoA (**1.10**). In the final step dephospho-CoA (**1.10**) is phosphorylated by dephospho-CoA kinase (**DPCK**) to form CoA (**1.11**). The CoA salvage pathway starts with the phosphorylation of pantetheine (**1.12**) by PanK and the 4'-phosphopantetheine (**1.9**) formed is then converted to CoA by PPAT and DPCK.

either eukaryotic or prokaryotic types. However, it soon became apparent that some bacterial PanKs have more in common with what was previously considered eukaryotic PanKs than other bacterial PanKs and therefore classification according to phylogeny was scrapped. Furthermore, the presence of two types of PanKs has also been found in some organisms like *Bacillus subtilis* and *Mycobacterium tuberculosis*. Next, the differentiating properties of each type of PanK will be discussed as well as the findings of drug development studies that have focused on PanK.

#### 1.3.4.1 Type I PanK

Type I PanK is considered to be the prototypical bacterial PanK and belongs to the family of P-loop kinases. The *E. coli* protein is a good representative example of type I PanKs and has been well studied.<sup>38</sup> It is the expression product of the *coaA* gene and has a homodimeric structure.<sup>39,40</sup> The reaction follows an ordered sequential mechanism where ATP binds first, followed by pantothenate. Cooperativity of ATP binding to the dimer has been observed in kinetic studies and a Hill coefficient of 1.46 has been reported.<sup>40</sup> Two characteristics of type I PanK has led to heightened interest in its potential as a drug target. First, PanK activity is modulated by feedback inhibition by CoA and to a far lesser extent by acetyl-CoA. Therefore PanK has been proposed to be a key regulatory point for the control of CoA production. It has been suggested that successful inhibition of this step would lead to effective inhibition of CoA synthesis.<sup>40</sup> Second, type I PanKs exhibit a low level of substrate specificity and are capable of binding and phosphorylating many types of pantothenate analogues including PanSH.  $K_M$  values for pantothenate have been reported in the range of 16.7–36  $\mu\text{M}$ <sup>31,32,40,41,42</sup> and for PanSH in the range of 19–91  $\mu\text{M}$ .<sup>41,43</sup> This indicates that there is little variation in the affinity for the two substrates. The reason for this becomes apparent when considering a cross-section view of the PanK active site where both pantothenic acid and ATP is bound (Figure 1.2). The active site is exposed as indicated by the arrow and this allows for variation in the carboxyl end of pantothenic acid. Hence, PanK can accept PanSH and other pantothenic acid analogues, like pantothenamides, as substrates for catalytic activity. A detailed review of the kinetic mechanism of *E. coli* PanK is given in Chapter 4 where the kinetic parameters are also discussed in detail.

Studies on the inhibition of type I PanKs have focused on the pantothenamide class of pantothenic acid analogues; however, strictly speaking they are not inhibitors of these PanKs but rather alternative substrates. These compounds substitute the carboxylic acid of pantothenate for an *N*-substituted amide. Compounds with *N*-pentyl or *N*-heptyl substituents

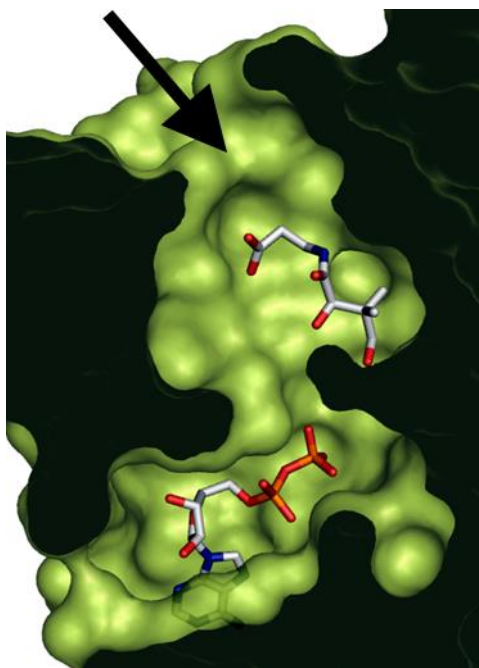


*Figure 1.2: Cross section of the active site of E. coli PanK (pdb:1SQ5). Pantothenic acid (top) and ATP (bottom) is bound in the active site. The active site is exposed to solvent, as indicated by the arrow, which allows for variation at the carboxyl end of pantothenic acid. Figure reproduced with permission from Wiley InterScience, Strauss, E., de Villiers M. and Rootman I. (2010) ChemCatChem 2, 929-937, <http://onlinelibrary.wiley.com/doi/10.1002/cctc.201000139/abstract> Copyright © 2010 Wiley-VCH Verlag GmbH&Co. KGaA, Weinheim*

have been well characterized<sup>31,44</sup> but a myriad of other substituents have also been prepared.<sup>45</sup> Type I PanKs often exhibit similar or better  $k_{cat}/K_M$  values for pantothenamides than for pantothenate and PanSH and therefore these PanKs do not distinguish between them catalytically; consequently the rate of pantothenate phosphorylation is reduced when these compounds are present.<sup>31</sup> *N*-pentyl pantothenamide (N5-Pan) was reported to inhibit *E. coli* growth with a minimum inhibitory concentration (MIC) of 2  $\mu$ M.<sup>46</sup> This observed inhibitory effect was due to the phosphorylation of N5-Pan by PanK with subsequent conversion to the corresponding CoA antimetabolite ethyldethia-CoA by PPAT and DPCK. Once the CoA antimetabolite is formed it can effectively inhibit the activity of CoA-dependent enzymes, particularly in fatty acid biosynthesis.<sup>31,44</sup> The pantothenamide class of compounds therefore only become active inhibitors because they are accepted as alternative substrates by type I PanK enzymes. In the context of drug development efforts, the ability to act on alternative substrates is one of the defining characteristics of the various PanK types. For example, the presence of a PanK with increased substrate specificity (one that does not allow pantothenate analogues to act as substrates) will exclude such organisms from being

targeted by strategies that aim to inhibit growth by exploiting the *in vivo* formation of CoA antimetabolites.

Only recently compounds have been discovered that inhibit the actual phosphorylation activity of type I PanKs. AstraZeneca have identified a range of specific inhibitors of *Mycobacterium tuberculosis* PanK (*MtPanK*) by high-throughput screening.<sup>47,48</sup> The majority of these compounds are ATP-competitive inhibitors which could mean that they are competitive inhibitors of other P-loop kinases as well. However, these compounds have not been tested with other kinases to determine their specificity. Several of these compounds displayed IC<sub>50</sub> values in the nanomolar range towards *MtPanK*, but failed to show any inhibitory effects in whole cell inhibition assays. Subsequently, vulnerability studies were performed using *MtPanK* overexpression- and knockdown-strains and it was found that PanK activity had to be reduced more than 95% to achieve growth inhibition.<sup>49</sup> This is likely due to the steady state pool of CoA being greatly in excess of what is required for survival. Thus to date, no inhibitor of PanK activity has been discovered that shows inhibitory activity of cell growth. These results also raise questions about the role of PanK in the regulation of CoA biosynthesis. If PanK controls the rate of CoA production as is suggested in the literature, it is expected that a reduction in CoA production and the resulting physiological effects would be observed at a lower percentage of inhibition of PanK. The requirement of a 95% reduction to see an effect is therefore an indication that PanK is not the main regulator of CoA production and therefore perhaps not the best drug target in the CoA biosynthesis pathway.

#### 1.3.4.2 Type II PanK

Type II PanKs are most often found in eukaryotic organisms and have been studied in fungi,<sup>50</sup> plants,<sup>51</sup> insects<sup>52</sup> and mammals.<sup>53</sup> More than one *coaA* gene encoding PanK type II is often present in these organisms, exhibiting tissue-specific expression. In humans there are four known PanK genes named *PANK1*, *PANK2*, *PANK3* and *PANK4*. *PANK1* is expressed mainly in the liver and kidneys while *PANK2* expression is localized to the mitochondria in most tissues.<sup>54,55</sup> *PANK 3* is expressed predominantly in the liver and to a lesser extent in the heart and skeletal muscles whereas *PANK 4* is mainly expressed in the heart.<sup>56</sup> Alternate initiation exons of some of the type II PanK genes can also result in two distinct isoforms. Human and mouse *PANK1* has two gene products, PanK1 $\alpha$  and PanK1 $\beta$ .<sup>57,53,58</sup> Therefore, an organism can harbour a variety of related PanKs due to the diversity of genes and the variety of expression patterns. For example, PKAN disease that was mentioned earlier has only been linked to mutations in the *PANK2* gene.<sup>56,59</sup> Type II

PanKs exhibit some similarities with the type I PanKs with regards to inhibition and substrate specificity. Type II PanKs are also inhibited by CoA but in contrast to type I, inhibition by CoA thioesters, especially acetyl-CoA, is more pronounced.<sup>60,58,53,61</sup> Low substrate specificity is also observed in type II PanKs with the pantothenamides also being accepted as alternative substrates.<sup>45</sup> Type I PanK and type II PanK have different primary sequence profiles and also different structural folds. The structures of human PanK1 $\alpha$  and PanK3 enzymes indicate that type II PanKs belong to the sugar kinase/heat-shock protein 70/actin (ASKHA) superfamily of kinases and not the P-loop kinases like type I PanKs.<sup>62,63,64</sup>

It has been reported that some Gram-positive bacteria express PanK proteins which are similar to type II PanKs in primary sequence. The type II PanK expressed by *Staphylococcus aureus* is the most notable example.<sup>65</sup> Despite its sequence similarity with type II PanKs, it differs from this class as well in that it has a greater affinity for ATP (34  $\mu$ M compared to values above 100  $\mu$ M) and it is not inhibited by CoA or its thioesters.<sup>66</sup> The reason for the lack of inhibition observed is a substitution of two residues known to be required for acetyl-CoA binding in the structure of human PanK3.<sup>63</sup> Steric bulk is introduced to the potential acetyl-CoA binding site by an Ala $\rightarrow$ Tyr substitution. A second substitution, Trp $\rightarrow$ Arg, causes disruption of the hydrophobic pocket which normally accommodates CoA's thiol or the acetyl group of acetyl-CoA. No other type I or type II PanKs have been found to be refractory to inhibition by CoA or its thio-esters and this characteristic of the *S. aureus* PanK may be a result of its distinctive redox biology. Aerobic eukaryotes and Gram-negative bacteria utilize glutathione (GSH) and an NADPH-dependent glutathione reductase enzyme to maintain the intracellular redox balance.<sup>67,68,69,70</sup>

*S. aureus* does not produce GSH and a glutathione reductase enzyme has not been identified in this organism. Instead, it employs CoA and a CoA disulfide reductase to maintain the intracellular reducing environment and neutralize oxidative stress. A much larger CoA pool is therefore required above what is needed for normal growth and metabolism in *S. aureus*. The reason that no feedback inhibition of PanK is observed is rationalized by the higher demand for CoA in *S. aureus*. Despite differences in the active site structure compared to other type II and type I PanKs, the *S. aureus* enzyme still phosphorylates some pantothenamides which have shown promise for the development of antistaphylococcal compounds.<sup>65</sup>

One pantothenamide in particular, *N*-heptyl pantothenamide (N7-Pan), has been reported to be the most potent inhibitor of *S. aureus* growth that has been discovered to date with an MIC of 78 nM.<sup>45</sup> Subsequent studies to elucidate the mode of action revealed that N7-Pan

binds to the type II PanK of *S. aureus* with high affinity but exhibits a slow turnover rate, indicating that it functions as an inhibitor of the enzyme but also as a substrate to a certain extent.<sup>71</sup> This is in contrast with the mode of action of *N*-pentyl pantothenamide (N5-Pan) for growth inhibition of *E. coli*, where it acts as an excellent substrate of the type I PanK and is converted to a CoA-antimetabolite. Variations in the dimethyl groups of the pantoic acid moiety of the pantothenamides were introduced in an attempt to increase the potency of N7-Pan towards *S. aureus* but failed to exhibit increased potency compared to N7-Pan.<sup>72</sup> These variations were further explored by a number of modifications made to the  $\beta$ -alanine moiety of the pantothenamide compounds. This moiety was replaced with  $\gamma$ -aminobutyric acid to yield homopantothenamides (ho-Pan). Studies have revealed that ho-Pan acts as a competitive inhibitor of the murine type II PanK and that *in vivo* CoA levels are decreased if administered to mice.<sup>73</sup> A similar reduction is seen when insect cells are treated with ho-Pan.<sup>74</sup> When the effects of ho-Pan on the activity of the *S. aureus* type II PanK were tested, it was found to be an inhibitor of activity but also exhibited substrate properties and consequently the mode of inhibition by ho-Pan is not clear at this stage.<sup>71</sup> However, *S. aureus* growth was not inhibited by ho-Pan, and this together with its inhibitory activity towards murine and mouse type II PanK raises questions about its utility for the development of anti-staphylococcal chemotherapeutic agents.

Investigation of inhibition of another type II PanK, the human PanK3 isoform was performed by high throughput screening (HTS) of a compound library containing 5600 biologically active compounds.<sup>75</sup> Three classes of inhibitors were identified, thiazolidinediones, sulfonylureas and steroids. Two thiazolidinediones were flagged in the screen, rosiglitazone and pioglitazone, and two sulfonylurea inhibitors were identified, glipizide and glyburide. The most potent inhibitor identified was a steroid-type compound, fusidic acid, which is known to inhibit growth of methicillin-resistant *S. aureus* and other Gram-positive bacteria but it is not commonly used to treat such infections due to hepatotoxic side effects.<sup>76,77</sup> Thiazolidinedione and sulfonylureas were shown to inhibit PanK3 activity by interaction with the acetyl-CoA binding site but structural studies suggests that it may not extend into the ATP binding site to prevent binding of the nucleotide.<sup>75</sup> This suggests that inhibition occurs due to allosteric binding to the acetyl-CoA binding site which indicates that inhibition may not be selective to this particular kinase and that others with similar acetyl-CoA binding sites may also be inhibited. The cross-reactivity of the thiazolidinedione and sulfonylurea scaffolds with PanK3 highlights the importance of testing PanK activity for potential off-target effects when the specificity of newly developed compounds is evaluated.

In another study a larger compound library was screened as inhibitors of the human type II PanK with the aim of developing tools to investigate the role of CoA in adult tissues and to accelerate the identification of bypass drugs for the treatment of PKAN disease.<sup>78</sup> HTS was also performed on the PanK3 isoform because it has a wide tissue distribution in mammals and high yields are obtained in purification. A number of compounds with a core tricyclic scaffold were identified as inhibitors during HTS and this scaffold was selected for the synthesis of more advanced lead compounds. Structure activity relationship experiments showed that the side chain of the tricyclic compound is tolerant to modifications and this would enable future expansion of the series in search of potent, drug-like compounds. One of the synthesized tricyclic compounds (referred to as compound 7 in the study) was tested as inhibitor of PanK3 and found to inhibit the enzyme with an  $IC_{50}$  value of 25 nM. Inhibition of PanK1 $\alpha$  and PanK1 $\beta$  was also observed with  $IC_{50}$  values of 70 nM and 92 nM respectively. Investigation of the kinetic mechanism of inhibition of PanK3 showed that the tricyclic compound 7 lowered both the maximal rate and  $K_M$  for ATP and a mixed inhibition pattern with respect to pantothenate was observed. It was also confirmed that compound 7 binds to the ATP-enzyme complex which could again raise the question of selectivity as other ATP-kinase enzyme complexes may also be inhibited by this mode of action, but this has not been tested. The ability of compound 7 to inhibit CoA biosynthesis in cultured C3A cells was confirmed by the observation of a dose-dependent decrease in pantothenate incorporation into CoA.

#### 1.3.4.2 Type III PanK

A third type of PanK was proposed to exist when genome-wide studies of certain bacteria, like *Helicobacter pylori* and *Pseudomonas aeruginosa*, allowed for the identification of homologues of all the CoA biosynthetic enzymes except PanK, regardless of whether type I or type II PanK sequences were used in the homology searches.<sup>20,79</sup> Subsequently, a gene distinct from those encoding the other PanK types was discovered in the Gram-positive *Bacillus subtilis*.<sup>80</sup> This second PanK-encoding gene was named *coaX* and homology searches based on sequence revealed that most bacteria where a PanK could not previously be identified, in fact contained CoaX homologues. The CoaX protein of *B. subtilis* and *H. pylori* was overexpressed and purified for full characterization; this indicated that these enzymes had a marked difference in kinetic parameters compared to other PanK types, in addition to the obvious differences in the primary sequence and structure.<sup>81</sup> The most notable of these kinetic parameter differences was the enzyme's  $K_M$  for ATP which was reported to be in the millimolar range (10 mM for *H. pylori* vs. 34  $\mu$ M and 100  $\mu$ M for type I and type II PanKs respectively). In addition, CoaX proteins do not experience feedback

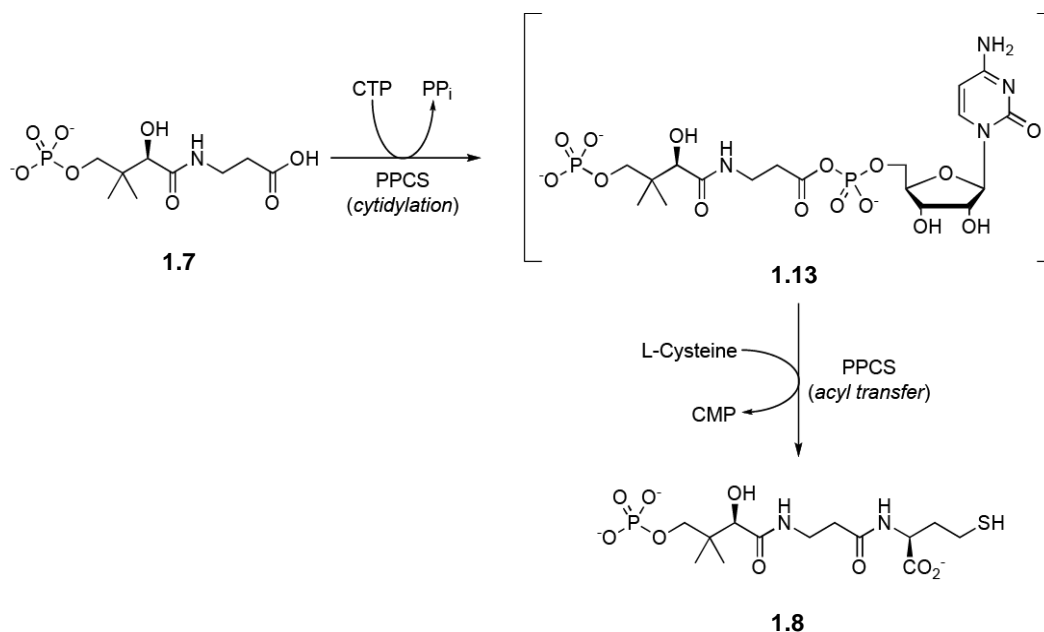
inhibition by CoA or acetyl-CoA and do not accept alternative substrates such as pantothenate analogues. CoaX proteins were deemed sufficiently different from type I and type II PanKs to constitute a third class, denoted as type III PanKs. Structural studies have confirmed that type III PanKs also belong to the ASKHA superfamily of kinases.<sup>82</sup> It is interesting to note that many pathogenic bacteria exclusively express type III PanKs, suggesting that these enzymes could be targets for the development of selective antimicrobial compounds considering the degree of difference with the type II PanKs found in humans.<sup>82</sup> The only inhibitors of type III PanKs that are currently known are nucleoside triphosphate mimetics of ATP that were identified by the synthesis and screening of a library of ATP structural analogues as inhibitors of *Bacillus anthracis* (*Ba*) PanK.<sup>83</sup> The triphosphate sidechains in the structure of ATP were replaced by uncharged methylene-triazole linked monosaccharide sidechains. One of these ATP analogues displayed competitive inhibition of *Ba*PanK with a  $K_i$  value of 164  $\mu\text{M}$  that is three-fold lower than the  $K_M$  value for ATP which is reported as 510  $\mu\text{M}$ . Although this indicates that the enzyme has a higher affinity for the inhibitor than ATP, the reported  $K_i$  value is too high to be of pharmaceutical interest, and no whole cell inhibition was reported. The low affinity of type III PanKs for ATP has raised questions of whether ATP really is the co-substrates of these enzymes.<sup>64,81</sup> This in turn, casts doubt on whether ATP mimetics is the best approach to pursue for the discovery of type III PanK inhibitors.

### 1.3.5 Phosphopantothenoylcysteine synthetase

PPCS is the second enzyme in the CoA biosynthesis pathway, catalysing the  $\text{Mg}^{2+}$ -dependent formation of 4'-phosphopantothenoylcysteine (PPC) (**1.8**) from 4'-phosphopantothenate (**1.7**) and L-cysteine with a nucleoside monophosphate and pyrophosphate ( $\text{PP}_i$ ) forming as side products.<sup>8</sup> Two forms of PPCS have been identified, namely bacterial PPCS and eukaryotic PPCS. Bacterial PPCS utilizes CTP for the activation of the carboxylate of 4'-phosphopantothenate through the formation of an acyl-cytidylate intermediate (**1.13**, Scheme 1.3).<sup>84</sup> The bacterial PPCS is normally fused to the next enzyme in the pathway, PPCDC, to form a bifunctional CoaBC protein (*coaBC* gene product). The eukaryotic enzyme on the other hand, is monofunctional (*coaB* gene product) and utilizes ATP for activation of the substrate carboxylate.<sup>85,86,87</sup>

The bacterial *coaBC* gene has been cloned and overexpressed and the CoaBC protein has been purified and characterized with a pyrophosphatase assay measuring  $\text{PP}_i$  formation.<sup>84</sup> The  $K_M$  for 4'-phosphopantothenate was determined to be 55  $\mu\text{M}$  with the  $K_M$  for CTP and L-cysteine given as 106  $\mu\text{M}$  and 109  $\mu\text{M}$  respectively.<sup>88</sup> Interestingly, studies have shown that

the product of the PPCS domain of the CoaBC protein, PPC, dissociates from the protein before binding to a different active site for transformation by the PPCDC domain.

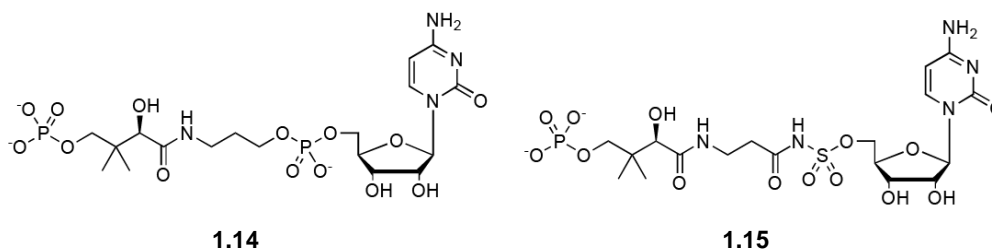


*Scheme 1.3: Reaction catalyzed by bacterial phosphopantothenoylcysteine synthetase (PPCS). 4'-Phosphopantothenate (1.7) is cytidylated to form the transient acyl-cytidylate intermediate (1.13) that subsequently yields 4'-phosphopantothenoylcysteine.*

This finding suggests that the fusion of these enzyme activities in bacteria is not mechanistically significant. From a physiological perspective, the fusion does ensure that the concentration of PPCS and PPCDC enzymes are always equal; this could be an important consideration in the distribution of the flux control among the pathway enzymes.<sup>89</sup> Both bacterial and eukaryotic PPCS proteins have dimeric structures with similar folds.<sup>90</sup> Another noteworthy characteristic of PPCS is the very high selectivity displayed for cysteine. Even in the presence of 500 000-fold excess serine, the structure of which closely resembles that of cysteine, only cysteine is incorporated into the product.<sup>91</sup> Since the structure of serine substitutes the thiol of cysteine for a hydroxyl group, this highly selective incorporation of cysteine is not surprising since condensation with serine would lead to the formation of oxy-CoA, a potentially toxic CoA analogue.<sup>92</sup>

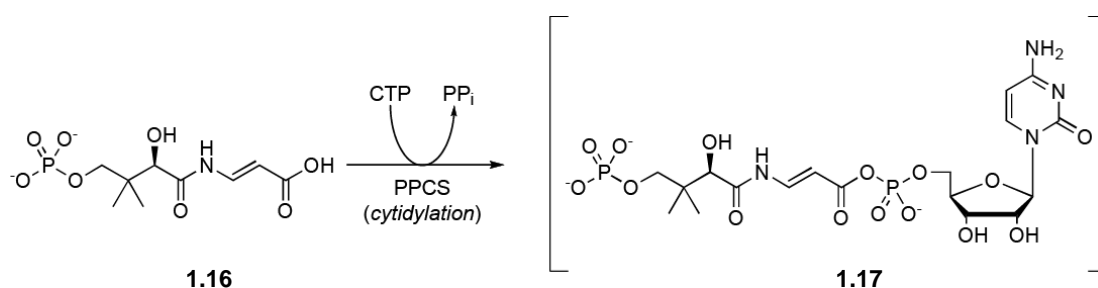
The above-mentioned differences the nucleotide requirement of bacterial vs. eukaryotic PPCS suggests that it is an excellent target for selective inhibition. Inhibitors of PPCS have been reported that mimic the structure of the acylcytidylate intermediate that forms during the catalytic cycle.<sup>93</sup> These inhibitors do not contain the reactive acyl-phosphate moiety but a phosphodiester (**1.14**, Scheme 1.4) or acyl-sulfonamide (**1.15**) isostere instead. This class of inhibitors were found to be non-competitive inhibitors and exhibited slow-onset tight-binding

inhibition. Nanomolar  $IC_{50}$  and  $K_i$  values have been reported for PPCS inhibition with up to 1000-fold selectivity over the human enzyme. These inhibitors failed to inhibit bacterial cell growth with poor cellular penetration cited as the cause.



*Scheme 1.4: Phosphopantothenoylcysteine synthetase (PPCS) inhibitors that mimic the acylcytidylate intermediate. Inhibitors substitute the acyl-phosphate moiety for a phosphodiester (**1.14**) or an acyl-sulfonamide (**1.15**)*

More success has been observed for the inhibitory properties of the natural product CJ-15,801 that was discovered by Pfizer in 2001.<sup>94</sup> This compound is structurally analogous to pantothenate but contains a trans-substituted double bond in the  $\beta$ -alanine moiety. It has been reported that CJ-15,801 inhibits the growth of drug resistant strains of *S. aureus* with MIC in the micromolar range without inhibiting the growth of other bacteria.<sup>94</sup> The reason is that it is phosphorylated by the uniquely selective PanK type II of *S. aureus* to yield the phosphorylated product **1.16** (Scheme 1.5) that is subsequently accepted as a substrate by PPCS.<sup>95</sup> Upon cytidylation, a structural mimic of the native acylcytidylate is formed (**1.17**) that functions as a tight-binding inhibitor of PPCS with nanomolar  $K_i$  values of the CoaBC protein in *S. aureus*.<sup>95</sup>



*Scheme 1.5: Cytidylation of phosphorylated CJ-15,801. *S. aureus* PanK phosphorylates CJ-15,801 to yield **1.16** that is subsequently cytidylated by phosphopantothenoylcysteine synthetase (PPCS) to form the structural mimic of the acylcytidylate intermediate (**1.17**) that acts as a tight binding inhibitor*

### 1.3.6 Phosphopantothenoylcysteine decarboxylase

As stated in the previous section, the activity of bacterial phosphopantothenoylcysteine decarboxylase (PPCDC) is fused to PPCS in the bifunctional CoaBC protein (*coaBC* gene product).<sup>84,96</sup> Bacterial CoaBC proteins form homododecamers (tetramers of trimers) through interaction of their CoaC domains. In eukaryotes PPCDC is expressed as a distinct monofunctional protein (*coaC* gene product) with a trimeric structure.<sup>97</sup> PPCDC catalyses the decarboxylation of the cysteine moiety of the substrate PPC to yield 4'-phosphopantetheine. This reaction causes a negative charge to be formed on the carbon adjacent to the amide nitrogen of PPC and the manner in which this charge was stabilized was elucidated using the *E. coli* CoaBC protein and by characterization of its PPCDC domain.<sup>96</sup> The enzyme was found to have a tightly bound flavin mononucleotide cofactor responsible for oxidation of the substrate cysteine thiol to form a thioaldehyde which undergoes spontaneous decarboxylation to yield an enethiol product. Reduction of this enethiol by the reduced flavin (using an active site cysteine as proton donor) yields the product 4'-phosphopantetheine to complete the catalytic cycle.<sup>98</sup>

Drug development efforts targeting PPCDC have been limited and only one inhibitor has been described so far. A cyclopropyl-substituted product analogue, 4'-phospho-*N*-(1-mercaptomethyl-cyclopropyl)-pantothenamide (PPan $\Delta$ SH), was discovered to be a mechanism-based inhibitor of the human PPCDC enzyme with a reported  $K_i$  of  $2.58 \pm 0.13$  mM.<sup>99</sup> It functions by alkylation of the active site cysteine that is required for enethiol reduction and product formation. This leads to the trapping of the covalently bound enethiolate intermediate. No inhibitors of the PPCDC domain of the bifunctional bacterial protein have been reported to date.

### 1.3.7 Phosphopantetheine adenylyltransferase

In the penultimate step of CoA biosynthesis, phosphopantetheine adenylyltransferase (*coaD* gene product) catalyses the reversible and  $Mg^{2+}$ -dependent adenylylation of PPanSH to yield dephospho-CoA and  $PP_i$  as products. In bacteria the protein is expressed as a single monofunctional protein with a homohexameric structure consisting of a dimer of distinct trimers.<sup>100</sup> Cloning of the *E. coli* PPAT protein has led to extensive kinetic characterization of this enzyme.<sup>101</sup> It has a random bi-bi mechanism and a ternary complex of PPanSH, ATP and enzyme is formed during the catalytic cycle. Like PanK, *E. coli* PPAT also experiences inhibition by CoA with a  $K_i$  reported in the range of 10–50  $\mu$ M. A detailed review of the

reaction mechanism of *E. coli* PPAT is given in Chapter 4 where the kinetic parameters are also discussed in detail.

In contrast, PPAT activity in eukaryotes is fused to the last enzyme in the pathway, dephospho-CoA kinase (DPCK).<sup>102</sup> This forms a bifunctional PPAT/DPCK protein that is also referred to as CoA synthase (CoASy). The PPAT domain of the eukaryotic protein reportedly shares little sequence similarity with the monofunctional bacterial enzyme, which suggests that PPAT may be a viable target for the development of novel and selective antimicrobial agents.<sup>85,103,104</sup> Structural studies of bacterial PPAT enzymes revealed that they display sequence homology to members of the nucleotidyltransferase  $\alpha/\beta$  phosphodiesterase superfamily of enzymes.<sup>105</sup> Little is known about the structure of the PPAT domain of the bifunctional protein in eukaryotes but preliminary studies suggest that it belongs to the same superfamily.<sup>106</sup>

Several PPAT inhibitors have previously been discovered but none of these showed any whole cell growth inhibition, raising questions about the suitability of PPAT as a target for inhibition.<sup>107,108</sup> Subsequently, a high-throughput screening of an AstraZeneca compound library identified a series of cycloalkyl pyrimidines that was optimized for effective inhibition of Gram-positive bacteria.<sup>109</sup> These compounds inhibited *S. aureus* and *S. pneumoniae* PPAT activity and inhibition was found to be competitive with respect to PPanSH binding. These compounds successfully inhibited growth of several clinical Gram-positive isolates but was not deemed suitable clinical candidates because their biological activity could not be reconciled with the necessary drug-like properties.

### 1.3.8 Dephospho-CoA kinase

In the final reaction of the CoA biosynthesis pathway, dephospho-CoA kinase (DPCK) catalyses the  $Mg^{2+}$ -ATP-dependent phosphorylation of DePCoA to yield CoA and ADP. As mentioned in the previous section, DPCK activity is fused to PPAT in eukaryotes as part of the bifunctional CoA synthase protein, but it is expressed as a monofunctional protein in bacteria (*coaE* gene product).<sup>97,102</sup> In contrast to PPAT, the eukaryotic DPCK domain exhibits good sequence homology with its bacterial counterpart.<sup>103,104</sup> Cloning, expression and characterization of the *E. coli* DPCK protein (*coaE* gene product) revealed that it is a monomer in solution with apparent  $K_M$  values of 140  $\mu M$  and 740  $\mu M$  for ATP and DePCoA respectively.<sup>110</sup> The DPCK domain of CoA synthase has a far higher affinity for DePCoA with a reported  $K_M$  of  $5.2 \pm 1.5 \mu M$ .<sup>103</sup> This leads to the normally reversible activity of PPAT to become effectively irreversible in the bifunctional CoA synthase protein. The DPCK domain

of CoA synthase displays similar affinity for ATP than the monofunctional bacterial enzyme with the  $K_M$  for ATP is reported as 192  $\mu\text{M}$ .<sup>103</sup> Structural studies of *E. coli* DPCK and the DPCK domain of *Mus musculus* CoA synthase show that DPCK belong to the P-loop kinase family of enzymes, just like pantothenate kinase.<sup>111</sup>

A limited amount of information is available on DPCK, creating some uncertainty about its kinetic parameters. Nothing is known about the catalytic mechanism, but it is thought that structural movement may occur during catalysis. The very low apparent affinity of *E. coli* (*EcDPCK*) for DePCoA remains an important question in the regulation of CoA production and consequently its potential as an antimicrobial drug target. Additionally, the basis for the relaxed substrate specificity seen in *EcDPCK* but not in *HsPPAT/DPCK* has not been elucidated. Structural factors may be behind both of these questions such as conformational changes upon substrate binding, differences in active site architecture and differences in quaternary structure. These structural factors and how they relate to the activity of *EcDPCK* will be discussed in detail in the following subsections.

#### 1.3.8.1 A conformational change of DPCK

The crystal structure of *EcDPCK* has been solved with only ADP bound but the structure determined for another bacterial DPCK from *Thermatoga maritima* (*TmDPCK*) had both DePCoA and ADP bound.<sup>111</sup> In Figure 1.3 an overlay of *EcDPCK* (PDB: 1VHL) with *TmDPCK* (PDB: 2GRJ) is shown, highlighting a clear difference in the conformation of the two enzymes. *TmDPCK* is shown in grey and appears to clamp down on DePCoA for a closed type of conformation. *EcDPCK* is shown in green and appears to have a more open conformation due to the unoccupied binding site of DePCoA. If DePCoA is modelled in the active site of *EcDPCK* in the open conformation containing either ATP or ADP, the distance between the 3'-OH group of the ribose moiety of DePCoA and the a  $\gamma$ -phosphate of ATP extends to about 7 Å. This is too far for phosphoryl transfer to occur and implies that the formation of a closed conformation is required when DPCK binds DePCoA to bring it closer to ATP for catalytic activity. Such a closed complex may also serve to protect bound ATP from hydrolysis during catalysis. Such substrate induced conformational changes are common in the P-loop kinase family of enzymes of which DPCK is a member.<sup>112</sup>

These structural studies of bacterial DPCKs indicate that *EcDPCK* binds to its substrate with low affinity and low specificity followed by a conformational change to a more closed structure with higher affinity and specificity to allow for catalysis to take place. This may account for the low affinity observed for DePCoA in *in vitro* initial rate assays of *EcDPCK*.

Another possible explanation for the low apparent affinity for DePCoA that is observed may be due to changes in the quaternary protein structure. *EcDPCK* has been identified as a monomer in solution<sup>110</sup> but surprisingly it crystallized as a trimer in the presence of sulfate.<sup>111</sup>

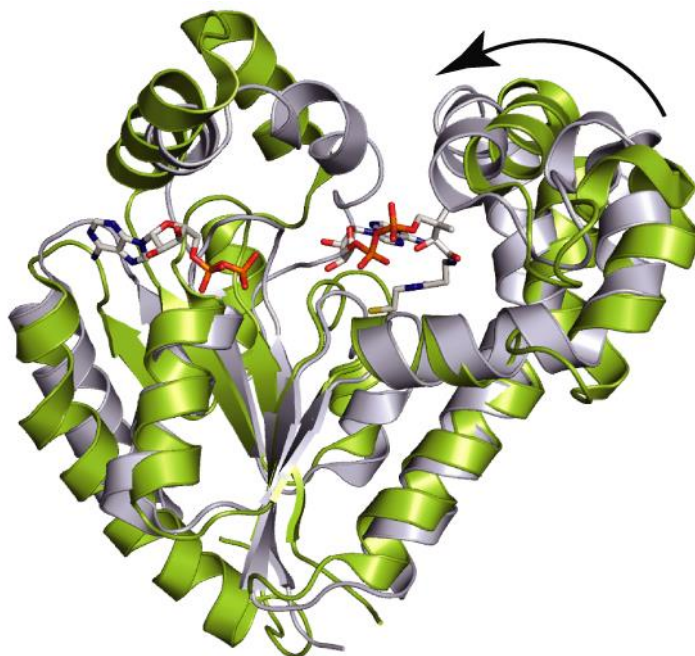
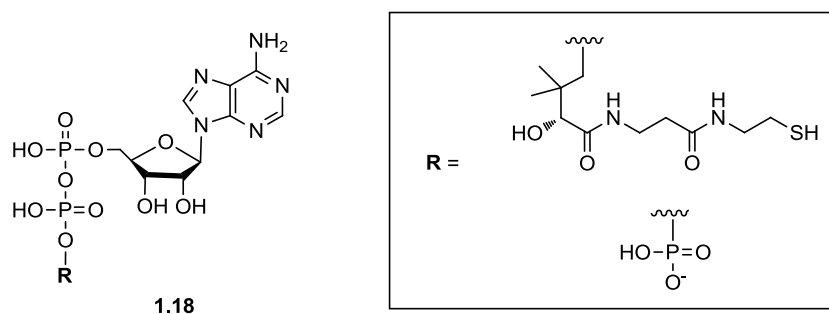


*Figure 1.3: Overlay of the crystal structures of TmDPCK (PDB: 2GRJ, grey) with EcDPCK (PDB: VHL, green). TmDPCK contains both ADP and DePCoA in the active sites and has a more closed conformation. Superimposition of EcDPCK that only has ADP bound reveals it has an open conformation. It is proposed that binding of DePCoA by EcDPCK will induce a conformational change, as indicated by the arrow, to yield a closed conformation for catalytic activity as is observed for TmDPCK. Figure reproduced with permission from Wiley InterScience, Strauss, E., de Villiers M. and Rootman I. (2010) ChemCatChem 2, 929-937, <http://onlinelibrary.wiley.com/doi/10.1002/cctc.201000139/abstract> Copyright © 2010 Wiley-VCH Verlag GmbH&Co. KGaA, Weinheim.*

Studies performed in our group on the monofunctional bacterial DPCK from *Corynebacterium ammoniagenes* (CaDPCK) revealed a far higher affinity for DePCoA with a dissociation constant ( $K_d$ ) of  $46.6 \pm 3.8 \mu\text{M}$  vs. a  $K_M$  of  $1550 \pm 510 \mu\text{M}$  determined for the *E. coli* protein under the same conditions. Furthermore, analysis of a Hill plot of CaDPCK activity exhibited positive cooperativity with a Hill coefficient of 3 which suggests an oligomeric structure. Consequently it has been proposed that the quaternary structure of *EcDPCK* may serve as a regulatory mechanism to switch from a low affinity monomer to a higher affinity oligomer. However, this remains speculation as the conditions that would cause such a switch to occur remain unknown.

### 1.3.8.2 Relaxed substrate specificity of *EcDPCK*

Two possible explanations for the low substrate specificity of *EcDPCK* have been proposed. First, PanSH and ATP may compete for their respective binding sites due to the high degree of similarity in their respective structures as highlighted in Scheme 1.6. This may lead to competitive inhibition of binding and catalytic activity.



*Scheme 1.6: An adenosine diphosphate moiety with a substitution make up the structures of both DePCoA and ATP. In the structure of ATP the substitution (R) is a phosphate group. In the case of DePCoA, R is a pantetheine moiety. The structural similarity afforded by the common adenosine diphosphate moiety may lead to substrate competition and inhibition of binding.*

The second possible explanation for the low substrate specificity of *EcDPCK* is the structure of the protein around the active site. If the protein structure is inspected where ADP and DePCoA have been modelled in the active site (Figure 1.4), an adjacent cleft can be seen as indicated by the arrow. This cleft can accommodate variations in the PanSH moiety of DePCoA but it can also allow DePCoA to bind in a reverse manner without affecting the binding of the adenosine moiety.<sup>111</sup> However, these explanations for the relaxed substrate specificity cannot be confirmed or excluded based in the structural information that is currently available.

The low substrate specificity exhibited by *EcDPCK* indicates that it should accept alternative substrates to be converted to CoA-antimetabolites for inhibition of CoA-dependent reactions. DPCK has not been the focus of any studies directed toward development of inhibitors because of the high degree of sequence homology between the monofunctional bacterial DPCK and the DPCK domain of the bifunctional CoASy protein in humans. This indicates that selective inhibitors will be hard to find.

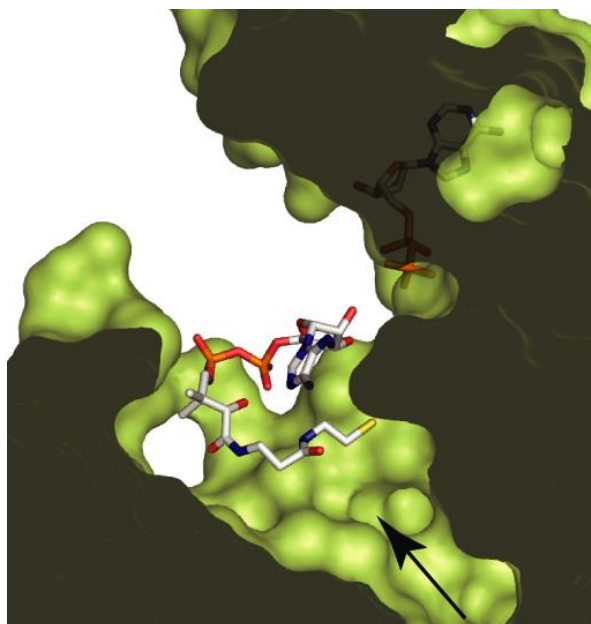


Figure 1.4: Cross-section revealing the active site of EcdPCK (PDB: 1VHL). DePCoA is modelled in the active site and the arrow indicates the presence of a cleft next to the binding site. This cleft could allow for variation in the PanSH moiety but also allow DePCoA to bind in a reverse mode where the PanSH moiety would then extend into the surrounding solvent represented by the white space above. Figure reproduced with permission from Wiley InterScience, Strauss, E., de Villiers M. and Rootman I. (2010) ChemCatChem 2, 929-937, <http://onlinelibrary.wiley.com/doi/10.1002/cctc.201000139/abstract> Copyright © 2010 Wiley-VCH Verlag GmbH&Co. KGaA, Weinheim

## 1.4 The demand for CoA

### 1.4.1 CoA degradation

Little is known about the purpose of CoA degradation but it is thought to be a mechanism for regulation of intracellular CoA levels. In mammals a nucleotide pyrophosphatase localized in the plasma membrane cleaves the pyrophosphate bonds of CoA to yield PPanSH and ADP.<sup>113,114</sup> However, this enzyme is considered non-specific for CoA degradation because of broad substrate selectivity and low affinity for unacylated CoA.<sup>115</sup>

Nudix hydrolases are a superfamily of enzymes that hydrolyse nucleoside diphosphates linked to other moieties and members of this family have been identified that act specifically as diphosphatases of CoA and its derivatives. Nudix hydrolases have been identified in bacteria<sup>116</sup> and mice<sup>117</sup> amongst other organisms, and have demonstrated activity to hydrolyse CoA and acyl-CoA thioesters to yield either PPanSH or an acyl-PPanSH product together with ADP.<sup>118</sup> It has been reported that in *E. coli* a rapid decrease in the acetate supply causes a dramatic reduction in the acetyl-CoA pool and a transient increase in free

CoA.<sup>119</sup> This is followed by the degradation of CoA to PPanSH, which is then excreted in the medium. It has been suggested that nudix hydrolases facilitates such rapid degradation of CoA.

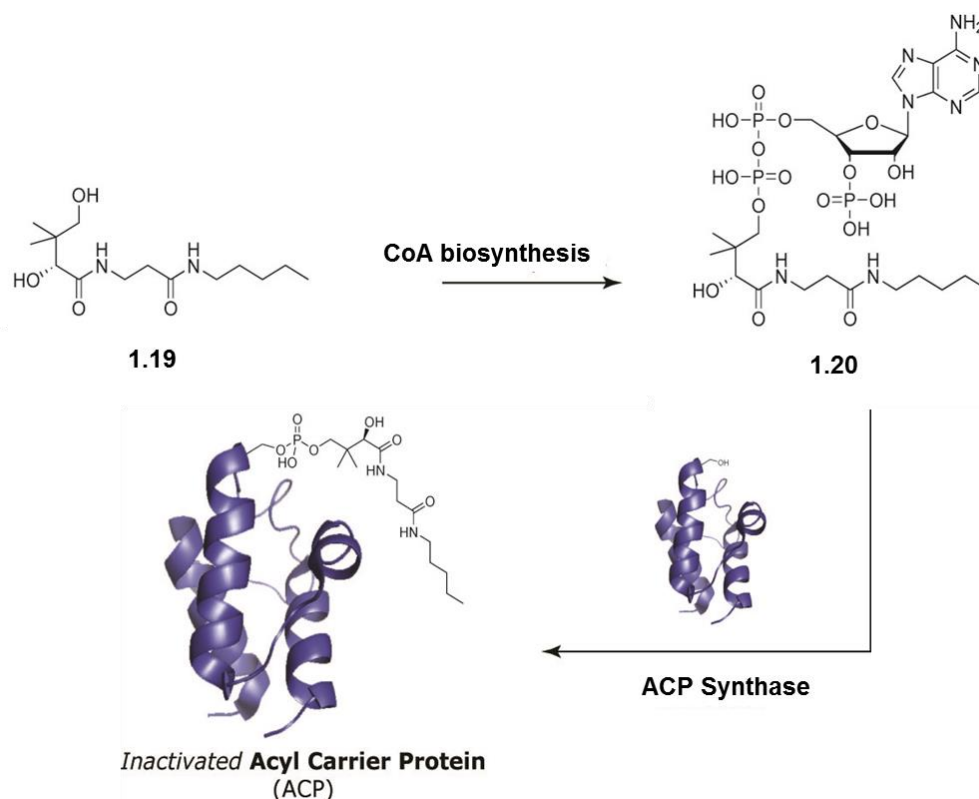
### 1.4.2 Synthesis of acyl carrier proteins

CoA consumption occurs with the transfer of its PPanSH moiety to carrier proteins such as acyl carrier proteins (ACP) in bacteria or fatty acid synthase (FAS) in eukaryotes. Transfer of the PPanSH prosthetic group activates these proteins to fulfil their function as acyl-group carriers. The thiol group of PPanSH enable these proteins to form thioester linkages with carboxylic acids. In bacteria, the transfer of PPanSH from CoA to the *apo*-ACP (inactive) to form the *holo*-ACP (active) is catalysed by ACP synthase.<sup>120,121</sup> The PPanSH prosthetic group is later removed from *holo*-ACP by ACP phosphodiesterase, which is a member of the HD phosphatase family.<sup>122</sup>

The mammalian FAS protein is activated by PPanSH transfer that is catalysed by cytoplasmic ACP synthase with broad substrate specificity.<sup>123</sup> These PPanSH transfer mechanisms provide a way to coordinate active ACP and FAS levels with CoA levels. ACP and FAS levels are typically much lower than the intracellular CoA level. The acyl-groups shuttled by ACP are required by the enzymes of fatty acid biosynthesis in bacteria. In eukaryotes FAS binds acetate and malonate to produce long-chain fatty acids. It has been reported that in bacteria recovering from CoA deprivation, the turnover of the ACP prosthetic group is four times faster than the rate of new ACP protein synthesis but in logarithmic growth when CoA levels are high, the turnover drops by an order of magnitude compared to when the CoA levels were low.<sup>124</sup> The physiological significance of *holo*-ACP synthesis and degradation is not known. The PPanSH generated in the synthesis and degradation cycle can either enter the CoA salvage pathway to be incorporated into CoA once again or it can be excreted to regulate CoA concentration.

When the pantothenamide class of inhibitors acts as antimetabolites, they exert their activity on the bacterial ACP as shown in Scheme 1.7. Following phosphorylation of *N*-pentyl pantothenamide (**1.19**) by Pank the resulting 4'-phosphopantothenamide is adenylylated by PPAT and 3'-phosphorylated by DPCK to form the CoA antimetabolite ethyldethia-CoA (**1.20**), which functions as an inhibitor of CoA-dependent enzymes, like ACP, that is involved in fatty acid biosynthesis.<sup>31,44</sup> Transfer of the 4'-phosphopantothenamide moiety by ACP synthase to ACP effectively inactivates the protein by replacing the terminal thiol with another functional group incapable of binding carboxylic acid groups. Therefore, when acting

as antimetabolites one of the major modes of action of the pantothenamides lies in their prevention of ACPs to act as acyl carriers.<sup>44,125</sup>



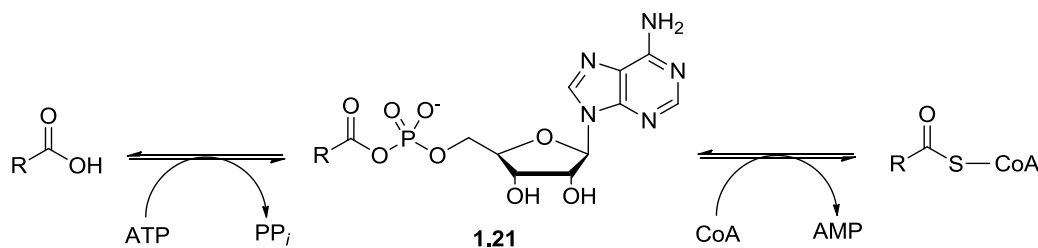
*Scheme 1.7: Mode of action of N-pentylpantothenamide.* The native CoA biosynthesis pathway converts N-pentylpantothenamide (**1.19**) to the CoA antimetabolite ethyldethia-CoA (**1.20**). Transfer of the phosphopantothenamide moiety to acyl carrier protein by ACP synthase effectively inactivates it.

### 1.4.3 Acyl-CoA synthesis

The bulk of CoA that is synthesised is converted to various acyl-CoA species and the enzymes that catalyse these conversions represent the largest demand for CoA. The various acyl-CoAs are synthesized by a number of ligases and oxidoreductases which are briefly described below.

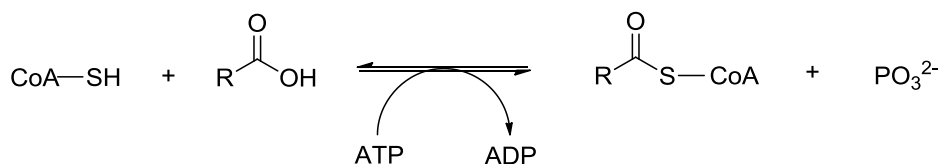
CoA ligases couple activated carboxylic acids directly to CoA. These include the acyl-CoA synthetases (ACS) that catalyse the formation of acyl-CoA thioesters from CoA and a free carboxylic acid in a reversible nucleoside triphosphate-dependent reaction. Two types of ACS can be distinguished based on the reaction mechanism. The first group utilizes ATP to activate the carboxylic acid (Scheme 1.8) by the formation of an acyl-adenylate intermediate (**1.21**) that reacts with CoA to yield the thioester and AMP.<sup>126,127</sup> This group of enzymes are

typically involved in the direct coupling of structurally diverse carboxylic acids to CoA including short-, medium, and long-chain fatty acids,<sup>128,129</sup> and amino acids.<sup>130</sup>



*Scheme 1.8: Coupling of activated carboxylic acid to CoA by AMP-forming acyl-CoA synthetase.* ATP is used for the initial activation of the carboxylic acid to form the acyl-adenylate intermediate (**1.21**) that subsequently reacts with CoA to give the thioester and AMP.

The second type of ACS also uses ATP for carboxylic acid activation but ADP and phosphate are produced as by-products of thioester formation (Scheme 1.9). In these reactions a phosphate is transferred from ATP to an active site histidine that subsequently transfers it to the substrate to yield an acyl-phosphate intermediate.<sup>131,132</sup> This intermediate is subsequently attacked by CoA's thiol to yield the acyl-CoA and phosphate. These reactions are reversible and the reverse reaction is a substrate level phosphorylation where a high-energy thioester bond is converted to the high-energy phosphoanhydride bond of a nucleoside triphosphate. With an equilibrium constant of approximately one, the reaction direction depends on the ATP/ADP ratio in the cell.<sup>133</sup>

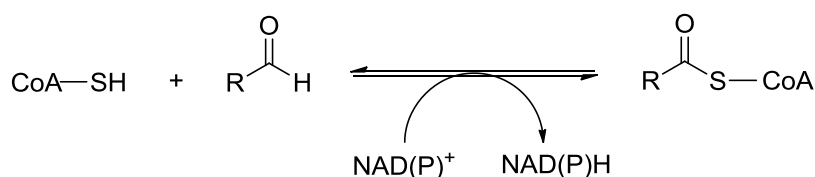


*Scheme 1.9: Coupling of activated carboxylic acid to CoA by ADP-forming acyl-CoA synthetase.* A phosphate group is transferred from ATP to the carboxylic acid group via an active site histidine to form an acyl-phosphate intermediate that is attacked by the CoA thiol to yield the acyl-CoA and phosphate.

Acetyl-CoA can be synthesised directly from acetic acid by ACS enzymes but the predominant reaction is determined by the concentration of acetate in the environment. This ensures that acetate can be used as a carbon- and energy source, regardless of the concentration in the environment. When low levels of acetate is present ( $\leq 10$  mM), the AMP-forming ACS reactions are active for the activation of acetate and the formation of acetyl-CoA.<sup>134,135</sup> ADP-forming ACS reactions are normally active in the reverse direction

and drive the formation of ATP from ADP with the hydrolysis of acetyl-CoA. When the environmental concentration of acetate is high, in excess of 30 mM, acetate kinase/phosphotransacetylase forms acetyl-CoA through the formation of acetyl phosphate. This reaction is also reversible and is used to maintain the steady-state concentration of CoA and conserve energy.<sup>136,137</sup>

Oxidoreductases catalyse the formation of acyl-CoA through aldehyde oxidation or oxidative decarboxylation of  $\alpha$ -keto acids. Aldehyde dehydrogenase (ALDH) enzymes catalyse the NAD(P)H-dependent oxidation of aldehydes to carboxylic acids for transfer to CoA (Scheme 1.10). An acyl-enzyme thioester intermediate forms when the active site cysteine residue acts as a nucleophile and attacks an aldehyde group. A CoA thioester is formed when the ALDH enzyme transfers the acyl group to the thiol of CoA. A reversible acetaldehyde dehydrogenase is found in the parasites *Giardia lamblia* and *Entamoeba histolytica* where it plays a central role in the utilization of glucose as energy source by fermentative pathways.<sup>138,139</sup>

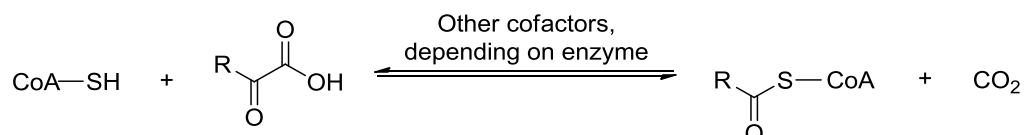


*Scheme 1.10: Acyl-CoA formation by the NAD(P)H dependent oxidation of an aldehyde by aldehyde dehydrogenase.* An acyl-enzyme thioester intermediate is formed and ALDH then transfers the acyl group to the thiol of CoA.

Oxidoreductases can also form acyl-CoA by oxidative decarboxylation reactions of  $\alpha$ -keto acids such as pyruvate and  $\alpha$ -ketoglutarate from which acetyl-CoA and succinyl-CoA are formed. Multienzyme complexes catalyse the oxidative decarboxylation of  $\alpha$ -keto acids under aerobic conditions (Scheme 1.11). These reactions require  $\text{NAD}^+$ , thiamin pyrophosphate (TPP), lipoic acid and CoA for activity. The  $\alpha$ -keto acid is decarboxylated by TPP to give an anionic hydroxyalkyl-TPP intermediate that reacts with the enzyme-bound lipoic acid to form acylated lipoamide. The acyl group is then transferred to CoA that acts as the final acceptor to form acetyl CoA.

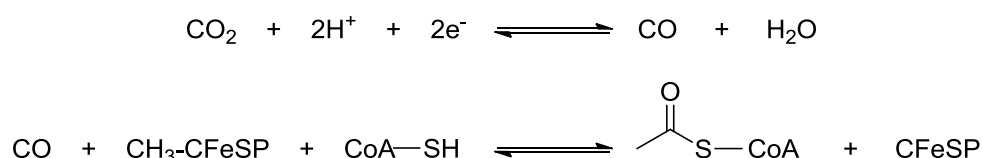
Under anaerobic conditions the same type of reaction is catalysed by ferredoxin-dependent 2-keto acid oxidoreductase enzymes such as pyruvate:ferredoxin oxidoreductase (PFOR). These enzymes also require TPP and CoA but have three  $[\text{Fe}_4\text{S}_4]^{2+/1+}$  clusters that act as

redox centres for the formation of a radical TPP intermediate. The exact mechanism which follows that finally forms the acyl-CoA product still has to be elucidated.<sup>140,141</sup> Acetyl-CoA is also formed by oxidative decarboxylation of pyruvate which is catalysed by the radical S-adenosyl methionine (SAM) enzyme pyruvate formate-lyase. The enzyme uses a [Fe<sub>4</sub>S<sub>4</sub>] cluster and SAM to form the catalytically active protein-based glycyl radical. The radical mediates a decarboxylation mechanism that forms an acetyl-enzyme thioester intermediate from which CoA accepts the acetyl group in a transthioesterification reaction.<sup>142,143</sup>



*Scheme 1.11: Acyl-CoA formation by oxidative decarboxylation of an  $\alpha$ -keto acid.* The  $\alpha$ -keto acid is decarboxylated and the acyl group transferred to CoA via TPP and lipoic acid in a reversible reaction.

The final group of reactions that catalyse the formation of acyl-CoA is carbon monoxide dehydrogenase (CODH)/acetyl-CoA synthase. This bifunctional enzyme is involved in the Wood-Ljungdahl pathway of carbon fixation present in anaerobic bacteria. The CODH functionality catalyses the reversible reduction of CO<sub>2</sub> to CO that is then transferred to the ACS active site to react with CoA and a methyl group donated by corrinoid iron-sulfur protein (CFeSP) to form acetyl-CoA (Scheme 1.12).

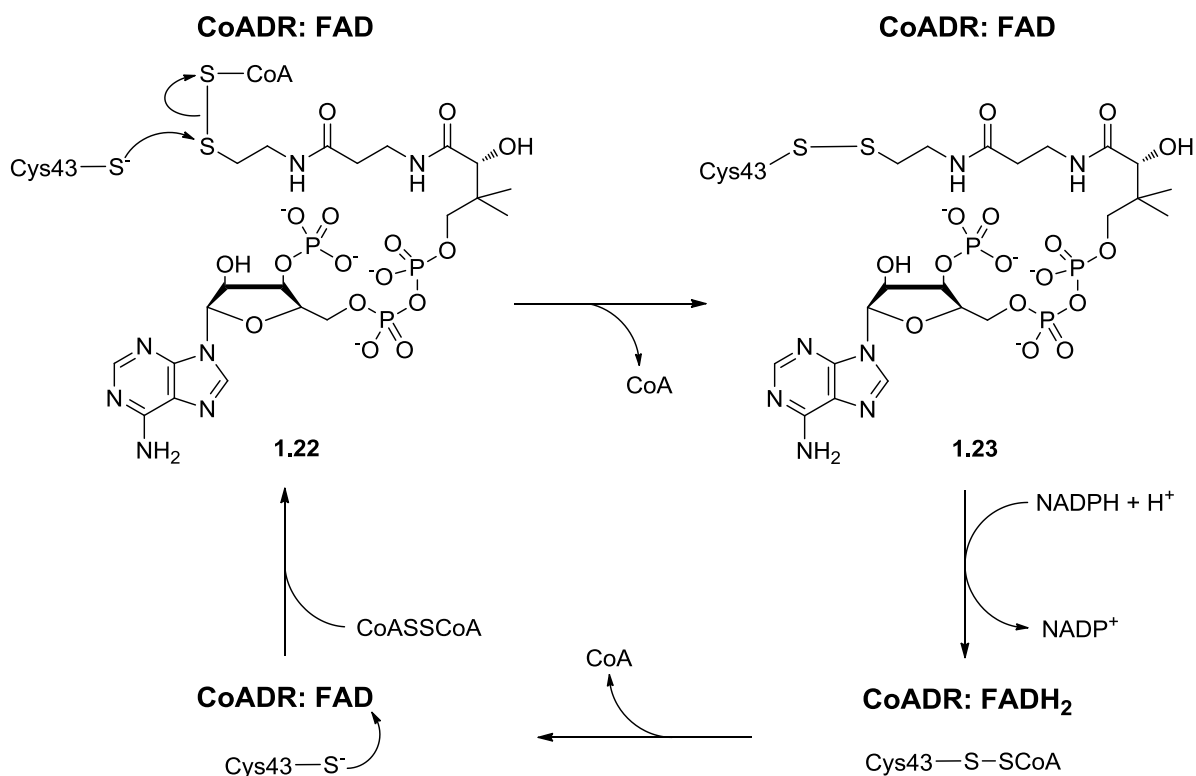


*Scheme 1.12: CODH/acetyl-CoA synthase mediated acetyl-CoA formation.* CO<sub>2</sub> is reduced to form CO by the CODH functionality and then reacts with CoA and a methyl from CFeSP in the ACS active site to form acetyl-CoA.

#### 1.4.4 CoA as redox buffer

CoA is used as a low molecular weight (LMW) thiol to mediate the effects of oxidative stress in some Gram-positive bacteria, most notably *S. aureus*. This is in contrast to eukaryotes and Gram-negative bacteria that use GSH to maintain the intracellular redox balance. CoA becomes oxidised in order to detoxify reactive oxygen species and *S. aureus* contains a dedicated CoA disulfide reductase (CoADR) enzyme to recycle free CoA in a NADPH dependent reaction. The proposed reaction mechanism for CoADR is shown in Scheme

1.13. CoADR uses an active site cysteine (Cys43) for catalysis and it has been shown that a mixed disulfide of Cys43 and CoA constitutes the redox centre during catalysis. FAD is reduced by NADPH and the resulting FADH<sub>2</sub> in turn reduces the Cys43:CoA disulfide and the liberated CoA is released.<sup>144,145</sup>



*Scheme 1.13: Reduction of CoA disulfide by CoA disulfide reductase (CoADR). CoA disulfide (1.22) undergoes nucleophilic attack by the catalytic Cys43 in the active site to form the Cys43:CoA mixed disulfide (1.23). Enzyme bound FAD is reduced by NADPH, forming FADH<sub>2</sub> that ultimately reduces the Cys43:CoA mixed disulfide and CoA is released.*

The distinction between the redox buffer system of *S. aureus* and eukaryotes make CoADR an attractive drug target. Pantothenamides containing a Michael-acceptor moiety have been designed and shown to be converted to the corresponding CoA-antimetabolites that subsequently inactivate CoADR.<sup>145</sup> However, the pantothenamide precursors of the CoA antimetabolites that showed effective inhibition of CoADR did not inhibit growth of *S. aureus*, with poor cell penetration being cited as the reason.

*S. aureus* is notoriously resistant to oxidative stress generated by neutrophils and macrophages during infection of the host and therefore the redox buffer system is vital to its growth and virulence. The presence of an additional LMW thiol, bacillithiol (BSH), has also been confirmed in *S. aureus* but its role in maintaining the intracellular redox balance is

currently unclear because no reductase enzyme has been identified to reduce BSH disulfides to constitute a separate redox buffer system.<sup>146</sup> The requirement of CoA in the known redox buffer system of *S. aureus* represents an additional demand for this cofactor in this organism and therefore intracellular concentrations are maintained in the millimolar range<sup>147</sup> as opposed to the micromolar range observed in *E. coli*<sup>39</sup> that uses a GSH based redox system. The regulation of increased intracellular CoA levels in *S. aureus* has been attributed to the lack of feedback inhibition of PanK by CoA as discussed earlier (Section 1.3.4.2). It stands to reason that redox-signalling may illicit a response in the form of increased CoA production when oxidative stress is encountered by *S. aureus* to enable the organism to adapt quickly to the oxidative environment created by the host immune system. However, such a redox-signalling mechanism has not been identified and it has not been tested whether CoA levels increase when oxidative stress is encountered.

## 1.5 Problem statement

The importance of CoA to all living organisms is well known and demonstrated by the essentiality of CoA production. If the ability to produce CoA is lost, cell viability is lost. While it is clear that CoA is essential, the specific life-sustaining function(s) of CoA has not been clearly defined. The essential roles of CoA in energy production by the Krebs cycle as well as in lipid biosynthesis are considered life sustaining processes. However, neither the Krebs cycle nor lipid biosynthesis pathways are active in blood stage malaria parasites and yet they display an essential requirement for pantothenate uptake and CoA biosynthesis.<sup>148,149,150,151,152</sup> Moreover, the specific life-sustaining function(s) are difficult to identify because of the multifaceted functions of CoA. The manner in which the essential functions of CoA determine the regulation of CoA levels (or vice versa) as well as the CoA:acetyl-CoA ratio is also unknown. These obscurities persist due to the lack of tools to study CoA production. The effects of factors that are thought to influence the regulation of CoA are difficult to test because the measurement of pathway intermediates for a holistic study are problematic so most investigations to date have focused on the measurement of CoA itself. However, such data do not provide the full picture and a better understanding of the CoA biosynthesis pathway would contribute significantly to our understanding of the relevance of maintaining specific CoA levels for survival. Our current understanding of the regulation of CoA production is based on studies of isolated enzymes, with PanK being identified as the so-called rate-limiting step. From a systems analysis perspective, it is unlikely that PanK alone controls the rate of CoA production; control is more likely distributed among all the steps. However, a systems analysis of CoA production has not been performed to evaluate this. Furthermore, because control distribution in the pathway has not

been assessed, the effects of different physiological or environmental states are unknown and these are questions that can only be answered by a systems analysis study of CoA production. In this study, oxidative stress is investigated as an environmental effector of CoA regulation in *S. aureus* because there is some information available on the role of CoA in the redox buffer system. The need for an analytical method to measure CoA biosynthesis intermediates as well as a systems analysis of CoA production will be addressed as outlined in the following objectives of this study.

### **1.5.1 Objective 1: Determine if CoA contributes to the oxidative stress resistance of the *S. aureus* USA300 strain**

CoA regulation by redox mediated signalling will be investigated by assessing whether CoA production is increased as a response to oxidative stress in *S. aureus* USA 300 and a bacillithiol deficient mutant USA300  $\Delta bshA$ . The importance of CoA to the overall oxidative stress resistance of *S. aureus* will be investigated by determining whether bacillithiol plays a significant role in resistance. This will be assessed by determining whether the strain that produces bacillithiol is less sensitive to oxidative stress than the bacillithiol deficient counterpart if CoA production is decreased by a known inhibitor of CoA production. The studies performed toward achieving this objective are described in Chapter 2.

### **1.5.2 Objective 2: Develop a method for the quantification of all the intermediates of the CoA salvage pathway**

Currently, no method exists for the quantification of all the intermediates of the CoA salvage pathway namely, PanSH, PPanSH, DePCoA and CoA. It will be determined if an analytical method can be developed for the measurement of the concentrations of these compounds based on derivatization with a fluorescent thiol probe and subsequent HPLC analysis. The main requirement of such an analysis method is simultaneous quantification of all the analytes of interest to enable analysis of the pathway. Validation of the method for accurate quantification is also vital to ensure credibility of the results and therefore statistical analyses will also be performed. These studies are reported in Chapter 3.

### **1.5.3 Objective 3: Systems analysis of the CoA salvage pathway in *E. coli***

The regulation of CoA production will be investigated by constructing the first kinetic model of the CoA salvage pathway. The current knowledge on the kinetic and regulatory properties of each enzyme will be reviewed to derive or identify the appropriate rate equation for each

step. Kinetic parameters from the literature will be used in the model of each reaction as well as parameters that were determined experimentally in this study. Validation of the model will be achieved by comparing time course predictions of the pathway made with the model to time courses of the reconstituted pathway measured under different conditions with the method developed in objective 1.5.2. A validated model will then enable control analysis to be performed to assess control distribution under different conditions and determine if PanK is a major controlling step under physiological conditions. Knowledge on the control distribution under physiological conditions will identify the most suitable target for the design of antimicrobial compounds that target CoA production. This objective was achieved through the studies described in Chapter 4.

## 1.6 References

1. Organization, W. H. *Antimicrobial Resistance: Global Report on Surveillance.*; WHO Press: Geneva, Switzerland, 2014.
2. Genschel, U., Coenzyme A Biosynthesis: Reconstruction of the Pathway in Archaea and an Evolutionary Scenario Based on Comparative Genomics. *Mol. Biol. Evol.* **2004**, *21* (7), 1242-1251.
3. Mishra, P. K.; Drueckhammer, D. G., Coenzyme A Analogues and Derivatives: Synthesis and Applications as Mechanistic Probes of Coenzyme A Ester-Utilizing Enzymes. *Chem. Rev.* **2000**, *100* (9), 3283-3309.
4. Yang, W.; Drueckhammer, D. G., Computational Studies of the Aminolysis of Oxoesters and Thioesters in Aqueous Solution. *Org. Lett.* **2000**, *2* (26), 4133-4136.
5. Yang, W.; Drueckhammer, D. G., Understanding the Relative Acyl-Transfer Reactivity of Oxoesters and Thioesters: Computational Analysis of Transition State Delocalization Effects. *J. Am. Chem. Soc.* **2001**, *123* (44), 11004-11009.
6. Abo Alrob, O.; Lopaschuk, Gary D., Role of CoA and acetyl-CoA in regulating cardiac fatty acid and glucose oxidation. *Biochem. Soc. Trans.* **2014**, *42* (4), 1043-1051.
7. Allfrey, V. G.; Faulkner, R.; Mirsky, A. E., Acetylation and methylation of histones and their possible role in the regulation of RNA synthesis. *Proc. Natl. Acad. Sci. USA* **1964**, *51* (5), 786-794.
8. Begley, T. P.; Kinsland, C.; Strauss, E., The biosynthesis of coenzyme A in bacteria. *Vitam. Horm.* **2001**, *61*, 157-171.
9. G M Brown, a.; Reynolds, J. J., Biogenesis of the Water-Soluble Vitamins. *Annu. Rev. Biochem.* **1963**, *32* (1), 419-462.
10. Williams, R. J.; Weinstock, H. H.; Rohrmann, E.; Truesdail, J. H.; Mitchell, H. K.; Meyer, C. E., Pantothenic Acid. III. Analysis and Determination of Constituent Groups. *J. Am. Chem. Soc.* **1939**, *61* (2), 454-457.
11. Leonardi, R.; Zhang, Y.-M.; Rock, C. O.; Jackowski, S., Coenzyme A: Back in action. *Prog. Lipid. Res.* **2005**, *44* (2-3), 125-153.
12. Maas, W. K., Pantothenate studies. III. Description of the extracted pantothenate-synthesizing enzyme of *Escherichia coli*. *J. Biol. Chem.* **1952**, *198* (1), 23-32.
13. Maas, W. K.; Novelli, G. D., Synthesis of pantothenic acid by depyrophosphorylation of adenosine triphosphate. *Arch. Biochem. Biophys.* **1953**, *43* (1), 236-8.
14. Maas, W. K.; Vogel, H. J., alpha-Ketoisovaleric acid, a precursor of pantothenic acid in *Escherichia coli*. *J. Bacteriol.* **1953**, *65* (4), 388-93.

15. Webb, M. E.; Smith, A. G.; Abell, C., Biosynthesis of pantothenate. *Nat. Prod. Rep.* **2004**, *21* (6), 695-721.
16. Sambandamurthy, V. K.; Wang, X.; Chen, B.; Russell, R. G.; Derrick, S.; Collins, F. M.; Morris, S. L.; Jacobs, W. R., A pantothenate auxotroph of *Mycobacterium tuberculosis* is highly attenuated and protects mice against tuberculosis. *Nat. Med.* **2002**, *8* (10), 1171-1174.
17. Sambandamurthy, V. K.; Derrick, S. C.; Hsu, T.; Chen, B.; Larsen, M. H.; Jalapathy, K. V.; Chen, M.; Kim, J.; Porcelli, S. A.; Chan, J., *Mycobacterium tuberculosis*  $\Delta$ RD1  $\Delta$ panCD: a safe and limited replicating mutant strain that protects immunocompetent and immunocompromised mice against experimental tuberculosis. *Vaccine* **2006**, *24* (37), 6309-6320.
18. Velaparthy, S.; Brunsteiner, M.; Uddin, R.; Wan, B.; Franzblau, S. G.; Petukhov, P. A., 5-tert-butyl-N-pyrazol-4-yl-4, 5, 6, 7-tetrahydrobenzo isoxazole-3-carboxamide derivatives as novel potent inhibitors of *Mycobacterium tuberculosis* pantothenate synthetase: initiating a quest for new antitubercular drugs. *J. Med. Chem.* **2008**, *51* (7), 1999-2002.
19. Mageed, S. N.; Cunningham, F.; Hung, A. W.; Silvestre, H. L.; Wen, S.; Blundell, T. L.; Abell, C.; McConkey, G. A., Pantothenic acid biosynthesis in the parasite *Toxoplasma gondii*: a target for chemotherapy. *Antimicrob. Agents Chemother.* **2014**, *58* (11), 6345-6353.
20. Gerdes, S. Y.; Scholle, M. D.; D'Souza, M.; Bernal, A.; Baev, M. V.; Farrell, M.; Kurnasov, O. V.; Daugherty, M. D.; Mseeh, F.; Polanuyer, B. M.; Campbell, J. W.; Anantha, S.; Shatalin, K. Y.; Chowdhury, S. A. K.; Fonstein, M. Y.; Osterman, A. L., From Genetic Footprinting to Antimicrobial Drug Targets: Examples in Cofactor Biosynthetic Pathways. *J. Bacteriol.* **2002**, *184* (16), 4555-4572.
21. Jackowski, S.; Alix, J. H., Cloning, sequence, and expression of the pantothenate permease (panF) gene of *Escherichia coli*. *J. Bacteriol.* **1990**, *172* (7), 3842-8.
22. Vallari, D. S.; Rock, C. O., Pantothenate transport in *Escherichia coli*. *J. Bacteriol.* **1985**, *162* (3), 1156-61.
23. Nakamura, H.; Tamura, Z., Pantothenate uptake in *Escherichia coli* K-12. *J. Nutr. Sci. Vitaminol.* **1973**, *19* (5), 389-400.
24. Reizer, J.; Reizer, A.; Saier, M. H., Jr., The Na<sup>+</sup>/pantothenate symporter (PanF) of *Escherichia coli* is homologous to the Na<sup>+</sup>/proline symporter (PutP) of *E. coli* and the Na<sup>+</sup>/glucose symporters of mammals. *Res. Microbiol.* **1990**, *141* (9), 1069-72.
25. Stolz, J.; Sauer, N., The fenpropimorph resistance gene FEN2 from *Saccharomyces cerevisiae* encodes a plasma membrane H<sup>+</sup>-pantothenate symporter. *J. Biol. Chem.* **1999**, *274* (26), 18747-52.

26. Prasad, P. D.; Wang, H.; Huang, W.; Fei, Y. J.; Leibach, F. H.; Devoe, L. D.; Ganapathy, V., Molecular and functional characterization of the intestinal Na<sup>+</sup>-dependent multivitamin transporter. *Arch. Biochem. Biophys.* **1999**, *366* (1), 95-106.
27. Prasad, P. D.; Ganapathy, V., Structure and function of mammalian sodium-dependent multivitamin transporter. *Curr. Opin. Clin. Nutr. Metab. Care* **2000**, *3* (4), 263-6.
28. Saliba, K. J.; Horner, H. A.; Kirk, K., Transport and metabolism of the essential vitamin pantothenic acid in human erythrocytes infected with the malaria parasite *Plasmodium falciparum*. *J. Biol. Chem.* **1998**, *273* (17), 10190-5.
29. Saliba, K. J.; Kirk, K., H<sup>+</sup>-coupled pantothenate transport in the intracellular malaria parasite. *J. Biol. Chem.* **2001**, *276* (21), 18115-21.
30. Jackowski, S.; Rock, C. O., Metabolism of 4'-phosphopantetheine in *Escherichia coli*. *J. Bacteriol.* **1984**, *158* (1), 115-120.
31. Strauss, E.; Begley, T. P., The Antibiotic Activity of N-Pentylpantothenamide Results from Its Conversion to Ethyldethia-Coenzyme A, a Coenzyme A Antimetabolite. *J. Biol. Chem.* **2002**, *277* (50), 48205-48209.
32. Meier, J. L.; Mercer, A. C.; Rivera, H.; Burkart, M. D., Synthesis and Evaluation of Bioorthogonal Pantetheine Analogues for in Vivo Protein Modification. *J. Am. Chem. Soc.* **2006**, *128* (37), 12174-12184.
33. Craig, J. A.; Snell, E. E., The comparative activities of pantetheine, pantothenic acid and coenzyme A for various microorganisms. *J. Bacteriol.* **1951**, *61* (3), 283-291.
34. Balibar, C. J.; Hollis-Symynkywicz, M. F.; Tao, J., Pantetheine Rescues Phosphopantothenoylcysteine Synthetase and Phosphopantothenoylcysteine Decarboxylase Deficiency in *Escherichia coli* but Not in *Pseudomonas aeruginosa*. *J. Bacteriol.* **2011**, *193* (13), 3304-3312.
35. Srinivasan, B.; Baratashvili, M.; van der Zwaag, M.; Kanon, B.; Colombelli, C.; Lambrechts, R. A.; Schaap, O.; Nollen, E. A.; Podgorsek, A.; Kosec, G.; Petkovic, H.; Hayflick, S.; Tiranti, V.; Reijngoud, D.-J.; Grzeschik, N. A.; Sibon, O. C. M., Extracellular 4[prime]-phosphopantetheine is a source for intracellular coenzyme A synthesis. *Nat. Chem. Biol.* **2015**, *11* (10), 784-792.
36. Jackowski, S.; Rock, C. O., Regulation of coenzyme A biosynthesis. *J. Bacteriol.* **1981**, *148* (3), 926-932.
37. Yang, K.; Eyobo, Y.; Brand, L. A.; Martynowski, D.; Tomchick, D.; Strauss, E.; Zhang, H., Crystal Structure of a Type III Pantothenate Kinase: Insight into the Mechanism of an Essential Coenzyme A Biosynthetic Enzyme Universally Distributed in Bacteria. *J. Bacteriol.* **2006**, *188* (15), 5532-5540.

38. Song, W. J.; Jackowski, S., Cloning, sequencing, and expression of the pantothenate kinase (coaA) gene of *Escherichia coli*. *J. Bacteriol.* **1992**, *174* (20), 6411-6417.
39. Vallari, D. S.; Rock, C. O., Isolation and characterization of temperature-sensitive pantothenate kinase (coaA) mutants of *Escherichia coli*. *J. Bacteriol.* **1987**, *169* (12), 5795-5800.
40. Song, W. J.; Jackowski, S., Kinetics and regulation of pantothenate kinase from *Escherichia coli*. *J. Biol. Chem.* **1994**, *269* (43), 27051-27058.
41. Worthington, A. S.; Burkart, M. D., One-pot chemo-enzymatic synthesis of reporter-modified proteins. *Org. Biomol. Chem.* **2006**, *4* (1), 44-46.
42. Mercer, A. C.; Meier, J. L.; Hur, G. H.; Smith, A. R.; Burkart, M. D., Antibiotic evaluation and *in vivo* analysis of alkynyl Coenzyme A antimetabolites in *Escherichia coli*. *Bioorg. Med. Chem. Lett.* **2008**, *18* (22), 5991-5994.
43. de Villiers, M. R., I.; Strauss, E., Unpublished results.
44. Zhang, Y.-M.; Frank, M. W.; Virga, K. G.; Lee, R. E.; Rock, C. O.; Jackowski, S., Acyl carrier protein is a cellular target for the antibacterial action of the pantothenamide class of pantothenate antimetabolites. *J. Biol. Chem.* **2004**, *279* (49), 50969-50975.
45. Virga, K. G.; Zhang, Y.-M.; Leonardi, R.; Ivey, R. A.; Hevener, K.; Park, H.-W.; Jackowski, S.; Rock, C. O.; Lee, R. E., Structure-activity relationships and enzyme inhibition of pantothenamide-type pantothenate kinase inhibitors. *Bioorg. Med. Chem.* **2006**, *14* (4), 1007-1020.
46. Clifton, G.; Bryant, S. R.; Skinner, C. G., N<sup>1</sup>-(substituted) pantothenamides, antimetabolites of pantothenic acid. *Arch. Biochem. Biophys.* **1970**, *137* (2), 523-8.
47. Venkatraman, J.; Bhat, J.; Solapure, S. M.; Sandesh, J.; Sarkar, D.; Aishwarya, S.; Mukherjee, K.; Datta, S.; Malolanarasimhan, K.; Bandodkar, B., Screening, identification, and characterization of mechanistically diverse inhibitors of the *Mycobacterium tuberculosis* enzyme, pantothenate kinase (CoaA). *J. Biomol. Screen* **2012**, *17* (3), 293-302.
48. Björkelid, C.; Bergfors, T.; Raichurkar, A. K. V.; Mukherjee, K.; Malolanarasimhan, K.; Bandodkar, B.; Jones, T. A., Structural and biochemical characterization of compounds inhibiting *Mycobacterium tuberculosis* PanK. *J. Biol. Chem.* **2013**, M113. 476473.
49. Reddy, B. K.; Landge, S.; Ravishankar, S.; Patil, V.; Shinde, V.; Tantry, S.; Kale, M.; Raichurkar, A.; Menasinakai, S.; Mudugal, N. V., Assessment of *Mycobacterium tuberculosis* pantothenate kinase vulnerability through target knockdown and mechanistically diverse inhibitors. *Antimicrob. Agents Chemother.* **2014**, *58* (6), 3312-3326.

50. Calder, R. B.; Williams, R. S.; Ramaswamy, G.; Rock, C. O.; Campbell, E.; Unkles, S. E.; Kinghorn, J. R.; Jackowski, S., Cloning and characterization of a eukaryotic pantothenate kinase gene (panK) from *Aspergillus nidulans*. *J. Biol. Chem.* **1999**, *274* (4), 2014-20.
51. Tilton, G. B.; Wedemeyer, W. J.; Browse, J.; Ohlrogge, J., Plant coenzyme A biosynthesis: characterization of two pantothenate kinases from *Arabidopsis*. *Plant. Mol. Biol.* **2006**, *61* (4-5), 629-42.
52. Yang, Y.; Wu, Z.; Kuo, Y. M.; Zhou, B., Dietary rescue of *fumble-a* *Drosophila* model for pantothenate-kinase-associated neurodegeneration. *J. Inherit. Metab. Dis.* **2005**, *28* (6), 1055-64.
53. Leonardi, R.; Zhang, Y. M.; Lykidis, A.; Rock, C. O.; Jackowski, S., Localization and regulation of mouse pantothenate kinase 2. *FEBS Lett.* **2007**, *581* (24), 4639-44.
54. Rock, C. O.; Calder, R. B.; Karim, M. A.; Jackowski, S., Pantothenate Kinase Regulation of the Intracellular Concentration of Coenzyme A. *J. Biol. Chem.* **2000**, *275* (2), 1377-1383.
55. Hortnagel, K.; Prokisch, H.; Meitinger, T., An isoform of hPANK2, deficient in pantothenate kinase-associated neurodegeneration, localizes to mitochondria. *Hum. Mol. Genet.* **2003**, *12* (3), 321-7.
56. Zhou, B.; Westaway, S. K.; Levinson, B.; Johnson, M. A.; Gitschier, J.; Hayflick, S. J., A novel pantothenate kinase gene (PANK2) is defective in Hallervorden-Spatz syndrome. *Nat. Genet.* **2001**, *28* (4), 345-9.
57. Ni, X.; Ma, Y.; Cheng, H.; Jiang, M.; Ying, K.; Xie, Y.; Mao, Y., Cloning and characterization of a novel human pantothenate kinase gene. *Int. J. Biochem. Cell Biol.* **2002**, *34* (2), 109-115.
58. Ramaswamy, G.; Karim, M. A.; Murti, K. G.; Jackowski, S., PPAR $\alpha$  controls the intracellular coenzyme A concentration via regulation of PANK1 $\alpha$  gene expression. *J. Lipid Res.* **2004**, *45* (1), 17-31.
59. Zhang, Y. M.; Rock, C. O.; Jackowski, S., Biochemical properties of human pantothenate kinase 2 isoforms and mutations linked to pantothenate kinase-associated neurodegeneration. *J. Biol. Chem.* **2006**, *281* (1), 107-14.
60. Rock, C. O.; Karim, M. A.; Zhang, Y. M.; Jackowski, S., The murine pantothenate kinase (Pank1) gene encodes two differentially regulated pantothenate kinase isozymes. *Gene* **2002**, *291* (1-2), 35-43.
61. Lehane, A. M.; Marchetti, R. V.; Spry, C.; van Schalkwyk, D. A.; Teng, R.; Kirk, K.; Saliba, K. J., Feedback inhibition of pantothenate kinase regulates pantothenol uptake by the malaria parasite. *J. Biol. Chem.* **2007**, *282* (35), 25395-405.

62. Cheek, S.; Ginalski, K.; Zhang, H.; Grishin, N., A comprehensive update of the sequence and structure classification of kinases. *BMC Struct. Biol.* **2005**, *5* (1), 6.
63. Hong, B. S.; Senisterra, G.; Rabeh, W. M.; Vedadi, M.; Leonardi, R.; Zhang, Y.-M.; Rock, C. O.; Jackowski, S.; Park, H.-W., Crystal Structures of Human Pantothenate Kinases: Insights into allosteric regulation and mutations linked to a neurodegeneration disorder. *J. Biol. Chem.* **2007**, *282* (38), 27984-27993.
64. Hong, B. S.; Yun, M. K.; Zhang, Y.-M.; Chohnan, S.; Rock, C. O.; White, S. W.; Jackowski, S.; Park, H.-W.; Leonardi, R., Prokaryotic Type II and Type III Pantothenate Kinases: The Same Monomer Fold Creates Dimers with Distinct Catalytic Properties. *Structure* **2006**, *14* (8), 1251-1261.
65. Choudhry, A. E.; Mandichak, T. L.; Broskey, J. P.; Egolf, R. W.; Kinsland, C.; Begley, T. P.; Seefeld, M. A.; Ku, T. W.; Brown, J. R.; Zalacain, M.; Ratnam, K., Inhibitors of pantothenate kinase: Novel antibiotics for staphylococcal infections. *Antimicrob. Agents Chemother.* **2003**, *47* (6), 2051-2055.
66. Leonardi, R.; Chohnan, S.; Zhang, Y.-M.; Virga, K. G.; Lee, R. E.; Rock, C. O.; Jackowski, S., A pantothenate kinase from *Staphylococcus aureus* refractory to feedback regulation by coenzyme A. *J. Biol. Chem.* **2005**, *280* (5), 3314-3322.
67. Sundquist, A. R.; Fahey, R. C., Evolution of antioxidant mechanisms: thiol-dependent peroxidases and thioltransferase among prokaryotes. *J. Mol. Evol.* **1989**, *29* (5), 429-435.
68. Fahey, R. C.; Sundquist, A., Evolution of glutathione metabolism. *Adv. Enzymol. Relat. Areas Mol. Biol.* **1991**, *64* (1), 53.
69. Fahey, R.; Brown, W.; Adams, W.; Worsham, M., Occurrence of glutathione in bacteria. *J. Bacteriol.* **1978**, *133* (3), 1126-1129.
70. Fahey, R. C., Glutathione analogs in prokaryotes. *Biochim. Biophys. Acta* **2013**, *1830* (5), 3182-3198.
71. de Villiers, M.; Barnard, L.; Koekemoer, L.; Snoep, J. L.; Strauss, E., Variation in pantothenate kinase type determines the pantothenamide mode of action and impacts on coenzyme A salvage biosynthesis. *FEBS Journal* **2014**, *281* (20), 4731-4753.
72. Akinnusi, T. O.; Vong, K.; Auclair, K., Geminal dialkyl derivatives of N-substituted pantothenamides: synthesis and antibacterial activity. *Bioorg. Med. Chem.* **2011**, *19* (8), 2696-2706.
73. Zhang, Y.-M.; Chohnan, S.; Virga, K. G.; Stevens, R. D.; Ilkayeva, O. R.; Wenner, B. R.; Bain, J. R.; Newgard, C. B.; Lee, R. E.; Rock, C. O., Chemical knockout of pantothenate kinase reveals

- the metabolic and genetic program responsible for hepatic coenzyme A homeostasis. *Chem. Biol.* **2007**, *14* (3), 291-302.
74. Siudeja, K.; Srinivasan, B.; Xu, L.; Rana, A.; de Jong, J.; Nollen, E. A.; Jackowski, S.; Sanford, L.; Hayflick, S.; Sibon, O. C., Impaired Coenzyme A metabolism affects histone and tubulin acetylation in *Drosophila* and human cell models of pantothenate kinase associated neurodegeneration. *EMBO Mol. Med.* **2011**, *3* (12), 755-766.
75. Leonardi, R.; Zhang, Y.-M.; Yun, M.-K.; Zhou, R.; Zeng, F.-Y.; Lin, W.; Cui, J.; Chen, T.; Rock, C. O.; White, S. W., Modulation of pantothenate kinase 3 activity by small molecules that interact with the substrate/allosteric regulatory domain. *Chem. Biol.* **2010**, *17* (8), 892-902.
76. Bode, K. A.; Donner, M. G.; Leier, I.; Keppler, D., Inhibition of transport across the hepatocyte canalicular membrane by the antibiotic fusidate. *Biochem. Pharmacol.* **2002**, *64* (1), 151-158.
77. Humble, M.; Eykyn, S.; Phillips, I., Staphylococcal bacteraemia, fusidic acid, and jaundice. *BMJ* **1980**, *280* (6230), 1495-1498.
78. Sharma, L. K.; Leonardi, R.; Lin, W.; Boyd, V. A.; Goktug, A.; Shelat, A. A.; Chen, T.; Jackowski, S.; Rock, C. O., A High-Throughput Screen Reveals New Small-Molecule Activators and Inhibitors of Pantothenate Kinases. *J. Med. Chem.* **2015**, *58* (3), 1563-1568.
79. Hong, B. S.; Yun, M. K.; Zhang, Y.-M.; Chohnan, S.; Rock, C. O.; White, S. W.; Jackowski, S.; Park, H.-W.; Leonardi, R., Prokaryotic Type II and Type III Pantothenate Kinases: The Same Monomer Fold Creates Dimers with Distinct Catalytic Properties. *Structure* **2006**, *14* (8), 1251-1261.
80. Yocum, R.; Patterson, T., Microorganisms and assays for the identification of antibiotics acting on the pantothenate kinase encoded by the *coaX* gene. *Omnigene Bioproducts, USA, ed.(USA)* **2002**.
81. Brand, L. A.; Strauss, E., Characterization of a New Pantothenate Kinase Isoform from *Helicobacter pylori*. *J. Biol. Chem.* **2005**, *280* (21), 20185-20188.
82. Yang, K.; Strauss, E.; Huerta, C.; Zhang, H., Structural basis for substrate binding and the catalytic mechanism of type III pantothenate kinase. *Biochemistry* **2008**, *47* (5), 1369-80.
83. Rowan, A. S.; Nicely, N. I.; Cochrane, N.; Wlassoff, W. A.; Claiborne, A.; Hamilton, C. J., Nucleoside triphosphate mimicry: a sugar triazolyl nucleoside as an ATP-competitive inhibitor of *B. anthracis* pantothenate kinase. *Org. Biomol. Chem.* **2009**, *7* (19), 4029-4036.
84. Strauss, E.; Kinsland, C.; Ge, Y.; McLafferty, F. W.; Begley, T. P., Phosphopantothenoylcysteine synthetase from *Escherichia coli*. Identification and characterization of the last unidentified coenzyme A biosynthetic enzyme in bacteria. *J. Biol. Chem.* **2001**, *276* (17), 13513-13516.

85. Kupke, T.; Hernandez-Acosta, P.; Culianez-Macia, F. A., 4'-phosphopantetheine and coenzyme A biosynthesis in plants. *J. Biol. Chem.* **2003**, *278* (40), 38229-37.
86. Daugherty, M.; Polanuyer, B.; Farrell, M.; Scholle, M.; Lykidis, A.; de Crécy-Lagard, V.; Osterman, A., Complete Reconstitution of the Human Coenzyme A Biosynthetic Pathway via Comparative Genomics. *J. Biol. Chem.* **2002**, *277* (24), 21431-21439.
87. Abiko, Y., [57] Pantothenic acid and coenzyme A: Phosphopantothenoylcysteine synthetase from rat liver (pantothenate 4'-phosphate: l-cysteine ligase, EC 6.3. 2.5). *Methods Enzymol.* **1970**, *18*, 350-354.
88. Strauss, E., *Thiols, radicals and antibiotics: mechanistic studies in Coenzyme A biosynthesis*. Cornell University, Jan.: 2003.
89. Strauss, E.; Begley, T. P., Mechanistic studies on phosphopantothenoylcysteine decarboxylase. *J. Am. Chem. Soc.* **2001**, *123* (26), 6449-50.
90. Stanitzek, S.; Augustin, M. A.; Huber, R.; Kupke, T.; Steinbacher, S., Structural basis of CTP-dependent peptide bond formation in coenzyme A biosynthesis catalyzed by *Escherichia coli* PPC synthetase. *Structure* **2004**, *12* (11), 1977-88.
91. Wang, S.; Eisenberg, D., Crystal structure of the pantothenate synthetase from *Mycobacterium tuberculosis*, snapshots of the enzyme in action. *Biochemistry* **2006**, *45* (6), 1554-1561.
92. Strauss, E.; Begley, T. P., The selectivity of cysteine over serine in coenzyme A biosynthesis. *Chembiochem* **2005**, *6* (2), 284-286.
93. Patrone, J. D.; Yao, J.; Scott, N. E.; Dotson, G. D., Selective inhibitors of bacterial phosphopantothenoylcysteine synthetase. *J. Am. Chem. Soc.* **2009**, *131* (45), 16340-16341.
94. Sugie, Y.; Dekker, K. A.; Hirai, H.; Ichiba, T.; Ishiguro, M.; Shioni, Y.; Sugiura, A.; Brennan, L.; Duignan, J.; Huang, L. H., CJ-15,801, a novel antibiotic from a fungus, *Seimatosporium* sp. *J. Antibiot.* **2001**, *54* (12), 1060-1065.
95. van der Westhuyzen, R.; Hammons, Justin C.; Meier, Jordan L.; Dahesh, S.; Moolman, Wessel J. A.; Pelly, Stephen C.; Nizet, V.; Burkart, Michael D.; Strauss, E., The Antibiotic CJ-15,801 Is an Antimetabolite that Hijacks and Then Inhibits CoA Biosynthesis. *Chem. Biol.* **2012**, *19* (5), 559-571.
96. Kupke, T.; Uebele, M.; Schmid, D.; Jung, G.; Blaesse, M.; Steinbacher, S., Molecular characterization of lantibiotic-synthesizing enzyme EpiD reveals a function for bacterial Dfp proteins in coenzyme A biosynthesis. *J. Biol. Chem.* **2000**, *275* (41), 31838-31846.

97. Daugherty, M.; Polanuyer, B.; Farrell, M.; Scholle, M.; Lykidis, A.; De Crecy-Lagard, V.; Osterman, A., Complete reconstitution of the human coenzyme A biosynthetic pathway via comparative genomics. *J. Biol. Chem.* **2002**, *277* (24), 21431-21439.
98. Strauss, E.; Begley, T. P., Stereochemical studies on phosphopantothencysteine decarboxylase from *Escherichia coli*. *Bioorg. Med. Chem. Lett.* **2003**, *13* (3), 339-42.
99. Strauss, E.; Zhai, H.; Brand, L. A.; McLafferty, F. W.; Begley, T. P., Mechanistic studies on phosphopantothencysteine decarboxylase: trapping of an enethiolate intermediate with a mechanism-based inactivating agent. *Biochemistry* **2004**, *43* (49), 15520-15533.
100. Martin, D. P.; Drueckhammer, D. G., Separate enzymes catalyze the final two steps of coenzyme A biosynthesis in *Brevibacterium ammoniagenes*: purification of pantetheine phosphate adenyltransferase. *Biochem. Biophys. Res. Commun.* **1993**, *192* (3), 1155-1161.
101. Miller, J. R.; Ohren, J.; Sarver, R. W.; Mueller, W. T.; de Dreu, P.; Case, H.; Thanabal, V., Phosphopantetheine adenyltransferase from *Escherichia coli*: Investigation of the kinetic mechanism and role in regulation of coenzyme a biosynthesis. *J. Bacteriol.* **2007**, *189* (22), 8196-8205.
102. Worrall, D. M.; Tubbs, P. K., A bifunctional enzyme complex in coenzyme A biosynthesis: purification of pantetheine phosphate adenyltransferase and dephospho-CoA kinase. *Biochem. J.* **1983**, *215* (1), 153-157.
103. Aghajanian, S.; Worrall, D. M., Identification and characterization of the gene encoding the human phosphopantetheine adenyltransferase and dephospho-CoA kinase bifunctional enzyme (CoA synthase). *Biochem. J.* **2002**, *365* (1), 13-18.
104. Zhyvoloup, A.; Nemazanyy, I.; Babich, A.; Panasyuk, G.; Pobigailo, N.; Vudmaska, M.; Naidenov, V.; Kukhareno, O.; Palchevskii, S.; Savinska, L.; Ovcharenko, G.; Verdier, F.; Valovka, T.; Fenton, T.; Rebholz, H.; Wang, M.-L.; Shepherd, P.; Matsuka, G.; Filonenko, V.; Gout, I. T., Molecular Cloning of CoA Synthase. *J. Biol. Chem.* **2002**, *277* (25), 22107-22110.
105. IZARD, T., The crystal structures of phosphopantetheine adenyltransferase with bound substrates reveal the enzyme's catalytic mechanism. *J. Mol. Biol.* **2002**, *315* (4), 487-495.
106. Bork, P.; Holm, L.; Koonin, E. V.; Sander, C., The cytidyltransferase superfamily: identification of the nucleotide-binding site and fold prediction. *PROTEINS* **1995**, *22* (3), 259-266.
107. Miller, J. R.; Thanabal, V.; Melnick, M. M.; Lall, M.; Donovan, C.; Sarver, R. W.; Lee, D. Y.; Ohren, J.; Emerson, D., The Use of Biochemical and Biophysical Tools for Triage of High-Throughput Screening Hits—A Case Study with *Escherichia coli* Phosphopantetheine Adenyltransferase. *Chem. Biol. Drug. Des.* **2010**, *75* (5), 444-454.

108. Zhao, L.; Allanson, N. M.; Thomson, S. P.; Maclean, J. K. F.; Barker, J. J.; Primrose, W. U.; Tyler, P. D.; Lewendon, A., Inhibitors of phosphopantetheine adenylyltransferase. *Eur. J. Med. Chem* **2003**, *38* (4), 345-349.
109. de Jonge, B. L.; Walkup, G. K.; Lahiri, S. D.; Huynh, H.; Neckermann, G.; Utlely, L.; Nash, T. J.; Brock, J.; San Martin, M.; Kutschke, A., Discovery of inhibitors of 4'-phosphopantetheine adenylyltransferase (PPAT) to validate PPAT as a target for antibacterial therapy. *Antimicrob. Agents Chemother.* **2013**, *57* (12), 6005-6015.
110. Mishra, P. K.; Park, P. K.; Drueckhammer, D. G., Identification of *yacE* (*coaE*) as the structural gene for dephosphocoenzyme A kinase in *Escherichia coli* K-12. *J. Bacteriol.* **2001**, *183* (9), 2774-2778.
111. O'Toole, N.; Barbosa Joao, A. R. G.; Li, Y.; Hung, L.-W.; Matte, A.; Cygler, M., Crystal structure of a trimeric form of dephosphocoenzyme A kinase from *Escherichia coli*. *Protein Sci.* **2003**, *12* (2), 327-36.
112. Schulz, G. E.; Muller, C. W.; Diederichs, K., Induced-fit movements in adenylate kinases. *J. Mol. Biol.* **1990**, *213* (4), 627-30.
113. Franklin, J. E.; Trams, E. G., Metabolism of coenzyme A and related nucleotides by liver plasma membranes. *Biochim. Biophys. Acta* **1971**, *230* (1), 105-116.
114. Trams, E. G.; Stahl, W. L.; Robinson, J., Formation of S-acyl pantetheine from acyl= coenzyme a by plasma membranes. *Biochim. Biophys. Acta* **1968**, *163* (4), 472-482.
115. Tahiliani, A. G.; Beinlich, C. J., Pantothenic acid in health and disease. *Vitam. Horm.* **1990**, *46*, 165-228.
116. Kang, L. W.; Gabelli, S. B.; Bianchet, M. A.; Xu, W. L.; Bessman, M. J.; Amzel, L. M., Structure of a coenzyme A pyrophosphatase from *Deinococcus radiodurans*: a member of the Nudix family. *J. Bacteriol.* **2003**, *185* (14), 4110-8.
117. Gasmi, L.; McLennan, A. G., The mouse *Nudt7* gene encodes a peroxisomal nudix hydrolase specific for coenzyme A and its derivatives. *Biochem. J.* **2001**, *357* (Pt 1), 33-8.
118. AbdelRaheim, S. R.; McLennan, A. G., The *Caenorhabditis elegans* Y87G2A.14 Nudix hydrolase is a peroxisomal coenzyme A diphosphatase. *BMC Biochem.* **2002**, *3*, 5.
119. Vallari, D. S.; Jackowski, S., Biosynthesis and degradation both contribute to the regulation of coenzyme A content in *Escherichia coli*. *J. Bacteriol.* **1988**, *170* (9), 3961-3966.
120. Elovson, J.; Vagelos, P. R., Acyl Carrier Protein X. Acyl Carrier Protein Synthetase. *J. Biol. Chem.* **1968**, *243* (13), 3603-3611.

121. Lambalot, R. H.; Walsh, C. T., Cloning, overproduction, and characterization of the *Escherichia coli* holo-acyl carrier protein synthase. *J. Biol. Chem.* **1995**, *270* (42), 24658-24661.
122. Thomas, J.; Rigden, D. J.; Cronan, J. E., Acyl Carrier Protein Phosphodiesterase (AcpH) of *Escherichia coli* Is a Non-Canonical Member of the HD Phosphatase/Phosphodiesterase Family. *Biochemistry* **2007**, *46* (1), 129-136.
123. Joshi, A. K.; Zhang, L.; Rangan, V. S.; Smith, S., Cloning, expression, and characterization of a human 4'-phosphopantetheinyl transferase with broad substrate specificity. *J. Biol. Chem.* **2003**, *278* (35), 33142-33149.
124. Jackowski, S.; Rock, C. O., Turnover of the 4'-phosphopantetheine prosthetic group of acyl carrier protein. *J. Bacteriol.* **1984**, *259* (3), 1891-5.
125. Mercer, A. C.; Burkart, M. D., The ubiquitous carrier protein—a window to metabolite biosynthesis. *Nat. Prod. Rep.* **2007**, *24* (4), 750-773.
126. Knights, K. M., Long-Chain-Fatty-Acid CoA Ligases: The Key to Fatty Acid Activation, Formation of Xenobiotic Acyl-CoA Thioesters and Lipophilic Xenobiotic Conjugates. *Curr. Med. Chem. Immunol. Endocr. Metab. Agents* **2003**, *3* (3), 235-244.
127. Londesborough, J. C.; Webster Jr, L. T., Fatty acyl-CoA synthetases. *Enzymes* **1974**.
128. Watkins, P. A., Fatty acid activation. *Prog. Lipid Res.* **1997**, *36* (1), 55-83.
129. Watkins, P. A., Very-long-chain acyl-CoA synthetases. *J. Biol. Chem.* **2008**, *283* (4), 1773-1777.
130. Linne, U.; Schäfer, A.; Stubbs, M. T.; Marahiel, M. A., Aminoacyl-coenzyme A synthesis catalyzed by adenylation domains. *FEBS Letters* **2007**, *581* (5), 905-910.
131. Fraser, M. E.; James, M. N.; Bridger, W. A.; Wolodko, W. T., Phosphorylated and dephosphorylated structures of pig heart, GTP-specific succinyl-CoA synthetase. *J. Mol. Biol.* **2000**, *299* (5), 1325-1339.
132. Fraser, M. E.; James, M. N.; Bridger, W. A.; Wolodko, W. T., A detailed structural description of *Escherichia coli* succinyl-CoA synthetase. *J. Mol. Biol.* **1999**, *285* (4), 1633-1653.
133. Galperin, M. Y.; Koonin, E. V., A diverse superfamily of enzymes with ATP-dependent carboxylate—amine/thiol ligase activity. *Protein Sci.* **1997**, *6* (12), 2639-2643.
134. Sánchez, L. B.; Galperin, M. Y.; Müller, M., Acetyl-CoA Synthetase from the Amitochondriate Eukaryote *Giardia lamblia* Belongs to the Newly Recognized Superfamily of Acyl-CoA Synthetases (Nucleoside Diphosphate-forming). *J. Biol. Chem.* **2000**, *275* (8), 5794-5803.
135. Musfeldt, M.; Schönheit, P., Novel type of ADP-forming acetyl coenzyme A synthetase in hyperthermophilic archaea: heterologous expression and characterization of isoenzymes

- from the sulfate reducer *Archaeoglobus fulgidus* and the methanogen *Methanococcus jannaschii*. *J. Bacteriol.* **2002**, *184* (3), 636-644.
136. Ingram-Smith, C.; Martin, S. R.; Smith, K. S., Acetate kinase: not just a bacterial enzyme. *Trends in Microbiol.* **2006**, *14* (6), 249-253.
137. Wolfe, A. J., The acetate switch. *Microbiol. Mol. Biol. Rev.* **2005**, *69* (1), 12-50.
138. Sánchez, L. B., Aldehyde dehydrogenase (CoA-acetylating) and the mechanism of ethanol formation in the amitochondriate protist, *Giardia lamblia*. *Arch. Biochem. Biophys.* **1998**, *354* (1), 57-64.
139. Chen, M.; Li, E.; Stanley, S. L., Structural analysis of the acetaldehyde dehydrogenase activity of *Entamoeba histolytica* alcohol dehydrogenase 2 (EhADH2), a member of the ADHE enzyme family. *Mol. Biochem. Parasitol.* **2004**, *137* (2), 201-205.
140. Furdui, C.; Ragsdale, S. W., The roles of coenzyme A in the pyruvate: ferredoxin oxidoreductase reaction mechanism: rate enhancement of electron transfer from a radical intermediate to an iron-sulfur cluster. *Biochemistry* **2002**, *41* (31), 9921-9937.
141. Mansoorabadi, S. O.; Seravalli, J.; Furdui, C.; Krymov, V.; Gerfen, G. J.; Begley, T. P.; Melnick, J.; Ragsdale, S. W.; Reed, G. H., EPR spectroscopic and computational characterization of the hydroxyethylidene-thiamine pyrophosphate radical intermediate of pyruvate: ferredoxin oxidoreductase. *Biochemistry* **2006**, *45* (23), 7122-7131.
142. Frey, P. A., Radical mechanisms of enzymatic catalysis. *Annu. Rev. Biochem.* **2001**, *70* (1), 121-148.
143. Ragsdale, S. W., Metals and their scaffolds to promote difficult enzymatic reactions. *Chem. Rev.* **2006**, *106* (8), 3317-3337.
144. Luba, J.; Charrier, V.; Claiborne, A., Coenzyme A-disulfide reductase from *Staphylococcus aureus*: evidence for asymmetric behavior on interaction with pyridine nucleotides. *Biochemistry* **1999**, *38* (9), 2725-2737.
145. van der Westhuyzen, R.; Strauss, E., Michael Acceptor-Containing Coenzyme A Analogues As Inhibitors of the Atypical Coenzyme A Disulfide Reductase from *Staphylococcus aureus*. *J. Am. Chem. Soc.* **2010**, *132*, 12853-12855.
146. Posada, A. C.; Kolar, S. L.; Dusi, R. G.; Francois, P.; Roberts, A. A.; Hamilton, C. J.; Liu, G. Y.; Cheung, A., Importance of Bacillithiol in the Oxidative Stress Response of *Staphylococcus aureus*. *Infect. Immun.* **2014**, *82* (1), 316-332.
147. Newton, G. L.; Arnold, K.; Price, M. S.; Sherrill, C.; Delcardayre, S. B.; Aharonowitz, Y.; Cohen, G.; Davies, J.; Fahey, R. C.; Davis, C., Distribution of thiols in microorganisms: mycothiol is a major thiol in most actinomycetes. *J. Bacteriol.* **1996**, *178* (7), 1990-5.

148. Fry, M.; Webb, E.; Pudney, M., Effect of mitochondrial inhibitors on adenosinetriphosphate levels in *Plasmodium falciparum*. *Comp. Biochem. Physiol. B-Biochem. Mol. Biol.* **1990**, *96* (4), 775-782.
149. Vaughan, A. M.; O'Neill, M. T.; Tarun, A. S.; Camargo, N.; Phuong, T. M.; Aly, A. S.; Cowman, A. F.; Kappe, S. H., Type II fatty acid synthesis is essential only for malaria parasite late liver stage development. *Cell. Microbiol.* **2009**, *11* (3), 506-520.
150. Yu, M.; Kumar, T. S.; Nkrumah, L. J.; Coppi, A.; Retzlaff, S.; Li, C. D.; Kelly, B. J.; Moura, P. A.; Lakshmanan, V.; Freundlich, J. S., The fatty acid biosynthesis enzyme FabI plays a key role in the development of liver-stage malarial parasites. *Cell Host Microbe* **2008**, *4* (6), 567-578.
151. Divo, A. A.; Geary, T. G.; Davis, N. L.; Jensen, J. B., Nutritional requirements of *Plasmodium falciparum* in culture. I. Exogenously supplied dialyzable components necessary for continuous growth. *J. Protozool.* **1985**, *32* (1), 59-64.
152. Saliba, K. J.; Kirk, K., CJ-15,801, a fungal natural product, inhibits the intraerythrocytic stage of *Plasmodium falciparum* in vitro via an effect on pantothenic acid utilisation. *Mol. Biochem. Parasitol.* **2005**, *141* (1), 129-131.

# Chapter 2

## CoA and oxidative stress resistance in *Staphylococcus aureus*

---

### 2.1 Introduction

*Staphylococcus aureus* is an opportunistic pathogen that has become a major threat because it has acquired resistance against last resort antibiotics.<sup>1</sup> Thus, novel anti-staphylococcal compounds are desperately needed. The virulence of *S. aureus* is exacerbated by its ability to evade the host immune system. During infection of the host, reactive oxygen species (ROS), reactive nitrogen species (NOS) and reactive chlorine species (RCS) are generated by neutrophils and macrophages which normally causes deleterious mutations, damage to proteins and membranes which leads to lysis and cell death of the invading organism.<sup>2,3</sup> *S. aureus* is notoriously resistant to oxidative stress, thereby enabling it to evade the immune system. While peroxidases are the primary reductants of hydrogen peroxide, organisms also make use of low molecular weight (LMW) thiols to mitigate the effects of oxidative stress, by reducing oxidised proteins for example, for recovery.<sup>4,5</sup> In general, aerobic organisms use LMW thiols together with disulfide reductases to help maintain the reduced state of the cytoplasm. This ensures proper protein function and helps to avoid oxidative damage to cellular components during metabolism and stress. Most Gram-positive bacteria including *S. aureus* do not employ the same glutathione (GSH) thiol/disulfide redox system used by eukaryotes and Gram-negative bacteria. Instead, both CoA (**2.1**, Figure 2.1) and bacillithiol (BSH) (**2.2**) have been suggested to fulfil the role of major LMW thiol in *S. aureus* as detailed below.<sup>6,7</sup>

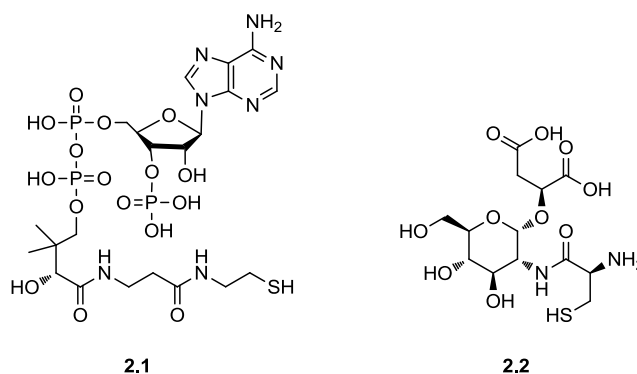


Figure 2.1: Structure of CoA (**2.1**) and BSH (**2.2**)

### 2.1.1 The role of CoA and BSH in *S. aureus*

In addition to CoA being a vital cofactor in many metabolic reactions, it has been proposed to perform the function of the major LMW thiol tasked with maintaining the reducing environment in *S. aureus*. This is supported by studies that have reported that *S. aureus* produces millimolar levels of CoA<sup>8</sup> as opposed to *E. coli* that produces micromolar levels of CoA and relies on GSH as its major LMW thiol.<sup>9</sup> The high intracellular CoA levels have been proposed to be due to the atypical type II PanK found in *S. aureus*. Unlike other type II PanKs it is refractory to feedback inhibition by CoA; this has been proposed to lead to increased levels of intracellular CoA levels compared to other organisms that harbour PanKs that do experience feedback inhibition.<sup>10</sup> A dedicated CoA disulfide reductase (CoADR) from *S. aureus* has also been isolated and characterized that recycles oxidized CoA back to the reduced form to complete this thiol/disulfide redox system.<sup>11</sup>

Resistance to the oxidative burst of neutrophils during phagocytosis contributes to the virulence of *S. aureus* and this resistance relies not only on the direct reducing activity of peroxidases but also on the thiol/disulfide redox system that enables it to recover from oxidative stress. Therefore recovery from oxidative stress is considered an integral part of oxidative stress resistance and consequently, the *S. aureus* CoADR has been identified as a target for inhibition for the development of anti-staphylococcal drugs. Pantothenamides have been designed specifically for the inactivation of CoADR by Van der Westhuyzen and Strauss (2010).<sup>12</sup> A Michael-acceptor moiety was incorporated into the pantothenamide structure which was shown to be converted to the corresponding CoA antimetabolite by the native CoA biosynthesis enzymes and subsequently inactivated the CoADR. However, the Michael-acceptor containing pantothenamide precursor of the CoA antimetabolite which showed the best inhibition of CoADR ( $k_{inact}/K_i \sim 40000 \text{ s}^{-1} \cdot \text{M}^{-1}$ ) failed to inhibit growth of *S. aureus* under normal growth conditions. The authors suggest that this may be due to CoADR only being essential under oxidative stress conditions (although this was not tested) or due to poor cell penetration of the pantothenamide precursors.

However, recent studies have shown that BSH and related S-transferases are likely candidates for an alternative or additional thiol/disulfide redox system.<sup>13,14</sup> Another study has shown the involvement of BSH in detoxification mechanisms whereby toxins and thiol-reactive antibiotics are converted to less potent mercapturic acids and are then transported out of the cell.<sup>15</sup> The intracellular concentration of CoA and BSH were measured among different *S. aureus* strains and found to vary with no clear predominant LMW thiol.<sup>7</sup> This suggests that CoA and BSH both contribute to the oxidative stress resistance of *S. aureus*. It

is therefore unlikely that inhibition of the CoA-based redox system alone will result in growth inhibition. Unlike CoA, BSH is not essential to the survival of *S. aureus* as not all strains of this organism produce it and mutants in which a gene encoding one of the BSH biosynthetic enzymes has been knocked-out are still viable.<sup>16</sup> Both BSH and CoA are therefore implicated in the efficient adaptation of *S. aureus* to the host environment that contributes to the virulence of this pathogen but the interplay between the systems is still poorly understood.

### 2.1.2 Regulation of CoA production under oxidative stress

In order to ascertain the role that the regulation of CoA production plays in the virulence of *S. aureus*, it will have to be determined which LMW thiol makes the largest contribution to its resistance to oxidative stress. It would be important to investigate how exposure to oxidative stress affects intracellular CoA levels and whether CoA production is up-regulated under such conditions. Oxidative stress is known to induce protein modifications, for example thiol oxidation of accessible cysteine residues. Such post-translational protein modifications could theoretically alter the kinetic and regulatory profile of the enzymes in question, and alter the flux in the pathway (and consequently CoA levels) in this manner. Establishing if this is the case would be important for the development of novel anti-staphylococcal agents.

The type II *S. aureus* PanK (SaPanK<sub>II</sub>) may provide the possible redox-sensing mechanism for up-regulation of CoA production under oxidative stress conditions. The crystal structure for this protein has been solved and shows that it is a dimer.<sup>17</sup> The sequence contains two cysteine residues at position 48 and 246. Generally protein cysteine thiols can be divided into four groups based on their reactivities. Some form permanent structural disulfide bonds, others co-ordinate metal ions. Some thiols remain in the reduced state and then there are those that are susceptible to reversible oxidation. These reversibly oxidized protein thiols (ROPTs) are often required for enzyme catalysis and activity regulation.<sup>18,19</sup> Agents that mediate oxidation of ROPTs include H<sub>2</sub>O<sub>2</sub> and hydroxyl radicals and these are released during the oxidative burst from activated neutrophils during the host immune response.<sup>20,21</sup> Oxidation of cysteine thiols yield Cys sulfenic acids which are reactive, unstable intermediates that readily react with other thiols to form intra- or intermolecular disulphide bonds. They can also react with LMW thiols like BSH or CoA in S-thiolation reactions to form mixed disulfides. If Cys sulfenic acids do not react with other thiols they can become overoxidized to sulphinic or sulphonic acids. Sulphinic acid can be reduced enzymatically by sulfiredoxin but oxidation to sulphonic acid is considered irreversible.<sup>22</sup> All oxidized states of the cysteine thiol can lead to changes in protein structure or activity.

In SaPanK<sub>II</sub>, Cys 246 has been identified as susceptible to oxidation to a sulfenic acid with the Cysteine Oxidation Prediction Algorithm (COPA) developed by Sanchez *et al.* (2008).<sup>23</sup> This algorithm predicts whether a protein sequence contains a cysteine residue that is susceptible to reversible oxidation based on the distance to the nearest cysteine sulfur atom, the solvent accessibility and the pKa. This is a possible redox sensitive switch that could change the kinetic and regulatory profile of the CoA biosynthesis pathway in response to oxidative stress and it supports the notion that CoA production in *S. aureus* should be studied under oxidative stress.

A better understanding of the regulation of CoA biosynthesis is required especially under oxidative stress because this is essential to the design of effective antimicrobial compounds aiming to stop or decrease CoA production in an attempt to inhibit cell growth. Despite the fact that all enzymes involved have been kinetically characterized little information is available on how the pathway is regulated, save for the proposed feedback inhibition of PanK by CoA in most organisms. Cellular metabolic states that trigger activation or suppression of CoA production are poorly understood. It has been observed that the intracellular CoA levels in *E. coli* vary depending on the carbon source.<sup>24</sup> Studies on pathway regulation and CoA homeostasis should be performed because it appears to vary with the metabolic state of the cell as well as the extracellular environment. It stands to reason that the environment created by activated macrophages during the host immune response to bacterial infection could also cause such variations and should be taken into account in the selection of the target enzyme and the design of inhibitory compounds.

### 2.1.3 Objective of this study

In order to ascertain the role that the regulation of CoA production plays in the virulence of *S. aureus*, it will have to be determined which LMW thiol makes the largest contribution to the resistance of oxidative stress and whether CoA levels are increased under oxidative stress conditions. We therefore set out to investigate these questions surrounding the redox system and CoA regulation in the USA 300 strain of *S. aureus* that is responsible for methicillin-resistant *S. aureus* (MRSA) infections in humans. Two *S. aureus* USA 300 strains were examined in this study, the wild type (*wt*) strain which produces CoA and BSH, as well as an isogenic  $\Delta bshA$  strain that does not produce BSH. The genotype of these strains were characterized in a previous study.<sup>16</sup> First, the viability of the two strains in the exponential growth phase was compared under conditions of oxidative stress to determine if there are any significant differences between them, thereby confirming the previously identified role of BSH in oxidative stress resistance.<sup>7</sup> Second, the viability of cells were assessed when they

are stressed by a known *S. aureus* growth inhibitor and CoA antimetabolite precursor, *N*-heptyl-pantothenamide (*N*7-Pan), in the absence and presence of oxidative stress.<sup>25</sup> This was done to determine whether inhibition of CoA production makes the cells less resistant to oxidative stress, in which case it would point to CoA making a contribution in this regard. Furthermore, the intracellular levels of CoA and its precursors, 3'-dephospho-CoA (DePCoA) and 4'-phosphopantetheine (PPanSH) was measured under the aforementioned conditions to determine whether CoA production is up-regulated when oxidative stress is encountered.

## 2.2 Results and discussion

The general strategy was to induce oxidative stress, N7-Pan or a combination of oxidative stress and N7-Pan in *S. aureus* strains in their exponential phase of growth. The culture viability and levels of CoA-related metabolites were subsequently tracked by harvesting culture aliquots for analysis at three intervals within the same growth phase to minimize metabolite variability associated with different growth phases. Harvested cells were subsequently washed and lysed to measure the intracellular concentration of the various metabolites by LC-MS using an analysis method previously developed for metabolomics studies.<sup>26</sup> Viability of cultures was assessed by measuring the adenylate energy charge (AEC). AEC is used as a scale of cell viability of a population and is calculated according to Equation 2.1.<sup>27</sup> For intact metabolizing cells the AEC is kept  $\geq 0.85$ .<sup>28</sup>

$$AEC = \frac{ATP + \frac{1}{2}ADP}{ATP + ADP + AMP} \quad \text{Eq. 2.1}$$

### 2.2.1 Cultivation and stress of *S. aureus* USA 300

Cultivation of *wt* and  $\Delta bshA$  strains of *S. aureus* USA 300 was performed in 100 ml RPMI media by dilution of an overnight starter culture to OD<sub>500</sub> of 0.05 followed by incubation at 37°C with vigorous agitation. Growth curves were established for both strains (Figure 2.1) to determine the range of exponential growth; this was found to be roughly between 0.5 and 2.5.

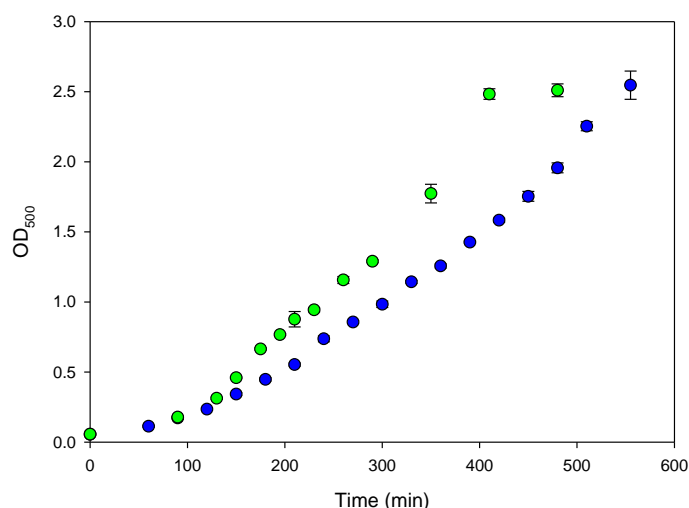


Figure 2.1: Growth curves of *S. aureus* USA 300. ● *wt* ●  $\Delta bshA$ . Exponential growth is observed between OD<sub>500</sub> of 0.5 and 2.5 for both strains. Measurements were made of triplicate cultures and data points represent the mean of the measurements with error bars denoting the standard deviation. Where no error bars are visible, the errors are smaller than the symbols.

Based on these growth curves, we decided to induce stress at OD<sub>500</sub> of 0.5 and to harvest the first aliquot directly thereafter ( $t_0$ ) with the subsequent harvests performed 15 minutes ( $t_{15}$ ) and 140 minutes ( $t_{140}$ ) after stress induction. To assess the effect of oxidative stress, H<sub>2</sub>O<sub>2</sub> was added to a final concentration of 20 mM to each culture. This concentration of H<sub>2</sub>O<sub>2</sub> was selected because it was used in a previous study investigating oxidative stress in *S. aureus*.<sup>29</sup> N7-Pan was added to a final concentration of 40 μM. A MIC of 78 nM determined by growth inhibition assays has been reported but since N7-Pan is added to exponentially growing cells in this study an excess concentration of 40 μM was selected. Combination experiments contained both 20 mM H<sub>2</sub>O<sub>2</sub> and 40 μM N7-Pan.

### **2.2.2 Harvest and metabolite extraction of *S. aureus***

The cell wall structure of *S. aureus* presents a challenge to the extraction and measurement of intracellular metabolites. Like other Gram-positive bacteria, the cell wall contains a thick layer of peptidoglycan and chemical or mechanical cell disruption techniques typically take longer than in the case of Gram-negatives. Therefore, cellular metabolism should be quenched before cell disruption and the time between sampling and quenching should be minimized to avoid changes in the metabolite levels due to enzyme activity. A protocol developed by Meyer *et al.* (2010) specifically for metabolomics studies of *S. aureus* was used to ensure that the samples analysed are in fact true representations of the biological state.<sup>30</sup> The general workflow is illustrated in Figure 2.2. Prior to each harvest, the OD<sub>500</sub> was measured to calculate the harvest volume that would contain 20 OD units. The time between harvest and quenching of metabolism was restricted to 60 seconds and the following three steps were performed in this time frame: 1) The appropriate volume was removed from the main culture and the media separated from the cells by fast vacuum filtration where the cells were retained on a mixed cellulose filter. 2) Residual media was removed by washing the cells on the filter with double the volume of a NaCl washing solution isotonic to the culture medium. 3) Metabolism was quenched by placing the filter, along with the cells, in a tube with ice cold extraction solution of 60% (w/v) ethanol and the tube was immediately submerged in liquid nitrogen to quench metabolism. The extraction mixture was thawed on ice and camphorsulfonic acid (CSA) was added as an internal standard. Repeated vortex of the tube ensured that all cells were washed from the filter. Glass beads were added to the extraction solution and cells were disrupted in a homogenizer. Following cell disruption, the glass beads and cell debris were removed by centrifugation. The supernatant was lyophilised and resuspended in ultrapure water for analysis.

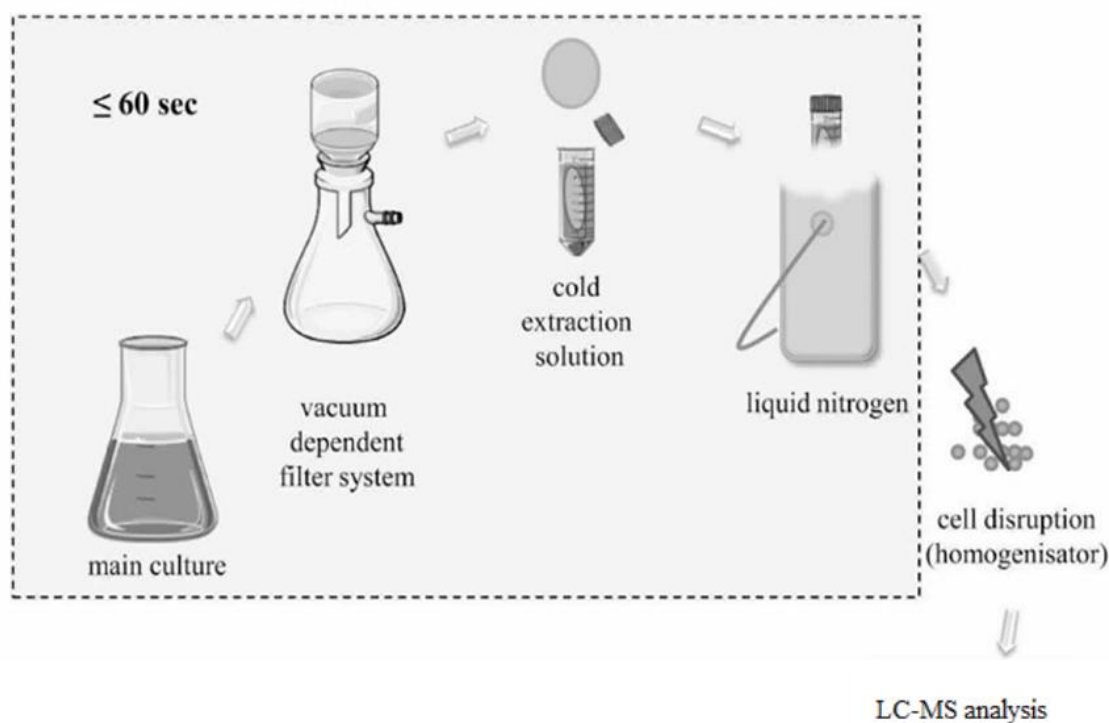


Figure 2.2: General workflow for harvesting *S. aureus*. Separation from media and washing of the cells is performed rapidly by vacuum filtration. Metabolism is effectively quenched by placing the filter with cells in ice cold extraction solution and flash-freezing the cells in liquid nitrogen. Cells are disrupted mechanically with glass beads in a homogenizer and lyophilised and resuspended for LC-MS analysis. Figure reproduced with permission from Elsevier, Meyer, H.; Liebeke, M.; Lalk, M., A protocol for the investigation of the intracellular *Staphylococcus aureus* metabolome. *Anal. Biochem.* **2010**, *401* (2), 250-259, <http://www.sciencedirect.com/science/article/pii/S0003269710001557>. Copyright © 2010 Elsevier Inc.

### 2.2.3 Analysis of *S. aureus* extracts

To determine the intracellular levels of ATP, ADP, AMP, CoA, DePCoA and PPanSH, LC-MS analysis of cell extracts was performed. These metabolites were identified by analytical standards and quantified by calibration curves.

#### 2.2.3.1 Adenylate energy charge

The adenylate energy charge (AEC) was calculated for each biological sample according to equation 2.1 and results are presented in Figure 2.3.<sup>27</sup> In this study the AEC was higher than 0.9 for *S. aureus* USA 300 *wt* and  $\Delta bshA$  control cultures throughout the experiment, as is expected for cells in the exponential growth phase. For *wt* cultures, a significant drop in the AEC is seen at  $t_0$  in the presence of 20 mM  $H_2O_2$  as well as the combination experiment

compared to the control ( $P \leq 0.001$ ). Here the AEC drops to  $\sim 0.5$  for  $H_2O_2$  alone and to  $\sim 0.4$  for the combination. These changes reported in AEC at  $t_0$  likely occur in the  $\leq 60$  second time period required for cell harvesting and quenching of metabolism. For growth the AEC has to be above 0.8; cells still retain viability between 0.5 and 0.8 but die below 0.5.<sup>28</sup> After 15 minutes of  $H_2O_2$  exposure the AEC levels returned to normal in the *wt* strain. For the  $\Delta bshA$  mutant an even stronger effect is seen in the presence of  $H_2O_2$ , with the AEC being decreased to  $\sim 0.2$  at  $t_0$ . After 15 minutes ( $t_{15}$ ) the AEC of the  $\Delta bshA$  strain had only increased marginally to 0.3, but at  $t_{140}$  the AEC levels were back to  $\sim 0.9$ . These results indicate that the *wt* strain is somewhat more resistant to oxidative stress than the  $\Delta bshA$  strain, where the decrease in AEC was found to be more pronounced. The *wt* population also recovers faster following oxidative stress with AEC levels returning to normal within 15 minutes. This is probably due to the *wt* population remaining viable throughout the decrease in AEC during oxidative stress whereas in the  $\Delta bshA$  population cell death occurs, leading to increased time required for recovery of the AEC of the population. Furthermore, no difference was observed in the viability of control cultures and cultures treated with N7-Pan, and the viability of  $H_2O_2$  treated cells did not decrease in the presence of N7-Pan. Taken together, the results obtained with N7-Pan indicate that CoA is not the major LMW thiol in *S. aureus*. However, all data from the N7-Pan stressed cultures are treated with caution since no decrease in viability was observed when treated with this known inhibitor of growth despite using a concentration far in excess ( $40\mu M$ ) of the reported MIC for *S. aureus* of 78 nM.<sup>31</sup>

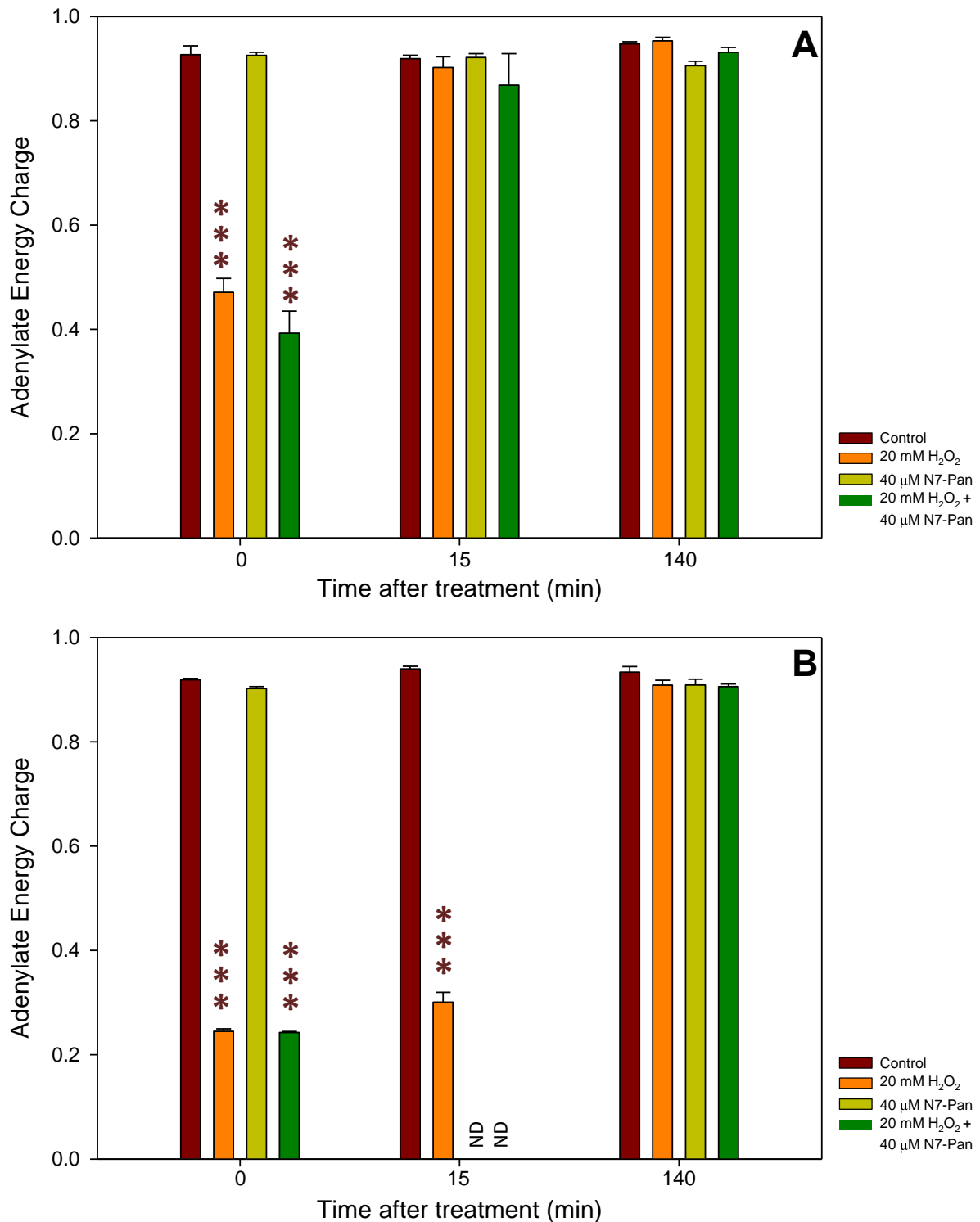


Figure 2.3: Adenylate energy charge in harvested *S. aureus*. **A)** USA 300 wt, **B)** USA 300  $\Delta bshA$ , \*\*\*  $P \leq 0.001$ ). A significant decrease in the AEC is observed at  $t_0$  for all cultures treated with H<sub>2</sub>O<sub>2</sub> and H<sub>2</sub>O<sub>2</sub> + N7-Pan compared to the control. This significant reduction in AEC persists up to 15 minutes for  $\Delta bshA$  cultures treated with H<sub>2</sub>O<sub>2</sub>. Bars represent the mean of the AEC measured in triplicate cultures, with the error bars denoting the standard deviation. ND denotes measurements Not Determined.

### 2.2.3.2 The impact of stress on levels of intracellular CoA and its precursors

At the same time intervals, the levels of PPanSH, DePCoA and CoA were measured by LC-MS and quantified from a standard curve. The intracellular levels of PPanSH measured in both strains are shown in Figure 2.4. For the *wt* strain, PPanSH levels stay consistent throughout the experiment in control cultures and in cultures stressed with 20 mM H<sub>2</sub>O<sub>2</sub> (panel A, Figure 2.4). There appears to be a slight decrease in PPanSH levels in the presence of N7-Pan but the difference is not significant. PPanSH levels in the  $\Delta bshA$  strain under control conditions exhibit some variability over the course of the experiment and also between the different replicate cultures (panel B, Figure 2.4). H<sub>2</sub>O<sub>2</sub>-treated cultures show significantly increased levels of PPanSH compared to the control at  $t_0$  when cultures were treated with 20 mM H<sub>2</sub>O<sub>2</sub>. This corresponds to the low cell viability observed in the AEC measurements. PPanSH levels are not increased in cultures treated with both H<sub>2</sub>O<sub>2</sub> and N7-Pan at  $t_0$ . This indicates that the increased PPanSH levels in cultures treated only with H<sub>2</sub>O<sub>2</sub> is not due to degradation of CoA when the population viability falls, since in such a case a similar increase would be apparent in the combination treated culture. Since CoA production is inhibited in the culture treated with H<sub>2</sub>O<sub>2</sub> and N7-Pan, and an increase in PPanSH is not observed it can be deduced that the increased levels of PPanSH seen in the H<sub>2</sub>O<sub>2</sub> culture is due to an increase in production. However, higher levels of PPanSH did not correlate with higher viability under oxidative stress as the AEC for cultures treated with H<sub>2</sub>O<sub>2</sub> alone and a combination of H<sub>2</sub>O<sub>2</sub> and N7-Pan had equally low viability.

DePCoA levels in control cultures remained consistent for the duration of the experiment in both the *wt* and  $\Delta bshA$  strains (Figure 2.5) although larger errors are apparent in DePCoA measurements of  $\Delta bshA$ . Stressed conditions induced in the *wt* and  $\Delta bshA$  culture did not lead to significant variations in the DePCoA levels. Although DePCoA levels of  $\Delta bshA$  treated with H<sub>2</sub>O<sub>2</sub> remained consistent up to 15 minutes, no DePCoA could be detected at  $t_{140}$  in any of the three cultures treated at any given time; this was not a significant difference of the DePCoA levels observed in the control at  $t_{140}$ . This strongly suggests that the levels of DePCoA in both strains remain largely constant, regardless of stress conditions or time after exposure to the stressors.

CoA levels in the *wt* strain was consistent for the duration of the experiment under control conditions (Panel A, Figure 2.6), with the only significant change being an increase in CoA at  $t_{15}$  after treatment with H<sub>2</sub>O<sub>2</sub> ( $P \leq 0.05$ ). Similar to PPanSH, the same response is not observed when cultures were treated with a combination of H<sub>2</sub>O<sub>2</sub> and N7-Pan, indicating the increase in CoA levels is due to increased production of the cofactor. The increase in CoA

coincides with the recovery of viability of the culture, but cultures treated with N7-Pan in the presence of H<sub>2</sub>O<sub>2</sub> stress recovers equally well without a significant increase in CoA levels. When cultures were treated with N7-Pan, culture viability was not decreased and the CoA measurements reflect levels similar to that of the control. Therefore CoA levels do not decrease when exponentially growing cultures are treated with 40 µM N7-Pan but that increased production of CoA is inhibited when the cultures are exposed to oxidative stress.

CoA levels in the  $\Delta bshA$  mutant remained unchanged for the duration of the experiment under control conditions, with the CoA levels being found to be very similar to those observed in the *wt* control. At  $t_0$ , cultures treated with either H<sub>2</sub>O<sub>2</sub> or H<sub>2</sub>O<sub>2</sub> and N7-Pan were found to have lower levels of CoA compared to the control and N7-Pan-treated samples, but the decrease was not found to be significant. At  $t_{15}$  however, the CoA levels measured in cultures treated with H<sub>2</sub>O<sub>2</sub> were significantly lower compared to the control even though it was only marginally less than at  $t_0$ . From these results, it seems that CoA levels do not increase when cultures of the  $\Delta bshA$  strain are treated with H<sub>2</sub>O<sub>2</sub>. This is probably due to the very low cell viability that predominates under these conditions, because CoA production cannot be increased if there is widespread cell death.

To summarize these findings, the only significant changes in metabolite levels relative to controls were observed for PPanSH in  $\Delta bshA$  at  $t_0$  with H<sub>2</sub>O<sub>2</sub> added and in the CoA levels of the *wt* at  $t_{15}$  after the addition of H<sub>2</sub>O<sub>2</sub>. The increases in these metabolites measured are attributed to increased production because similar increases are not seen under the same conditions when N7-Pan is added.

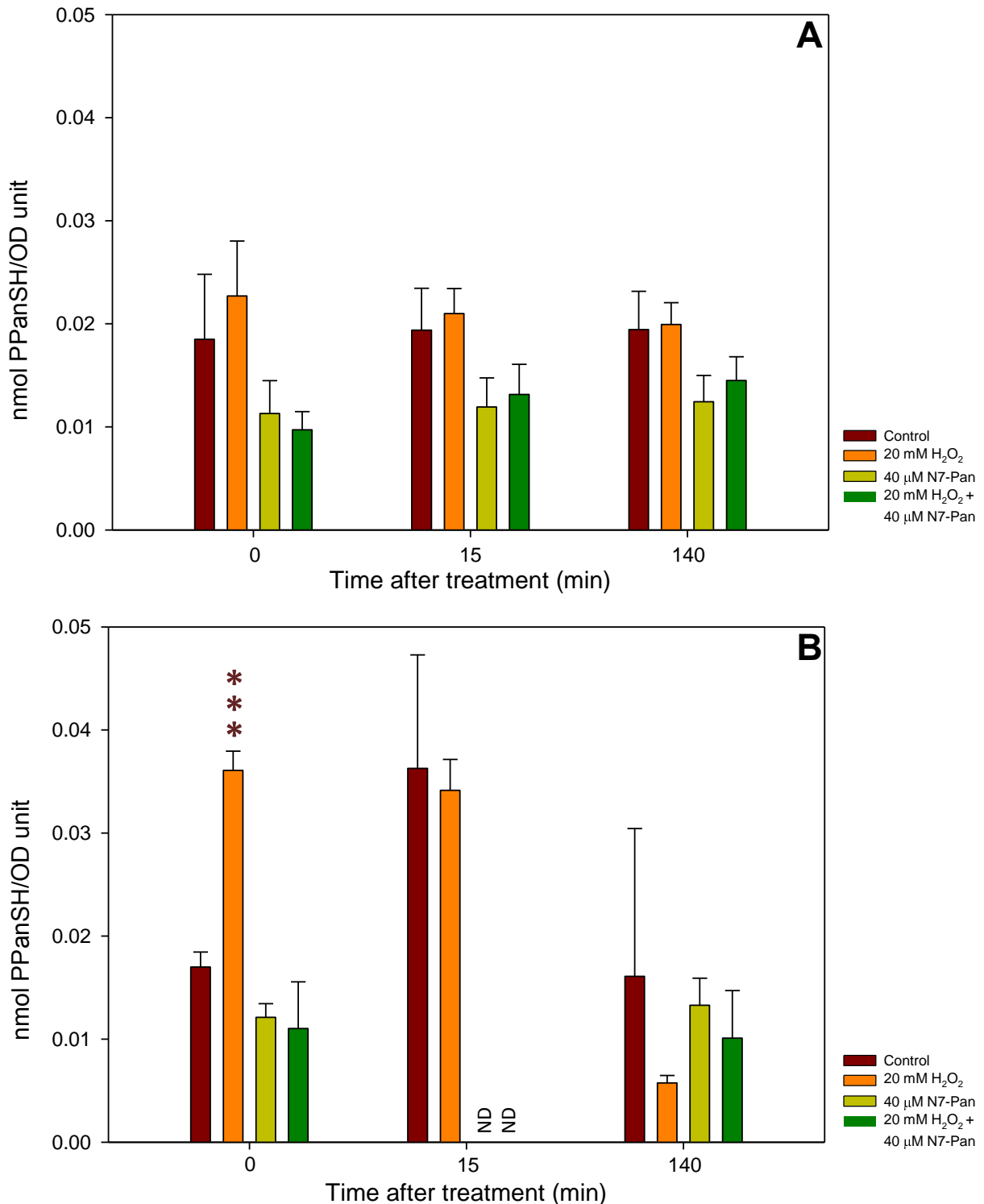


Figure 2.4: PPanSH levels in *S. aureus*. **A**) USA 300 Wt **B**) USA 300  $\Delta bshA$ . (\*\*\*)  $P \leq 0.001$  ). PPanSH levels do not vary significantly under all conditions tested for the wt strain. A significant increase in the level of PPanSH of  $\Delta bshA$  is observed at  $t_0$  in cultures treated with H<sub>2</sub>O<sub>2</sub> but not in cultures treated with H<sub>2</sub>O<sub>2</sub> and N7-Pan, which suggests that the increase in PPanSH under oxidative stress conditions is due to increased production of PPanSH. Bars represent the mean of PPanSH measured in triplicate cultures, with the error bars denoting the standard deviation. ND denotes measurements Not Determined.

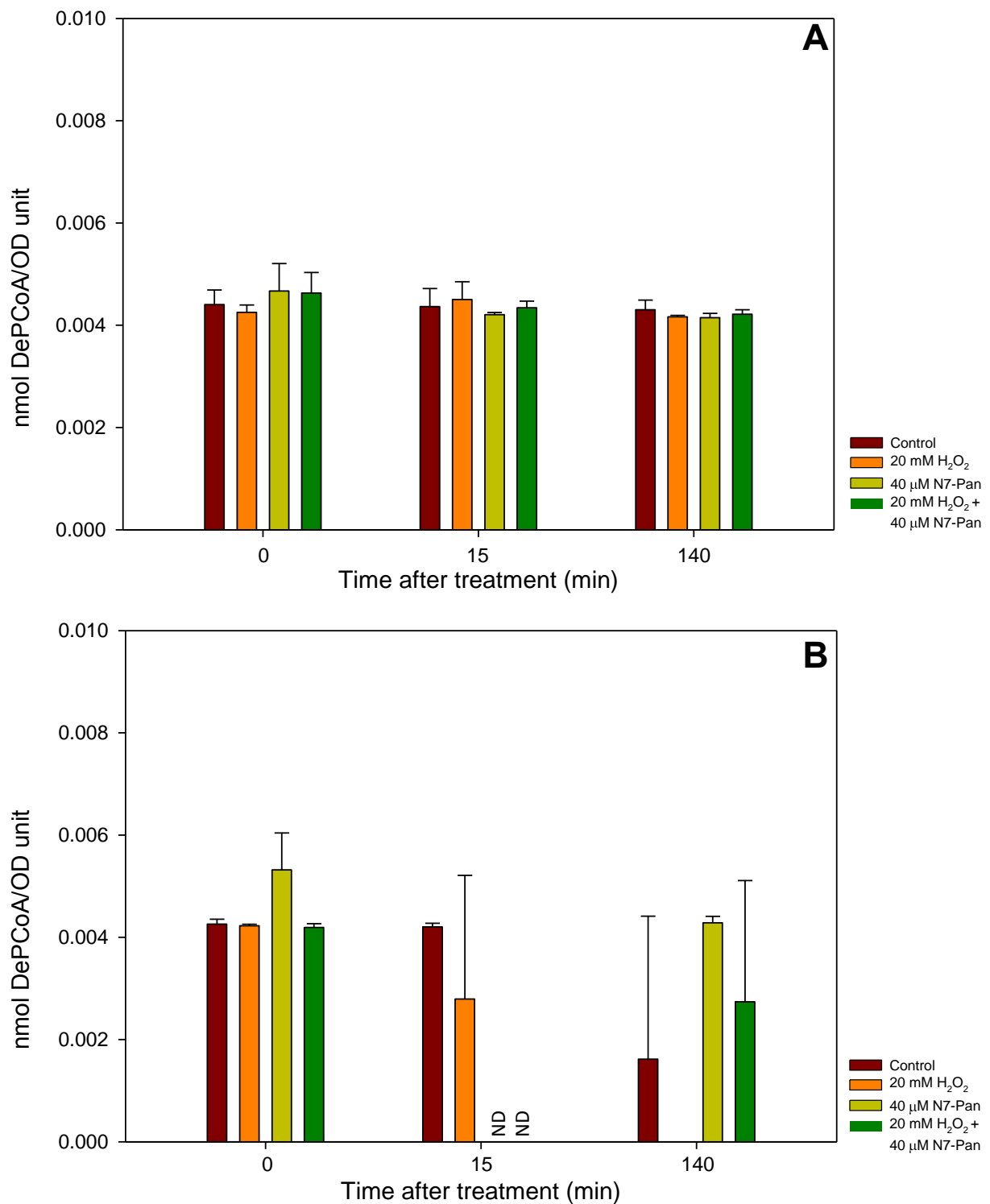


Figure 2.5: DePCoA levels in *S. aureus*. **A**) USA 300 wt **B**) USA 300  $\Delta bshA$ . No significant changes in DePCoA levels were observed in both strains under control conditions or after treatment with H<sub>2</sub>O<sub>2</sub>, N7-Pan or a combination of the two. Bars represent the mean of PPanSH measured in triplicate cultures, with the error bars denoting the standard deviation. ND denotes measurements Not Determined.

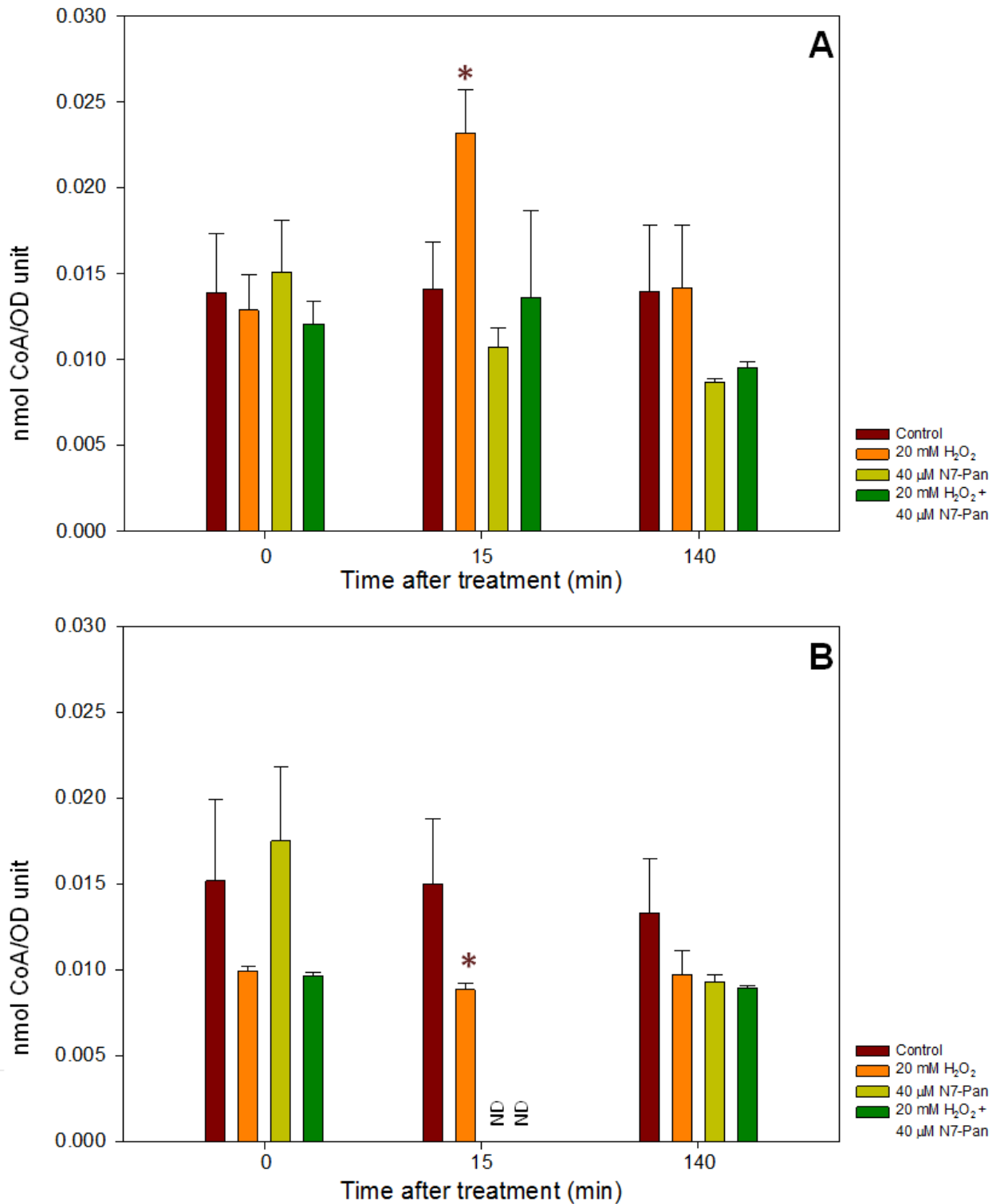


Figure 2.6: CoA levels in *S. aureus*. **A**) USA 300 wt **B**) USA 300  $\Delta bshA$ . \*  $P \leq 0.05$  CoA levels are increased significantly at  $t_{15}$  in the presence of H<sub>2</sub>O<sub>2</sub> but return to levels comparable to the control at  $t_{140}$ . CoA levels remain consistent in the  $\Delta bshA$  strain for the different conditions tested, but there is a significant decrease in CoA at  $t_{15}$  in cultures treated with H<sub>2</sub>O<sub>2</sub>. ND denotes measurements Not Determined.

## 2.3 Conclusion

In this study, it was investigated if the regulation of CoA production plays a role in the oxidative stress resistance of *S. aureus* USA 300. It was found that the *wt* strain that produces CoA and BSH is more resistant to oxidative stress than the BSH-deficient mutant  $\Delta bshA$ . This is in line with studies that have shown the importance of BSH in the oxidative stress response of *S. aureus* USA 300.<sup>7</sup> Results also indicate that the production of CoA is up-regulated under oxidative stress conditions where increased levels of CoA were measured in *wt S. aureus*. This indicates that a redox-signal may change the normal regulation of CoA production to an activated state, supporting the idea of a redox-switch in the pathway. Confirming whether this is the case is beyond the scope of this study but should be investigated in future studies. Although a similar response of increased GSH production under conditions of oxidative stress has been observed in plants and humans, there is no evidence of a redox switch responsible for the up-regulation.<sup>32,33,34</sup>

The up-regulation in CoA production is not correlated with the up-regulation of the immediate CoA biosynthetic precursors, DePCoA and PPanSH. An increase in flux is not necessarily expected to be accompanied by an increase in the steady state concentration of the intermediates. However, metabolite concentrations are the chemical key that can be measured to provide insight into the regulation of the pathway and the steps that it consists of. To explore in-depth regulation of the pathway, time course analysis where all pathway intermediates are measured under controlled conditions during CoA production is required and will be investigated in the following chapters.

A conclusion that can be made from the observation of increased CoA levels is that oxidative stress increased the demand for free CoA as a redox buffer. If another CoA dependent process increased the demand for CoA an increase in the steady state CoA concentration would not be expected because it would be consumed due to the increased demand. Interestingly, it was only the *wt* that showed a significant increase in CoA levels following oxidative stress induction; a similar response is not observed in  $\Delta bshA$ . A more pronounced increase in CoA levels is expected in the absence of BSH. However, such a response may have been masked by cell death as indicated by the extremely low viability observed for the  $\Delta bshA$  strain when H<sub>2</sub>O<sub>2</sub> was added. In future studies it would also be worthwhile to measure the levels of CoA and CoA disulfide as well as BSH and BSH disulfide under oxidative stress conditions with a range of oxidants and concentrations to determine whether these redox buffers have complimentary actions.

The results also indicate that N7-Pan, the known growth inhibitor and CoA-antimetabolite precursor, failed to decrease the viability of exponentially growing cells of both strains—in spite of it being added to the culture at a concentration far in excess of the reported MIC. This may be due to a large intracellular CoA pool already being established upon addition of N7-Pan. Viability of H<sub>2</sub>O<sub>2</sub> treated cultures did not decrease in the presence of N7-Pan and taking these findings together it is concluded that although CoA plays a role as a redox buffer it is not the major LMW thiol in *S. aureus*. BSH most likely makes a significant contribution as an additional redox buffer although the mechanism of recycling of reduced BSH from the disulfide remains to be discovered. N7-Pan negated the increase in CoA production of the *wt* under oxidative stress conditions but viability was not decreased further in spite of the lack of the CoA response. This suggests that the increased CoA response may be more important to the recovery of viability following oxidative stress, than direct reduction of oxidative stress.

In summary, these results indicate that the production of CoA can indeed be up-regulated in *S. aureus* under oxidative stress conditions. However, it seems that this is not the only factor responsible for the oxidative stress resistance of *S. aureus* because BSH was found to play an important role as a redox buffer as well. Oxidative stress resistance and subsequent recovery can therefore be attributed to both the presence of BSH and higher levels of CoA that is produced as a response to oxidative stress. From a drug development perspective, it is unlikely that inhibition of CoADR in the CoA redox buffer system will result in growth inhibition under oxidative stress conditions because of the increase seen in the production of CoA. If CoADR is inhibited and CoA disulfide accumulates, there would still be an increased demand for CoA and consequently increased production. In order to make *S. aureus* more vulnerable to the effects of oxidative stress BSH biosynthesis should be targeted directly. Increased vulnerability to oxidative stress can also be accomplished by inhibiting the recovery of viability following exposure. This may be achieved by targeting CoA production directly in combination with inhibition of CoADR. Inhibition of the production of CoA and the ability to recycle oxidised CoA would lead to the available CoA pool becoming trapped in the disulfide state. This would affect all CoA dependent processes, not just oxidative stress resistance resulting in inhibition of growth. Effective inhibition of CoA production is difficult considering the current poor understanding of the regulation of the rate of CoA production but this will be addressed in the following chapters.

## 2.4 Experimental procedures

All chemicals, solvents and media were purchased from Sigma-Aldrich and were of the highest purity. Centrifugation was carried out in a Heraeus Multifuge 3S/3S-R centrifuge. Small scale centrifugation was performed on a Heraeus Biofuge pico centrifuge.

### 2.4.1 *S. aureus* strains and growth conditions

*S. aureus* USA 300 *wt* and  $\Delta bshA$  strains were cultured at 37°C with vigorous agitation in RPMI-1640 medium (Sigma-Aldrich) which was supplemented with the following: 0.51  $\mu\text{M}$   $\text{ZnCl}_2$ , 0.5  $\mu\text{M}$   $\text{MnCl}_2$ , 0.097  $\mu\text{M}$   $\text{H}_3\text{BO}_3$ , 1.46  $\mu\text{M}$   $\text{CoCl}_2$ , 0.015  $\mu\text{M}$   $\text{CuCl}_2$ , 0.1  $\mu\text{M}$   $\text{NiCl}_2$ , 0.148  $\mu\text{M}$   $\text{NaMoO}_4$ , 0.75  $\mu\text{M}$   $\text{FeCl}_3$  and 2.05 mM L-glutamine. Main cultures were made by inoculating 100 ml medium in a 500 ml Erlenmeyer culture flask with exponentially growing overnight starter culture for an initial optical density at 500 nm ( $\text{OD}_{500}$ ) of 0.05. At an OD of 0.5, cultures were treated with 20 mM  $\text{H}_2\text{O}_2$  or 40  $\mu\text{M}$  of N7-Pan, or both 20 mM  $\text{H}_2\text{O}_2$  and 40  $\mu\text{M}$  N7-Pan. For the control, cultures were incubated without the addition of  $\text{H}_2\text{O}_2$  or N7-Pan. Cultivation was performed in triplicate to obtain three independent biological replicates. For the analysis of intracellular metabolites, samples containing 20 OD units were taken directly after treatment with  $\text{H}_2\text{O}_2$  or N7-Pan ( $t_0$ ) and 15 minutes ( $t_{15}$ ) and 140 minutes ( $t_{140}$ ) later. The OD was measured prior to every sampling to calculate the appropriate culture aliquot to be harvested.

### 2.4.2 Cell harvest and quenching of metabolism

At each sampling time point, 20  $\text{OD}_{500}$  units of culture was harvested with the vacuum-dependent fast-filtration approach of Meyer et al.<sup>30</sup> The vacuum filtration system consisted of a large glass funnel (90 mm diameter), a glass filter holder with a stainless steel mesh screen, a glass tubulated base and a vacuum filter flask, all obtained from Merck-Millipore. A mixed cellulose ester filter membrane with 0.45  $\mu\text{m}$  pore sizes obtained from Whatman was used to retain the cells while the media was filtered into the vacuum flask. Residual media was removed from the cells retained on the filter with double the volume of an ice cold washing solution. The washing solution was isotonic to the RPMI growth media and contained 0.85% (w/v) NaCl. After washing, the filter with the cells was immediately transferred to a tube filled with 5 ml of ice cold extraction solution consisting of 60% ethanol (w/v). The tube was shaken and submerged in liquid nitrogen to flash-freeze the cells and effectively quench metabolism. The time between removal of an aliquot from the main culture until quenching in liquid nitrogen was kept below 60 seconds to ensure that the levels of intracellular metabolites do not change significantly during the sampling procedure.

Frozen extraction samples were stored at -80°C until cell disruption and extraction could be performed.

### **2.4.3 Extraction of intracellular metabolites**

The frozen extraction solution with the filter and cells was thawed on ice and all subsequent steps of the extraction procedure were performed on ice. 5 nmol Camphorsulfonic acid (CSA) was added to the extraction mixture as internal standard for LC-MS analysis. Cells were washed from the filter by shaking and vortexing the tube 10 times for 10 seconds. The extraction solution containing the resuspended cells was transferred to a tube containing ~ 3 ml of glass beads 0.1-0.11 mm in diameter (Sigma-Aldrich). Mechanical cell disruption was performed with a FastPrep-24 homogenizer (MP Biomedicals, LLC) for two cycles of 40 seconds each at 6.0 m/s. The ethanol cell extracts were transferred to 15 ml tubes and the glass beads and cell debris was washed with 5 ml ultrapure water for a second extraction step. The aqueous and ethanol extracts were combined and centrifuged for 5 min at 10 000 x *g* and 4°C to remove remaining cell debris and glass beads. The supernatant was collected and stored at -80°C for lyophilisation. Blank samples were obtained with the same extraction protocol by adding a filter without cells to the extraction solution.

### **2.4.4 Analysis and quantification of metabolites**

Cell extracts were lyophilised to complete dryness and redissolved in 100 µl ultrapure water. Samples were centrifuged for 5 min at 17900 x *g* and 4°C and the supernatant removed to a clean tube and centrifuged again to remove residual cell debris. Ion-pairing HPLC-MS analysis was performed to quantify the metabolites of interest. Analyses were performed on an Agilent 1100 series HPLC consisting of a degasser and quaternary pump with a manual injector connected to a micro-time of flight (microTOF) mass spectrometer (Bruker Daltonics). Samples were analysed by injecting 25 µl on to a SymmetryShield reverse phase C18 column (4.6 mm x 150 mm x 3.5 µm) (Waters) protected by a SecurityGuard C18 guard column (3 mm x 4 mm) (Phenomenex). A binary mobile phase was used for chromatographic separation that consisted of A) 95% H<sub>2</sub>O, 15 mM acetic acid, 5% methanol and 10 mM tributylamine (pH 4.9) as the ion-pairing reagent, and B) 100% methanol. The column was equilibrated at 100% A with a flow rate of 0.5 ml/min. The gradient elution method started with a linear increase in B to 31% in the first two minutes and continued with an increase to 50% in 18.5 minutes, from 50 to 60% in 2.5 minutes and 60% to 100% B in 1 minute, isocratic at 100% B for 7 minutes followed by return to initial conditions with A increasing from 0 to 100% A in 1 minute. The column was re-equilibrated for 10 minutes in 100% A. MS analysis was carried out by using electrospray ionization and negative-ion

polarity with full scan mode being used over the mass range of 50 to 3000 m/z. Calibration of the MS was achieved with 16 different masses ranging from 112.98 to 1132.79 m/z from a sodium formate solution in 49.4% H<sub>2</sub>O, 49.4 % isopropanol, 0.2 % formic acid and 10 mM NaOH that was used as a tune mix that was injected at the beginning of each run.

#### **2.4.5 LC-MS data analysis**

Metabolites were identified by matching retention time and m/z values of the peaks detected in samples to those of analytical standards of the metabolites of interest. The area of m/z of [M-H]<sup>-</sup> or [M-H]<sup>2-</sup> of each metabolite was integrated. These areas were then normalized to the integral area of m/z of [M-H] of the internal standard by using QuantAnalysis v1.8 software (Bruker Daltonik GmbH) resulting in the relative metabolite amount per 20 OD units. For absolute quantification, the ratio of metabolite area/internal standard area was substituted into the calibration equation for each metabolite of interest. Calibration curves were set up for each metabolite separately in the range of 0.001 to 0.5 mM, based on 11 calibration points and linear regression. Blank extraction samples were also analysed and masses detected in these samples were excluded from the data analysis of biological samples. For the calculation of the adenylate energy charge, concentrations of AMP, ADP and ATP were determined in each biological sample and calculations performed according to the method of Atkinson (Eq 2.1).<sup>27</sup> Statistical significance of the difference in AEC and other metabolite levels between the control and treated cultures were determined from the mean value for three biological replicates by performing the unpaired t test in Sigmaplot 11.0 (Systat Software, Inc.) with P values ≤ 0.05 indicating significance.

## 2.5 References

1. Livermore, D. M., Antibiotic resistance in staphylococci. *Int. J Antimicrob. Agents* **2000**, *16 Suppl 1*, S3-10.
2. Babior, B. M.; Kipnes, R. S.; Curnutte, J. T., Biological defense mechanisms. The production by leukocytes of superoxide, a potential bactericidal agent. *J. Clin. Invest* **1973**, *52* (3), 741.
3. Iyer, G.; Islam, M.; Quastel, J., Biochemical aspects of phagocytosis. *Nature* **1961**, *192*, 535-41.
4. Winterbourn, C. C.; Hampton, M. B., Thiol chemistry and specificity in redox signaling. *Free Radic. Biol. Med.* **2008**, *45* (5), 549-561.
5. Winterbourn, C. C., Are free radicals involved in thiol-based redox signaling? *Free Radic. Biol. Med.* **2015**, *80*, 164-170.
6. Fahey, R. C., Glutathione analogs in prokaryotes. *Biochim. Biophys. Acta* **2013**, *1830* (5), 3182-3198.
7. Posada, A. C.; Kolar, S. L.; Dusi, R. G.; Francois, P.; Roberts, A. A.; Hamilton, C. J.; Liu, G. Y.; Cheung, A., Importance of Bacillithiol in the Oxidative Stress Response of *Staphylococcus aureus*. *Infect. Immun.* **2014**, *82* (1), 316-332.
8. Newton, G. L.; Arnold, K.; Price, M. S.; Sherrill, C.; Delcardayre, S. B.; Aharonowitz, Y.; Cohen, G.; Davies, J.; Fahey, R. C.; Davis, C., Distribution of thiols in microorganisms: mycothiol is a major thiol in most actinomycetes. *J. Bacteriol.* **1996**, *178* (7), 1990-5.
9. Vallari, D. S.; Jackowski, S.; Rock, C. O., Regulation of pantothenate kinase by coenzyme A and its thioesters. *J. Biol. Chem.* **1987**, *262* (6), 2468-71.
10. Leonardi, R.; Chohan, S.; Zhang, Y. M.; Virga, K. G.; Lee, R. E.; Rock, C. O.; Jackowski, S., A pantothenate kinase from *Staphylococcus aureus* refractory to feedback regulation by coenzyme A. *J Biol Chem* **2005**, *280* (5), 3314-22.
11. delCardayré, S. B.; Stock, K. P.; Newton, G. L.; Fahey, R. C.; Davies, J. E., Coenzyme A Disulfide Reductase, the Primary Low Molecular Weight Disulfide Reductase from *Staphylococcus aureus*: Purification and characterization of the native enzyme. *J. Biol. Chem.* **1998**, *273* (10), 5744-5751.
12. van der Westhuyzen, R.; Strauss, E., Michael Acceptor-Containing Coenzyme A Analogues As Inhibitors of the Atypical Coenzyme A Disulfide Reductase from *Staphylococcus aureus*. *J. Am. Chem. Soc.* **2010**, *132*, 12853-12855.
13. Sharma, S. V.; Arbach, M.; Roberts, A. A.; Macdonald, C. J.; Groom, M.; Hamilton, C. J., Biophysical features of bacillithiol, the glutathione surrogate of *Bacillus subtilis* and other firmicutes. *Chembiochem* **2013**, *14* (16), 2160-2168.

14. Chi, B. K.; Roberts, A. A.; Huyen, T. T. T.; Bäsell, K.; Becher, D.; Albrecht, D.; Hamilton, C. J.; Antelmann, H., S-bacillithiolation protects conserved and essential proteins against hypochlorite stress in firmicutes bacteria. *Antioxid. Redox Signal.* **2013**, *18* (11), 1273-1295.
15. Newton, G. L.; Fahey, R. C.; Rawat, M., Detoxification of toxins by bacillithiol in *Staphylococcus aureus*. *Microbiology* **2012**, *158* (Pt 4), 1117-1126.
16. Rajkarnikar, A.; Strankman, A.; Duran, S.; Vargas, D.; Roberts, A. A.; Barretto, K.; Upton, H.; Hamilton, C. J.; Rawat, M., Analysis of mutants disrupted in bacillithiol metabolism in *Staphylococcus aureus*. *Biochem. Biophys. Res. Commun.* **2013**, *436* (2), 128-133.
17. Hong, B. S.; Yun, M. K.; Zhang, Y.-M.; Chohnan, S.; Rock, C. O.; White, S. W.; Jackowski, S.; Park, H.-W.; Leonardi, R., Prokaryotic Type II and Type III Pantothenate Kinases: The Same Monomer Fold Creates Dimers with Distinct Catalytic Properties. *Structure* **2006**, *14* (8), 1251-1261.
18. Finkel, T., Oxidant signals and oxidative stress. *Curr. Opin. Cell Biol.* **2003**, *15* (2), 247-254.
19. Linke, K.; Jakob, U., Not Every Disulfide Lasts Forever: Disulfide Bond Formation as a Redox Switch. *Antioxid. Redox Signal.* **2003**, *5* (4), 425-434.
20. Åslund, F.; Zheng, M.; Beckwith, J.; Storz, G., Regulation of the OxyR transcription factor by hydrogen peroxide and the cellular thiol—disulfide status. *Proc. Natl. Acad. Sci.* **1999**, *96* (11), 6161-6165.
21. Fuangthong, M.; Helmann, J. D., The OhrR repressor senses organic hydroperoxides by reversible formation of a cysteine-sulfenic acid derivative. *Proc. Natl. Acad. Sci.* **2002**, *99* (10), 6690-6695.
22. Biteau, B.; Labarre, J.; Toledano, M. B., ATP-dependent reduction of cysteine—sulphinic acid by *S. cerevisiae* sulphiredoxin. *Nature* **2003**, *425* (6961), 980-984.
23. Sanchez, R.; Riddle, M.; Woo, J.; Momand, J., Prediction of reversibly oxidized protein cysteine thiols using protein structure properties. *Protein Sci.* **2008**, *17* (3), 473-481.
24. Vallari, D. S.; Rock, C. O., Isolation and characterization of temperature-sensitive pantothenate kinase (coaA) mutants of *Escherichia coli*. *J. Bacteriol.* **1987**, *169* (12), 5795-5800.
25. de Villiers, M.; Barnard, L.; Koekemoer, L.; Snoep, J. L.; Strauss, E., Variation in pantothenate kinase type determines the pantothenamide mode of action and impacts on coenzyme A salvage biosynthesis. *FEBS J.* **2014**, *281* (20), 4731-4753.
26. Dörries, K.; Schlueter, R.; Lalk, M., Impact of antibiotics with various target sites on the metabolome of *Staphylococcus aureus*. *Antimicrob. Agents Chemother.* **2014**, *58* (12), 7151-7163.

27. Atkinson, D. E., Energy charge of the adenylate pool as a regulatory parameter. Interaction with feedback modifiers. *Biochemistry* **1968**, *7* (11), 4030-4034.
28. Chapman, A. G.; Fall, L.; Atkinson, D. E., Adenylate energy charge in *Escherichia coli* during growth and starvation. *J. Bacteriol.* **1971**, *108* (3), 1072-1086.
29. Pöther, D.-C.; Gierok, P.; Harms, M.; Mostertz, J.; Hochgräfe, F.; Antelmann, H.; Hamilton, C. J.; Borovok, I.; Lalk, M.; Aharonowitz, Y.; Hecker, M., Distribution and infection-related functions of bacillithiol in *Staphylococcus aureus*. *Int. J. Med. Microbiol.* **2013**, *303* (3), 114-123.
30. Meyer, H.; Liebeke, M.; Lalk, M., A protocol for the investigation of the intracellular *Staphylococcus aureus* metabolome. *Anal. Biochem.* **2010**, *401* (2), 250-259.
31. Virga, K. G.; Zhang, Y.-M.; Leonardi, R.; Ivey, R. A.; Hevener, K.; Park, H.-W.; Jackowski, S.; Rock, C. O.; Lee, R. E., Structure-activity relationships and enzyme inhibition of pantothenamide-type pantothenate kinase inhibitors. *Bioorg. Med. Chem.* **2006**, *14* (4), 1007-1020.
32. Kimura, Y.; Goto, Y.-I.; Kimura, H., Hydrogen sulfide increases glutathione production and suppresses oxidative stress in mitochondria. *Antioxid. Redox Signal.* **2010**, *12* (1), 1-13.
33. Queval, G.; Thominet, D.; Vanacker, H.; Miginiac-Maslow, M.; Gakière, B.; Noctor, G., H<sub>2</sub>O<sub>2</sub>-activated up-regulation of glutathione in *Arabidopsis* involves induction of genes encoding enzymes involved in cysteine synthesis in the chloroplast. *Molecular. Plant.* **2009**, *2* (2), 344-356.
34. Zhou, W.; Freed, C. R., DJ-1 up-regulates glutathione synthesis during oxidative stress and inhibits A53T  $\alpha$ -synuclein toxicity. *J. Biol. Chem.* **2005**, *280* (52), 43150-43158.

# Chapter 3

## Measuring CoA salvage intermediates

---

### 3.1 Introduction

Studies investigating the regulation of CoA biosynthesis are currently limited by the lack of a sensitive quantitative method to measure all intermediates without incorporating radioactive isotopes.<sup>1</sup> In order to realize a holistic study of the CoA salvage pathway by time course analysis, a method had to be developed that could simultaneously quantify PanSH, PPanSH, DePCoA and CoA. The LC-MS method that was used for the quantification of intracellular PPanSH, DePCoA and CoA in *S. aureus* in Chapter 2 could not be used for the quantification of PanSH as well. A very low intensity signal is obtained for PanSH by MS detection due to a lack of ionizable groups which leads to a far higher limit of detection than the other intermediates of the CoA salvage pathway to such an extent that simultaneous quantification is not possible. Therefore a different method is required.

In addition to the study of biosynthesis regulation, reliable and robust methods are also required to measure CoA and related metabolites in biological samples as highlighted in a recent review on the role of CoA and its derivatives in cellular metabolism and disease.<sup>2</sup> Therefore, our aim was to develop a novel method suited to measuring CoA and its precursors in a simple matrix (e.g. when the pathway is reconstituted *in vitro*) as well as in complex matrices, such as those encountered in biological samples. Numerous methods have been developed specifically to measure CoA and its precursors, but success has been rather limited. A review was recently published on methods available to measure CoA and its thioester derivatives, such as enzymatic assays, paper and thin-layer chromatography as well as HPLC techniques.<sup>3</sup> Other techniques that have been used to measure PanSH, PPanSH, DePCoA and CoA include enzymatic degradation and microbiological assays, coupled chemical and enzymatic reactions, HPLC and MS detection of native metabolites as well as chemical derivatization prior to HPLC and/or MS. Due to the variety of techniques that have been employed in attempts to measure these metabolites a short review is presented here in which the suitability of these methods for simultaneous quantification of PanSH, PPanSH, DePCoA and CoA is evaluated.

## 3.2 Methods currently available for measuring CoA and its precursors

One of the earliest methods for quantifying PPanSH and CoA was based on their differential enzymatic degradation to PanSH by prostate and intestinal phosphatases followed by a microbiological growth assay with *Lactobacillus helveticus* or *L. arabinosus* to measure the products.<sup>4</sup> However, CoA and DePCoA could not be quantified explicitly with this method because there is no separation step and the quantitative data for CoA is actually the sum of DePCoA and CoA. Even though this method was published in 1958, subsequent methods that were developed failed to overcome the same obstacles encountered by this relatively rudimentary method *i.e.* separation of the metabolites and sensitive detection.

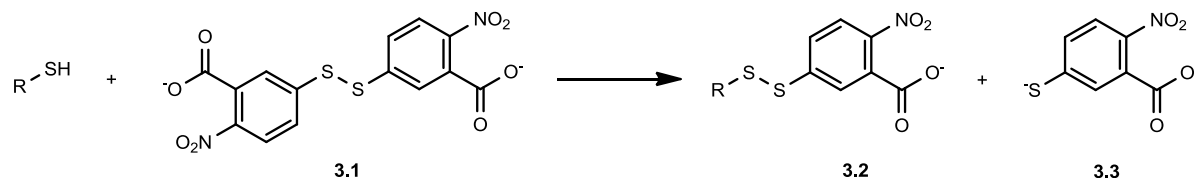
In the following subsections methods will be reviewed that have been used for the quantification of CoA and the possibility of adaptation to measure CoA precursors. The first group of methods reviewed involves direct or indirect measurement of CoA using spectrophoto- or spectrofluorometry in conjunction with coupled enzymatic or chemical reactions to facilitate detection. The second group of methods make use of a chromatographic separation step with various detection methods that will be discussed in greater detail.

### 3.2.1 Spectrophoto- and spectrofluorometric methods

These methods rely on an enzyme or chemical agent to link CoA to the fate of a spectrophoto- or spectrofluorometrically detectable product. Coupled enzyme reactions have been used to measure CoA directly and DePCoA and PanSH indirectly. Molnos *et al.* assayed the activity of malonyl-CoA:acyl carrier protein transacylase (MCAT) by measuring CoA with  $\alpha$ -ketoglutarate dehydrogenase ( $\alpha$ -KGDH). This involves the CoA-dependent oxidation of  $\alpha$ -ketoglutarate, accompanied by the reduction of  $\text{NAD}^+$  to NADH which can be measured at 340 nm as outlined in scheme 3.1.<sup>5</sup> This method is not useful for measuring CoA salvage intermediates because it is too specific:  $\alpha$ -KGDH only utilizes CoA and not any of its precursors and therefore it is not of use to this study. A similar enzyme-coupled technique was developed by Allred and Guy and subsequently modified that in effect amplifies CoA for measurement by a CoA recycling assay.<sup>6,7,8</sup> Here phosphotransacylase links the CoA concentration to NADH generation. This approach proved to be very sensitive but suffers from the same limitation of being too specific for the purpose of this study.



These reactions are not useful for determining metabolite concentrations, because it is not specific enough. All the metabolites of interest in this study contain a thiol group and therefore individual concentrations cannot be determined in a mixture without a prior separation step, because the same product is produced for the coupled reactions with all metabolites.



*Scheme 3.3: Reaction of DTNB with a thiol group.* The thiol cleaves the disulfide bond of DTNB (**3.1**) to yield  $\text{TNB}^{-1}$  (**3.3**) that ionizes in water and causes an increase in absorption at 412 nm.

### 3.2.2 Chromatographic methods

Quantitative methods based on HPLC and MS techniques have had limited success in measuring the four metabolites in their native state. LC techniques provide the means whereby the metabolites can be separated but sensitive detection for quantification still presents a significant challenge. A gradient HPLC method has enabled the separation and quantification of DePCoA and CoA by UV absorbance at 254 nm of the adenosine moiety in the respective structures.<sup>12</sup> However, this group is not present in PanSH and PPanSH structures. All four metabolites contain another UV-active group, the amide bond that absorbs at 214 nm. However, the molar extinction coefficient of the amide bond is  $923 \text{ M}^{-1}\text{cm}^{-1}$  which is very low compared to  $14\,200 \text{ M}^{-1}\text{cm}^{-1}$  for adenosine.<sup>13</sup> Hence, the absorbance of amide bonds at 214 nm is not strong enough to permit detection of low concentrations of the metabolites.

Due to these detection limitations, the four metabolites of the CoA salvage pathway have not been successfully measured in any of the bacterial metabolomics studies reported in recent years. Bajad *et al.* identified 141 metabolites of interest to be measured in *E. coli*, including DePCoA and CoA.<sup>14</sup> The metabolites were selected based on importance to core metabolic processes common to eukaryotic organisms. The HPLC-MS/MS technique that was developed in the study was successful at measuring DePCoA and CoA concentrations in standard mixtures but not cell extracts. Later the method was refined and CoA (but not DePCoA) was successfully quantified in cell extracts.<sup>15</sup> Similar results were reported in another study where ion-paired LC-ESI-MS was used for separation and quantification.<sup>16</sup> A number of methods have been established for the analysis of CoA and some of its

precursors based on chemical derivatization with a fluorophore followed by separation and detection of the products by HPLC. These methods are well suited for the detection of CoA salvage pathway metabolites from the same mixture or biological extracts and will be discussed in greater detail.

### 3.2.3 Pre-column derivatization and chromatographic analysis

A promising approach for measuring CoA and its intermediates is based on derivatization with a chemical agent followed by separation and detection of the derivatized product by HPLC. The thiol group of CoA is generally targeted for alkylation by chemical derivatization agents. There are two structural features common to good derivatization agents: a functional group that readily reacts with said thiol group (reacting group) and a fluorophore signalling group with a high quantum yield which translates to a high detector response factor and ultimately sensitive detection. A myriad of different combinations of reacting groups and signalling groups are available as fluorescent thiol probes. Published HPLC-based methods seem to favour two classes of thiol derivatization agents, namely halides and *N*-substituted maleimides. Those that have been used for pre-column derivatization of CoA or related thiols will be discussed in detail in the following sections.

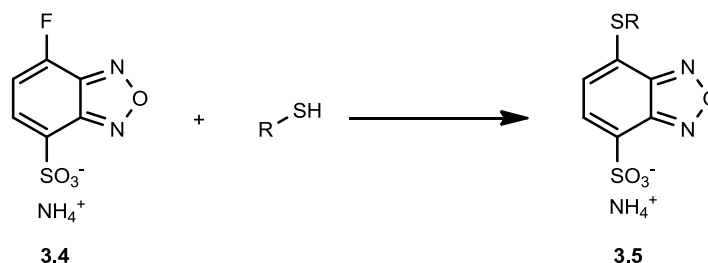
#### 3.2.3.1 Halides

##### 3.2.3.1.1 Ammonium 7-Fluorobenzo-2-oxa1,3-diazole-4-sulfonate (SBD-F)

SBD-F is a fluorogenic compound that has been used as a pre-column thiol derivatization reagent for the detection of biological thiols and for the quantification of CoA.<sup>17,18</sup> Its structure (scheme 3.3) consists of a benzofurazan moiety with a fluorine as reacting group but also an electron withdrawing aminosulfonyl group to further increase its reactivity.<sup>19</sup> The benzofurazan moiety exhibits fluorescence with excitation and emission maxima at 395 nm and 520 nm after derivatization and acts as a good signalling group. This reagent was found to be highly selective towards thiols with the derivatization reaction shown in Scheme 3.4 occurring rapidly. The thiol adducts formed were found to be stable if refrigerated but significant hydrolysis of SBD-F adducts occur at higher temperatures, with extended time and at high pH.

Due to the previous use of SBD-F for the sensitive quantification of CoA it was considered a good candidate for derivatization of the metabolites focused on in this study. However, a recent study by Sibon *et al.* used SBD-F specifically for the derivatization of PPanSH and

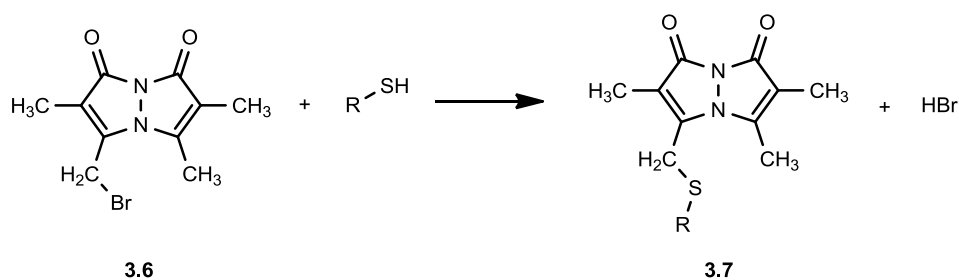
CoA.<sup>20</sup> These analytes could be detected qualitatively following separation by HPLC but absolute quantification could not be achieved. The reason quantification was not possible was not stated in the publication but in general there is some difficulty associated with the preparation of standards for calibration and reproducibility of results when fluorescent probes are used.



*Scheme 3.4: Reaction of SBD-F with a thiol group.* The benzofurazan moiety of **3.4** reacts with a thiol group to produce a fluorescent product (**3.5**) with excitation and emission maxima at 381 nm and 512 nm respectively.

### 3.2.3.1.2 Monobromobimane (mBBr)

Monobromobimane (mBBr) has been used with great success for the derivatization and detection of biological thiols. mBBr was the derivatization agent of choice in a qualitative study by Fahey *et. al.* that identified the four CoA salvage pathway metabolites by chromatographic separation and fluorescence detection in 1987.<sup>21</sup> mBBr is a heterocyclic bimane compound (scheme 3.5) that forms a fluorescent thioether derivatization product upon alkylation of thiols with excitation and emission maxima at 400 nm and 475 nm.<sup>22</sup> The alkylation reaction is rapid and complete in 10 minutes when mBBr is in two-fold excess but the thioether derivatization products formed are susceptible to photodegradation requiring the reaction and analysis of samples to be carried out in the dark. The study by Fahey *et. al.* noted some additional undesirable characteristics of mBBr and its derivatization products that were observed during chromatographic analysis, such as high levels of background noise. This was attributed to residual fluorescence of unreacted mBBr as well as non-specific binding of mBBr to carboxylates, amines and phosphates. Consequently, an uneven chromatographic baseline hindered accurate peak integration and metabolite quantification, resigning the study to qualitative data only.



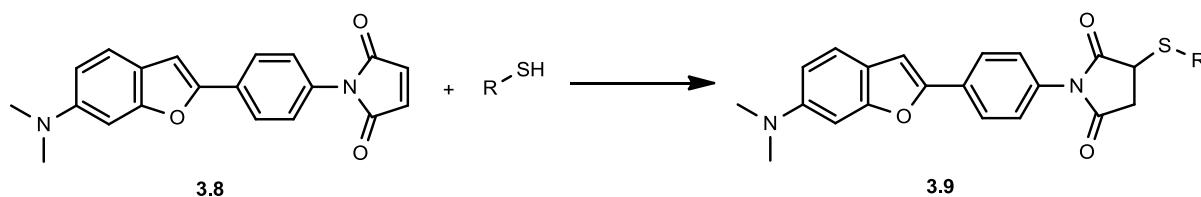
*Scheme 3.5: Reaction of mBBr with a thiol group.* mBBr (**3.6**) reacts with a thiol group to form a fluorescent thioether product (**3.7**) with excitation and emission maxima at 400 nm and 475 nm respectively.

### 3.2.3.2 *N*-substituted maleimides

Maleimide moieties contain a reactive double bond that allows for a rapid and specific reaction with thiols by facile addition.<sup>23</sup> Many different fluorophores have been coupled to the *N*-position of maleimide functional groups and are known to become fluorescent only after binding of a thiol group to the maleimide.<sup>24</sup> The following sections will focus on two specific *N*-substituted maleimides which have been useful for the detection of CoA.

#### 3.2.3.2.1 *N*-6[4-(6-dimethylamino-2-benzofuranyl)phenyl]-maleimide (DBPM)

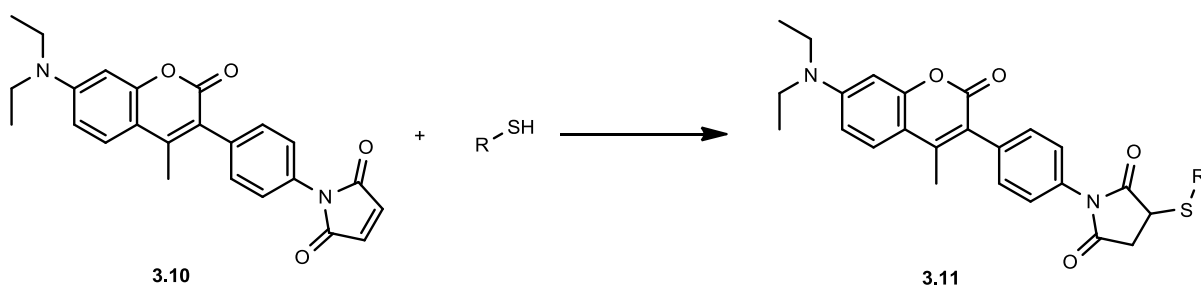
DBPM was one of the first *N*-substituted maleimides to contain a dimethylamino residue as part of the fluorophore moiety. The presence of this residue markedly improved the solubility of this reagent, something that was problematic for earlier *N*-substituted maleimides.<sup>25</sup> DBPM was used successfully for the determination of CoA by Nakashima *et. al.*<sup>26</sup> It binds to the CoA thiol by simple covalent bond formation as shown in scheme 3.6, to yield a fluorescent product with excitation and emission maxima at 355 nm and 457 nm. Optimal conditions for the derivatization reaction were found to be at a 1.5-fold excess of DBPM with incubation at 60°C for 20 minutes. No background fluorescence or side-reactions were reported and HPLC analysis enabled the quantification of CoA but this method has not been evaluated for the quantification of the thiolated CoA precursors.



*Scheme 3.6: Reaction of DBPM with a thiol group.* Thiol addition to the maleimide moiety of DBPM (**3.8**) yields a fluorescent product (**3.9**) with excitation and emission maxima at 355 nm and 457 nm respectively.

### 3.2.3.2.2 7-Diethylamino-3-(4-maleimidophenyl)-4-methylcoumarin (CPM)

Previous studies that have made use of CPM for the detection and quantification of CoA, among other biological thiols, have enjoyed great success.<sup>27,28</sup> Similar to other *N*-substituted maleimides, CPM contains a maleimide moiety as the reacting group but in this case the signalling group is a methylcoumarin moiety. Thiol group addition to the maleimido double bond (scheme 3.7) occurs very rapidly and derivatization is reportedly complete within 30 seconds if a 1.5-fold excess of CPM is used. The fluorescent adduct formed has a high quantum yield with excitation and emission maxima at 387 nm and 465 nm. Other favourable characteristics of CPM derivatives are their stability at room temperature and ambient light. Under these conditions the observed fluorescence of CPM derivatization products were reported to remain stable for several days.



*Scheme 3.7: Reaction of CPM with a thiol group.* Thiol addition to the maleimido double bond of CPM (**3.10**) yields a fluorescent product (**3.11**) with excitation and emission maxima at 387 nm and 465 nm respectively.

## 3.3 Objective of this study

From a review of the literature it was concluded that the derivatization of CoA and its thiol precursors with CPM followed by HPLC separation presented the best strategy for developing a novel method for quantification. The practical aspects surrounding derivatization and chromatographic separation will be discussed in detail in the results and

discussion section to highlight the factors that were found to be key to the development of a quantitative method. Here we report the simultaneous quantification of PanSH, PPanSH, DePCoA and CoA to meet the objective of performing the first time course analysis of the CoA salvage pathway reconstituted *in vitro*. This method was also applied to biological samples and CoA salvage intermediates were also measured in *E. coli* and *S. aureus*.

## 3.4 Results and Discussion

### 3.4.1 CPM derivatization of CoA and its thiol precursors

The desirable characteristics of CPM as a thiol probe were highlighted in the previous section but several factors relating to its reactivity, specificity and the stability of derivatives were encountered that affected its practical use in the proposed strategy for the quantification of the CoA salvage pathway intermediates. These factors are discussed in the following subsections.

#### 3.4.1.1 Reactivity of CPM

Reactivity of CPM with the thiols targeted for derivatization is crucial to ensure complete derivatization and accurate quantification. In this regard, the pH of samples to be derivatized was found to be of critical importance. CPM does not react with free thiols at an acidic pH but requires a near neutral environment for optimal reactivity. At higher pH levels it has been reported that hydrolysis of the maleimide moiety can occur before derivatization takes place. Hence the pH has to be closely controlled in the preparation of samples to be derivatized with CPM. This is not so trivial if the source of reaction- and biological samples are considered. Acids are often used for the rapid quenching of *in vitro* reactions when collecting time course samples as well as in biological extraction solutions. Therefore it is important to incorporate the neutralization of samples into the workflow of sample preparation.

#### 3.4.1.2 Specificity of CPM

Complete derivatization of thiol metabolites also require that the thiols be in the free, reduced form because CPM is not reactive towards the oxidized disulfides. Particularly PanSH is known to readily oxidize to its disulfide, pantethine. Treating samples with a reducing agent is required to ensure all thiols are in the reduced form for complete derivatization. For this purpose tris(2-carboxyethyl) phosphine (TCEP) was selected because it is an effective reducing agent and only a small excess relative to the thiol/disulfide content is required compared to other commonly used reductants such as NaBH<sub>4</sub>, dithiothreitol (DTT), and β-mercaptoethanol (BME). In addition DTT and BME both also contain thiol groups that are derivatized by CPM to form fluorescent products. Due to the specificity of CPM for thiols it was surprising to find that fluorescent products were also formed with TCEP and NaBH<sub>4</sub> that do not contain thiol groups (Figure 3.1). Regardless of the type of reducing agent used, the background fluorescence is increased by the presence

of their CPM adducts and the onus falls to the chromatographic method to separate it from the compounds of interest.

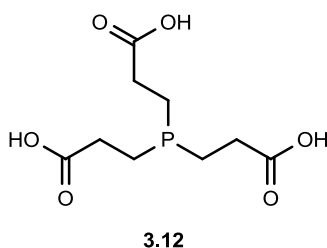
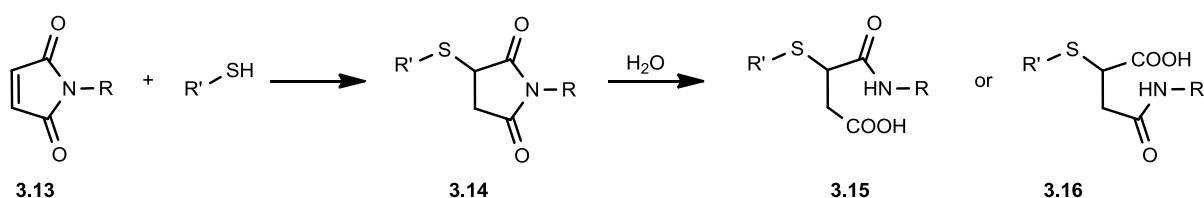


Figure 3.1: Structure of TCEP. TCEP (**3.12**) contains no reactive thiol groups but forms a fluorescent adduct with CPM.

### 3.4.1.3 Stability of CPM derivatives

It is known that the maleimide moiety of CPM-thiol adducts are unstable, undergoing hydrolysis to form two ring-cleaved fluorophores at the N-C=O position as shown in Scheme 3.8.<sup>25</sup> No effect on the fluorescence quantum yield of the coumarin signalling group has been reported following maleimide hydrolysis. However, the presence of both non-hydrolysed and hydrolysed forms leads to two peaks being observed for the CPM adduct in HPLC analysis. Prolonged incubation of derivatization reactions were found to ensure complete hydrolysis and elution of CPM derivatives in a single peak.



Scheme 3.8: Maleimide hydrolysis of CPM derivatives. The maleimide moiety of CPM adducts hydrolyse without affecting fluorescence. Incomplete hydrolysis of CPM derivatives leads to a mixture of two fluorophores with distinct chromatographic elution profiles.

### 3.4.2 Sample preparation for derivatization and analysis of CoA and its thiol precursors

Taking all the factors discussed in this section into consideration, we developed a general sample preparation method presented in Figure 3.2. Aliquots collected from a reaction mixture are quenched with 15% trichloroacetic acid (TCA) to precipitate proteins. In the case of biological samples, acetonitrile with 1 M formic acid is used for extraction. The reducing agent TCEP is also added to each sample to ensure that all thiols are in the reduced form.

Next, the samples are neutralized and precipitated proteins and cellular material are collected by centrifugation. The supernatant is removed and added to the derivatization reaction that contains 30% acetonitrile and one and a half times more CPM than its derivatization targets (thiols plus TCEP). The derivatization reaction is incubated overnight to ensure complete hydrolysis of CPM derivatives before analysis by HPLC. Each of these factors: reduction, neutralization and prolonged derivatization by CPM were central to obtaining consistent results to meet our objective of establishing a sensitive quantitative method.

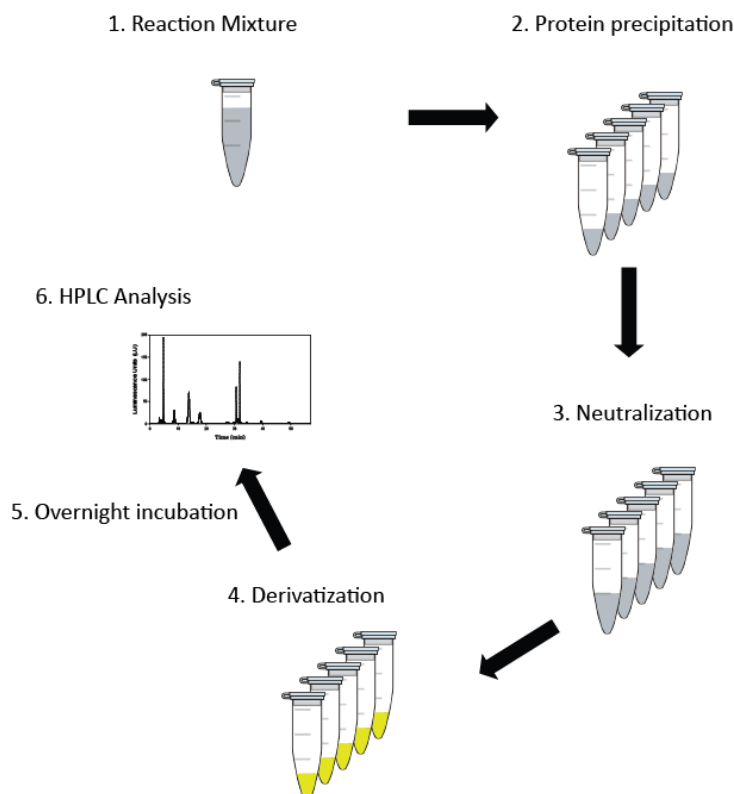


*Figure 3.2: Sample preparation for the analysis of CPM derivatives. Samples obtained by acid quenching of a reaction mixture or acidic biological extraction have to be neutralized to ensure successful derivatization. A prolonged incubation is further required to ensure that all CPM adducts are in the hydrolysed form so only one fluorophore is observed in HPLC analysis.*

### 3.4.3 Resolving the analytes of interest

The next step towards quantification of the analytes is chromatographic separation by HPLC. Our strategy was to identify the column stationary phase best capable of retaining CPM derivatized compounds so that their elution can be manipulated by a mobile phase gradient. A reverse phase column with a di-phenyl bonded phase was selected because it exhibits superior retention of aromatic groups compared to the more common C18 phase. Pi-pi

interactions between stationary phase phenyl groups and the aromatic groups in the coumarin moiety permit retention of a variety of CPM derivatives.

Next, the structures and chemical properties of the four analytes of interest in our study were inspected as they represent the variable part of the structure of CPM adducts to be resolved. Among the four metabolites the variable number of phosphate groups and pyrophosphate moieties account for the most important determinant of differences in polarity between them. PanSH has no ionizable groups whereas PPanSH has one phosphate group with two ionizable groups. DePCoA on the other hand has one pyrophosphate moiety which also contains two ionizable groups. CoA has both a phosphate group and a pyrophosphate moiety, giving it a total of four ionizable groups. Conversely, the adenosine moieties of DePCoA and CoA add to the hydrophobicity of the CPM adducts which are already rich in aromatic groups.

These differences in polarity and hydrophobicity can be quantitatively assessed by calculating the specific partition coefficient ( $P$ ) for each analyte of interest.<sup>29</sup> The log of the calculated octanol/water partition coefficient,  $\text{clog}P$ , for the analytes were calculated using the Calculator Plugin for partitioning of Marvin Sketch and are presented in Table 3.1. Hydrophobicity is directly proportional to these values, *i.e.* the larger the value, the more hydrophobic the compound. Since analytes elute in order of increasing hydrophobicity in reverse phase chromatography, these values also served as an indication of the elution order and what mobile phase conditions would be required to resolve them. CoA and DePCoA derivatives display considerably lower  $\text{clog}P$  values than PanSH and PPanSH indicating that a lower organic solvent content in the mobile phase would be required for their elution. In contrast, the high values calculated for the PanSH- and PPanSH-CPM adducts indicate that these analytes should be strongly retained in a reverse phase system and would require a much higher proportion of organic solvent in the mobile phase for elution.

*Table 3.1: Calculated log partition coefficients of CoA salvage intermediates.\**

Compound	PanSH	PPanSH	DePCoA	CoA
<b>clogP</b>	1.98	1.86	0.24	0.12

\* Partition Calculator Plugin was used for  $\text{clog}P$  calculation, Marvin 6.0.2, 2013, ChemAxon (<http://www.chemaxon.com>)

Taking these findings together, a gradient HPLC method was developed to separate the analytes of interest; this method is presented schematically in Figure 3.3. A ternary solvent system consisting of 50 mM potassium phosphate buffer (pH 6.8), 60% acetonitrile and 100% acetonitrile was employed.

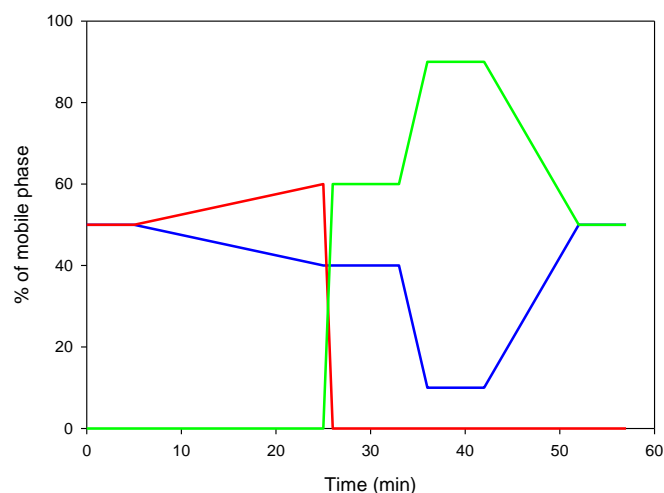


*Figure 3.3: Gradient method for elution of CPM derivatized intermediates of the CoA salvage pathway. A ternary solvent system was employed consisting of 50 mM potassium phosphate buffer, pH 6.8 (in blue —), 60% acetonitrile (in red —) and 100% acetonitrile (in green —).*

Analyte standards for HPLC method development were prepared by treating commercial standards by the same five steps as described in Figure 3.2. Pure PPanSH could not be obtained commercially, and therefore its standard was prepared by phosphorylation of PanSH by purified PanK. The retention time (Rt) of each analyte was established by separately injecting CPM-derivatized standards. Successful separation from one another as well as the TCEP based background was accomplished. A typical chromatogram resulting from the sample preparation and analysis methods described in this section is shown in Figure 3.4. An unidentified compound with a Rt of 15.8 minutes was also present in the chromatogram, and was thought to be cysteine. This was confirmed by the derivatization and analysis of a cysteine standard as the Rt was found to correspond with that of the unidentified peak. The quantification strategy employed to relate the integrated peak areas to analyte concentrations is detailed in the following section.

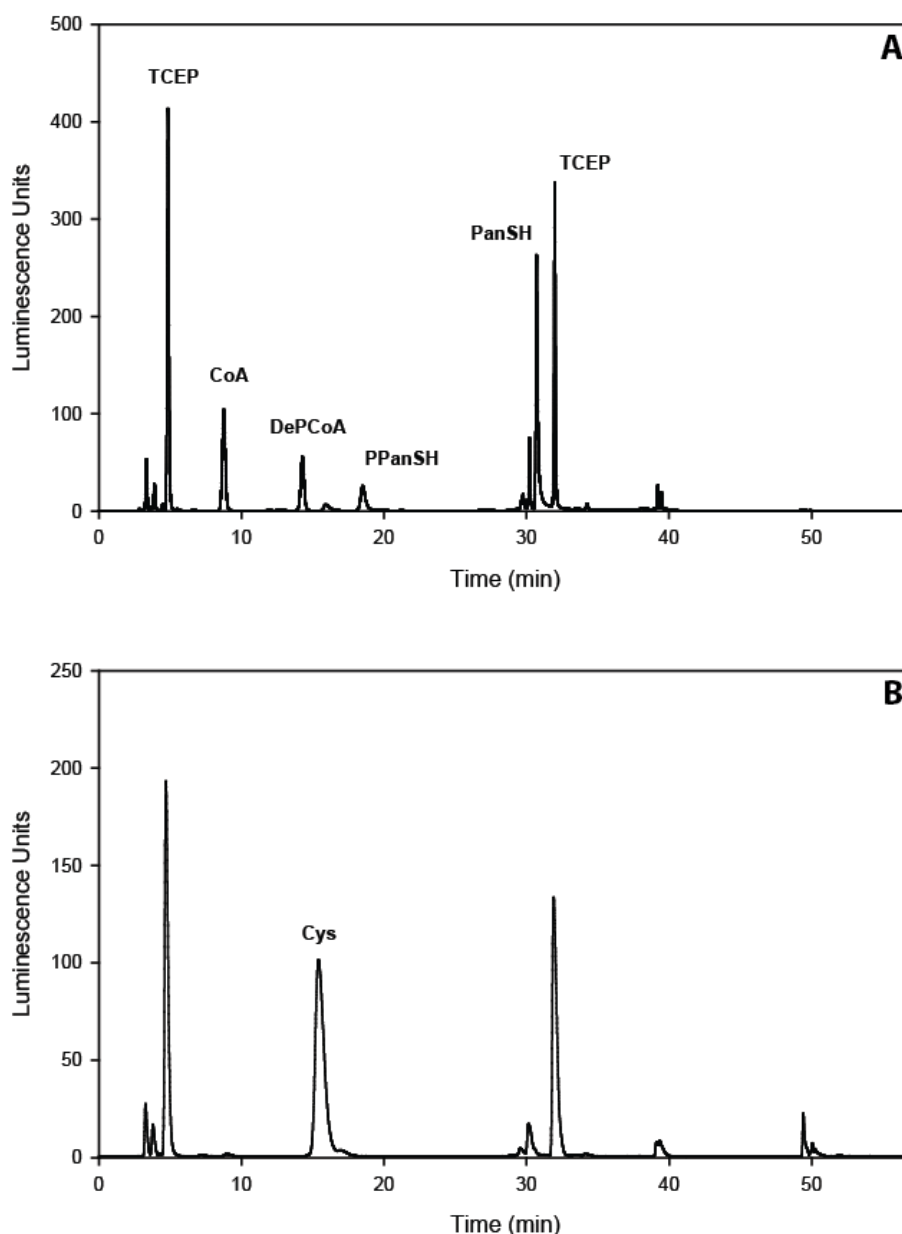


**Figure 3.4: Chromatographic analysis of CPM derivatized thiols. A** A typical chromatogram resulting from the sample preparation and analysis method described in this section. The analytes of interest are resolved from the TCEP based background which elute as multiple peaks between 3.3 and 4.4 minutes as well as at 29.7, 30.2 and 31 minutes. CoA elutes first at 8.7 minutes followed by DePCoA at 14.2 minutes. PPanSH elutes at 18.5 minutes and PanSH in between TCEP related peaks at 30.7 minutes. An unidentified peak eluted at 15.8 minutes, thought to be the CPM derivative of cysteine. **B** CPM derivatized cysteine standard. The  $R_t$  of cysteine corresponded to the  $R_t$  of the unidentified peak in panel A.

### 3.4.4 Quantification strategy

Three different methods are generally used for the quantification of analytes from chromatographic peak areas, *i.e.* the standard addition method, the internal standard

method and the external standard or calibration method. The most suitable approach is determined by the practicality of its application and the resulting accuracy. Both the standard addition method and the internal standard method were deemed to be unsuitable for practical application in this study, albeit for different reasons which will be discussed briefly.

The standard addition method requires two steps for the quantification of analytes. The sample mixture containing the unknown amount of analyte is analysed after which a known amount of the analyte of interest is added to the sample before a second round of analysis is performed. The resulting increase in peak area is proportional to the amount of analyte that was added and hence allows for the unknown concentration of the analyte in the original sample to be calculated. This method is impractical for this study due to low availability of specifically PPanSH and the high cost that would result from adding commercially available standards to every sample. Also, two analysis steps are not ideal if a large number of samples have to be analysed in an experimental setup such as time course analysis of CoA salvage biosynthesis.

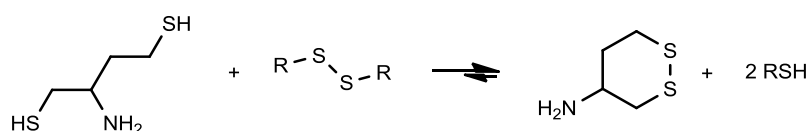
The internal standard method has found widespread application and is a very useful technique for performing quantitative chromatographic analyses. This method requires that a known quantity of a reference standard be added to all samples before analysis. The ratio of peak areas of the unknowns relative to that of the internal standard can then be used to calculate unknown concentrations. Success of the internal standard method heavily depends on the availability of a suitable compound that can be used as the internal standard. In this case it would have to be a thiol compound that can be derivatized with CPM to yield a fluorescent product that does not co-elute or overlap with any other analyte in the sample and is not present in biological samples. Due to multiple peaks already present in the chromatograms for the analytes of interest in this study as well as the TCEP based background it was concluded that the standard addition method was not ideal as it would convolute results.

The external standard or calibration method was selected for quantification of analytes in this study. It requires that a calibration curve of peak area vs. concentration be set up for each analyte of interest. These calibration curves have to exhibit a linear response over the concentration range where quantification of unknowns is expected, because fluorescence quenching can occur at high concentrations leading to inaccurate quantification. The slope of each calibration curve is determined by linear regression and subsequently used for quantification of the respective analytes. This method was favoured due to its simplicity in the sense that a calibration curve has to be set up once and can then be used for numerous

subsequent analyses of unknown samples until eventual column aging necessitates a repeat. Standardization of analyte calibration standards also proved to be vital for accurate quantification and the manner in which this was achieved will be discussed in the following section.

### 3.4.4.1 Standardizing the concentrations of the external standards

Standardizing calibration standards by an independent method is essential for accurate quantification. The DTNB assay outlined in section 3.2.1 was selected as the independent method whereby this could be achieved because it is a simple and widely-used thiol quantification assay. Additionally, for the purpose of standardization the various analytes would be assayed separately, meaning that the assay in question would not have to differentiate between the analytes. However, the reducing agent TCEP was found to react with DTNB, leading to very high levels of background absorbance. It was therefore necessary to remove the reducing agent from the sample immediately before derivatization. This was done in a manner similar to the method developed by Lukesh *et al.*<sup>30</sup> TCEP was replaced as reducing agent by dithiobutylamine (DTBA), a structural analogue of DTT but with a free amine group (Scheme 3.9). It is this amine group that allows for the effective removal of both oxidised and unreacted DTBA from the sample mixture by cation exchange chromatography before quantification by the DTNB assay. Following independent standardization of the analyte standard solutions, they were used to establish calibration curves for the four analytes of interest in this study.



*Scheme 3.9: Disulfide reduction by DTBA.* DTBA is an effective reducing agent with a free amine group and both free and oxidized forms can be removed by cation exchange chromatography.

### 3.4.4.2 Preparing calibration curves of analyte standards

Metabolite standards were prepared in the concentration range of 9.7 – 218.4 pmol and analysed in triplicate to establish calibration curves (Fig. 3.5). A linear response was observed in this concentration range and linearity was assessed by linear regression. The resulting  $R^2$  values, which ranged from 0.995 to 0.999, are reported in Table 3.2. The equations of the straight lines obtained from the linear regression analysis were

subsequently used to convert the relative fluorescence units of analyte peak areas obtained in the analysis of unknown samples to the corresponding metabolite concentration.

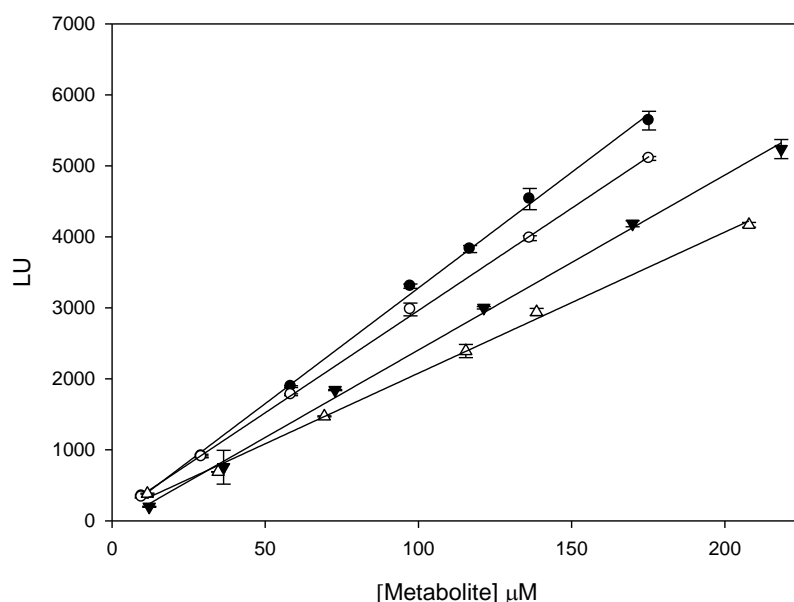


Figure 3.5: Calibration curves of CPM derivatives of ● PanSH, ○ PPanSH, ▼ DePCoA, Δ CoA. All data points represent the mean of triplicate values, with the error bars denoting the standard deviation. Where errors are not visible they are smaller than the symbol.

Table 3.2: Linear regression parameters of the calibration curves. Errors denote the standard deviation in the regression parameters determined for seven calibration levels, in triplicate.

Metabolite	Calibration	R <sup>2</sup>
PanSH	$y = (32.58 \pm 0.39) x + (21.91 \pm 40.41)$	0.997
PPanSH	$y = (28.81 \pm 0.23) x + (81.34 \pm 24.05)$	0.999
DePCoA	$y = (24.64 \pm 0.43) x - (58.34 \pm 54.22)$	0.995
CoA	$y = (19.88 \pm 0.30) x - (91.14 \pm 35.50)$	0.997

### 3.4.5 Method validation

Analytical figures of merit were calculated according to the International Conference on Harmonization (ICH) guidelines for the validation of analytical procedures.<sup>31</sup> The consistency in  $R_t$ , limits of detection (LOD), limits of quantification (LOQ), accuracy and precision of the newly developed method was assessed and data is shown in Table 3.3. The standard deviation in  $R_t$  reported was calculated from at least three different concentrations analysed in triplicate ( $N = 9$ ).  $R_t$ 's did not vary by more than eight seconds with the exception of DePCoA where the  $R_t$  varied by 31 seconds. LOD and LOQ were calculated by considering  $\sigma$ , which is the residual standard deviation of the regression line. Based on a 95% confidence level, the LOD is usually calculated as  $3.3 \sigma$  divided by the slope of the regression line and LOQ as  $10 \sigma$  divided by the slope. LOD and LOQ values for all CoA salvage pathway intermediates were calculated from the calibration curves in this manner. LOD values were found to be in the range of 6.27–16.44 pmol and LOQ values were in the range of 19–50 pmol. Commercially available kits that specifically measure CoA such as ELISA by BioSource and Amplite by AAT Bioquest, claim the lowest LOD for CoA, reported by the suppliers as 18.3 fmol and 4 pmol respectively. CoA has also been determined by derivatization with SBD-F with a reported LOD of 120 pmol.<sup>18</sup> Coulier *et al.* has reported a LOD value for CoA measured by a LC-MS based technique of 1.3 nmol.<sup>16</sup> We also evaluate our results against detection methods for CoA esters and our LOD and LOQ values compare well with values reported for the detection of short- and long chain CoA species by HPLC methods which range from 3–12 pmol.<sup>32,33,34,35</sup> MS-based techniques have proven more sensitive for the detection of CoA esters and reported LOD values range from 10 fmol to 0.5 pmol.<sup>36,37,38,39,40</sup>

Accuracy is evaluated based on the % recovery of at least nine determinations representing three concentration levels, determined in triplicate. Similarly, precision is assessed based on repeatability where at least nine determinations covering the concentration range are analysed and the coefficient of variation % calculated. All analytical figures of merit were found to be within the acceptable range for accurate determination of metabolite concentrations.

Table 3.3: Analytical figures of merit for the newly developed quantitative method

Parameter	PanSH	PPanSH	DePCoA	CoA
SD in Rt (min)	0.12	0.09	0.51	0.08
LOD (pmol)	9.40	6.33	16.44	12.30
LOQ (pmol)	28.49	19.19	49.82	37.28
Precision: Repeatability CV %	1.90	1.43	1.26	1.11
Accuracy: Recovery %	99.91	98.47	100.59	99.57

### 3.4.6 Measuring intermediates of CoA salvage in *E. coli* and *S. aureus*

The newly developed method was used to measure the intracellular concentration of CoA and its precursor metabolites in *Escherichia coli* and *Staphylococcus aureus*, representing Gram-negative and Gram-positive bacteria respectively. Cells were harvested in stationary phase as described in the methods section. Cold acidic acetonitrile was used to lyse cells and precipitate proteins to quench metabolism followed by neutralization and CPM derivatization. Due to the large variation in the intracellular concentration among metabolites, different volumes of the derivatized extract were analysed to ensure accurate quantification of each metabolite in the linear range. The amount of each metabolite measured is reported as nmol/g dry cell weight (dcw) and is shown in Table 3.4. For *S. aureus*, values range from 44.47 nmol/g dcw for PanSH to 658.19 nmol/g dcw for CoA.

The most notable result here is the detection of PanSH in *S. aureus* at levels above the LOQ. It was previously suggested that *S. aureus* does not contain PanSH and that it does not make use of the CoA salvage pathway. *S. aureus* contains an atypical type II PanK that does not readily phosphorylate PanSH. The presence of PanSH in *S. aureus* is therefore very intriguing. A typical chromatogram resulting from cell extract analysis is shown in Figure 3.6, panel A. In addition to the CoA-related analytes of interest, an additional unidentified peak eluted at 10.5 minutes. To determine the identity of the compound corresponding to this Rt, standards of other biologically-relevant thiols were analysed using the same protocol. In this manner it was found that the Rt of glutathione (GSH) corresponds to the peak at 10.5 minutes (see panel C, Figure 3.8). It was surprising that GSH was also detected since *S. aureus* does not have the biosynthetic machinery to produce it *de novo*. However GSH

*Table 3.4: Determination of the amount of intracellular CoA and CoA salvage intermediates in S. aureus RN4220 and E. coli K12. Values for S. aureus represent the mean of triplicate derivatization reactions and analyses with the standard deviation as error. In E. coli only PPanSH and CoA could be quantified and the values reported are for a single determination.*

Analyte	<i>S. aureus</i> (nmol/g dcw)	<i>E. coli</i> (nmol/g dcw)
PanSH	44.47 ± 3.88	-
PPanSH	146.44 ± 5.40	151.15
DePCoA	155.62 ± 1.89	-
CoA	658.19 ± 4.25	293.12

import was confirmed by Pöther *et al.* where it was found that intracellular accumulation of GSH occurs after GSH-supplementation of chemically defined culture medium.<sup>41</sup> It was also found that in tryptic soy broth (TSB) media *S. aureus* starts to accumulate GSH in the post-exponential phase with increasing levels in the stationary phase. The TSB culture medium in which the cells were grown therefore likely acts as the source of GSH; however, it should be pointed out that GSH transport system capable of importing this molecule is not known to exist in *S. aureus*.

The same extraction and analysis method was also tested on *E. coli* cells. CoA and PPanSH could be successfully quantified with PPanSH found at a similar level of 151.15 nmol/g cdw compared to the PPanSH detected in *S. aureus*. CoA was detected at 293.12 nmol/g cdw which is less than half the CoA content measured in *S. aureus*. In order to compare the CoA content measured in *E. coli* with values reported in previous studies, the amount of CoA per cdw was converted to concentration by employing the ratio of aqueous cell volume to cellular dry weight for *E. coli* of 0.0023 L/g.<sup>42</sup> The intracellular concentration of CoA is calculated as 127.44 µM in this study. In a similar range, the intracellular CoA concentration of exponentially growing *E. coli* cultures with different carbon sources (glucose, acetate and glycerol) have been reported between 56 and 108 µM.<sup>43</sup> However, a more recent study has reported exponentially growing *E. coli* cultures to contain between 1.37 mM and 4.54 mM CoA, depending on the carbon source (glucose, acetate and glycerol).<sup>15</sup> The values reported by the latter study are high considering that the total CoA pool (including CoA esters) is reported to be 500 µM.<sup>43</sup>

PanSH was also detected in *E. coli* above the LOD but below the LOQ and therefore it could not be quantified. GSH is known to be the major low molecular weight thiol in *E. coli* and therefore a large peak was expected at 10.5 minutes. It was found that the GSH content of *E. coli* cells is so high, compared to CoA and its precursors, that it overlaps with the DePCoA peak preventing its accurate quantification. It is important to keep this in mind if cell extracts are analysed that contain high levels of GSH. A solution to this problem may be to treat these cell extracts with glutathione S-transferase (GST) and 1-chloro-2,4-dinitrobenzene (CDNB). GST will conjugate CDNB to the thiol group of GSH specifically and it will no longer react with CPM to produce an interfering background signal.

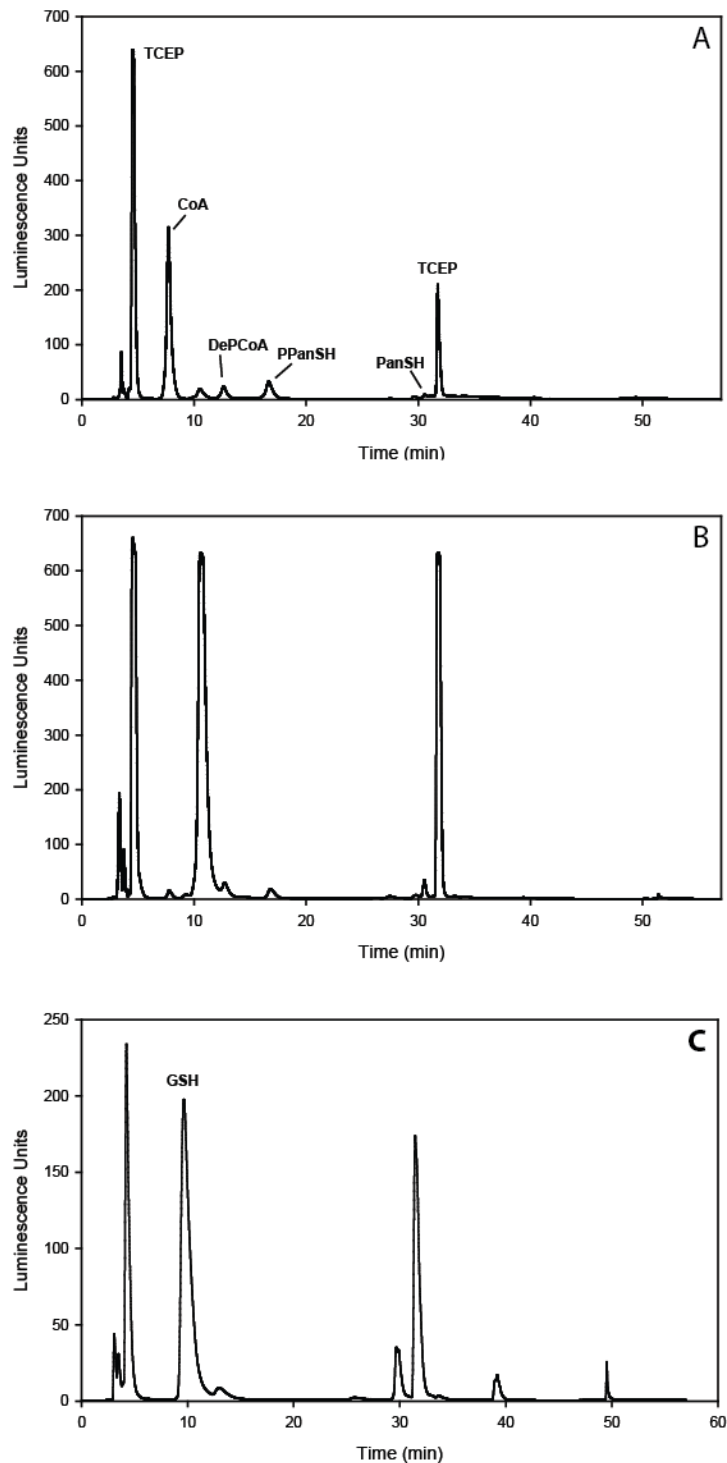


Figure 3.6: Chromatographic analysis of CPM derivatized intermediates of CoA salvage. Emission of fluorescent derivatives was detected at 465 nm with excitation at 387 nm. **A** Intracellular thiol metabolites of *S. aureus*. In addition to CoA and precursor metabolites, an unconfirmed thiol thought to be glutathione (GSH) eluted at 10.5 min. **B** Intracellular thiol metabolites of *E. coli*. CoA and precursor metabolites were detected in much lower abundance than glutathione. **C** Derivatized GSH standard. The  $R_t$  of derivatized GSH corresponds to the unconfirmed thiol metabolite eluting at 10.5 min in *S. aureus* and *E. coli* cell extracts.

### 3.4.7 Application of the method for time course analysis of CoA salvage biosynthesis

The newly developed method for the quantification of CoA salvage pathway intermediates was applied to perform the first time course analysis of CoA salvage biosynthesis by reconstituting the pathway *in vitro*. Reconstitution was achieved by adding 900  $\mu\text{M}$  PanSH to a mixture containing 0.1  $\mu\text{g}/\mu\text{l}$  pure (as confirmed by SDS-PAGE analysis, see Figure 3.7) PanK, PPAT and DPCK. Also present in the mixture was 5 mM ATP, 0.04 U/ $\mu\text{l}$  with pyruvate kinase and 1.8 mM phosphoenolpyruvate (PEP) to recycle ADP, as well as 1.75 mM TCEP, 10 mM  $\text{MgCl}_2$  and 20 mM KCl in 50 mM Tris-HCl buffer pH 7.6. The mixture was incubated at 37°C and at various time points aliquots were removed and quenched by TCA precipitation of the enzymes. These samples were subsequently prepared and analysed according to the newly developed method. Finally, the calibration curves were used to calculate the concentration of each intermediate at every time point to yield the time course shown in Figure 3.8. To evaluate the robustness of the method we calculated the sum of all intermediates measured at every time point and then determined the mean for all the time points as  $857 \pm 43 \mu\text{M}$ . The error denotes standard deviation of the sum of intermediates between 21 time points. The sum of intermediates is expected to be 900  $\mu\text{M}$  at every time point and by taking the total we calculate the measured total as a percentage of the expected total to find that  $95.2 \pm 4.8\%$  of the expected total is recovered. This demonstrates that the method can effectively measure changing levels of every intermediate.

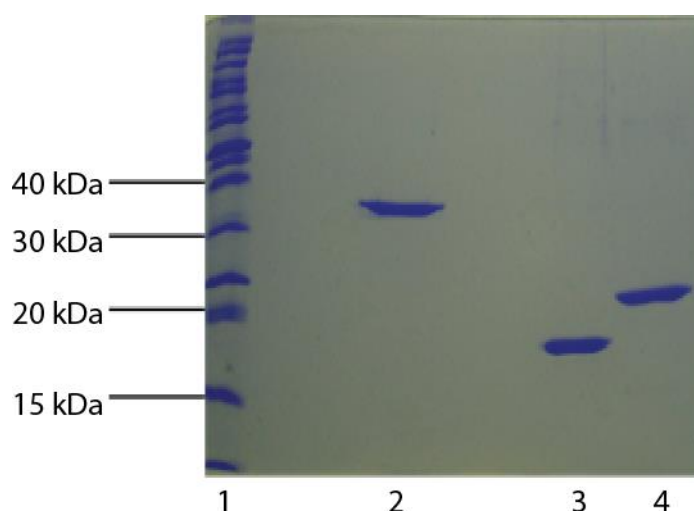
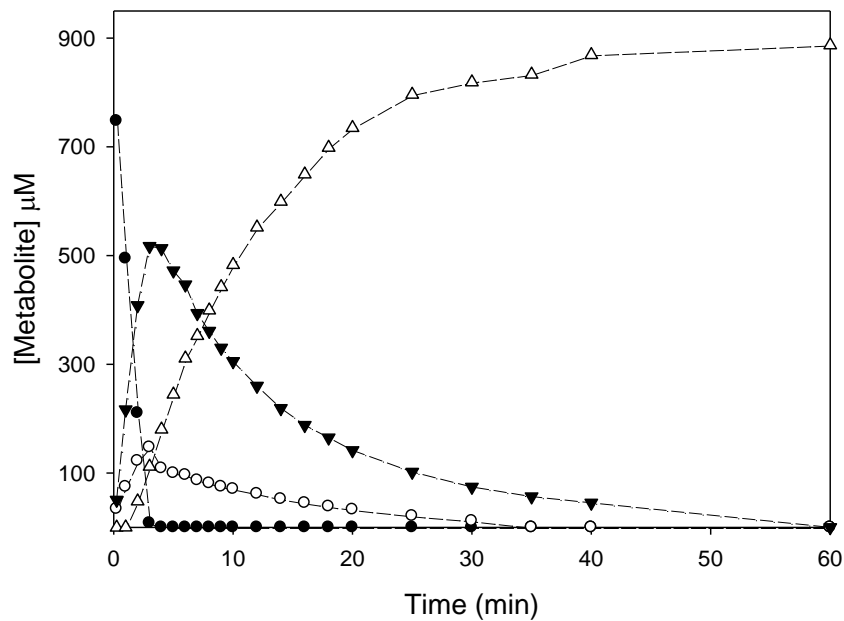


Figure 3.7 SDS-PAGE analysis of purified CoA salvage enzymes. 1) Molecular weight marker; 2) PanK (38 kDa); 3) PPAT (19 kDa); DPCK (24 kDa). All protein bands corresponded to the expected enzyme molecular weight.



*Figure 3.8: Time course analysis of CoA salvage biosynthesis as performed by the in vitro reconstituted CoA salvage pathway. ● PanSH, ○ PPanSH, ▼ DePCoA, Δ CoA. The CoA salvage pathway was reconstituted by addition of the 0.1 μg/μl pure PanK, PPAT and DPCK enzymes to a reaction mix containing 900 μM PanSH, 5 mM ATP, 0.04 U/μl with pyruvate kinase, 1.8 mM phosphoenolpyruvate (PEP), as well as 1.75 mM TCEP, 10 mM MgCl<sub>2</sub> and 20 mM KCl in 50 mM Tris-HCl buffer pH 7.6. The reaction was incubated at 37°C and aliquots were collected over the course of 60 minutes. Aliquots of the reaction mix were removed at various time points and quenched and derivatized with CPM prior to analysis by the HPLC method developed. The standard curve for each metabolite was used to relate peak area to the concentration of the metabolite in each aliquot.*

### 3.5 Conclusion

A method was developed for the quantification of the CoA salvage intermediates, PanSH, PPanSH, DePCoA and CoA. Existing methods were found to be inadequate or impractical for quantitative analysis of a mixture of these compounds. The best approach for the development of a quantitative method was deemed to be derivatization with the fluorescent thiol probe CPM and subsequent HPLC analysis with quantification by standard calibration curves.

Two factors were found to be important for the successful derivatization of intermediates by CPM. First, sample treatment with TCEP ensured that any intermediates in the oxidized disulfide form were reduced and free to bind CPM for complete derivatization. Second, a neutralization step is required prior to the addition of CPM to avoid incomplete derivatization at lower pH.

A HPLC method was developed to separate the derivatized analytes by employing a reverse phase di-phenyl column and a ternary solvent system consisting of potassium phosphate buffer, 60% acetonitrile and 100% acetonitrile. For successful separation of the analytes a prolonged incubation of the derivatization reaction was required to ensure that each analyte of interest eluted as a single peak. Derivatized analytes were successfully resolved by a gradient method with an increasing acetonitrile component in the mobile phase.

The quantification of derivatized intermediates was achieved by standard calibration curves. LOD's and LOQ's were calculated indicating suitable sensitivity for the purpose of this study. The method was assessed for repeatability and accuracy and the analytical figures of merit reported were satisfactory.

The method developed proved to be successful for the purpose of tracing metabolite concentrations when the CoA salvage pathway was reconstituted *in vitro* to yield the first time course of the pathway. The method was also successfully used to measure the intracellular concentrations of CoA and its precursor metabolites in *S.aureus*.

In conclusion, CoA salvage intermediates can now be quantified in a mixture for the first time. This method will aid various future studies on the biocatalytic production of CoA and CoA metabolism, especially systems biology orientated studies aimed in identifying the regulatory events that govern CoA homeostasis in different organisms.

## 3.6 Experimental procedures

All chemicals and solvents were purchased from either Fluka or Sigma-Aldrich and were of the highest purity. Expression vectors and competent cell strains (BL21, *E. coli*) for overexpression were purchased from Novagen. HiTrap™ chelating columns for protein purification were from Amersham Biosciences. All protein purifications were performed on a ÄKTAprime protein purification system. The Quick Start Bradford Protein Assay Kit (Bio-Rad) containing Bradford reagent and a Bovine Serum Albumin standard set was used for protein determinations. Large scale centrifugation was carried out in a Beckman Coulter Avanti J-26 XPI centrifuge. Medium scale centrifugation was carried out in a Heraeus Multifuge 3S/3S-R centrifuge. Small scale centrifugation was performed on a Heraeus Biofuge pico centrifuge.

### 3.6.1 Overexpression and purification of CoA salvage pathway proteins

To reconstitute the CoA salvage pathway, pure PanK, PPAT and DPCK enzymes were obtained by overexpression of the respective *E. coli* genes *coaA*, *coaD* and *coaE* contained in available pET-28a(+) expression vectors.<sup>44,45</sup> The gene sequence of the plasmids have been checked and are available from Addgene (plasmid # 50386, 50388 and 50390) The base vector encodes an N-terminal histidine tag that allows for nickel based immobilised metal affinity chromatography (IMAC) after overexpression. Overexpression and purification was done as previously reported.<sup>46</sup> Glycerol was added to purified fractions to a final concentration of 5%. Protein stocks were divided into 50 µl aliquots and stored at -80°C.

### 3.6.2 CoA salvage reactions, quenching and sample treatment

Reconstituting the CoA salvage pathway *in vitro* entailed the addition of the starting substrate PanSH to a reaction mixture containing PanK, PPAT and DPCK enzymes along with an excess of ATP. A 10 mM PanSH stock solution was prepared by a 10 min reduction reaction of 5 mM pantethine with 7.5 mM TCEP. The CoA salvage pathway reaction mix contained 50 mM Tris-HCl buffer (pH 7.6), 10 mM MgCl<sub>2</sub>, 20 mM KCl, 5 mM ATP, 1.75 mM TCEP, 0.04 U/µl pyruvate kinase, 1.8 mM phosphoenolpyruvate (PEP) and 0.1 µg/µl each of PanK, PPAT and DPCK respectively in a total reaction volume of 1 ml. The reaction was initiated by the addition of PanSH to a final concentration of 900 µM. The reaction mixture was incubated at 37°C for 60 minutes and mixed by rotation. During incubation, 50 µl aliquots were removed from the reaction mixture at various time points and added to 10 µl TCA for precipitation of the proteins to quench the reaction. The 60 µl acid precipitation mixture contained 15% TCA, and the precipitation reaction was incubated for 10 min at 4 °C. Following acid precipitation, the 60 µl mixture was neutralized by the addition of 40 µl 2.75 M

ammonium acetate. The precipitated proteins were removed by centrifugation at  $10\,000 \times g$  for 10 min.

Metabolites in neutralized samples were derivatized with CPM in reaction mixtures that contained 30% MeCN and a total concentration of  $45\ \mu\text{M}$  metabolites and  $67.5\ \mu\text{M}$  TCEP from the reaction mixture. The derivatization mix also contained  $187.5\ \mu\text{M}$  CPM and was incubated overnight at room temperature to ensure complete derivatization. In order to set up calibration curves, standard solutions of PanSH, PPanSH, DePCoA and CoA were prepared respectively.

### 3.6.3 Standardization of standards

The concentration of PanSH, DePCoA and CoA standards were determined according to the method of Lukesh *et al.*<sup>30</sup> First, the metabolite standards were treated with the reducing agent dithiobutylamine (DTBA) to ensure all thiols were in the reduced form so that the concentrations could be measured with DTNB after removal of DTBA. The reduction reaction contained  $500\ \mu\text{M}$  of the standard and  $500\ \mu\text{M}$  DTBA in a total volume of  $280\ \mu\text{l}$  made up with DTNB assay buffer ( $0.1\ \text{M}$  sodium phosphate buffer, pH 8 and  $1\ \text{mM}$  EDTA). The reaction was incubated at room temperature for 15 minutes to allow for complete reduction. DTBA contains two free thiol groups and will also react with DTNB and therefore had to be removed after the reduction reaction. This was accomplished by the addition of  $7\ \text{mg}$  Dowex 50WX4-400 cation exchange resin to the reduction reaction. The mixture was swirled for 5 minutes before the resin with DTBA bound was removed by centrifugation at  $10\,000 \times g$  for 1 minute.  $25\ \mu\text{l}$  of the reduced sample was immediately added to the DTNB assay mixture and incubated at room temperature for 15 minutes. The DTNB assay mixture consisted of  $250\ \mu\text{l}$  reaction buffer and  $5\ \mu\text{l}$  DTNB reagent solution. The DTNB reagent solution was prepared by the addition of  $4\ \text{mg}$  DTNB to  $1\ \text{ml}$  reaction buffer. The TNB produced by the reaction of DTNB with free thiols was measured spectrophotometrically at  $412\ \text{nm}$  and quantified using an extinction coefficient of  $14\,150\ \text{M}^{-1}\text{cm}^{-1}$  to determine the thiol content in the metabolite standard.<sup>47</sup>

### 3.6.4 Calibration curves of analyte standards

Metabolite standards for HPLC calibrations were prepared in the same manner as described for the salvage pathway samples, with only the enzymes being omitted from the reaction mixture prior to acidification, neutralization, and derivatization. Calibration standard solutions were prepared in triplicate in the range of  $2.5$  to  $45\ \mu\text{M}$  of the respective metabolites. PPanSH standards were prepared by allowing a phosphorylation reaction of PanSH by

PanK to run to completion (confirmed by HPLC analysis) and dilution of the PPanSH produced to the appropriate standard concentrations. The PanK reaction mixture contained 900  $\mu\text{M}$  PanSH, 5 mM ATP, 1 mM TCEP, 0.1  $\mu\text{g}/\mu\text{l}$  PanK in a total volume of 1 ml and was incubated for 20 minutes.

### 3.6.5 Extraction and derivatization of CoA salvage intermediates in *E. coli* and *S. aureus*

The extraction of CoA salvage intermediates was performed similarly for both *S. aureus* RN4220 and *E. coli* K12 with the exception that *S. aureus* was cultured in 500 ml TSB and *E. coli* in 500 ml LB media, both at 37°C with shaking. Cells were harvested in stationary phase ( $\text{OD}_{600} = 1.75$ ) by the removal of 100 ml culture from the main culture and then split into two 50 ml aliquots where one was used for dry cell weight determination and the other for metabolite extraction and derivatization. Both 50 ml culture aliquots were centrifuged at 4500 x g and 4°C for 20 minutes to remove growth media. Cells were washed twice to remove residual media by resuspension in 50 ml ice cold PBS followed by centrifugation under the same conditions. The cell pellet used for dry cell weight determination was dried on a SpeedVac system until constant weight was recorded, normally after 18-20 hours. Cells earmarked for metabolite extraction were resuspended in ice cold extraction solution consisting of 80% MeCN and 0.1 M formic acid in water using a ratio of 50  $\mu\text{l}$  extraction solution per 20 mg wet cells harvested. The extraction mixture was shaken at 4°C for 30 minutes to complete cell lysis and metabolite extraction. Next, cell debris was removed from the cell extract by centrifugation at 4°C and 10 000 x g for 15 minutes. The supernatant was then filtered by centrifugation through Nanosep 3K membrane filtration tubes for 10 min at 10 000 x g. The filtered cell extracts were neutralized and reduced prior to derivatization with CPM. The 140 $\mu\text{l}$  derivatization mixture consisted of 44.62  $\mu\text{l}$  cell extract, 50 mM Tris pH 7.6 and 1 mM TCEP that was incubated for 10 minutes at room temperature to ensure complete reduction of all disulfides. CPM was added last to a final concentration of 450  $\mu\text{M}$  and samples were incubated at room temperature overnight to ensure complete derivatization and maleimide hydrolysis.

### 3.6.6 HPLC analysis of CPM-derivatized CoA salvage intermediates

High performance liquid chromatography (HPLC) analyses were performed on an Agilent 1100 series system equipped with an in line FLD-fluorescence detector. Chromatograms were traced, generated, integrated and analysed with the software package Chemstation for LC, Rev. A.10.02[1757]. A Supelcosil LC-DP (250 x 4.60 mm, 5  $\mu\text{m}$  particle size) reverse phase column was used for analysis and was obtained from Supelco. The column was

protected by a Supelcosil LC-DP Supelguard cartridge obtained from Sigma-Aldrich. All graphical and statistical analyses were performed with SigmaPlot 11.0 (Systat Software, Inc.).

A 57 minute analysis method with a flow rate of 1 mL/min was used to analyse a 5 µl sample injection. A ternary solvent system was used that consisted of A) 50 mM potassium phosphate buffer, pH 6.8; B) 60 % acetonitrile (MeCN) and C) 100% MeCN. The method started with 50% A and 50% B and the following elution protocol was followed to achieve separation: 5 min isocratic, 50% A and 50% B; 20 min linear gradient, 40% A and 60% B; 1 min linear gradient, 40% A and 60% C; 6 min isocratic, 40% A and 60% C; 3 min linear gradient, 10 % A and 90% C; 6 min isocratic, 10% A and 90% C; 10 min linear gradient back to initial conditions, 50% A and 50% B; 5 min isocratic, 50% A and 50% B. Fluorescence was monitored as emission at 465 nm with excitation at 387 nm

### 3.7 References

1. Jackowski, S.; Rock, C. O., Regulation of coenzyme A biosynthesis. *J. Bacteriol.* **1981**, *148* (3), 926-932.
2. Theodoulou, Frederica L.; Sibon, Ody C. M.; Jackowski, S.; Gout, I., Coenzyme A and its derivatives: renaissance of a textbook classic. *Biochem. Soc. Trans.* **2014**, *42* (4), 1025-1032.
3. Tsuchiya, Y.; Pham, U.; Gout, I., Methods for measuring CoA and CoA derivatives in biological samples. *Biochem. Soc. Trans.* **2014**, *42* (4), 1107-1111.
4. Brown, G. M., Assay and Distribution of Bound Forms of Pantothenic Acid. *J. Biol. Chem.* **1959**, *234* (2), 379-382.
5. Molnos, J.; Gardiner, R.; Dale, G. E.; Lange, R., A continuous coupled enzyme assay for bacterial malonyl-CoA:acyl carrier protein transacylase (FabD). *Anal. Biochem.* **2003**, *319* (1), 171-176.
6. Allred, J. B.; Guy, D. G., Determination of coenzyme A and acetyl CoA in tissue extracts. *Anal. Biochem.* **1969**, *29* (2), 293-299.
7. Kato, T., CoA cycling: An enzymatic amplification method for determination of CoASH and acetyl CoA. *Anal. Biochem.* **1975**, *66* (2), 372-392.
8. Szutowicz, A.; Bielarczyk, H., Elimination of CoASH interference from acetyl-CoA cycling assay by maleic anhydride. *Anal. Biochem.* **1987**, *164* (2), 292-296.
9. Rootman, I.; de Villiers, M.; Brand, L. A.; Strauss, E., Creating Cellulose-Binding Domain Fusions of the Coenzyme A Biosynthetic Enzymes to Enable Reactor-Based Biotransformations. *Chemcatchem* **2010**, *2* (10), 1239-1251.
10. Grassetti, D. R.; Murray Jr, J. F., Determination of sulfhydryl groups with 2,2'- or 4,4'-dithiodipyridine. *Arch. Biochem. Biophys.* **1967**, *119* (0), 41-49.
11. Yamato, S.; Nakajima, M.; Wakabayashi, H.; Shimada, K., Specific detection of acetyl-coenzyme A by reversed-phase ion-pair high-performance liquid chromatography with an immobilized enzyme reactor. *J. Chromatogr. A* **1992**, *590* (2), 241-245.
12. Shibata, K.; Nakai, T.; Fukuwatari, T., Simultaneous high-performance liquid chromatography determination of coenzyme A, dephospho-coenzyme A, and acetyl-coenzyme A in normal and pantothenic acid-deficient rats. *Anal. Biochem.* **2012**, *430* (2), 151-155.
13. Kuipers, B. J. H.; Gruppen, H., Prediction of Molar Extinction Coefficients of Proteins and Peptides Using UV Absorption of the Constituent Amino Acids at 214 nm To Enable Quantitative Reverse Phase High-Performance Liquid Chromatography–Mass Spectrometry Analysis. *J. Agric. Food Chem.* **2007**, *55* (14), 5445-5451.

14. Bajad, S. U.; Lu, W.; Kimball, E. H.; Yuan, J.; Peterson, C.; Rabinowitz, J. D., Separation and quantitation of water soluble cellular metabolites by hydrophilic interaction chromatography-tandem mass spectrometry. *J. Chromatogr. A* **2006**, *1125* (1), 76-88.
15. Bennett, B. D.; Kimball, E. H.; Gao, M.; Osterhout, R.; Van Dien, S. J.; Rabinowitz, J. D., Absolute metabolite concentrations and implied enzyme active site occupancy in *Escherichia coli*. *Nat. Chem. Biol.* **2009**, *5* (8), 593-599.
16. Coulier, L.; Bas, R.; Jespersen, S.; Verheij, E.; van der Werf, M. J.; Hankemeier, T., Simultaneous Quantitative Analysis of Metabolites Using Ion-Pair Liquid Chromatography–Electrospray Ionization Mass Spectrometry. *Anal. Chem.* **2006**, *78* (18), 6573-6582.
17. Yamato, S.; Sugihara, H.; Shimada, K., Enzymic assay of chloramphenicol coupled with fluorescence reaction. *Chem. Pharm. Bull.* **1990**, *38* (8), 2290-2292.
18. Imai, K.; Toyo'oka, T.; Watanabe, Y., A novel fluorogenic reagent for thiols: Ammonium 7-fluorobenzo-2-oxa-1,3-diazole-4-sulfonate. *Anal. Biochem.* **1983**, *128* (2), 471-473.
19. Toyo'oka, T.; Imai, K., High-performance liquid chromatography and fluorometric detection of biologically important thiols, derivatized with ammonium 7-fluorobenzo-2-oxa-1,3-diazole-4-sulphonate (SBD-F). *J. Chromatogr. A* **1983**, *282* (0), 495-500.
20. Srinivasan, B.; Baratashvili, M.; van der Zwaag, M.; Kanon, B.; Colombelli, C.; Lambrechts, R. A.; Schaap, O.; Nollen, E. A.; Podgorsek, A.; Kosec, G.; Petkovic, H.; Hayflick, S.; Tiranti, V.; Reijngoud, D.-J.; Grzeschik, N. A.; Sibon, O. C. M., Extracellular 4[prime]-phosphopantetheine is a source for intracellular coenzyme A synthesis. *Nat. Chem. Biol.* **2015**, *11* (10), 784-792.
21. Fahey, R. C.; Newton, G. L., Determination of low-molecular-weight thiols using monobromobimane fluorescent labeling and high-performance liquid chromatography. In *Methods Enzymol.* **1987** Vol. 143, pp 85-96.
22. Demoz, A.; Netteland, B.; Svardal, A.; Mansoor, M. A.; Berge, R. K., Separation and detection of tissue CoASH and longchain acyl-CoA by reversed-phase high-performance liquid chromatography after precolumn derivatization. *J. Chromatogr. A* **1993**, *635* (2), 251-256.
23. Cecil, R., Neurath, H., *The Proteins*. 2 ed.; Academic Press: New York, 1963; Vol. 1.
24. Kanaoka, Y.; Machida, M.; Ando, K.; Sekine, T., Fluorescence and structures of proteins as measured by incorporation of fluorophore: IV. Synthesis and fluorescence characteristics of N-(p-(2-benzimidazolyl)phenyl) maleimide. *Biochim. Biophys. Acta* **1970**, *207* (2), 269-277.
25. Shimada, K.; Mitamura, K., Derivatization of thiol-containing compounds. *J. Chromatogr. B Biomed. Sci. Appl.* **1994**, *659* (1-2), 227-241.

26. Nakashima, K.; Umekawa, C.; Yoshida, H.; Nakatsuji, S. i.; Akiyama, S., High-performance liquid chromatography-fluorometry for the determination of thiols in biological samples using N-4-(6-dimethylamino-2-benzofuranyl)phenyl]-maleimide. *J. Chromatogr. B Biomed. Sci. Appl.* **1987**, *414* (0), 11-17.
27. Steenkamp, D. J., Simple methods for the detection and quantification of thiols from *Crithidia fasciculata* and for the isolation of trypanothione. *Biochem. J.* **1993**, *292* (1), 295-301.
28. Chung, C. C.; Ohwaki, K.; Schneeweis, J. E.; Stec, E.; Varnerin, J. P.; Goudreau, P. N.; Chang, A.; Cassaday, J.; Yang, L.; Yamakawa, T.; Kornienko, O.; Hodder, P.; Inglese, J.; Ferrer, M.; Strulovici, B.; Kusunoki, J.; Tota, M. R.; Takagi, T., A fluorescence-based thiol quantification assay for ultra-high-throughput screening for inhibitors of coenzyme A production. *Assay. Drug. Dev. Technol.* **2008**, *6* (3), 361-374.
29. Yamagami, C.; Araki, K.; Ohnishi, K.; Hanasato, K.; Inaba, H.; Aono, M.; Ohta, A., Measurement and prediction of hydrophobicity parameters for highly lipophilic compounds: Application of the HPLC column-switching technique to measurement of log P of diarylpyrazines. *J. Pharm. Sci.* **1999**, *88* (12), 1299-1304.
30. Lukesh, J. C.; Palte, M. J.; Raines, R. T., A Potent, Versatile Disulfide-Reducing Agent from Aspartic Acid. *J. Am. Chem. Soc.* **2012**, *134* (9), 4057-4059.
31. *ICH Harmonized Tripartite Guideline, Validation of analytical procedures: Text and methodology (Q2R1)*, International Conference on Harmonization, ICH, Ed. ICH: 2012.
32. King, M. T.; Reiss, P. D., Separation and measurement of short-chain coenzyme-A compounds in rat liver by reversed-phase high-performance liquid chromatography. *Anal. Biochem.* **1985**, *146* (1), 173-179.
33. Corkey, B. E.; Brandt, M.; Williams, R. J.; Williamson, J. R., Assay of short-chain acyl coenzyme a intermediates in tissue extracts by high-pressure liquid chromatography. *Anal. Biochem.* **1981**, *118* (1), 30-41.
34. Demoz, A.; Garras, A.; Asiedu, D. K.; Netteland, B.; Berge, R. K., Rapid method for the separation and detection of tissue short-chain coenzyme A esters by reversed-phase high-performance liquid chromatography. *J. Chromatogr. B Biomed. Sci. Appl.* **1995**, *667* (1), 148-152.
35. Mangino, M. J.; Zografakis, J.; Murphy, M. K.; Anderson, C. B., Improved and simplified tissue extraction method for quantitating long-chain acyl-coenzyme A thioesters with picomolar detection using high-performance liquid chromatography. *J. Chromatogr. B Biomed. Sci. Appl.* **1992**, *577* (1), 157-162.

36. Haynes, C. A.; Allegood, J. C.; Sims, K.; Wang, E. W.; Sullards, M. C.; Merrill, A. H., Quantitation of fatty acyl-coenzyme As in mammalian cells by liquid chromatography-electrospray ionization tandem mass spectrometry. *J. Lipid. Res.* **2008**, *49* (5), 1113-1125.
37. Kasuya, F.; Oti, Y.; Tatsuki, T.; Igarashi, K., Analysis of medium-chain acyl-coenzyme A esters in mouse tissues by liquid chromatography–electrospray ionization mass spectrometry. *Anal. Biochem.* **2004**, *325* (2), 196-205.
38. Gao, L.; Chiou, W.; Tang, H.; Cheng, X.; Camp, H. S.; Burns, D. J., Simultaneous quantification of malonyl-CoA and several other short-chain acyl-CoAs in animal tissues by ion-pairing reversed-phase HPLC/MS. *J. Chromatogr. B* **2007**, *853* (1–2), 303-313.
39. Tamvakopoulos, C. S.; Anderson, V. E., Detection of acyl-coenzyme a thioester intermediates of fatty acid  $\beta$ -oxidation as the N-acylglycines by negative-ion chemical ionization gas chromatography—Mass spectrometry. *Anal. Biochem.* **1992**, *200* (2), 381-387.
40. Kopka, J.; Ohlrogge, J. B.; Jaworski, J. G., Analysis of in Vivo Levels of Acyl-Thioesters with Gas Chromatography-Mass Spectrometry of the Butylamide Derivative. *Anal. Biochem.* **1995**, *224* (1), 51-60.
41. Pöther, D.-C.; Gierok, P.; Harms, M.; Mostertz, J.; Hochgräfe, F.; Antelmann, H.; Hamilton, C. J.; Borovok, I.; Lalk, M.; Aharonowitz, Y.; Hecker, M., Distribution and infection-related functions of bacillithiol in *Staphylococcus aureus*. *Int. J. Med. Microbiol.* **2013**, *303* (3), 114-123.
42. Bennett, B. D.; Yuan, J.; Kimball, E. H.; Rabinowitz, J. D., Absolute quantitation of intracellular metabolite concentrations by an isotope ratio-based approach. *Nat. Protoc.* **2008**, *3* (8), 1299-1311.
43. Vallari, D. S.; Jackowski, S.; Rock, C. O., Regulation of pantothenate kinase by coenzyme A and its thioesters. *J. Biol. Chem.* **1987**, *262* (6), 2468-71.
44. Brand, L. A.; Strauss, E., Characterization of a New Pantothenate Kinase Isoform from *Helicobacter pylori*. *J. Biol. Chem.* **2005**, *280* (21), 20185-20188.
45. Strauss, E.; Begley, T. P., The Antibiotic Activity of N-Pentylpantothenamide Results from Its Conversion to Ethyldethia-Coenzyme A, a Coenzyme A Antimetabolite. *J. Biol. Chem.* **2002**, *277* (50), 48205-48209.
46. Choudhry, A. E.; Mandichak, T. L.; Broskey, J. P.; Egolf, R. W.; Kinsland, C.; Begley, T. P.; Seefeld, M. A.; Ku, T. W.; Brown, J. R.; Zalacain, M.; Ratnam, K., Inhibitors of pantothenate kinase: Novel antibiotics for staphylococcal infections. *Antimicrob. Agents Chemother.* **2003**, *47* (6), 2051-2055.

47. Riddles, P. W.; Blakeley, R. L.; Zerner, B., Ellman's reagent: 5,5'-dithiobis(2-nitrobenzoic acid)—a reexamination. *Anal. Biochem.* **1979**, *94* (1), 75-81.

# Chapter 4

## Systems analysis of the regulation of the CoA salvage pathway in *E. coli*<sup>†</sup>

---

### 4.1 Introduction

As an essential metabolic cofactor, the biosynthesis of CoA needs to be regulated to prevent the unnecessary expenditure of cellular energy on the production of CoA beyond what is needed for growth under current conditions. Such regulation can be achieved in a number of ways, such as through transcriptional control of expression of the CoA biosynthetic enzymes, through inhibition of their activity by related or unrelated metabolites, or by the specific kinetic characteristics of the enzymes (such as cooperativity). Much research has been performed on the regulation of the activity of two of the CoA enzymes in *E. coli*: pantothenate kinase (PanK) and phosphopantetheine adenylyltransferase (PPAT). In addition, our group has also done some investigation on the possible regulation of dephospho-CoA kinase (DPCK). Together, these three enzymes constitute the CoA salvage pathway as described in Chapter 1. In addition to isolated enzyme studies, some studies have also investigated the effect of perturbing CoA biosynthesis through mutation or overexpression of some of the CoA enzymes, particularly PanK. The combined results of these studies have consequently been used as the basis for making conclusions regarding the physiological regulation of CoA biosynthesis by directly correlating CoA levels with PanK activity, particularly in *E. coli*. In spite of this body of work, a systems-based analysis of CoA biosynthesis has not been performed where all components of the system are considered to contribute to the regulation, and much of the conclusions drawn in the current literature have therefore not been tested in such a context to establish their validity.

In this part of the study we set out to use the CoA salvage pathway of *E. coli*, which provides for a minimal system for the study of the regulation of CoA, to perform such a systems analysis. This entailed first revisiting our current knowledge of the kinetic mechanisms of the enzymes in question, as well as the observations made to date on CoA regulation in whole cell experiments, and to evaluate the utility of this knowledge as a starting-point for this

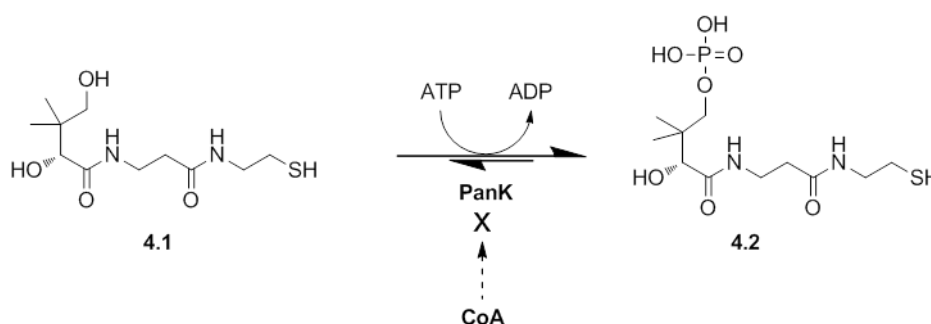
---

<sup>†</sup> Practical implementation of rate equations for modelling in Mathematica was performed by Prof. J.L. Snoep

analysis. In the following sections a summary of this information, as well as a critical analysis of the claims that were made, are provided. Finally, an overview of the information that would be required for a systems analysis is given in light of the shortcomings that were identified in the current knowledge.

#### 4.1.1 Regulation of *E. coli* pantothenate kinase (*EcPanK*) activity

PanK catalyses the Mg-ATP-dependent phosphorylation of pantothenic acid. However, type I or II PanKs can also phosphorylate pantetheine (PanSH) (**4.1**, Scheme 4.1) to form 4'-phosphopantetheine (PPanSH) (**4.2**), allowing organisms that contain these enzymes to also make use of the CoA salvage pathway as discussed in Chapter 1.



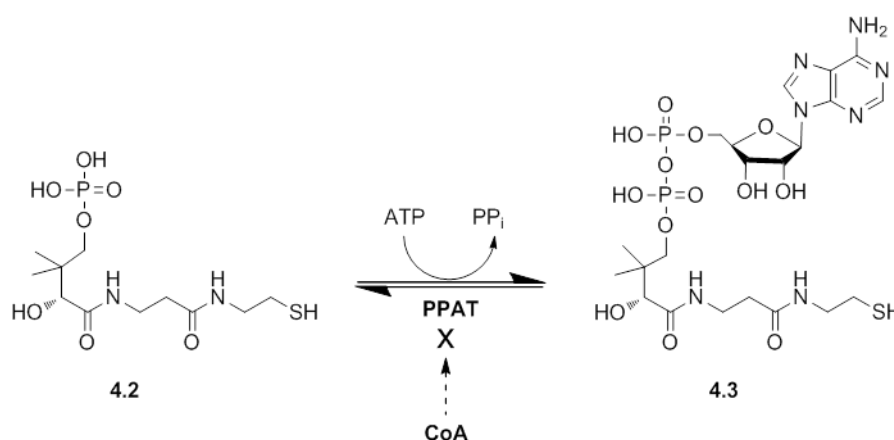
*Scheme 4.1: ATP dependent phosphorylation of PanSH by PanK.* The first step in the CoA salvage pathway is the phosphorylation of PanSH (**4.1**) by PanK to yield PPanSH (**4.2**). PanK is inhibited by CoA where CoA binding is competitive with ATP binding as well as PanSH binding.

Regardless of the substrate, *EcPanK* activity is proposed to be regulated by feedback inhibition by CoA (and to a far lesser extent by acyl-CoAs such as acetyl-CoA), a phenomenon that has been investigated in isolated enzyme studies.<sup>1</sup> Specifically, kinetic inhibition assays showed that the binding of CoA was competitive with ATP binding.<sup>2</sup> This study reported the  $K_i$  for CoA inhibition as  $24.5 \pm 5 \mu\text{M}$ , but no details of how this value was derived, or under which conditions, were provided. Such information — particularly, the ATP concentration at which it was determined — is highly relevant, since CoA binding (and its  $K_i$ ) will vary with ATP concentration. Such measurements are complicated further by the known cooperative nature of ATP binding to *EcPanK*.<sup>2</sup> The same study also reported  $K_d$  values for ATP and CoA binding derived from equilibrium dialysis experiments. These found the  $K_d$  for ATP to be  $2.1 \pm 0.1 \mu\text{M}$ , and  $6.7 \pm 1.4 \mu\text{M}$  for CoA. The similar, but slightly higher affinity of the enzyme for ATP suggests that CoA may not be a potent inhibitor of *EcPanK* activity at high ATP concentrations. However, this important deduction was not considered in the authors' analysis, which led them to the conclusion that CoA exerts potent inhibition on

*EcPanK* under all circumstances. No recognition was given that competition by ATP determines the potency of the inhibitory effect of CoA. These factors have not been addressed in any study performed to date and therefore PanK's inhibition by CoA has not been fully characterized.

#### 4.1.2 Regulation of *E. coli* phosphopantetheine adenylyltransferase (*EcPPAT*) activity

PPAT catalyses the reversible adenylylation of PPanSH (4.3 Scheme 4.2) yielding dephospho-CoA (DePCoA) (4.4) and pyrophosphate. It is currently the best kinetically characterized enzyme in the pathway.



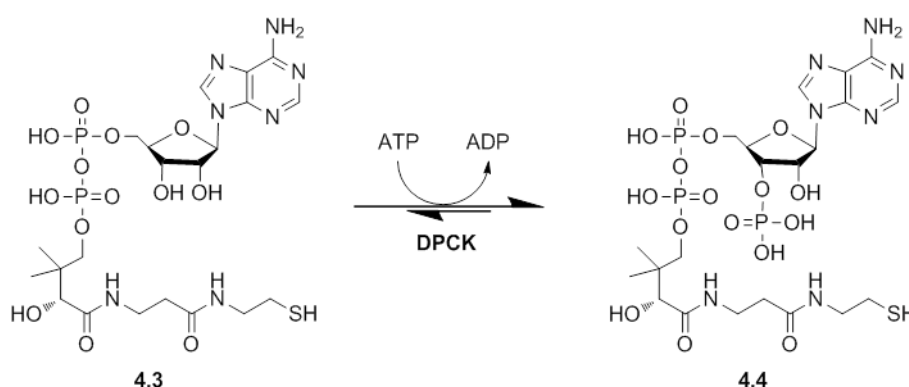
*Scheme 4.2: The ATP dependent adenylylation of PPanSH by PPAT. PPAT adenylylates PPanSH (4.2) to form DePCoA (4.3) in a fully reversible reaction. PanK is inhibited by CoA where CoA binding is competitive with PPanSH and ATP binding.*

The  $K_{eq}$  for the *EcPPAT* reaction was determined by following the approach to equilibrium and was reported to be in the range of 1.25-1.95. The protein was purified with CoA tightly bound, suggesting that *EcPPAT* activity is also regulated by CoA feedback inhibition.<sup>3</sup> Subsequent kinetic characterization of *EcPPAT* revealed that CoA binding is competitive with PPanSH and ATP binding in the forward reaction, with  $K_i$  values in the range of 10–50  $\mu\text{M}$ .<sup>4</sup> The affinity of *EcPPAT* for CoA was determined by isothermal titration calorimetry (ITC) and its  $K_d$  reported as 65 nM, indicating a very high affinity for CoA compared to PPanSH and ATP for which values of  $0.27 \pm 0.04 \mu\text{M}$  and  $1.85 \pm 0.22 \mu\text{M}$  were determined respectively. The authors of this study attributed the large discrepancy between the  $K_d$  and  $K_i$  values for CoA to competition by the substrates in the kinetic determination of  $K_i$ , and also to a proposed dual binding mode for CoA to *EcPPAT*. This conclusion was supported by ITC measurements which revealed two thermodynamically distinct binding modes of CoA with low and high affinity. From ligand binding data it was suggested that PPanSH concentration

modulates *Ec*PPAT's binding of CoA between high affinity and lower affinity binding modes. The regulation of *Ec*PPAT's activity by CoA feedback inhibition was therefore proposed to only be relevant when CoA levels are high and PPanSH levels are low. No inhibitory effect was observed with acetyl-CoA up to 500  $\mu$ M suggesting that only free CoA acts as an inhibitor of *Ec*PPAT.

#### 4.1.3 Regulation of *E. coli* dephospho-coenzyme A kinase (DPCK) activity

DPCK phosphorylates DePCoA (**4.3**, Scheme 4.3) in an ATP-dependent manner to yield CoA (**4.4**) and ADP. *Ec*DPCK is the least studied enzyme in the CoA pathway and limited information is available on the regulation of its activity.



*Scheme 4.3: ATP dependent phosphorylation of DePCoA by DPCK. In the final step of CoA biosynthesis, DePCoA (4.3) is phosphorylated to yield CoA (4.4).*

Product inhibition by CoA has not been assessed. Kinetic studies of *Ec*DPCK demonstrated high  $K_M$  values for DePCoA and has been reported to range between 650 and 740  $\mu$ M.<sup>5,6,7</sup> In Chapter 1 we suggested that *Ec*DPCK affinity for DePCoA may be modulated by switching between a low affinity monomer and a high affinity trimer. However, this has not been confirmed experimentally due to the difficulties associated with simultaneously assessing oligomeric structure and activity. Consequently such proposals currently remain largely speculative.

#### 4.1.4 Observations on the regulation of CoA production *in vivo*

PanK is not only the first enzyme of the CoA pathway, but it was also the first pathway enzyme in *E. coli* to be identified, characterized and studied in isolation. One of the major findings of these studies was the inhibition of the enzyme's activity by CoA. This led to the suggestion that feedback inhibition of *Ec*PanK by different CoA species controls the overall concentration of CoA. Indeed, since there is no evidence yet for transcriptional control of *Ec*PanK, all indications are that CoA levels are mainly controlled by biochemical regulation.<sup>8</sup>

The results of several studies that have been conducted in *E. coli in vivo* have been interpreted to support the conclusion that the flux through the CoA pathway is controlled by *EcPanK*. For example, the CoA pool in *E. coli* mainly consists of acetyl-CoA but the size of the CoA pool and distribution of the CoA species are dependent on the carbon source on which it is cultured.<sup>1</sup> The size of the CoA pool was reported to halve, from 400  $\mu\text{M}$  to 200  $\mu\text{M}$ , when the carbon source is shifted from glucose to acetate. Following the shift, the ratio of CoA:acetyl-CoA is increased with an accompanying decline in ATP levels.<sup>1,9</sup> It has been reported that *E. coli* growing on glucose-containing media produces 15 times more pantothenic acid than what is utilized for CoA production, with the excess being excreted.<sup>10</sup> From this finding the authors concluded that pantothenic acid utilization controls the rate of CoA biosynthesis and not the supply, and that *EcPanK* must therefore catalyze the “rate-limiting step” in the pathway. They also suggested that the reduction in the CoA pool is a direct consequence of *EcPanK* activity being reduced in response to the shift in carbon source from glucose to acetate. This reduction in activity was proposed to occur because *EcPanK* is less sensitive to inhibition by acetyl-CoA, the major CoA species in cells grown on glucose, and more sensitive to inhibition by CoA, which predominates in cells grown on acetate. The physiological significance of variance in inhibition by these two forms of CoA was proposed to allow the CoA pool to increase and meet the metabolic demands of cells dividing rapidly when glucose can be utilized as carbon source.

In a subsequent study, a single residue in the *EcPanK* protein was mutated to yield an enzyme refractory to inhibition by CoA species *in vitro*.<sup>11</sup> Cells expressing this mutated *EcPanK* at single copy levels were found to produce double the amount of CoA compared to when the wild-type protein was expressed at single copy levels in a temperature sensitive *PanK* deficient strain, *coaA15(T)*. Similar results were obtained with overexpression of *EcPanK* to a concentration level 76-fold higher compared to that found in wild-type *E. coli* cells; in this case, only a 1.5-fold increase in intracellular CoA was observed.<sup>12</sup> These results were taken as proof that biochemical feedback inhibition of *EcPanK* functions *in vivo* to limit the amount of CoA that is produced. Additionally, the finding that CoA-binding is competitive with ATP-binding suggested that CoA production can also be coordinated with the energy state of the cell, where reduced ATP levels would allow more CoA to inhibit *EcPanK* activity.<sup>2,1,13</sup> From these results it was concluded that the changes in the predominant CoA species as well as changes in ATP levels function in concert to regulate the rate of CoA biosynthesis mainly by modulating *EcPanK* activity. As a consequence of these reports and their findings, *EcPanK* has been referred to as the “rate-limiting” enzyme of CoA biosynthesis in all subsequent studies.

In a similar vein other studies have suggested that *EcPPAT* acts as a secondary regulatory point of CoA biosynthesis based on the finding that *E. coli* excretes the PPAT substrate PPanSH.<sup>10,14</sup> It was proposed that regulation at the level of *EcPPAT* may become relevant when regulation by *EcPanK* is disrupted or when *EcPanK* levels are increased by overexpression.<sup>11,12</sup> Under both these conditions the amount of intracellular and extracellular PPanSH was found to be increased, and the authors ascribed this to restricted flux through the *EcPPAT*-catalysed step in the CoA biosynthesis pathway. Importantly, it was found that in *E. coli*, the excreted PPanSH cannot be transported back into the cells.<sup>14</sup> Years later, kinetic studies of the purified enzyme showed that although *EcPPAT* activity is also regulated by inhibition by CoA, its higher affinity for PPanSH causes this to only become relevant when CoA levels are high and PPanSH levels are low.<sup>4</sup> From these findings it was concluded that CoA inhibition of *EcPPAT* does not play a significant role in regulating CoA production under physiological conditions. Interestingly, a recent study showed that PPanSH can pass through eukaryotic cell membranes by unassisted passive diffusion, but this has not been observed in bacteria.<sup>15</sup>

To summarize the current view of the regulation of CoA biosynthesis: *EcPanK* activity determines the rate of CoA production due to strong feedback inhibition by CoA, with a secondary control point at *EcPPAT*. This is based on a reductionist approach to pathway regulation where the perceived potent inhibition of *EcPanK* in isolated studies is used to describe the behaviour of the system. *EcPPAT* activity displayed weaker inhibition in isolated studies and was therefore considered a secondary control point.

#### **4.1.5 Shortcomings of currently accepted view of the regulation of CoA production**

The classic reductionist approach to interpret pathway control relies on the identification of a single rate-limiting enzyme, usually loosely defined as the slowest step in the pathway. In the case of CoA biosynthesis, the identification of the so-called “rate-limiting” enzyme as outlined above was made based on which enzyme experiences the strongest inhibition by CoA in isolated enzyme studies. This led to *EcPanK* being branded as the “rate-limiting” enzyme due to the perceived potency of inhibition by CoA based on the inhibitory constant determined in the kinetic studies discussed in Section 4.1.1.

Such a conclusion would imply that varying the activity of *EcPanK* alone would change the flux through the pathway as a whole. This is a highly unlikely occurrence in most systems, and such a phenomenon is seldom observed even in the absence of feedback inhibition.<sup>16</sup>

From the specific experimental results cited above, it becomes clear that a systems approach to explaining the findings was never considered. For example, the change observed in the steady state concentration of CoA in the carbon shift experiments discussed above is completely ascribed to *EcPanK* and its inhibition by CoA while the rest of the components of the system are completely ignored. Similarly, the studies in which the PanK activity in *E. coli* cells were effectively modified—by making it refractory to inhibition by CoA and by overexpressing the enzyme— did not result in an unlimited increase in intracellular CoA concentration because the control point was removed. This does not necessarily mean that the flux through the pathway was not affected as CoA utilization and degradation (i.e. the demand for CoA) were not taken into account at all in the experimental design. The conclusion that *EcPPAT* must become the next rate-limiting reaction when *EcPanK* activity is altered in these ways is also based only on the observation that its substrate accumulates, and not because of a systems analysis. The apparent central role assigned to *EcPanK* in the regulation of CoA production may also be a consequence of the historical timeline, where for 10–15 years (until the late 90s) *EcPanK* was the only isolated and characterized enzyme of the pathway.

While these deductions may not be explicitly wrong, the idea of a single rate-limiting enzyme is conceptually problematic. In addition, the manner in which *EcPanK* was identified as the rate-limiting enzyme, mainly based on the perceived potent inhibition by CoA, is wholly inadequate. We need an alternative approach to move away from the idea of a unique rate-limiting step. We need to shift from the qualitative (“is this step rate-limiting or not?”) to the quantitative (“how much does the metabolic flux vary if the activity of the enzyme in question is varied?”). Such an approach is described by metabolic control analysis (MCA) because it sets out to quantify the distribution of control among the steps of a pathway.<sup>17</sup> With MCA it becomes apparent that even the rate of a sequence of simple chemical reactions depends on the rate constants of all the reactions. Flux control is not a unique property of a single “rate-limiting” enzyme in the pathway. Flux control is a property of the system—a distributed property—that is shared among all the enzymes.<sup>18</sup> This is illustrated by the failed strategy of many biotechnology studies where the “rate-limiting” enzyme in a pathway is identified so that it can be overexpressed in the hope of increasing the yields of the desired product. Moreno-Sanchez suggests that such efforts have often been unsuccessful because the “rate-limiting” enzyme as it is classically conceived does not exist; as such, the approach is therefore fundamentally misconceived.<sup>16</sup> The rationale behind the failure of such strategies is that overexpression of the one “rate-limiting” step leads to flux control redistribution in which case other steps become “rate-limiting”. Therefore, any attempt to modify or manipulate metabolism cannot be based on the notion of a “rate-limiting” enzyme. The same concept

also applies to rational drug design strategies where the aim is to modify an essential metabolic pathway by inhibiting the pathway flux with a specific enzyme inhibitor.<sup>19</sup> In CoA biosynthesis, for example, identifying the single “rate-limiting” step with the aim of inhibiting that step to inhibit CoA production will not aid in developing a successful inhibitor by rational design because it is highly unlikely that such an enzyme exists in the pathway. By performing metabolic control analysis of the target pathway with the help of a computational model of the system, it is possible to determine to what extent an enzyme in the pathway has to be inhibited to achieve a 50% reduction in pathway flux for example. This creates a more realistic view of what is required to achieve the objective.

#### **4.1.6 Requirements for a systems analysis of CoA production**

In light of the shortcomings of the currently accepted view of CoA synthesis, it is clear that some form of holistic study is required. We have discussed the control that an enzyme exerts on the pathway flux is a system property that cannot be determined or predicted when only some properties of the enzyme have been studied in isolation. Intuitively, there must be a link between the kinetic properties of the isolated enzyme and its potential for flux control. Computational modelling can serve as a tool to link what is observed on the single reaction level with what is observed on the systems level by simulating the interdependency of the constituent reactions. Due to the lack of information on the control of CoA production and the errors pointed out in some of the information that is available, we considered the requirements for a systems analysis of CoA production. These included knowledge of the stoichiometry of the pathway, so that all the role players in the pathway—enzymes, substrates, products and effectors—can be accounted for. In addition, specific data must be available to allow for the construction of a kinetic model for such a holistic study of the pathway, as outlined below.

##### *4.1.6.1 Modelling the reaction components of the system*

Enzyme rate equations are required to mathematically describe the dependency of each reaction rate on the concentration of substrates, products and effectors. The rate equation is therefore a function of reactant concentrations and parameters that specify how fast the reaction will proceed. Rate equations can be derived from detailed kinetic enzyme studies that provide information on the enzyme mechanism. Such detailed rate equations often contain a large number of parameters that are either not available or hard to determine. Generic rate equations do not contain the mechanistic information but only captures the essential detail of the reaction to illustrate the dependence of rate on substrates, products

and effectors. These types of equations are frequently preferred for modelling as they are often found to describe the enzyme reaction with the same accuracy as detailed mechanistic rate equations, but they require fewer parameters to be known. To turn the rate equation into a useful model that can describe the reaction, values for all the parameters have to be included.

Parameters such as the  $K_M$  and  $K_i$  for example can be determined by isolated enzyme studies. Initial-rate kinetic assays are typically performed to determine these parameters by coupling the reaction of interest, via intermediate enzymes, to a chromogenic reaction that can be monitored by spectrophotometry. A tangent line is fitted to the first few data points to approximate the initial rate. Initial-rate data is collected for various substrate concentrations and irreversible kinetic equations like the Michaelis-Menten<sup>20,21</sup> or Hill<sup>22</sup> equations are fitted to determine the kinetic parameters. An alternative approach involves global fits of complete progress curves of enzyme-catalysed reactions.<sup>23</sup> Here the rate equation is integrated, making the substrate and product concentrations implicit.

Initial-rate kinetic assays can be complicated by burst- or lag-phases that alter the initial velocity measurements and the requirement for coupling enzymes could lead to experimental artefacts. Since initial rates are extracted from only the first few data points, a large number of these experiments have to be performed to generate relatively little kinetic data.<sup>24</sup> Progress curves on the other hand, are acquired while substrate and product concentrations are changing during a reaction, thereby yielding a large amount of data per experiment on the dependence of the reaction rate on the substrate and product concentrations.<sup>25</sup> However, the progress curve approach is limited by the perturbations that can be studied because the substrate concentrations are not controlled for the duration of the experiment and it is not always known which parameter is affecting the reaction rate. The analysis of time course data also becomes significantly more complex if the enzyme of interest is not stable for the duration of the time course as this would augment perceived product inhibition.<sup>26</sup> Both approaches are useful but it is often analytical constraints in measuring reactants for reaction progress curves that limits the use of this approach.

Thermodynamic data such as the equilibrium constant of each reaction is required in the model to capture the degree of reversibility of each enzymatic reaction. The value of  $V_M$  for each reaction is also required under the conditions for which the model is being built because this value depends on the enzyme concentration. If biological protein extracts are used, the  $V_M$  should be determined in those samples if each enzyme concentration is not known. Other parameters that are required for a model of the pathway are the initial

concentrations of all the variables contained in the model if the goal is a time course simulation. If a steady state is simulated it is required that the concentration of terminal source and sink metabolites be entered as fixed parameters.

#### 4.1.6.2 Linking components for a model of the pathway

Once all the rate equations are defined and all the parameters determined, the model can be assembled by combining the rate equations in a set of ordinary differential equations (ODEs). Since we know the network structure and the stoichiometry of the reactions, the formulation of the set of ODEs is straightforward and is shown in Scheme 4.4.

$$\begin{aligned}\frac{d(\text{PanSH})}{d(t)} &= -v_{\text{PanK}} \\ \frac{d(\text{PPanSH})}{d(t)} &= v_{\text{PanK}} - v_{\text{PPAT}} \\ \frac{d(\text{DePCoA})}{d(t)} &= v_{\text{PPAT}} - v_{\text{DPCK}} \\ \frac{d(\text{CoA})}{d(t)} &= v_{\text{DPCK}}\end{aligned}$$

*Scheme 4.4: Set of ordinary differential equations (ODEs) representing the CoA salvage pathway.*

For determination of a pathway time course the ODEs are numerically integrated. For a steady state calculation the set of ODEs are set to zero and solved for the variable concentrations. To assess the quality of the model it has to be validated by comparing the model output with independent data that was not used in the construction of the model. The independent dataset usually entails the measured fluxes or metabolite concentrations from the complete pathway and are directly comparable with model outputs. Data for validation are typically system data whereas the data for model construction are usually mechanistic properties of the isolated components. This is termed the “bottom up” approach to modelling but it is sometimes not a feasible approach because not enough data are available or some parameters cannot be determined because of assay limitations. The “top down” approach can then be used as an alternative where missing parameters can be fitted by iterative adjustment in an optimization routine so that the model output matches an experimentally determined value. The drawback of this approach is that the fitted parameters are no longer mechanistically derived from enzyme properties and this may lead to errors in the model if an over-simplified generic rate equation was used where the parameters also have limited mechanistic interpretation. If the “top down” approach is used it would therefore be advisable

to use mechanistically derived rate equations to ensure that mechanistic information is incorporated into the model. Models constructed by the “top down” approach may fail to describe the pathway flux or concentrations under conditions that are far removed from those under which the parameters were fitted. Validation under different conditions is therefore especially important when the “top down” approach is used.

#### **4.1.7 Objective of this study**

The aim of this study is to perform the first holistic study of CoA production by systems analysis of the salvage pathway. The goal of this system analysis is to provide updated information on the biochemical regulation of CoA production to assist rational drug development efforts. A kinetic model of the salvage pathway in *E. coli* will be constructed because the system components are best characterized in this model organism with all proteins being cloned and characterized. This study will focus on the salvage pathway because it represents a simplified version of the five step pathway where we are able to measure all the metabolites. This is important when it comes to generating system data required for model validation. Control in the salvage pathway is also especially relevant to drug development efforts because this is actually the pathway targeted in organisms that contain type I or type II PanKs. Inhibition of either one of the other two enzymes found in the full pathway can easily be overcome by CoA production via the salvage pathway. As for the approach used for model construction in our study, a combination of “bottom up” and “top down” strategies are employed for model construction. The best approach was determined on a case-by-case basis for each enzyme and will be discussed in detail in the results section.

## 4.2 Results and Discussion

The objective of performing computational modelling of the CoA salvage pathway was achieved by first performing a critical evaluation of the available information on the reaction mechanism, rate equation and kinetic parameters of each of the three enzymes involved in the pathway, to obtain new data where necessary and to use this as basis for obtaining parameterized rate equations that describe the activity of each enzyme. Next, these rate equations were combined to construct a model of the pathway, which was then tested for its ability to describe the progress of CoA salvage biosynthesis in terms of each of the metabolites concerned, and under various conditions. Finally, having validated the model in this manner, it was used to predict the conditions under which certain factors take control of the flux in the pathway.

### 4.2.1 *EcPanK* kinetics

#### 4.2.1.1 *Literature survey of the kinetic parameters and mechanistic properties of EcPanK*

*EcPanK* has been overexpressed, purified and its kinetic parameters determined in several studies. These have reported  $K_M$  values for pantothenate of between 17 and 36  $\mu\text{M}$ , for PanSH of between 19 and 91  $\mu\text{M}$  and for ATP of 136  $\mu\text{M}$ .<sup>2,27</sup> The similar  $K_M$  values reported for pantothenate and PanSH and the fact that the enzyme also exhibits similar  $k_{\text{cat}}$  values for both substrates at saturating ATP indicate that the enzyme does not make a catalytic distinction between them (as explained in more detail in Chapter 1). This suggests that the two substrates can be used interchangeably in determining the parameterized rate equation of the enzyme. The inhibition of *EcPanK* activity by CoA and its thioesters were also determined, but only at one set of enzyme, pantothenic acid and ATP concentration. As explained in section 4.1.1, a  $K_i$  value for CoA inhibition has also been reported, but no information was provided on how this was determined.

The *EcPanK* kinetic parameters cited above were determined using two different assays. The first uses radiolabelled pantothenate in a discontinuous, end-point assay which measures the amount of product formed after five or ten minutes. The second is a standard continuous kinase assay based on coupling the production of ADP to the consumption of NADH using pyruvate kinase and lactate dehydrogenase (PK/LDH) as coupling enzymes. However, in the majority of the studies in which the kinetic mechanism and the inhibition by CoA was studied, the discontinuous assay was used without providing clear evidence that

the reaction rate remained linear for the duration of the assay. Consequently, it is uncertain if the parameters that were obtained in these studies are indeed based on the true initial rates of the reactions in question. This suggested that a re-evaluation of these parameters were required for the construction of a suitable kinetic model.

The kinetic mechanism of *EcPanK* can be deduced from the extensive studies of the protein. Structural studies have shown that it has a homo-dimeric structure.<sup>13</sup> Kinetic studies have indicated also that it has an ordered mechanism where ATP binds first, and that ATP binding to the *EcPanK* dimer exhibits positive cooperativity with a Hill coefficient of 1.46.<sup>2</sup> Site-directed mutagenesis and kinetic studies have shown that CoA binding is competitive with ATP binding.<sup>1,2</sup> This finding is supported by a study where the crystal structure of *EcPanK* in complex with either CoA or the non-hydrolyzable ATP analogue, AMPPNP, was solved.<sup>13</sup> Alignment of these structures show that these molecules bind in pockets located close to one another and in such a manner that the pyrophosphate moiety of CoA occupies the same space as the  $\beta$ - and  $\gamma$ -phosphates of AMPPNP. This overlap of the ATP and CoA binding sites explain the competition as well as the inhibition of *EcPanK* activity when CoA is bound. Structural studies have also reported that when CoA is bound, its PanSH moiety overlaps with the pantothenic acid/PanSH binding site.<sup>28</sup> Taken together, this implies that when CoA is bound, neither ATP nor PanSH can bind to their respective active sites. In addition, structural studies have shown that a significant conformational change occurs when pantothenic acid binds to *EcPanK*. There is a large movement of the helix-H/loop region, corresponding to amino acids 243-263, that acts as a lid that closes over the pantothenate binding site.<sup>13</sup>

Our strategy was to define the enzyme's kinetic mechanism using this information, and to derive a mechanistically appropriate rate equation based on it. This would be followed by the execution of detailed kinetic studies using isolated *EcPanK* to determine all the kinetic parameters by performing a global fit of the newly derived rate equation to the data.

#### *4.2.1.2 Proposed EcPanK kinetic mechanism and rate equation*

We propose the detailed *EcPanK* kinetic mechanism presented in Figure 4.1. Subunits that are active (shown in green in Figure 4.1) are derived in several ways. Considering its ordered mechanism, the enzyme only becomes active when PanSH binds (with the binding constant denoted by  $K_{\text{PanSH}}$ ) to a sub-unit that has ATP bound. Since ATP binding to the *EcPanK* dimer is cooperative, the binding constant of the first ATP is denoted by  $K_{\text{ATP}}$  while the binding constant of ATP to the second subunit is denoted by  $K_{\text{ATP}}/\alpha$ . We assumed that

the catalytic activities of subunits are independent in all cases—i.e. that once ATP is bound to one subunit it can bind PanSH and react to form product without the need for ATP binding at the other subunit—as there is no information in the literature to the contrary. However, if both subunits have ATP bound and PanSH binds to one subunit with the binding constant  $K_{\text{PanSH}}$ , we propose that binding of PanSH to the second subunit may occur cooperatively with a binding constant denoted by  $K_{\text{PanSH}}/\beta$ .

Similarly, inactive subunits (shown in dark grey in Figure 4.1) can also be obtained in different ways. It is assumed that at high PanSH concentrations, it can bind sub-units that have no ATP bound with a binding constant denoted by  $K_{\text{PanSH}}^i$ ; it then induces the same conformational change that “closes” the active site that was mentioned earlier. This would block ATP from entering its binding site, thereby making the sub-unit inactive. PanSH has to dissociate and leave the active site to allow ATP to bind first, followed by PanSH, for catalytic activity to occur. CoA has been shown to be a competitive inhibitor of ATP binding, indicating competition for the same binding site.<sup>2</sup> Structural studies have also indicated that CoA overlaps with the PanSH binding site and therefore we assumed that when CoA binds to a free subunit it blocks both the ATP and PanSH binding sites, rendering the subunit inactive.<sup>28</sup> The binding constant of CoA is denoted by  $K_{\text{CoA}}$ . In this scenario, it is also assumed that CoA binding by one subunit does not have an effect on the other subunit.

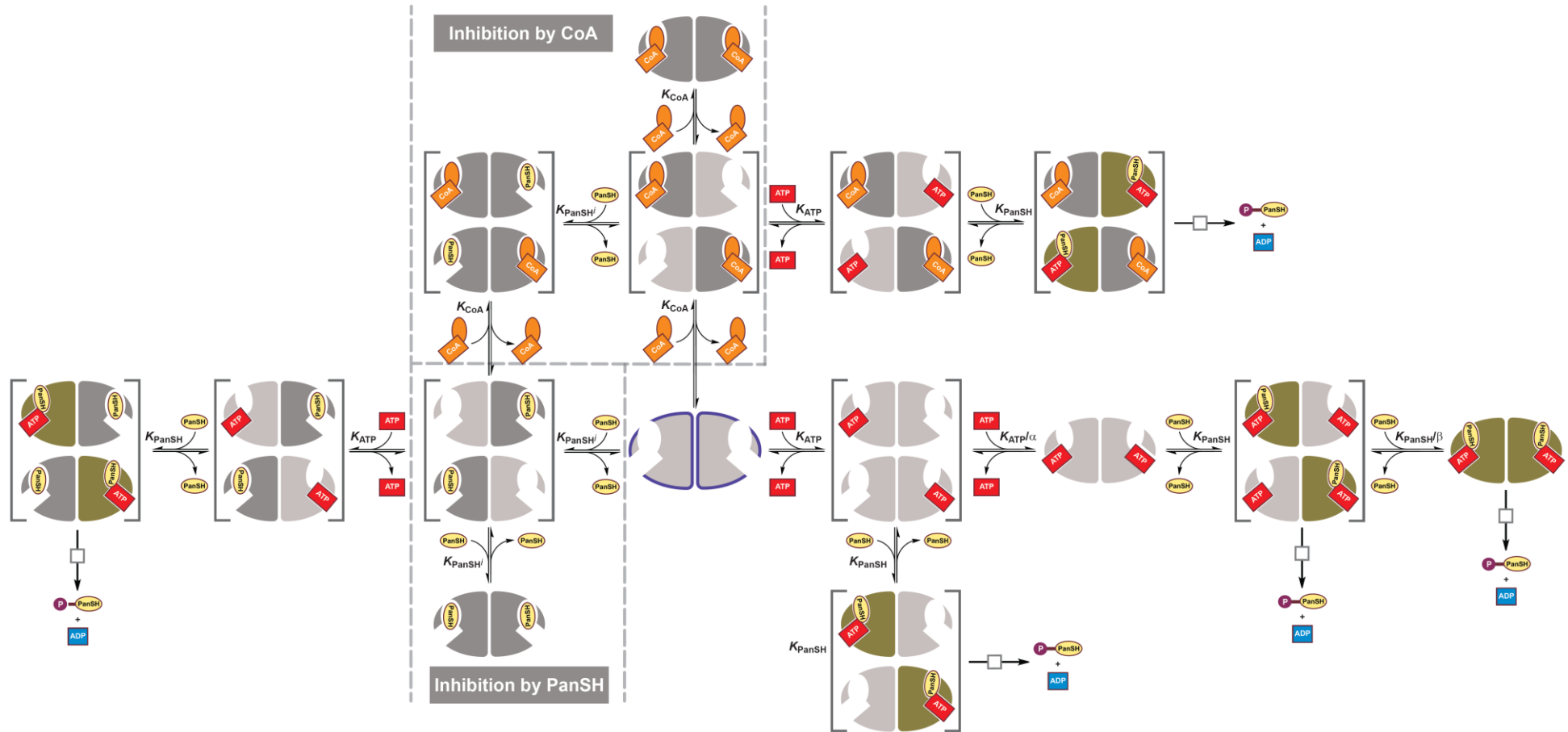


*Figure 4.1: Proposed kinetic mechanism for EcPanK.* Active subunits are shown in green, and based on the enzyme's ordered mechanism are obtained when ATP binds first to one subunit's active site, followed by the cooperative binding of ATP to the second subunit which occurs with a different binding constant ( $K_{ATP}/\alpha$ ). When both subunits have ATP bound it is proposed that once PanSH binds to one of the subunits, binding to the second subunit will also occur with a distinct binding constant ( $K_{PanSH}/\beta$ ). Inactive subunits are shown in dark grey, and are formed when PanSH binds first, binding in a different conformation to prevent ATP binding. It is assumed the other subunit is not affected. Similarly, CoA binding to a subunit prevents both ATP and PanSH binding at that subunit without affecting the other subunit.

From the proposed mechanism for *EcPanK*, Equation 4.1 is derived (details in appendix) to describe the reaction rate.

$$v_{PanK} = \frac{e_{PanK} \cdot V_M \cdot \frac{ATP}{K_{ATP}} \cdot \frac{PanSH}{K_{PanSH}} \left(1 + \alpha \cdot \frac{ATP}{K_{ATP}} \left(1 + \beta \cdot \frac{PanSH}{K_{PanSH}}\right) + \frac{CoA}{K_{iCoA}} + \frac{PanSH}{K_{iPanSH}}\right)}{1 + 2 \cdot \frac{ATP}{K_{ATP}} \cdot \left(1 + \frac{PanSH}{K_{PanSH}}\right) + \alpha \cdot \left(\frac{ATP}{K_{ATP}}\right)^2 \left(1 + \frac{2 \cdot PanSH}{K_{PanSH}} + \beta \cdot \left(\frac{PanSH}{K_{PanSH}}\right)^2 + \left(\frac{CoA}{K_{iCoA}} + \frac{PanSH}{K_{iPanSH}}\right) \cdot \left(2 + \frac{CoA}{K_{iCoA}} + \frac{PanSH}{K_{iPanSH}} + \frac{2 \cdot ATP}{K_{ATP}} \cdot \left(1 + \frac{PanSH}{K_{PanSH}}\right)\right)\right)}$$

Eq. 4.1

Next, a detailed kinetic study of *EcPanK* was performed to determine all the parameters contained in the proposed rate equation.

#### 4.2.1.3 Kinetic studies of *EcPanK* to determine its kinetic parameters

The shortcomings of the discontinuous, end-point assay employed previously for the kinetic characterization of *EcPanK* was overcome by using the continuous PK/LDH assay (discussed above and in Chapter 3) that couples the production of ADP to the oxidation of NADH. Our assays were performed at a dilute *EcPanK* concentration of 0.005 mg/ml (129.8 nM) and the reaction was followed for 10 minutes. Initial rates were determined by linear regression analysis of the linear portions of the progress curves as identified by visual inspection. It is important to note that in these kinetic studies, the enzyme was not pre-incubated with ATP, PanSH or CoA prior to the initiation of the reaction. This was done to ensure that not one particular enzyme form is favoured, for example, by saturating it with ATP before the reaction is initiated by the addition of PanSH. Consequently, all parameters were determined from reactions in which the substrates and/or inhibitor were mixed and then simultaneously added to the assay mixture containing the enzyme to initiate the reaction.

*EcPanK* activity was assessed by measuring the initial rate at various concentrations of ATP and PanSH. When the ATP concentration is varied up to 5 mM with the initial rate measured at various fixed concentrations of PanSH, data points form a sigmoidal curve confirming the positive cooperativity of ATP binding (Figure 4.2A). When the concentration of PanSH is varied up to 766  $\mu$ M at various fixed concentrations of ATP, data points displayed a hyperbolic relationship, reaching a plateau at saturating concentrations of PanSH (Figure 4.2 B) However, the observed rate profile deviates from the standard Michaelis-Menten profile at the highest concentration of 766  $\mu$ M PanSH, where lowered activity is observed (profile not shown for the sake of clarity in the combined data set). This is in agreement with the proposed mechanism of inhibition by PanSH when it binds first, a situation that is more likely at high PanSH concentrations. However, from the rate profiles it seems that dissociation of

PanSH occurs quite rapidly as the activity is only slightly lowered at such high levels of PanSH.

Inhibition of *EcPanK* activity by CoA was also assessed at various concentrations of ATP and PanSH (Figure 4.3). First, the concentration of CoA was varied at 100  $\mu\text{M}$  PanSH and a high concentration of ATP (5000  $\mu\text{M}$ ). This was followed by determining inhibition using the same concentration range of CoA in combination with 100  $\mu\text{M}$  PanSH but a lowered ATP concentration of 500  $\mu\text{M}$ . Finally, inhibition by CoA was also assessed at a lowered PanSH concentration of 25  $\mu\text{M}$  and lowered ATP concentration of 500  $\mu\text{M}$ . Taken together, these data indicate that a high concentration of ATP better protects *EcPanK* against inhibition by CoA. This is in agreement with the equilibrium dialysis experiments described in the literature which reported that the enzyme has a stronger affinity for ATP than CoA and suggested that inhibition by CoA at high ATP concentrations would become less potent.<sup>2</sup>

Taking all the results of these kinetic experiments together, a global fit of Eq. 4.1 to all the obtained data was performed to determine all the kinetic parameters. The fitted rates are indicated by the various solid lines in Figures 4.2 and 4.3. The parameter values that were determined in this manner are shown in Table 4.1, including the standard error of the fit.

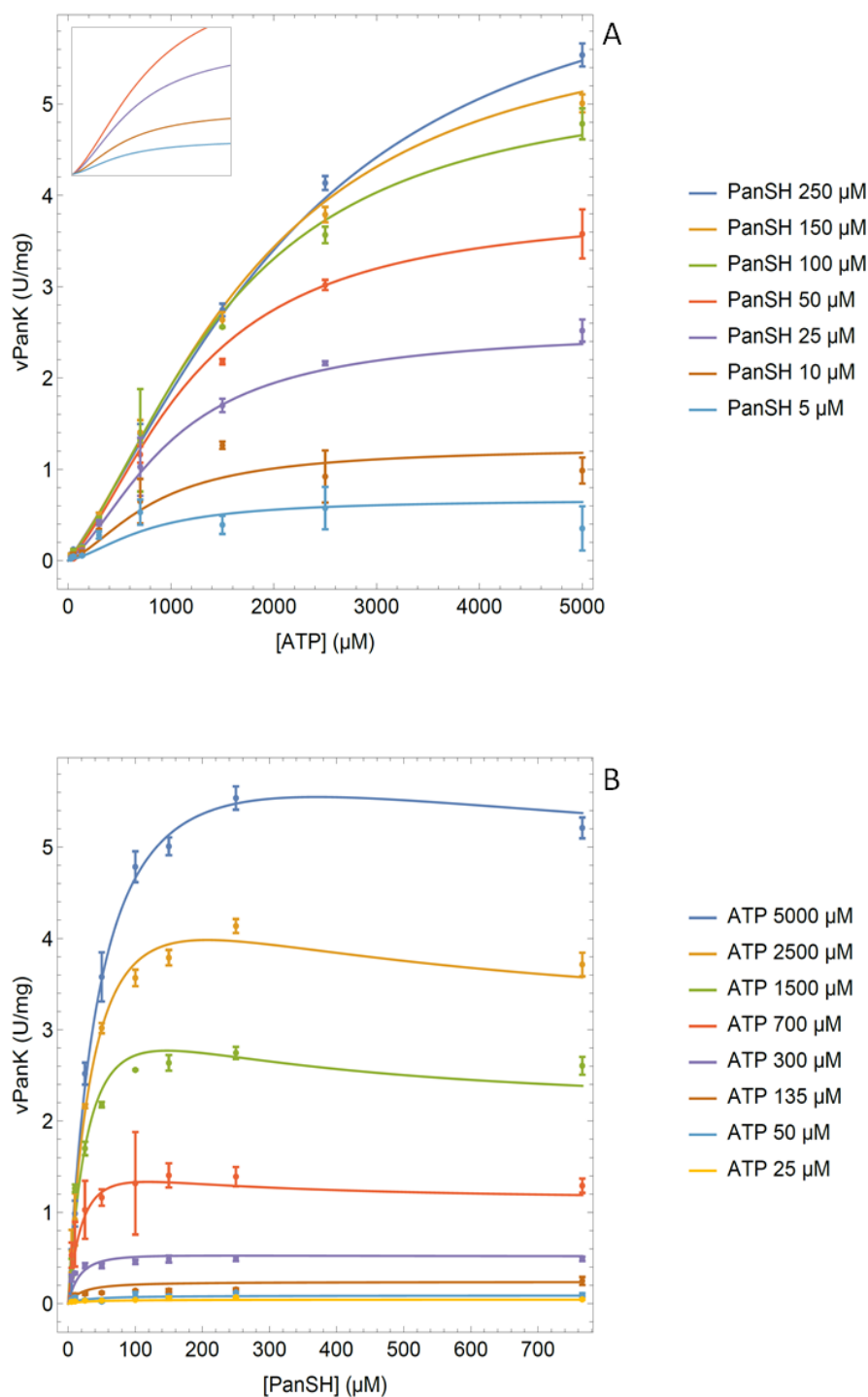


*Figure 4.2: EcPanK activity as a function of ATP and PanSH concentration.* The kinetic profile with variable ATP concentrations at 766  $\mu\text{M}$  PanSH was determined but not shown in the figure (A) for the sake of clarity. An enlarged insert was added to panel A to point out the sigmoidal shape of the graphs. Initial rates were determined with the PK/LDH coupled assay containing 0.005 mg/ml *EcPanK*, 0.01 U/ $\mu\text{l}$  PK, 0.01 U/ $\mu\text{l}$  LDH, 0.3 mM NADH, 0.5 mM PEP, 50 mM Tris buffer pH 7.6, 20 mM KCl, 10 mM  $\text{MgCl}_2$  and 250  $\mu\text{M}$  TCEP (or 1 mM TCEP for the 766  $\mu\text{M}$  PanSH reaction). 1 Unit = 1  $\mu\text{mol}$  PanSH consumed per minute at 37°C. Assay data is represented by the dots and represent the mean of triplicate determinations with the error bars denoting the standard deviation. Solid lines represent the rate profiles obtained by performing a global fit of Eq. 4.1 to the data.

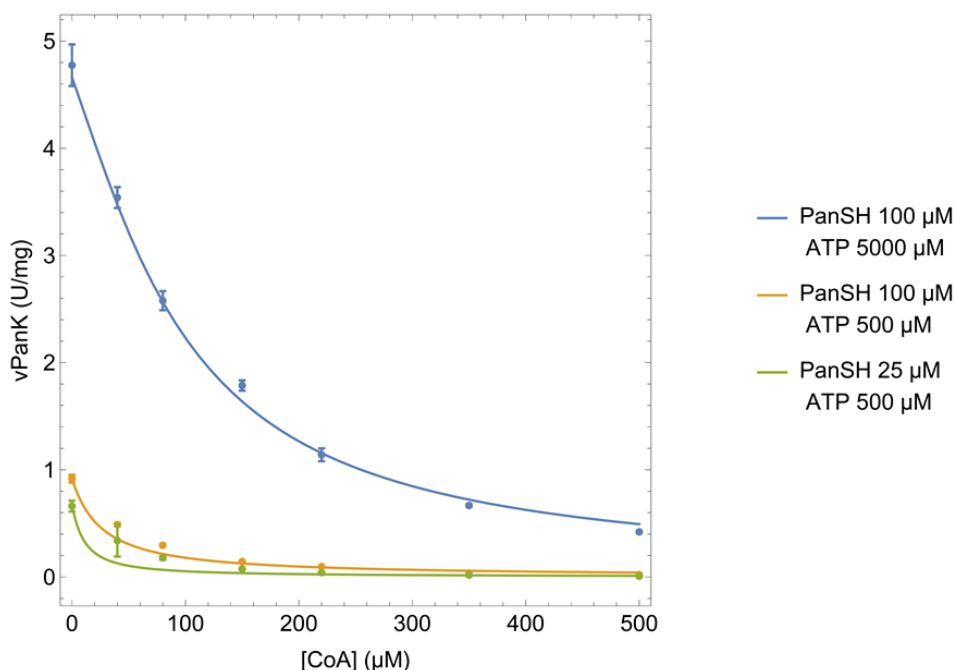


Figure 4.3: Inhibition of *EcPanK* activity by CoA. Initial rates were determined with the PK/LDH coupled assay containing 0.005 mg/ml *EcPanK*, 0.01 U/ $\mu$ l PK, 0.01 U/ $\mu$ l LDH, 0.3 mM NADH, 0.5 mM PEP, 50 mM Tris buffer pH 7.6, 20 mM KCl, 10 mM MgCl<sub>2</sub> and 250  $\mu$ M TCEP (or 1 mM TCEP for the 766  $\mu$ M PanSH reaction). 1 Unit = 1  $\mu$ mol PanSH consumed per minute at 37°C. Assay data is represented by the dots and represent the mean of triplicate determinations with the error bars denoting the standard deviation. Solid lines represent the rate profiles obtained by performing a global fit of Eq. 4.1 to the data.

Table 4.1: Kinetic parameters of *EcPanK*. Parameters were determined by performing a global fit of Eq. 4.1 to all the initial rate assay data sets. Errors represent the standard error of parameters obtained by the fit.

Parameter	Estimate and Standard Error
$V_M$	$16.67 \pm 0.89$ U/mg
$K_{ATP}$	$2696 \pm 547$ $\mu$ M
$K_{PanSH}$	$112.7 \pm 11$ $\mu$ M
$K_{i_{PanSH}}$	$33.16 \pm 5.6$ $\mu$ M
$K_{i_{CoA}}$	$7.692 \pm 1.1$ $\mu$ M
$\alpha$	$15.04 \pm 3.1$
$\beta$	$0 \pm 0$

A few points regarding the parameters obtained in this manner should be highlighted. First, the value for  $K_{ATP}$  seems high if it is considered similar to a  $K_M$  value. However, due to the cooperative binding of ATP this is not the case, and the value of the parameter should be

adjusted by taking into account the value of  $\alpha$ . This would similarly be the case for the value of  $K_{PanSH_i}$ ; however, the best fit was obtained when  $\beta$  was estimated to be zero and  $K_{PanSH}$  as 112.7  $\mu$ M. This implies a very low affinity for PanSH when both subunits have ATP bound which suggests that the scenario where PanSH is bound by both subunits along with ATP is not observed. With  $\beta$  estimated as zero, Eq. 4.1 reduces to Eq. 4.2.

$$v_{PanK} = \frac{e_{PanK} \cdot V_M \cdot \frac{ATP}{K_{ATP}} \cdot \frac{PanSH}{K_{PanSH}} \left(1 + \alpha \cdot \frac{ATP}{K_{ATP}} + \frac{CoA}{K_{iCoA}} + \frac{PanSH}{K_{iPanSH}}\right)}{1 + 2 \cdot \frac{ATP}{K_{ATP}} \cdot \left(1 + \frac{PanSH}{K_{PanSH}}\right) + \alpha \cdot \left(\frac{ATP}{K_{ATP}}\right)^2 \left(1 + \frac{2 \cdot PanSH}{K_{PanSH}} + \left(\frac{CoA}{K_{iCoA}} + \frac{PanSH}{K_{iPanSH}}\right) \cdot \left(2 + \frac{CoA}{K_{iCoA}} + \frac{PanSH}{K_{iPanSH}} + \frac{2 \cdot ATP}{K_{ATP}} \cdot \left(1 + \frac{PanSH}{K_{PanSH}}\right)\right)\right)}$$

Eq. 4.2

#### 4.2.1.5 Confirming the $V_M$ for *EcPanK* under model conditions

While the initial rate kinetic assays performed using the PK/LDH assay in a microplate format were ideal for obtaining the various kinetic parameters as outlined in the previous section, we wanted to experimentally confirm the maximal rate ( $V_M$ ) under conditions identical to those that will be used for the *in vitro* reconstruction of the CoA salvage pathway. This was done for two reasons: First, in the reconstructed pathway reactions higher concentrations of *EcPanK* are typically used; we wanted to confirm that this change made no difference to the  $V_M$ . Second, for analysis of the progress of the reconstructed pathway an offline assay will be used, specifically the HPLC-based assay described in Chapter 3. We therefore wanted to ensure that the two assays gave the same result.

To this end, PanSH conversion reactions were performed by incubation with two different concentrations of *EcPanK*. PanSH and PPanSH concentrations were measured at various time points during the incubation by using the method that was developed in Chapter 3 to yield progress curves of the conversion reaction (Figure 4.4). The PanSH consumption rate and PPanSH production rate were then used to calculate  $V_M$  by fitting Eq. 4.1 to the data. Time is not explicit in the equation because analytical integration was not performed in order to fit the equation. Instead, numerical integration of the Eq. 4.1 was carried out by a minimized function in Mathematica to find the optimal parameter values that gave the best fit to the progress curve of the PanSH conversion reaction. This gave a value of 47.3 U/mg, which is three-fold higher than the value of ~16.7 U/mg obtained from the initial rate kinetic assay data (Table 4.1).

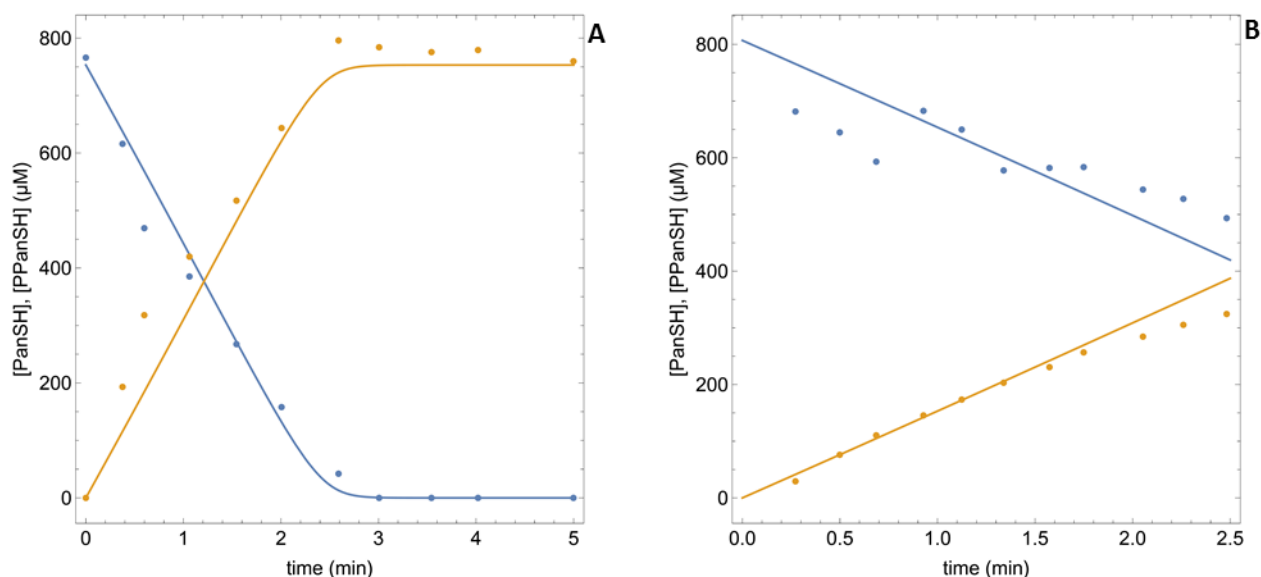


**Figure 4.4:** Conversion of PanSH to PPanSH by EcPanK. ● PanSH ● PPanSH; PanSH conversion reactions contained 0.02 mg/ml (A) and 0.01 mg/ml (B) EcPanK, 766  $\mu\text{M}$  PanSH 0.01 U/ $\mu\text{l}$  PK, 1.8 mM PEP, 50 mM Tris buffer pH 7.6, 20 mM KCl, 10 mM  $\text{MgCl}_2$  and 1 mM TCEP. A  $V_M$  of 47.3 U/mg was estimated by fitting Eq. 4.1 to the progress curves. 1 Unit = 1  $\mu\text{mol}$  PanSH consumed per minute at 37°C.

We considered two possible reasons for the differences in obtained  $V_M$  values, the first of which was that the coupling enzymes were limiting the rate in the continuous assay. In order to ensure that this was not the case, three additional assays were performed with 0.5, 0.75, and 1.25 equivalents of the amount of EcPanK used in the original assay; all other components were kept constant. If coupling enzymes are not limiting the observed  $V_M$ , it is expected that the  $V_M$  obtained for the different equivalents of EcPanK should correspond to 50%, 75% and 125% respectively of the originally determined  $V_M$  value taken as 100%. However, to simplify the analysis the activity with the different equivalents of EcPanK was measured at a single saturating concentration of PanSH (766  $\mu\text{M}$ ) at a fixed concentration of 5 mM ATP and the values compared (Figure 4.5). These show a clear linear relationship, indicating that the coupling reactions were not limiting the observed  $V_M$  in the initial rate kinetic studies performed at 0.005 mg/ml EcPanK.

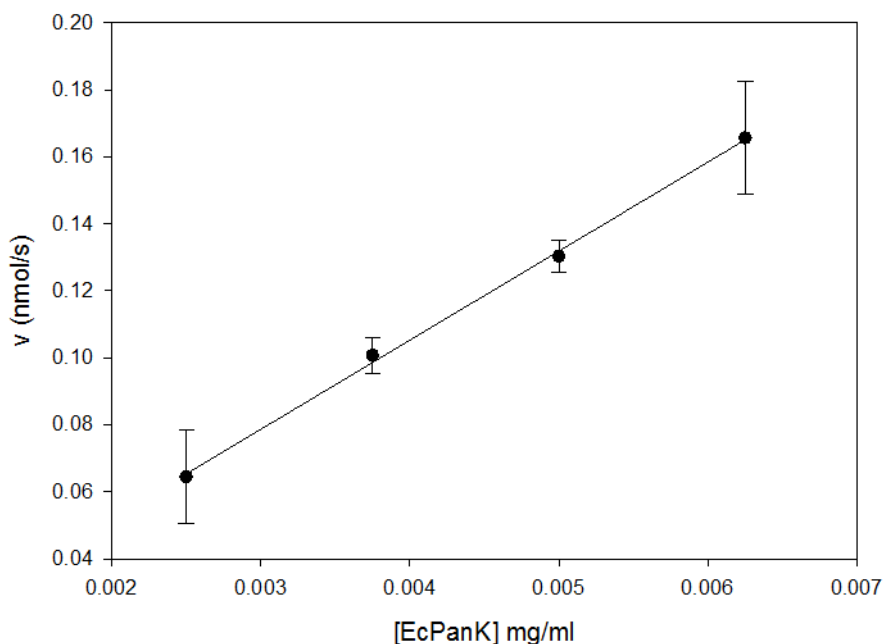
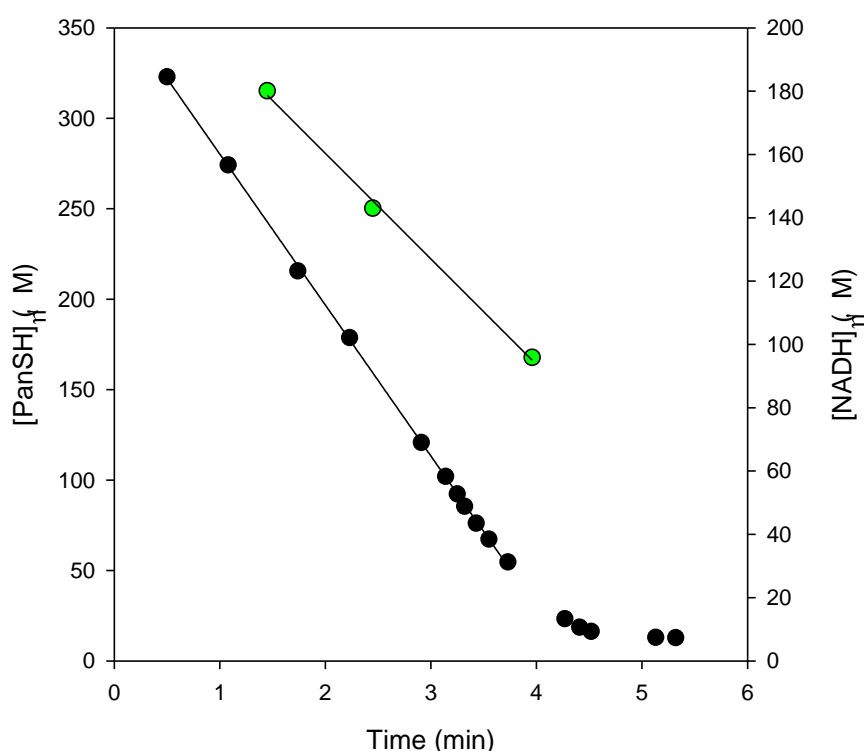


Figure 4.5: Activity of various concentrations of *EcPanK*. Rates were measured at four different *EcPanK* concentrations while all other assay components were kept constant at 766  $\mu\text{M}$  PanSH, 5 mM ATP, 0.01 U/ $\mu\text{l}$  PK, 0.01 U/ $\mu\text{l}$  LDH, 0.3 mM NADH, 0.5 mM PEP, 50 mM Tris buffer pH 7.6, 20 mM KCl, 10 mM  $\text{MgCl}_2$  and 1 mM TCEP. A linear relationship between the measured rates and the concentration of *EcPanK* was observed ( $R^2 = 0.9457$ ) which indicate that the coupling reactions do not limit the observed  $V_M$  in assays performed at 0.005 mg/ml PanK. Data-points represent the mean of triplicate determinations with the error bars denoting the standard deviation

We next considered that the different  $V_M$  values were due to inherent differences in the assays. All kinetic assays were performed in a 96-well plate format in a total volume of 300  $\mu\text{l}$ , and analysed by spectrophotometry. The PanSH conversion reactions were performed in a larger volume (1.1 ml) and was analysed off-line by HPLC analysis. To directly compare the two assays, both techniques were used to determine the reaction rate in the same sample. To achieve this, a reaction was set up to contain 0.005 mg/ml *EcPanK*, 5mM ATP and 400  $\mu\text{M}$  PanSH with coupling enzymes and other reaction components kept the same as in the previous kinetic assays. The reaction was performed in a 1 ml cuvette with a pathlength of 1 cm to avoid the need for a pathlength correction as is required when the assay is performed in 96-well plates. This made it possible to measure the decrease in absorbance at 340 nm while at the same time intermittently removing aliquots from the reaction mixture to determine the PanSH and PPanSH content by HPLC. The reaction mixture was therefore treated in a manner identical to the previous assays, except for the maintenance of temperature: like the previous assays the reaction mixture was heated up to 37°C before the reaction was initiated, but the temperature could not be maintained thereafter due to instrument limitations. While this factor would not influence the comparison

of the two assays, it did mean that the absolute value of the determined rates could not be used. The results of these combined assays are shown in Figure 4.6. The decrease in PanSH concentration as measured by the HPLC method is shown together with the decrease in NADH concentration as measured by the spectrophotometer and it can be seen that very similar rates are obtained for the two methods of analysis with measured rates of 9.69 U/mg and 9.54 U/mg respectively. Although 0.3 mM NADH was added to the reaction mixture, the first measurement at 340 nm could only be performed more than a minute after the reaction was initiated and therefore the concentration of NADH had decreased to 180  $\mu$ M when the first measurement was taken.



*Figure 4.6: Progress curve of an EcPanK reaction measured by spectrophotometry and HPLC. 0.005 mg/ml EcPanK was incubated with 5mM ATP, 400  $\mu$ M PanSH, 0.01 U/ $\mu$ l PK, 0.01 U/ $\mu$ l LDH, 0.3 mM NADH, 0.5 mM PEP, 50 mM Tris buffer pH 7.6, 20 mM KCl, 10 mM MgCl<sub>2</sub> and 1 mM TCEP. ● PanSH concentration measured by HPLC; ● NADH measured by spectrophotometry. A similar reaction rate is measured by both techniques.*

We concluded that the discrepancy in rates observed between kinetic assays performed in a 96-well plate and the rates measured in conversion reactions by progress curve analysis with HPLC, was due to the difference in reaction volume, since when it is kept constant identical reaction rates are measured. Consequently, we opted to use the  $V_M$  for EcPanK determined by fitting Eq. 4.1 to the progress curve data from the PanSH conversion

reactions (Figure 4.4), as the conditions used for this reaction is identical to those that will be used for the time course analyses of the reconstituted CoA salvage pathway.

In summary: a parameterized rate equation for the *EcPanK* reaction was established by first deriving a rate equation (Eq. 4.1) based on what is known about the enzyme mechanism from the literature. Kinetic characterization of *EcPanK* was performed with a spectrophotometric assay to determine all parameters by performing a global fit of Eq 4.1. All parameters were determined in this manner except for the  $V_M$  that was fitted to progress curves of PanSH conversion reactions performed at different concentrations of *EcPanK*.

#### 4.2.1.5 Validation of *EcPanK* rate equation

To validate the parameterized rate equation of *EcPanK*, two additional PanSH conversion reactions were performed, one at a lower enzyme concentration of 0.005 mg/ml, and the other at 0.02 mg/ml but in the presence of 100  $\mu$ M CoA. Both reactions were performed in the presence of 5 mM ATP. Progress curves of these reactions are well predicted by the *EcPanK* rate equation, although a better fit is possible (Figure 4.7). We considered the predictions sufficiently close for inclusion of the rate equation in the system model that would be validated independently upon completion.

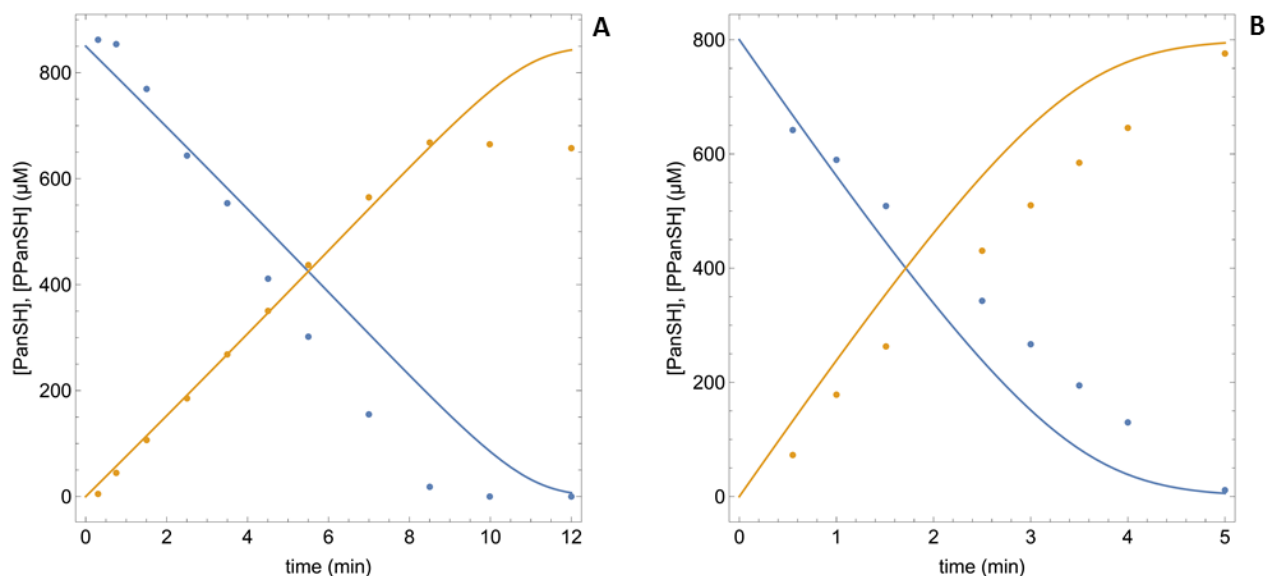


**Figure 4.7: Conversion of PanSH to PPanSH by *EcPanK*.** ● PanSH ● PPanSH; PanSH conversion assays were performed at 5 mM ATP and 0.005 mg/ml *EcPanK* (A) and 0.02 mg/ml *EcPanK* with 766  $\mu$ M PanSH, 0.01 U/ $\mu$ l PK, 1.8 mM PEP, 50 mM Tris buffer pH 7.6, 20 mM KCl, 10 mM MgCl<sub>2</sub> and 1 mM TCEP in the presence of 100  $\mu$ M CoA (B). Dots represent concentrations measured. The lines represent the rate equation predictions for the progress curves and were not fitted to the data.

## 4.2.2 EcPPAT kinetics

### 4.2.2.1 Literature survey of the kinetic parameters of EcPPAT

PPAT catalyses the reversible adenylation of PPanSH yielding DePCoA and pyrophosphate. EcPPAT was the second enzyme in the CoA biosynthesis pathway to be cloned and characterized.<sup>3</sup> A comprehensive kinetic study of EcPPAT was performed by Miller *et al.* to elucidate its kinetic mechanism and parameters by steady-state kinetic analysis.<sup>4</sup> The complete set of kinetic parameters that were determined is summarized in Table 4.2. It should be highlighted that although Miller *et al.* reported a low  $K_M$  of  $4.7 \pm 0.5$   $\mu\text{M}$  for PPanSH, an earlier study reported a much larger value of  $119.8 \pm 30.4$   $\mu\text{M}$ , creating some uncertainty about the enzyme's affinity for PPanSH.<sup>5</sup> Miller *et al.* also studied the inhibition of both the forward and reverse reactions, with  $K_i$  values of between 10-120  $\mu\text{M}$  being determined depending on which substrate was being varied. No inhibitory effect was observed with several acyl-CoAs, including acetyl-CoA, at concentrations up to 500  $\mu\text{M}$ .

Table 4.2 Kinetic characterization data for *E. coli* PPAT as determined by Miller *et al.*<sup>4</sup>

Substrate	Assay direction	$K_M$ ( $\mu\text{M}$ )	$k_{\text{cat}}$ ( $\text{s}^{-1}$ )	$k_{\text{cat}} / K_M$ ( $\text{s}^{-1} \text{mM}^{-1}$ )
PPanSH	Forward	$4.7 \pm 0.5$	$1.37 \pm 0.03$	$(2.9 \pm 0.1) \times 10^5$
ATP	Forward	$220 \pm 10$	$1.59 \pm 0.01$	$(7.1 \pm 0.2) \times 10^3$
DePCoA	Reverse	$17 \pm 2$	$1.4 \pm 0.1$	$(4.4 \pm 0.3) \times 10^4$
Pyrophosphate	Reverse	$230 \pm 10$	$1.4 \pm 0.1$	$(6.1 \pm 0.4) \times 10^3$

Finally, the authors also measured the EcPPAT equilibrium constant at various starting concentrations of substrate. Equilibrium constants between 1.2 and 2 were reported. These constants were determined by measuring the concentrations of ATP and DePCoA by HPLC using UV detection at 260 nm, with ATP eluting in the void volume. Due to the low sensitivity of the detection technique and the possibility that the ATP co-eluted with other ATP-degradation products, these equilibrium constants should be investigated again.

### 4.2.2.2 EcPPAT mechanism and proposed rate equation

From their kinetic studies, Miller *et al.* deduced that EcPPAT has a random bi-bi mechanism whereby a ternary complex is formed that consists of enzyme and both substrates, ATP and PPanSH.<sup>4</sup> DePCoA binding was shown to be competitive with both ATP and PPanSH binding, while pyrophosphate binding was competitive with ATP binding. These findings are

in agreement with what would be expected based on the chemical reaction catalysed by PPAT. Additionally, CoA binding was found to be competitive with PPanSH, ATP and DePCoA binding. Structural studies indicate that CoA exerts its inhibitory effect on *Ec*PPAT by binding to the same site as DePCoA but in a different mode. Only the 5'-phosphate groups of DePCoA and CoA occupy the same space. The 3'-phosphate group of CoA causes its adenylyl moiety to bind to a different site than that of DePCoA.

Taking all the available information together, we decided to use a general rate equation that describes a standard reversible reaction to describe the *Ec*PPAT activity (Eq. 4.3). We decided not to include the inhibition of CoA into the rate equation because the primary focus of this study was the impact of CoA inhibition on PanK, and consequently we wanted to first exclude the effects that CoA might have on the other pathway enzymes. Also the inhibition of PPAT by CoA has little physiological relevance as a control point in the pathway due to reversibility of the reaction. Therefore we opted to use the simplest rate equation that could describe the enzyme, and we considered it the best starting point for inclusion in the pathway model.

$$v_{PPAT}(t) = \frac{e_{PPAT} \cdot V_{M_{forward}} \left( \frac{ATP(t) \cdot PPanSH(t)}{K_{ATP} \cdot K_{PPanSH}} - \frac{DePCoA(t) \cdot PP_i(t)}{K_{DePCoA} \cdot K_{PP_i}} \right)}{\left( \frac{PPanSH(t)}{K_{PPanSH}} + 1 \right) \cdot \left( \frac{ATP(t)}{K_{ATP}} + \frac{PP_i(t)}{K_{PP_i}} + 1 \right) + \frac{DePCoA(t) \left( \frac{PP_i(t)}{K_{PP_i}} + 1 \right)}{K_{DePCoA}}} \quad \text{Eq. 4.3}$$

#### 4.2.2.3 Kinetic parameters of *Ec*PPAT included in the rate equation

The  $K_M$  values reported by Miller *et al.* for ATP, DePCoA and  $PP_i$  (Table 4.3) were used to parameterize this rate equation. However, since an earlier study of *Ec*PPAT reported a much larger  $K_M$  for PPanSH ( $4.7 \pm 0.5 \mu\text{M}$  vs.  $119.8 \pm 30.4 \mu\text{M}$ ) we chose to calculate this parameter using the Haldane relation (Eq 4.4). This relationship can be used to calculate one of the kinetic constants ( $K_{PPanSH}$ ) by substituting the equilibrium constant ( $K_{eq}$ ).

$$K_{eq} = \frac{V_f \cdot K_{DePCoA} \cdot K_{PP_i}}{V_r \cdot K_{PPanSH} \cdot K_{ATP}} \quad \text{Eq. 4.4}$$

We determined the  $K_{eq}$  and  $V_M$  independently by performing progress curve analysis of equilibrium approximation reactions. Since we could not measure ATP and  $PP_i$  concentrations in these reactions equal amounts of ATP and PPanSH (or ADP and

DePCoA) were used for the incubations as they react in a 1:1 ratio. These reactions were performed by incubating 0.05 mg/ml *EcPPAT* with either 500  $\mu$ M PPanSH and 500  $\mu$ M ATP (substrates of the forward reaction), or 500  $\mu$ M DePCoA and 500  $\mu$ M PP<sub>i</sub> (substrates of the reverse reaction). The progress curves were followed as the reactions approached equilibrium. Equation 4.3 was fitted to the experimental data shown in Figure 4.8 and values of 16.5 U/mg and 1.25 were obtained for the  $V_M$  and  $K_{eq}$  respectively from these fits.

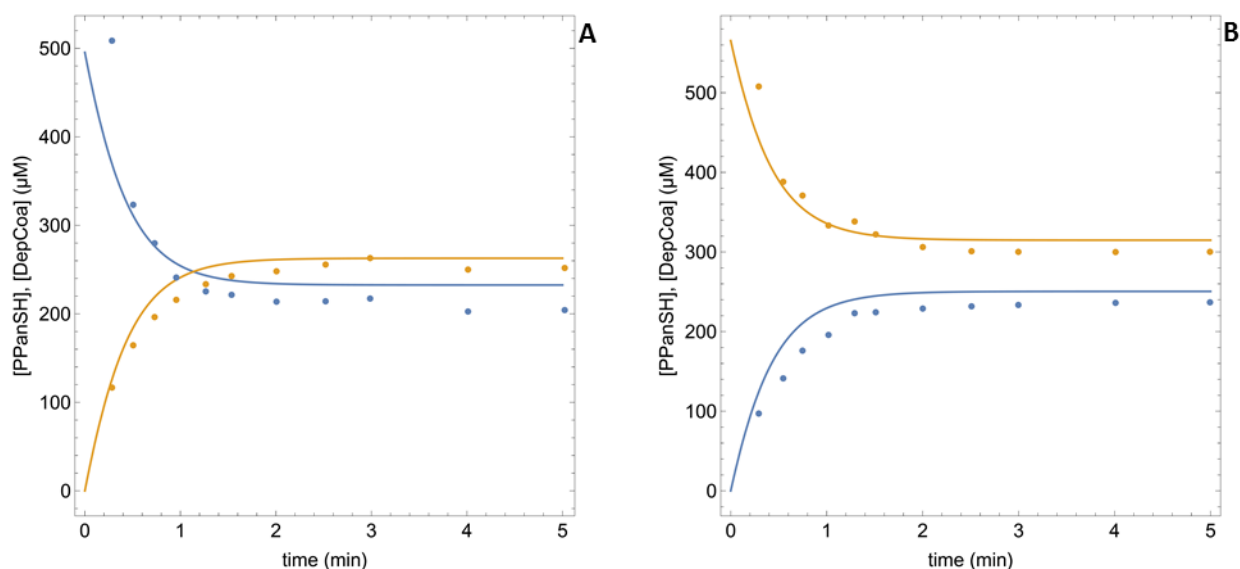


**Figure 4.8:** *EcPPAT* approach to equilibrium. ● PPanSH ● DePCoA. Reactions were performed at 0.05 mg/ml *EcPPAT* with either 500  $\mu$ M PPanSH and 500  $\mu$ M ATP (**A**) or 500  $\mu$ M DePCoA and 500  $\mu$ M PP<sub>i</sub> (**B**) in 50 mM Tris-HCl buffer (pH 7.6), 20 mM KCl and 10 mM MgCl<sub>2</sub>. Dots represent concentrations measured and the lines represent the fitted rate equation.

The Haldane relation was then used to determine the  $K_M$  for PPanSH. The  $K_{eq}$  determined from the equilibrium approximation reactions was used along with equal maximal rates for the forward and reverse reactions as suggested by Miller *et. al.* The  $K_M$  for PPanSH was calculated as 14.2  $\mu$ M, slightly higher than the value of 4.7  $\mu$ M reported by Miller *et al.*<sup>4</sup> A summary of the kinetic parameters used to parameterize the rate equation of *EcPPAT* is presented in Table 4.3.

Table 4.3: *EcPPAT* kinetic parameters. The binding constant for PPanSH was determined from the Haldane relation with an equilibrium approximation reaction.

Parameter	Estimate	Source
$K_{ATP}$	$220 \pm 10$	Miller et. al. <sup>4</sup>
$K_{PPanSH}$	$4.7 \pm 0.5$	Miller et. al. <sup>4</sup>
$K_{i_{DePCoA}}$	$17 \pm 2$	Miller et. al. <sup>4</sup>
$K_{PPanSH}$	14.2	This study

#### 4.2.2.4 Validation of the *EcPPAT* rate equation

The parameterized rate equation was validated by performing progress curve analysis of a PPanSH conversion reaction to test the model's prediction of the conversion of PPanSH to DePCoA. To be able to perform this reaction, excess pyrophosphatase was added to the reaction mixtures. This enzyme cleaves the pyrophosphate that is produced in the forward reaction, thereby making the reaction irreversible. Experimental data of the progress curve is shown in Figure 4.9 along with the progress curve predicted by the rate equation, with the amount of pyrophosphate formed set to zero. The rate equation predicted the experimental data very well, and was therefore used for inclusion in the model of the CoA salvage pathway.

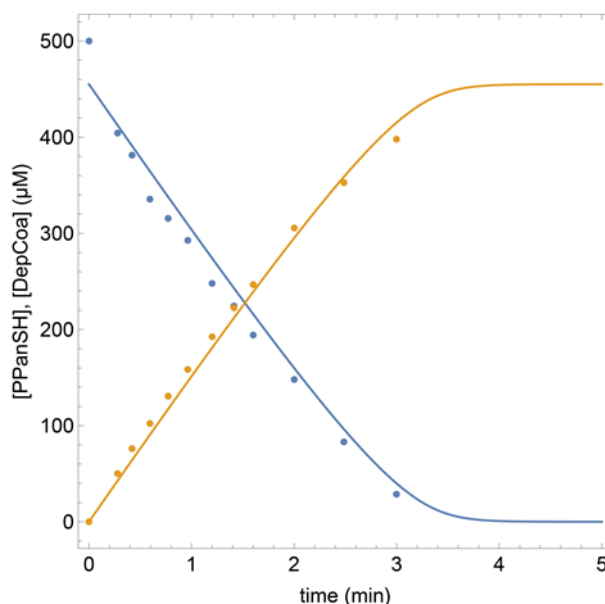


Figure 4.9: Conversion of PPanSH to DePCoA by *EcPPAT*. ● PPanSH ● DePCoA; Reactions were performed at 0.01 mg/ml *EcPPAT* with 50 mM Tris-HCl buffer (pH 7.6), 20 mM KCl and 10 mM MgCl<sub>2</sub>, 1 mM TCEP, 500 μM PPanSH and 5 mM ATP in the presence of 0.04 U/μl pyrophosphatase to make the reaction irreversible and to test the model's prediction of the conversion of PPanSH to DePCoA by *EcPPAT*. Dots represent concentrations measured. The lines represent the rate equation predictions for the progress curves and were not fitted to the data.

### 4.2.3 *EcDPCK* kinetics

#### 4.2.3.1 Overview of the current knowledge of the properties of *EcDPCK*

*EcDPCK* phosphorylates DePCoA in an ATP-dependent manner to yield CoA and ADP. Due to limited information available on *EcDPCK* there is uncertainty about its kinetic parameters, catalytic mechanism and whether structural movement of the protein occurs during catalysis as discussed in Chapter 1. High  $K_M$  values for DePCoA in the range of 650-740  $\mu\text{M}$  has been reported for *EcDPCK* in the literature.<sup>5,6,7</sup> The  $K_M$  for ATP was determined in only one of these studies and is reported to be 140  $\mu\text{M}$ .<sup>6</sup> Gel-filtration studies have showed that *EcDPCK* has a monomeric structure in solution.<sup>6,29,30</sup> Surprisingly, structural studies have shown *EcDPCK* to crystallize as a trimer in the presence of sulfate ions and gel-filtration experiments performed in the presence of 0.2 M ammonium sulfate confirmed the presence of both monomeric and trimeric forms under these conditions.<sup>29</sup> The role of quaternary structure in the activity of bacterial DPCKs was highlighted by kinetic studies of *Corynebacterium ammoniagenes* (Ca) DPCK performed in previous unpublished studies in our group. Initial rate assays led to a sigmoidal kinetic profile that was accurately described by the Hill equation indicating positive cooperativity was at play during the catalytic cycle. By fitting the Hill equation to the data a Hill coefficient of  $n \approx 3$  was calculated. This indicated that CaDPCK is most likely a trimer in solution. It also exhibited a much lower apparent  $K_M$  ( $K_M^{app}$ ) of  $46.6 \pm 3.81 \mu\text{M}$  for DePCoA vs. a  $K_M^{app}$  of  $1551 \pm 507$  for DePCoA determined for *EcDPCK* under the same conditions (using 0.7 mM ATP).

In light of these findings we conducted kinetic studies of *EcDPCK* to assess whether the presence of  $\text{MgSO}_4$  would have an effect on activity by promoting the formation of trimers. The affinity for DePCoA increased in the presence of 10 mM  $\text{MgSO}_4$  and the  $K_M^{app}$  was reduced from  $1551 \pm 507 \mu\text{M}$  to  $424 \pm 71 \mu\text{M}$  in combination with 0.7 mM ATP, with all other factors being kept constant. These results suggest that *EcDPCK* may assume a trimeric structure with a higher affinity for DePCoA than the monomer. The physiological significance of this sulfate induced increase in affinity is questionable because sulfate is not known to be present at such high concentrations in *E. coli* cells. Therefore we investigated if the same effect is seen in the presence of phosphate because it is known to be present at a concentration of 10 mM in *E. coli* and has a tetrahedral shape with two negative charges at physiological pH, similar to sulfate.<sup>31</sup> *EcDPCK* activity was assessed in Tris-HCl buffer, Tris-HCl buffer supplemented with 10 mM  $\text{MgSO}_4$  or 50 mM phosphate buffer using a range of DePCoA concentrations at fixed ATP concentrations of either 0.7 mM or 1.5 mM. The

resulting kinetic profiles are shown in Figure 4.10. A summary of the kinetic parameters (determined by fitting the Michaelis-Menten equation to the data) is shown in Table 4.4.

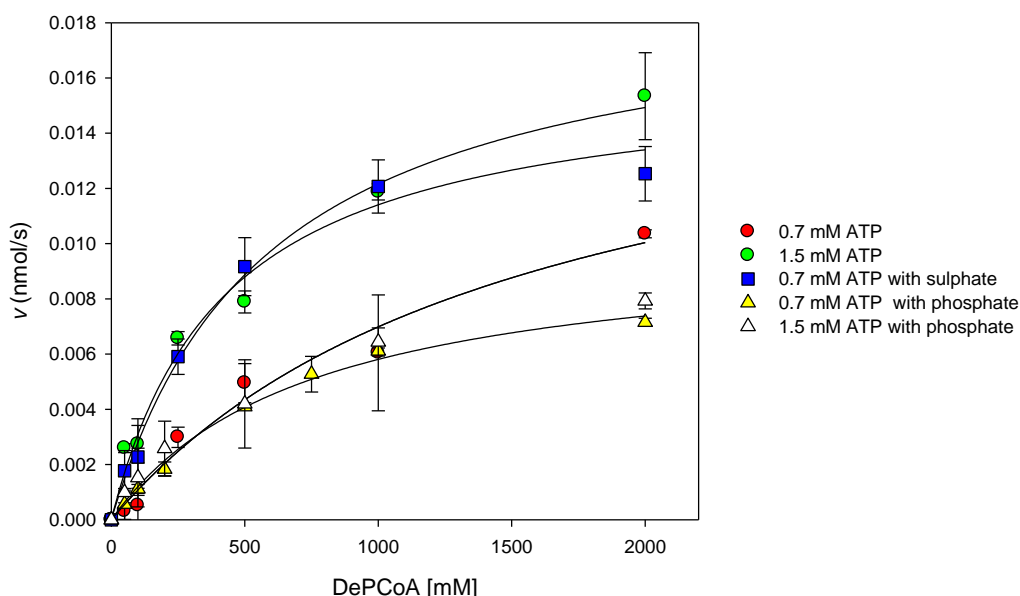


Figure 4.10: *EcDPCK* activity in the absence and presence of sulfate and phosphate. Initial rates were determined for increasing DePCoA concentrations at 0.7 mM ATP or 1.5 mM ATP in either Tris-HCl, Tris-HCl + MgSO<sub>4</sub> or phosphate buffer, all at pH 7.6 with 20 mM KCl and 10 mM MgCl<sub>2</sub>, 0.01 U/μl PK, 0.01 U/μl LDH with 0.005 mg/ml *EcDPCK*. Data-points represent the mean of triplicate determinations with the error bars denoting the standard deviation. The Michaelis-Menten equation was fitted to the data as indicated by the lines.

Table 4.4: Kinetic parameters of *EcDPCK* in the presence and absence of phosphate and sulfate

Enzyme	ATP Concentration	Buffer	$K_M^{app}$ (μM)	$k_{cat}$ (s <sup>-1</sup> )	$k_{cat}/K_M$ (mM <sup>-1</sup> .s <sup>-1</sup> )	<i>n</i>
<i>CαDPCK</i>	0.7 mM ATP	50 mM Tris-HCl, 10 mM MgCl <sub>2</sub> , pH 7.6	46.6 ± 3.8	2.52 ± 0.13	54.2 ± 34.3	2.59 ± 0.44
<i>EcDPCK</i>	0.7 mM ATP	50 mM Tris-HCl, 10 mM MgCl <sub>2</sub> , pH 7.6	1550 ± 510	0.59 ± 0.11	0.38 ± 0.21	-
<i>EcDPCK</i>	0.7 mM ATP	50 mM Tris-HCl, 10 mM MgSO <sub>4</sub> , pH 7.6	424 ± 71	0.54 ± 0.03	1.26 ± 0.47	-
<i>EcDPCK</i>	0.7 mM ATP	50 mM potassium phosphate, 10 mM MgCl <sub>2</sub> , pH 7.6	742 ± 86	0.33 ± 0.02	0.45 ± 0.19	-
<i>EcDPCK</i>	1.5 mM ATP	50 mM Tris-HCl, pH 7.6	589 ± 86	0.64 ± 0.04	1.08 ± 0.42	-
<i>EcDPCK</i>	1.5 mM ATP	50 mM potassium phosphate, 10 mM MgCl <sub>2</sub> , pH 7.6	651 ± 168	0.35 ± 0.02	0.53 ± 0.24	-

The results suggest that the presence of 50 mM phosphate does not have a major effect on *EcDPCK* activity. In fact, based on the lower  $k_{cat}$ -values it appears that phosphate reduces the activity. The  $K_M$  values are mostly unchanged which leads to lower specificity constants ( $k_{cat}/K_M$ ) in the presence of phosphate. Fitting the Hill equation to this data pointed to a Hill coefficient of  $n \approx 1$ , which suggests that trimerization and positive cooperativity most likely does not occur. These results indicate that phosphate does not modulate *EcDPCK* activity by inducing trimerization of the enzyme monomers. It seems that only the addition of sulfate caused an increased affinity for DePCoA but since this observation has limited physiological relevance it was not investigated further. Clearly the kinetic and catalytic mechanism of *EcDPCK* warrants further in-depth study, but such studies are beyond the scope of the study at hand.

#### 4.2.3.2 Proposed rate equation for *EcDPCK*

Due to the limited amount of information that is available on the *EcDPCK* catalytic mechanism and kinetic parameters we proposed to use a general irreversible product insensitive rate equation (Eq. 4.5) to describe the *EcDPCK* reaction. We opted for the product insensitive equation because no study conducted to date has suggested that CoA inhibits *EcDPCK* activity.

$$v_{DPCK}(t) = \frac{V_M (ATP(t) \cdot DePCoA(t))}{(K_{ATP} \cdot K_{DePCoA}) \left( \left( \frac{ATP(t)}{K_{ATP}} + 1 \right) \cdot \left( \frac{DePCoA(t)}{K_{DePCoA}} + 1 \right) \right)} \quad \text{Eq. 4.5}$$

#### 4.2.3.3 Kinetic parameters of *EcDPCK* included in the rate equation

We incorporated kinetic parameters reported in the literature for *EcDPCK* into the model as shown in Table 4.5. Although several values for  $K_{DePCoA}$  has been reported in the literature as outlined in Chapter 1 and described above, we decided to use the first value reported for this enzyme because we obtained a similar value of  $589 \pm 86 \mu\text{M}$  at 1.5 mM ATP (in Tris-HCl buffer, Table 4.4).

Table 4.5: Kinetic parameters of *EcDPCK* included in our model.

Parameter	Estimate	Source
$K_{ATP}$	140	Mishra <i>et. al.</i> <sup>6</sup>
$K_{DePCoA}$	645	Strauss <i>et. al.</i> <sup>5</sup>

The  $V_M$  of *EcDPCK* was estimated from the progress curves of two DePCoA conversion reactions. These reactions contained 0.1 mg/ml and 0.2 mg/ml respectively data is shown in Figure 4.11. Equation 4.5 was fitted to the experimental data, resulting in a relatively low  $V_M$  of 0.83 U/mg that was included in the model. Validation of the *EcDPCK* rate equation was not performed in isolation but rather evaluated upon reconstitution of the *E. coli* CoA salvage pathway.

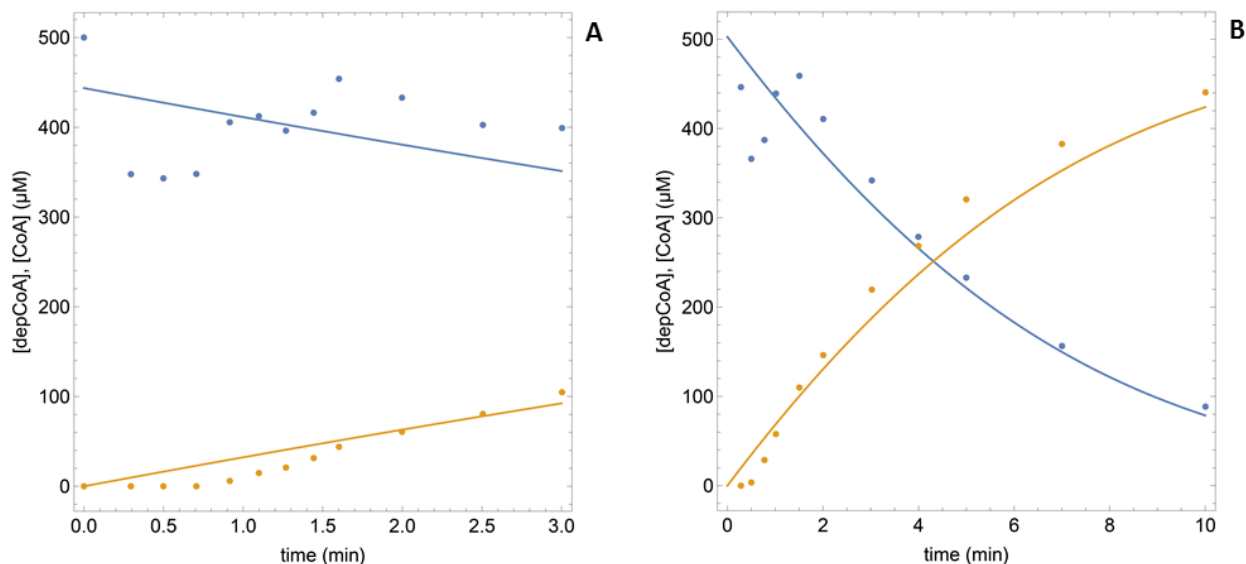


Figure 4.11: Conversion of DePCoA to CoA by DPCK. ● PPanSH ● DePCoA; Conversion reactions contained 0.1 mg/ml DPCK (A) and 0.2 mg/ml DPCK (B) in 50 mM Tris-HCl buffer (pH 7.6) with 20 mM KCl, 10 mM MgCl<sub>2</sub>, 1 mM TCEP, 18 mM PEP and 0.04 U/μl PK. A  $V_M$  of 0.83 U/mg was obtained by fitting Eq. 4.5 to the data.

#### 4.2.4 In vitro reconstitution of the CoA salvage pathway and validation of the model

The parameterized rate equations established for the individual reactions were assembled to constitute our system model of the CoA salvage pathway. Next, time course analyses of the reconstituted pathway were followed under various conditions of initial metabolite concentrations and enzyme ratios. Not only does time course analysis provide the information to visually interpret control of the pathway but it is also used to validate the model for system analysis; these results are presented in the following subsections.

##### 4.2.4.1 Reactions with equivalent amounts of *EcPanK*, *EcPPAT* and *EcDPCK*

The CoA salvage pathway was reconstituted by incubation of the three purified CoA salvage biosynthesis enzymes with PanSH and excess ATP. ATP levels could effectively be kept constant with the addition of an ATP recycling system consisting of pyruvate kinase and

phosphoenolpyruvate. In the first set of experiments, equal amounts of each of the three enzymes were used in the reaction mixture, and the amount of CoA present initially was increased. Our goal with these experiments was to establish if under such simple conditions it would already be possible to determine if PanK limits the amount of CoA produced, and whether the initial CoA concentration amplifies the control by PanK as proposed by much of the literature published to date.

The conditions tested were as follows: *EcPanK*, *EcPPAT* and *EcDPCK* at 0.1 mg/ml each, 5 mM ATP (kept constant by addition of 1.8 mM PEP and 0.04 U/ $\mu$ l PK) and A) 766  $\mu$ M PanSH; B) 525  $\mu$ M PanSH with 225  $\mu$ M DePCoA; C) 575  $\mu$ M PanSH with 225  $\mu$ M CoA; D) 383  $\mu$ M PanSH with 225  $\mu$ M DePCoA and 225  $\mu$ M CoA. Reaction mixtures were incubated at 37 °C and sampled at regular intervals to determine the composition thereof (using the analysis method described in Chapter 3) in a time-dependent fashion. Reactions were followed for 1 hour, at which point all the substrate was found to have been converted to CoA. The resulting time course profiles (Figure 4.12) show that under these conditions the consumption of PanSH is very fast, with complete depletion within two to three minutes. In the presence of CoA, with a small but noteworthy reduction in rate of conversion is observed (Figure 4.12, C and D). The concentrations of PPanSH and DePCoA are essentially kept in equilibrium by PPAT, except for the first minutes when there is a rapid influx of PanSH. From these results it is evident that under these conditions CoA production is not limited by PanK due to its fast rate. Instead, it seems to be limited at the last step, i.e. by *EcDPCK*, as the rate of conversion of DePCoA to CoA controls the rate of CoA production.

The assembled model of the CoA salvage pathway was used to predict the various time courses under the same conditions; these predictions are represented by the solid lines in various panels in Figure 4.12. The lines therefore do not represent a fit of the data, but the model predictions. The model was able to predict the time course of conversion of PanSH to CoA very well. Specifically, the dynamics of PanSH, DePCoA and CoA were predicted very accurately, with the exception of the DePCoA concentration changes during the first few minutes of the reaction. This might be partly due to the concentrations of PPanSH consistently being slightly underpredicted by the model, i.e. the model predicted that the conversion of PPanSH to DePCoA would be faster than what was found in reality. A possible reason for this could be the exclusion of the inhibitory effect of CoA on the PPAT kinetic mechanism. However, since the predicted PPanSH to DePCoA conversion rate is faster than is found in reality even in the absence of CoA (Figure 4.12A), this cannot be the only

factor at play. Nonetheless, as the rate of CoA production is predicted well, these experiments provide good validation of the model for use in a systems analysis.

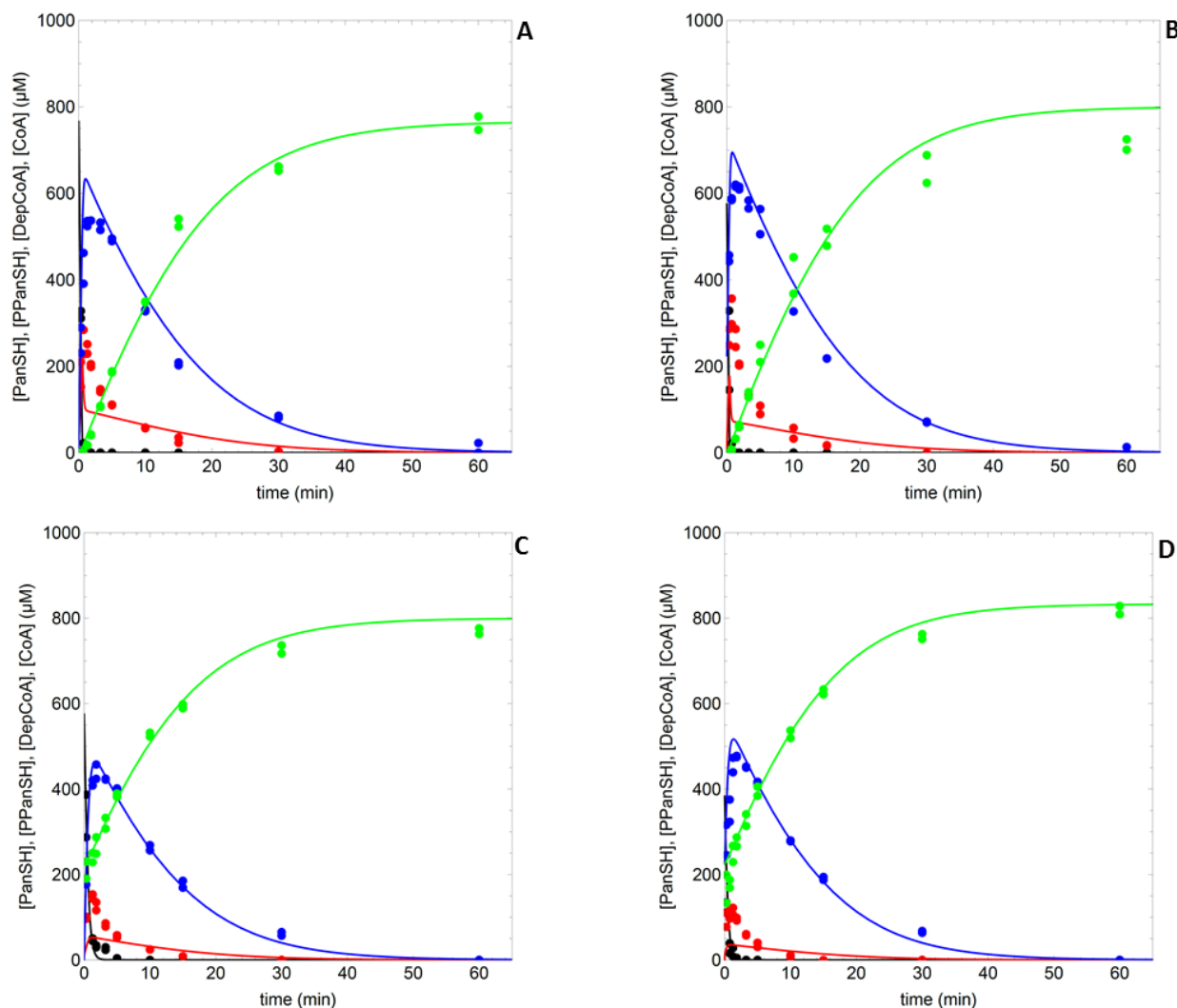


**Figure 4.12:** Time course of conversion of PanSH to CoA by the reconstituted CoA salvage system under various starting conditions of substrate and product. ● PanSH ● PPanSH ● DepCoA ● CoA; *EcPanK*, *EcPPAT* and *EcDPCCK* were present at equal concentrations of 0.1 mg/ml with 5 mM ATP and 50 mM Tris-HCl buffer (pH 7.6), 10 mM MgCl<sub>2</sub>, 20 mM KCl, 1.75 mM TCEP, 0.04 U/μl pyruvate kinase, 1.8 mM PEP and variable initial concentrations of other reactants: (A) 766 μM PanSH, other reactants 0 μM; (B) 525 μM PanSH, 225 μM DepCoA, other reactants 0 μM; (C) 575 μM PanSH, 225 μM CoA, other reactants 0 μM; (D) 383 μM PanSH, 225 μM DepCoA, 225 μM CoA, other reactants 0 μM. Dots represent concentrations measured of the intermediates and lines are the model simulations of the respective reaction conditions and were not fitted to the data. Reactions were performed at least in duplicate, with both data sets being shown for each conversion profile.

#### 4.2.4.2 Reduced *EcPanK* concentrations in reconstitution of the CoA salvage pathway

The reactions in which equivalent amounts of each CoA salvage enzyme were present and excess ATP were used, indicated that *EcDPCK* controls the rate at which CoA is produced. Since many studies have pointed to *EcPanK* as the so-called “rate-limiting” enzyme in the pathway, we next investigated the conditions that would enable it to do so. The *EcPanK* concentration was decreased relative to the other enzymes, which were kept constant at 0.1 mg/ml, to test its effect on the CoA production rate. In the case in which the *EcPanK* concentration was reduced 10-fold reduction to 0.01 mg/ml, the rate of PanSH consumption was observed to be much slower as expected (approximately 10-fold slower) (Figure 4.13 A). However, this decreased rate in PanSH consumption only had a small effect on CoA synthesis, which showed production rates very similar to the rates observed previously. Only when the concentration of *EcPanK* was 20-fold lower (at 0.005 mg/ml) compared to that of *EcPPAT* and *EcDPCK*, was an effect on the rate of CoA production observed (Figure 4.13 B).

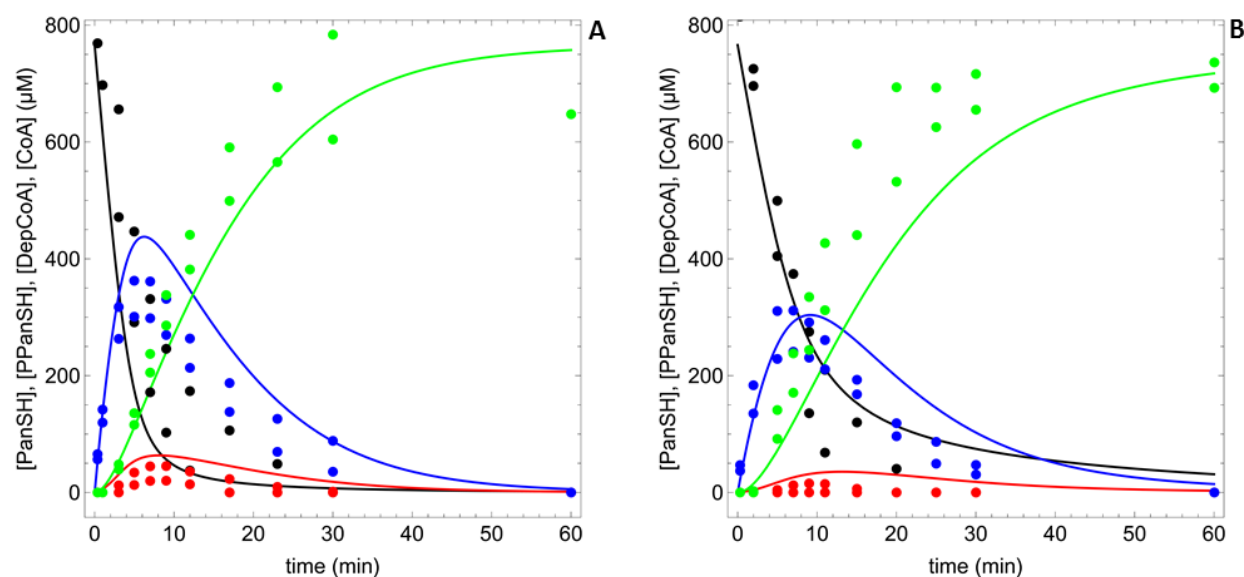


**Figure 4.13:** Time course of conversion of PanSH to CoA by the reconstituted CoA salvage system with a lower concentration of *EcPanK*. ● PanSH ● PPanSH ● DePCoA ● CoA; *EcPanK* concentrations were varied: (A) 0.01 mg/ml and (B) 0.005 mg/ml, with *EcPPAT* and *EcDPCK* kept constant at 0.1 mg/ml and with 50 mM Tris-HCl buffer (pH 7.6), 10 mM  $\text{MgCl}_2$ , 20 mM KCl, 1.75 mM TCEP, 0.04 U/ $\mu\text{l}$  pyruvate kinase, 1.8 mM PEP. Initial concentrations of 766  $\mu\text{M}$  PanSH and 5 mM ATP were used. Dots represent concentrations measured of the intermediates and lines are the model simulations for the time course of the reconstituted CoA salvage pathway and were not fitted to the data.

Overall the model predicts the data well although a better fit is possible (Figure 4.12). Experimental error is likely the cause of any discrepancy because some variability is also observed between the duplicate datasets of each of these two time course experiments.

#### 4.2.4.3 Reconstitution of the CoA salvage pathway with physiological ratios of the enzymes

Ultimately, we are interested in biochemical control of the rate of CoA production under physiological conditions. Ideally, this would be assessed by time course analysis of PanSH conversion to CoA by protein extracts from *E.coli*. Though many attempts were made, such time course profiles could not be obtained, presumably due to the very low expression levels of the three enzymes. This is consistent with the findings of a previous study of the *coaA* gene (that encodes PanK) which reported poor homology of this gene with the consensus *E. coli* promoter sequences and that the *coaA* coding sequence is populated largely by low usage codons.<sup>12</sup> This suggests that PanK is found in low abundance relative to the average *E. coli* protein. We therefore decided to again use purified proteins to reconstitute the reaction *in vitro* at concentrations that would allow us to effectively measure intermediates, but to combine the enzymes in a ratio that recapitulates the physiological conditions of the *E. coli* cytosol. To obtain the relative ratio of *EcPanK*, *EcPPAT* and *EcDPCK* values reported in the proteomics database *Version 4.0 of PaxDb: Protein abundance data, integrated across model organisms, tissues, and cell-lines* (PaxDb4) were used.<sup>32</sup> PaxDb4 is a comprehensive absolute protein abundance database which contains whole genome protein abundance information. It presents an integrated dataset of protein abundance by weighted averages of the data of numerous proteomics studies. The PaxDb4 integrated dataset reports the abundance of CoA salvage pathway proteins as follows: *EcPanK*, 14.2 ppm; *EcPPAT*, 148 ppm; *EcDPCK*, 7.84 ppm. This translates to a PanK:PPAT:DPCK ratio of approximately 2:20:1, which was the ratio of amount of enzymes used in the last set of time course analysis experiments.

For these experiments, enzyme quantities were defined as mg/ml rather than molar concentrations because the values reported in PaxDb4 are relative amounts and not relative concentrations. The *EcDPCK* concentration was fixed at 0.1 mg/ml, with the concentrations of the other enzymes adjusted accordingly. In the first case, 5 mM ATP (a relatively high amount) was used as before. Under these conditions, PanK was again found to rapidly consume the available PanSH, while PPAT is essentially in equilibrium for the duration of the time course of conversion (Figure 4.14 A). Consequently, the rate of CoA production is once again controlled by *EcDPCK*. To determine if this still is the case in the presence of CoA (i.e.

when feedback inhibition of PanK is possible) and also when the amount of ATP is lowered to levels closer to that expected to be found in exponentially growing *E. coli*, the experiment was repeated with 1.5 mM ATP and 320  $\mu\text{M}$  CoA (the concentration of the total CoA pool—including all major acyl-CoAs—in glucose fed *E. coli* was reported as 500  $\mu\text{M}$ .<sup>1</sup> (Figure 4.14 B). Although conversion of PanSH is much slower under these conditions, control of the CoA production rate was found to still lie with *EcDPCK*.

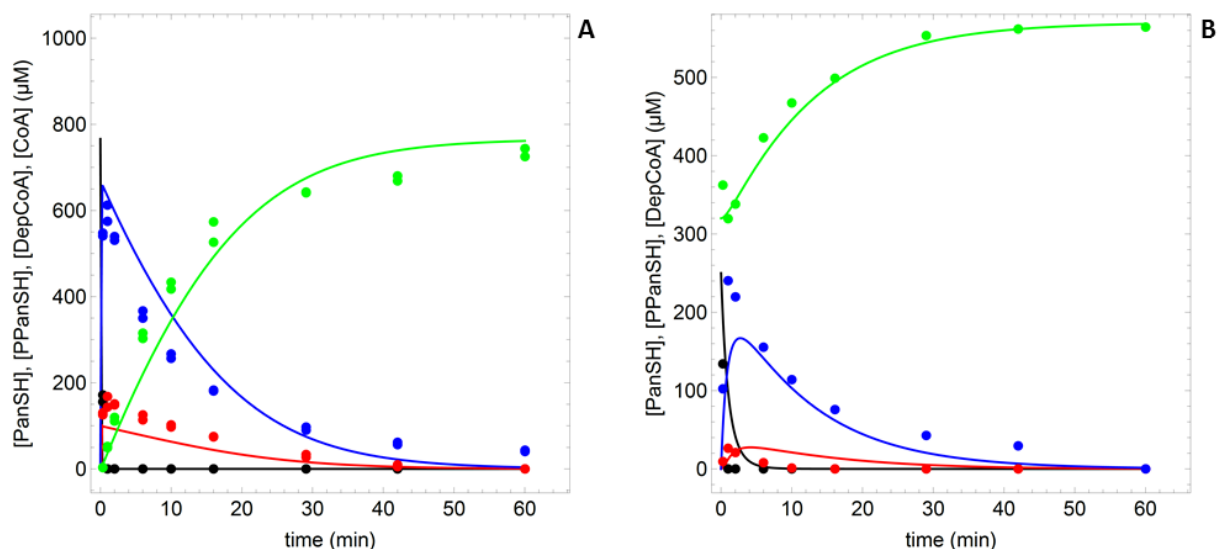


**Figure 4.14:** Time course of conversion of PanSH to CoA by the reconstituted CoA salvage system with physiological ratios of enzymes. ● PanSH ● PPanSH ● DePCoA ● CoA; *EcPanK*, *EcPPAT* and *EcDPCK* were present at physiological ratios of 0.2 mg/ml, 2 mg/ml, 0.1 mg/ml respectively with 50 mM Tris-HCl buffer (pH 7.6), 10 mM  $\text{MgCl}_2$ , 20 mM KCl, 1.75 mM TCEP, 0.04 U/ $\mu\text{l}$  pyruvate kinase, 1.8 mM PEP and variable initial concentrations of reactants: (A) 766  $\mu\text{M}$  PanSH, 5 mM ATP, other reactants 0  $\mu\text{M}$ ; (B) 250  $\mu\text{M}$  PanSH, 1.5 mM ATP, 320  $\mu\text{M}$  CoA, other reactants 0  $\mu\text{M}$ . Dots represent concentrations measured of the intermediates and lines are the model simulations for the time course of the reconstituted CoA salvage pathway and were not fitted to the data.

Model predictions describe these data sets well although a better fit is possible. From the results shown in Figure 4.14 A, it seems that activity of *EcPPAT* is slightly lower than predicted by the model with PPanSH concentrations higher than predicted and DePCoA concentrations lower than expected. The opposite is seen in the presence of CoA (Figure 4.14 B) where the rate of the PPAT reaction is slightly underestimated by the model with PPanSH concentrations lower than predicted and DePCoA concentrations higher than predicted by the model.

#### 4.2.4.4 Validation of the CoA salvage pathway model

Taking together all time course data collected from reactions where the CoA salvage pathway was reconstituted along with the predictions made by the model, we concluded that our computational model was able to predict each of the different reaction conditions tested with accurately. Thus, the model is validated for different enzyme concentrations and ratios and varying initial concentrations of reactants.

#### 4.2.5 Applying the model to evaluate the contribution of PanK to the control of the rate of CoA synthesis

Model predictions of the conversion of PanSH to CoA by the reconstituted salvage pathway were fairly accurate when different *EcPanK* concentrations were tested at fixed levels of *EcPPAT* and *EcDPCK*. Therefore, to test the effect of *EcPanK* on the CoA production directly, we simulated a range of *EcPanK* concentrations at constant concentrations of *EcPPAT* and *EcDPCK* (0.1 mg/ml). The time required for conversion of 95% of PanSH to CoA was taken as a measure of the conversion rate. Figure 4.15 shows the conversion rate as a function of *EcPanK* concentration and from this graph it becomes apparent that the concentration of *EcPanK* must be reduced to less than 10% (0.01 mg/ml) of the concentration of *EcPPAT* and *EcDPCK* before a marked effect on the conversion of PanSH to CoA is observed. Furthermore, the effect of CoA on the conversion rate was also tested and since CoA inhibits *EcPanK* it is expected that lowering this enzyme concentration would have a larger effect at increased concentrations of CoA. This is indeed observed as shown in Figure 4.15 but the effect of CoA does not appear to be very strong. For example, at a CoA concentration of 1 mM, lowering the *EcPanK* concentration to 20% of the concentration of the other enzymes only leads to a 1.5 fold increase in the time required for 95% conversion of PanSH to CoA. Therefore, under the conditions that we tested it seems that CoA is not such a strong inhibitor of *EcPanK* activity as is suggested in the literature.

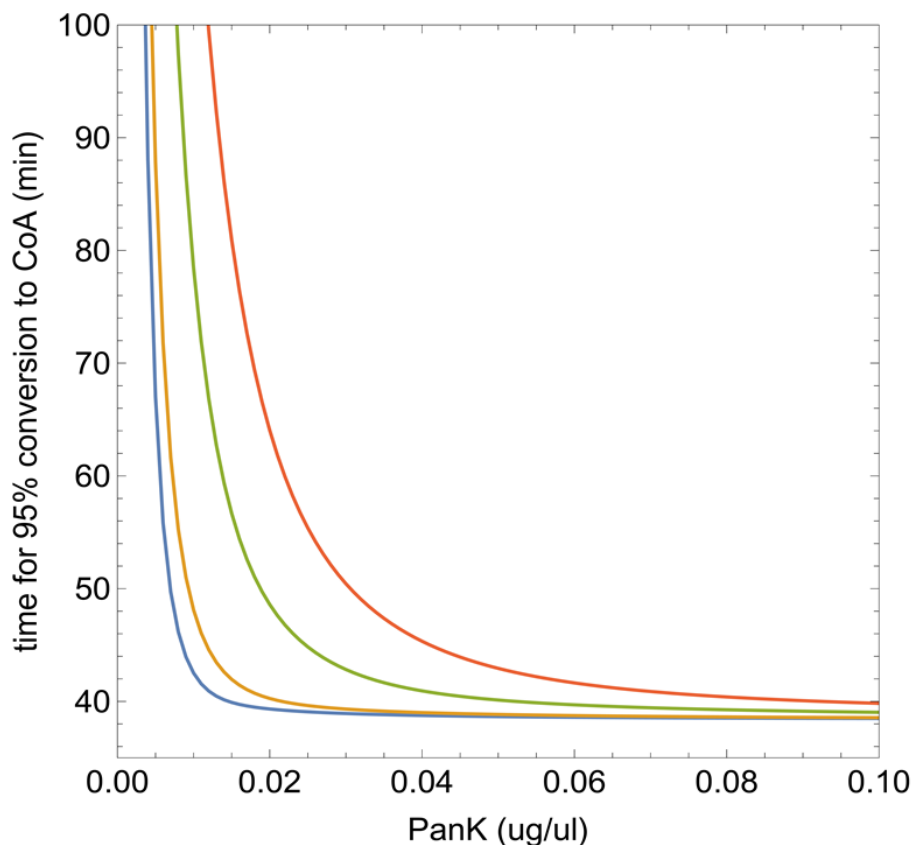


Figure 4.15: Conversion of PPanSH to CoA in the reconstituted system with different concentrations of *EcPanK* and CoA. PPAT and DPCK were kept constant at 0.1 mg/ml with 5 mM ATP and variable initial concentrations of CoA: — 0  $\mu$ M; — 100  $\mu$ M; — 500  $\mu$ M; — 1000  $\mu$ M

In addition, the control distribution of the CoA production rate was calculated by using MCA. It is clear that in the reactions where the CoA salvage pathway was reconstituted, a steady state is not reached and therefore we cannot apply a standard steady state control analysis. However, control analysis for the conversion to CoA can still be performed, specifically on the time period to 95% conversion of substrate to product as has been described in the literature for dynamic metabolic control analysis.<sup>33,34</sup> Control coefficients were calculated under different reaction conditions and are reported in Table 4.6. At equal concentrations of the three enzymes (A, Table 4.6), *EcDPCK* has full control over the conversion time and when the concentration of *EcPanK* is reduced 10-fold there is only a marginal increase in the control of *EcPanK* with the vast majority of control still residing with *EcDPCK* (B, Table 4.6). Only when the concentration of *EcPanK* is 10% of the concentrations of *EcPPAT* and *EcDPCK* and 1 mM of CoA is added does control shift to *EcPanK* (C, Table 4.6).

*Table 4.6: Control coefficients determined by dynamic control analysis*

	Reaction conditions	$C_{vPanK}^{t95\%}$	$C_{vPAT}^{t95\%}$	$C_{vDPCK}^{t95\%}$
A	0.1 mg/ml PanK, PPAT, DPCK	-0.003	-0.004	-0.992
B	0.01 mg/ml PanK, 0.1 mg/ml PPAT and DPCK	-0.272	-0.000	-0.728
C	0.01 mg/ml PanK, 0.1 mg/ml PPAT and DPCK, 1 mM CoA	-0.967	-0.000	-0.033
D	0.02 mg/ml PanK, 0.2 mg/ml PPAT, 0.01 mg/ml DPCK	-0.002	0.000	-0.997
E	0.02 mg/ml PanK, 0.2 mg/ml PPAT, 0.01 mg/ml DPCK, 320 $\mu$ M CoA	-0.007	0.000	-0.992

To evaluate the control of CoA production under physiological conditions, the control coefficients were calculated for the time course experiments discussed in Section 4.2.4.3 where incubations were performed with *EcPanK*, *EcPPAT* and *EcDPCK* in the ratio of 2 : 20 : 1 in the absence (D, Table 4.6) and presence (E, Table 4.6) of 320  $\mu$ M CoA. Under these conditions the production of CoA is completely controlled by *EcDPCK* as confirmed by a  $C_{vDPCK}^{t95\%}$  of -0.997 in the absence of CoA and a  $C_{vDPCK}^{t95\%}$  of -0.992 in the presence of 320  $\mu$ M CoA.

Although a steady state analysis or supply and demand analysis was not performed on the system where the removal or demand for CoA was incorporated into our analysis the extreme scenario of CoA build-up was ideal to determine the control distribution in this case. This is because the basis for the argument that *EcPanK* controls the rate of CoA production is based on feedback inhibition by CoA. If this was indeed the case, the effect of CoA would be very clearly seen in the results of our experiments and the simulations of the model especially because CoA is not removed from the system. Therefore, these results confirm that *EcPanK* does not make the largest contribution to the control of CoA production under physiological conditions but rather that it is *EcDPCK*.

### 4.3 Conclusion

Understanding the regulation of CoA production is vital to the design of antimicrobial compounds that target the production of CoA. PanK is currently considered the most attractive target in the pathway due to the commonly accepted view that PanK stands central to the control of CoA production due to strong feedback inhibition by CoA. This misconception was addressed in this study. By constructing the first kinetic model of CoA production a systems analysis approach was applied to correct the mistaken belief that PanK is the “rate-limiting” step of the pathway. Time course analysis as well as predictions made by the validated model indicated that control only shifts to PanK when the concentration of this enzyme is very low and the CoA concentration is very high to such an extent that it is highly unlikely for PanK to make a contribution to the control of flux under physiological conditions. Instead, our study revealed that DPCK is the major role-player in the control of flux under most of the conditions that were tested especially under physiological conditions. This indicates that DPCK would make a more appropriate drug target because it is more likely to be in control of the rate of CoA production under physiological conditions.

## 4.4 Experimental procedures

### 4.4.1 Materials and methods

All chemicals and solvents were purchased from Sigma-Aldrich and were of the highest purity. Competent cell strains (BL21, *E.coli*) and expression vectors for overexpression were purchased from Novagen. Rabbit pyruvate kinase (10128155001) and lactate dehydrogenase (10127876001) were purchased from Sigma-Aldrich. Large scale centrifugation was performed in a Beckman Coulter Avanti J-26 XPI centrifuge. Medium scale centrifugation was performed in a Heraeus Multifuge 3S/3S-R centrifuge. Small scale centrifugation was carried out on a Heraeus Biofuge pico centrifuge.

HiTrap high performance chelating columns for protein purification were from GE Healthcare. All protein purifications were performed on a ÄKTA<sup>prime</sup> protein purification system. The Quick Start Bradford Protein Assay Kit (Bio-Rad) containing a bovine serum albumin (BSA) standard set and Bradford reagent was used for protein determinations. Flat bottom 96-well plates for protein determination and enzyme activity assays were from Greiner Bio-One International GmbH. Kinetic enzyme activity assays were performed on a Varioscan multiplate spectrophotometer from Thermo Labsystems. All graphical and statistical analyses were performed with SigmaPlot 11.0 (Systat Software, Inc.).

An Agilent 1100 series system equipped with an in line FLD-fluorescence detector was used for high performance liquid chromatography (HPLC) analyses. Chromatograms were generated, integrated and analysed with the software package Chemstation for LC, Rev. A.10.02[1757]. A Supelcosil LC-DP reverse phase column (250 x 4.60 mm, 5 µm particle size) was used in combination with a Supelcosil LC-DP Supelguard cartridge (2 cm length, 4.0 mm internal diameter, 5 µm particle size) for all HPLC analyses and both were obtained from Supelco. All graphical and statistical analyses for calibration were performed with SigmaPlot 11.0 (Systat Software, Inc.).

### 4.4.2 Expression and purification of *EcPanK*, *EcPPAT* and *EcDPCK*

#### 4.4.2.1 Expression conditions

Available pET28a-*EcCoaA*, pET28a-*EcCoaD* and pET28a-*EcCoaE* expression vectors that encode *EcPanK*, *EcPPAT* and *EcDPCK* enzymes respectively were transformed into competent BL21 *E. coli* cells for overexpression. This particular expression vector encodes a

kanamycin resistance gene as well as an *N*-terminal histidine tag that allows for nickel based immobilised metal affinity chromatography (IMAC) after overexpression. Transformed cells were cultured at 37°C in 500 ml Luria Bertani (LB) broth media in a two litre culture flask also containing 30 mg/l kanamycin sulphate. Following inoculation, cells were incubated with shaking until an OD<sub>600</sub> of about 0.6 was observed. At this point expression was induced by the addition of Isopropyl β-D-1-thiogalactopyranoside (IPTG). Expression of the *EcCoaA* gene was induced with 800 μM IPTG, while *EcCoaD* and *EcCoaE* were both induced with 1 mM IPTG. After induction, expression of *EcCoaA* and *EcCoaD* continued at 37°C for three hours but expression of *EcCoaE* continued overnight at 25°C. Cells were harvested by centrifugation at 10 000 x *g* for 20 minutes and cell pellets were dried and stored at -20°C.

#### 4.4.2.1 Purification conditions

Cell pellets were thawed and re-suspended in sonication buffer (20 mM Tris buffer, 500 mM NaCl, pH 7.4). Cells were disrupted by performing 6x60 second sonication cycles. The sonicated cell extract mixture was centrifuged at 15 000 x *g* for 30 minutes to remove cellular debris. Expressed proteins were purified from the crude cell extract by IMAC, using a 1 ml HisTrap chelating column. The column was preloaded with 100 mM NiSO<sub>4</sub> and the purification was performed on an ÄKTAprime system. Weakly bound proteins were washed from the column with sonication buffer followed by another wash step with sonication buffer containing 75 mM imidazole. The protein of interest was eluted by increasing the imidazole concentration to 500 mM. Protein fractions were identified by monitoring the eluent at A<sub>280</sub> and then pooled and loaded onto a HiTrap desalting column equilibrated in gel filtration buffer (25 mM Tris buffer, 5 mM MgCl<sub>2</sub>, pH 7.4). Imidazole was removed from the protein fractions by elution with gel filtration buffer and protein fractions were identified in the same manner as previously. These fractions were pooled and glycerol was added to a final concentration of 5%. After addition of glycerol, all protein stocks were divided into 50 μl aliquots and stored at -80°C. Aliquots were for single use with the leftovers being disposed to ensure a uniform single freeze and thaw for each protein aliquot used. Purity of the *EcPanK*, *EcPPAT* and *EcDPCK* proteins expressed was confirmed by SDS-PAGE using 12% gel.

#### 4.4.2.2 Protein determinations

Purified protein concentrations were determined by Bradford protein determination performed with the Quick Start Bradford protein assay kit. Proteins are bound with Coomassie Brilliant Blue R-250 dye to form a blue, stable, unprotonated product that can be measured by absorbance at 595nm. Bovine serum albumin (BSA) was used as the protein

standard for calibration curves with a linear range of 125-1000 µg/ml. A volume of 5 µl of each BSA standard was added to a 96-well microtitre plate followed by the addition of 250 µl Bradford reagent. All measurements were performed in triplicate and distilled H<sub>2</sub>O was used as a blank. After addition of the Bradford reagent, the plate was incubated for 5 minutes at room temperature to ensure complete binding. Absorbance was measured at 280 nm and the Beer-Lambert law was used to convert the measurements to concentrations.

### 4.4.3 Spectrophotometric activity assays

#### 4.4.3.1 *EcPanK* activity assays

*EcPanK* activity was measured by the pyruvate kinase/lactate dehydrogenase coupled assay in a 96-well plate. The ADP that is produced from the *EcPanK* reaction is coupled to the dephosphorylation of phosphoenolpyruvate (PEP) by pyruvate kinase to form pyruvate. Lactate dehydrogenase then converts pyruvate to lactate with the concomitant oxidation of NADH to NAD<sup>+</sup>.

Each assay contained 50 mM Tris-HCl buffer, pH 7.6, 20 mM KCl, 10 mM MgCl<sub>2</sub>, 250 µM TCEP, 0.3 mM NADH, 0.5 mM PEP, 0.01 U/µl pyruvate kinase, 0.01 U/µl lactate dehydrogenase and 1.5 µg *EcPanK*. PanSH concentration was varied up to a maximum of 766 µM at various fixed ATP concentrations and the ATP concentration was varied up to a maximum of 5 mM at various fixed PanSH concentrations. All assay components except PanSH and ATP were present in a master mix that was incubated at 37°C for five minutes before addition to the wells containing the substrates to initiate the reaction. A PanSH stock solution was prepared fresh prior to every run by the reduction of pantethine by 1.5 equivalents TCEP. A 100 µl substrates solution was prepared for each concentration level in the specific assay. PanSH was added last to the substrates solution before 30 µl was transferred to the wells of triplicate concentration levels. This was done shortly before the assay was initiated by the addition of 270 µl master mix to avoid re-oxidation of PanSH to pantethine. Blank reactions were the same as assay reactions, except that PanSH was omitted from the substrates mix. The decrease in NADH was measured at 340 nm at five second intervals over a period of 10 minutes at 37°C. All measurements were taken in triplicate. Initial rates were plotted against PanSH and ATP concentrations respectively and Eq 4.2 was fitted to all data sets. For CoA inhibition assays, the same procedure was followed except that CoA was added to the substrates solution along with various fixed concentrations of PanSH and ATP. CoA concentrations were varied up to a maximum of 500 µM.

#### 4.4.3.2 *EcDPCK activity assays*

Each assay contained 50 mM Tris-HCl buffer, pH 7.6 (or 50 mM phosphate buffer), 20 mM KCl, 10 mM MgCl<sub>2</sub> (or 10 mM MgSO<sub>4</sub>), 1 mM DTT, 0.3 mM NADH, 0.5 mM PEP, 0.01 U/μl units pyruvate kinase, 0.01 U/μl lactic dehydrogenase, 0.75 μg *EcDPCK*, ATP (0.7 mM or 1.5 mM) and DePCoA (varied concentrations) in a final volume of 150 μl. The decrease in NADH was measured at 340 nm over a period of 5 minutes at 25°C. All measurements were taken in triplicate. Initial rates were plotted against DePCoA concentration and the Michaelis-Menten equation (Eq. 4.6) was fitted to all data sets. The general Hill equation (Eq. 4.7) was also fitted to the data sets obtained for assays performed in the presence of excess phosphate.

$$v = \frac{V_{max} \times [S]}{K_M + [S]} \quad (\text{Eq. 4.6})$$

$$v = \frac{V_{max} \times [S]^n}{K_M^n + [S]^n} \quad (\text{Eq. 4.7})$$

#### 4.4.4 Single enzyme progress curves

##### 4.4.4.5 *EcPanK progress curves*

PanSH conversion reactions each contained 50 mM Tris-HCl buffer (pH 7.6), 5 mM ATP, 1 mM TCEP, 1.8 mM PEP, 0.04 U/μl pyruvate kinase in a reaction volume of 1.1 ml. 766 μM PanSH was converted to PPanSH by 0.02 mg/ml and 0.01 mg/ml and 0.005 mg/ml *EcPanK* respectively. The reaction with 0.02 mg/ml *EcPanK* was incubated for five minutes while the reaction with 0.01 mg/ml *EcPanK* was incubated for two and a half minutes and the reaction containing 0.005 mg/ml was incubated for 12 minutes. An additional reaction with 0.02 mg/ml PanK was performed with 100 μM CoA present at the start of the reaction which was incubated for five minutes. At various time points during the each of the incubations, 50 μl aliquots were removed from the reactions and quenched by protein precipitation with 15% trichloroacetic acid so that PanSH and PPanSH could be measured by derivatization with 7-Diethylamino-3-(4-maleimidophenyl)-4-methylcoumarin (CPM) and HPLC analysis.

##### 4.4.4.6 *EcPPAT progress curves*

Progress curves were determined for equilibrium approximation reactions that each contained 50 mM Tris-HCl buffer (pH 7.6), 1 mM TCEP and 0.05 mg/ml *EcPPAT* with 500

$\mu\text{M}$  PPanSH and 500  $\mu\text{M}$  ATP or 500  $\mu\text{M}$  DePCoA and 500  $\mu\text{M}$   $\text{PP}_i$  in a reaction volume of 1.1 ml. The progress curve determined for the conversion of PPanSH to DePCoA by *EcPPAT* contained 50 mM Tris-HCl buffer (pH 7.6), 1 mM TCEP, 500  $\mu\text{M}$  PPanSH, 5 mM ATP with 0.01 mg/ml *EcPPAT* and 0.04 U/ $\mu\text{l}$  pyrophosphatase added in a reaction volume of 1.1 ml. All reactions were incubated for five minutes and at various time points during the incubation 50  $\mu\text{l}$  aliquots were removed from the reactions and quenched by protein precipitation with 15% trichloroacetic acid so that PPanSH and DePCoA concentrations could be measured by derivatization with CPM and HPLC analysis.

#### 4.4.4.6 *EcDPCK* progress curves

DePCoA conversion reactions each contained 50 mM Tris-HCl buffer (pH 7.6), 1 mM TCEP, 18 mM PEP and 0.04 U/ $\mu\text{l}$  pyruvate kinase in a reaction volume of 1.1 ml. 500  $\mu\text{M}$  DePCoA was converted to CoA by 0.1 mg/ml and 0.2 mg/ml *EcDPCK* respectively. The reaction with 0.01 mg/ml *EcDPCK* was incubated for three minutes while the reaction with 0.2 mg/ml *EcDPCK* was incubated for 10 minutes. At various time points during the incubation 50  $\mu\text{l}$  aliquots were removed from the reactions and quenched by protein precipitation with 15% trichloroacetic acid so that DePCoA and CoA concentrations could be measured by derivatization with CPM and HPLC analysis.

### 4.4.6 Reconstituted pathway time courses

#### 4.4.6.1 Equivalent amounts of enzymes

Pathway reconstitution was performed as described in Chapter 3. Each reaction contained 50 mM Tris-HCl buffer (pH 7.6), 10 mM  $\text{MgCl}_2$ , 20 mM KCl, 5 mM ATP, 1.75 mM TCEP 0.04 U/ $\mu\text{l}$  pyruvate kinase, 1.8 mM PEP and 0.1  $\mu\text{g}/\mu\text{l}$  each of *EcPanK*, *EcPPAT* and *EcDPCK* respectively in a total reaction volume of 600  $\mu\text{l}$ . PanSH stock was prepared fresh prior to every reaction by reduction with 1.5 equivalents TCEP. Reactions were initiated by the addition of substrate mixtures consisting of the following: A) 766  $\mu\text{M}$  PanSH; B) 575  $\mu\text{M}$  PanSH, 225  $\mu\text{M}$  DePCoA; C) 575  $\mu\text{M}$  PanSH, 225  $\mu\text{M}$  CoA; D) 383  $\mu\text{M}$  PanSH, 225  $\mu\text{M}$  DePCoA, 225  $\mu\text{M}$  CoA. Each reaction mixture was incubated at 37°C for 60 minutes during which 50  $\mu\text{l}$  aliquots were removed from the reaction mixture at various time points and quenched by protein precipitation with 15% trichloroacetic acid so all intermediates could be measured by derivatization with CPM followed by HPLC analysis.

#### 4.4.6.2 Reduced *EcPanK* concentrations

The CoA salvage pathway was reconstituted in the same manner as described above with 766  $\mu\text{M}$  PanSH and 5 mM ATP, except that the concentration of *EcPanK* was lowered to 0.01 mg/ml and 0.005 mg/ml respectively whilst keeping *EcPPAT* and *EcDPCK* the same at 0.1 mg/ml. These reactions were incubated for 60 minutes at 37°C and 50  $\mu\text{l}$  aliquots collected and quenched for derivatization and HPLC analysis to measure all intermediates.

#### 4.4.6.3 Physiological enzyme ratios

The CoA salvage pathway was reconstituted with *EcPanK*, *EcPPAT* and *EcDPCK* in the ratio of 2:20:1 as is expected under physiological conditions in *E. coli*. Both reactions were performed under the same general conditions as described above with the following exceptions: each reaction contained 0.2 mg/ml *EcPanK*, 2 mg/ml *EcPPAT* and 0.1 mg/ml *EcDPCK* in a total reaction volume of 250  $\mu\text{l}$ . Reaction A contained 766  $\mu\text{M}$  PanSH and 5 mM ATP and reaction B contained 250  $\mu\text{M}$  PanSH, 1.5 mM ATP and 320  $\mu\text{M}$  CoA. Reactions were incubated for 60 minutes at 37°C and 50  $\mu\text{l}$  aliquots collected and quenched for derivatization and HPLC analysis to measure all intermediates.

#### 4.4.7 Measuring PanSH, PPanSH, DePCoA and CoA

Aliquots collected from single enzyme reactions and reactions where the CoA salvage pathway was reconstituted, were neutralized and derivatized with CPM as described in Chapter 3. HPLC analysis was also performed according to the method developed in Chapter 3. The peak areas of interest were integrated with the Chemstation for LC software and calibration curves were used to calculate the concentrations of the analytes of interest. For calibration curves, metabolite standards were prepared and standardized by reduction with DTBA, removal of DTBA by cation exchange, followed by the DTNB assay for thiol quantification as described in Chapter 3. These standards were used to set up calibration curves for the quantification of the analytes of interest from peak areas following HPLC analysis of CPM derivatized samples. Standards for calibration were derivatized in binary combinations *i.e.* PanSH and CoA calibrations were prepared in combination and PPanSH and DePCoA were prepared in combination. This was done to reduce the number of calibration samples and analysis time to allow for more frequent calibration (once a month) to ensure quantification remains accurate as the column ages.

#### **4.4.8 Computational methods**

All computational analyses were performed in Mathematica 10 ([www.wolfram.com](http://www.wolfram.com)). For parameterisation of the rate equation we used the NonLinearModelFit method. For estimation of  $V_M$  values in the conversion assays we used the NMinimize method. The ODEs were integrated using the NDSolve method.

## 4.5 References

1. Vallari, D. S.; Jackowski, S.; Rock, C. O., Regulation of pantothenate kinase by coenzyme A and its thioesters. *J. Biol. Chem.* **1987**, *262* (6), 2468-71.
2. Song, W. J.; Jackowski, S., Kinetics and regulation of pantothenate kinase from *Escherichia coli*. *J. Biol. Chem.* **1994**, *269* (43), 27051-27058.
3. Geerlof, A.; Lewendon, A.; Shaw, W. V., Purification and characterization of phosphopantetheine adenylyltransferase from *Escherichia coli*. *J. Biol. Chem.* **1999**, *274* (38), 27105-27111.
4. Miller, J. R.; Ohren, J.; Sarver, R. W.; Mueller, W. T.; de Dreu, P.; Case, H.; Thanabal, V., Phosphopantetheine adenylyltransferase from *Escherichia coli*: Investigation of the kinetic mechanism and role in regulation of coenzyme a biosynthesis. *J. Bacteriol.* **2007**, *189* (22), 8196-8205.
5. Strauss, E.; Begley, T. P., The Antibiotic Activity of N-Pentylpantothenamide Results from Its Conversion to Ethyldethia-Coenzyme A, a Coenzyme A Antimetabolite. *J. Biol. Chem.* **2002**, *277* (50), 48205-48209.
6. Mishra, P. K.; Park, P. K.; Drueckhammer, D. G., Identification of yacE (coaE) as the structural gene for dephosphocoenzyme A kinase in *Escherichia coli* K-12. *J. Bacteriol.* **2001**, *183* (9), 2774-2778.
7. Rootman, I.; de Villiers, M.; Brand, L. A.; Strauss, E., Creating Cellulose-Binding Domain Fusions of the Coenzyme A Biosynthetic Enzymes to Enable Reactor-Based Biotransformations. *Chemcatchem* **2010**, *2* (10), 1239-1251.
8. Leonardi, R.; Zhang, Y.-M.; Rock, C. O.; Jackowski, S., Coenzyme A: Back in action. *Prog. Lipid. Res.* **2005**, *44* (2-3), 125-153.
9. Lowry, O. H.; Carter, J.; Ward, J. B.; Glaser, L., The Effect of Carbon and Nitrogen Sources on the Level of Metabolic Intermediates in *Escherichia coli*. *J. Biol. Chem.* **1971**, *246* (21), 6511-6521.
10. Jackowski, S.; Rock, C. O., Regulation of coenzyme A biosynthesis. *J. Bacteriol.* **1981**, *148* (3), 926-932.
11. Rock, C. O.; Park, H.-W.; Jackowski, S., Role of Feedback Regulation of Pantothenate Kinase (CoaA) in Control of Coenzyme A Levels in *Escherichia coli*. *J. Bacteriol.* **2003**, *185* (11), 3410-3415.
12. Song, W. J.; Jackowski, S., Cloning, sequencing, and expression of the pantothenate kinase (coaA) gene of *Escherichia coli*. *J. Bacteriol.* **1992**, *174* (20), 6411-6417.

13. Yun, M.; Park, C.-G.; Kim, J.-Y.; Rock, C. O.; Jackowski, S.; Park, H.-W., Structural basis for the feedback regulation of *Escherichia coli* pantothenate kinase by coenzyme A. *J. Biol. Chem.* **2000**, *275* (36), 28093-28099.
14. Jackowski, S.; Rock, C. O., Metabolism of 4'-phosphopantetheine in *Escherichia coli*. *J. Bacteriol.* **1984**, *158* (1), 115-120.
15. Srinivasan, B.; Baratashvili, M.; van der Zwaag, M.; Kanon, B.; Colombelli, C.; Lambrechts, R. A.; Schaap, O.; Nollen, E. A.; Podgorsek, A.; Kosec, G.; Petkovic, H.; Hayflick, S.; Tiranti, V.; Reijngoud, D.-J.; Grzeschik, N. A.; Sibon, O. C. M., Extracellular 4'-phosphopantetheine is a source for intracellular coenzyme A synthesis. *Nat Chem Biol* **2015**, *11* (10), 784-792.
16. Moreno-Sánchez, R.; Saavedra, E.; Rodríguez-Enríquez, S.; Olín-Sandoval, V., Metabolic Control Analysis: A Tool for Designing Strategies to Manipulate Metabolic Pathways. *J. Biomed. Biotechnol.* **2008**, *2008*, 597913.
17. Fell, D., *Understanding the control of metabolism*. Portland press London: 1997; Vol. 2.
18. Rohwer, J. M., Kinetic modelling of plant metabolic pathways. *J. Exp. Bot.* **2012**, *63* (6), 2275-2292.
19. Cascante, M.; Boros, L. G.; Comin-Anduix, B.; de Atauri, P.; Centelles, J. J.; Lee, P. W.-N., Metabolic control analysis in drug discovery and disease. *Nat. Biotechnol.* **2002**, *20* (3), 243-249.
20. Michaelis, L.; Menten, M. L., Die kinetik der invertinwirkung. *Biochem.* **1913**, *49* (333-369), 352.
21. Briggs, G. E.; Haldane, J. B. S., A note on the kinetics of enzyme action. *Biochem. J.* **1925**, *19* (2), 338.
22. Hill, A. V., The possible effects of the aggregation of the molecules of haemoglobin on its dissociation curves. *J. Physiol.* **1910**, *40*, 4-7.
23. Schnell, S.; Chappell, M. J.; Evans, N. D.; Roussel, M. R., The mechanism distinguishability problem in biochemical kinetics: The single-enzyme, single-substrate reaction as a case study. *C. R. Biol.* **2006**, *329* (1), 51-61.
24. Goudar, C. T.; Harris, S. K.; McInerney, M. J.; Suflita, J. M., Progress curve analysis for enzyme and microbial kinetic reactions using explicit solutions based on the Lambert W function. *J. Microbiol. Methods* **2004**, *59* (3), 317-326.
25. Duggleby, R. G., [3] Analysis of enzyme progress curves by nonlinear regression. In *Methods Enzymol.* **1995** Vol. 249, pp 61-90.
26. Orsi, B. A.; Tipton, K. F., Kinetic analysis of progress curves. *Methods Enzymol.* **1979**, *63*, 159-183.

27. Strauss, E.; de Villiers, M.; Rootman, I., Biocatalytic Production of Coenzyme A Analogues. *Chemcatchem* **2010**, *2* (8), 929-937.
28. Ivey, R. A.; Zhang, Y.-M.; Virga, K. G.; Hevener, K.; Lee, R. E.; Rock, C. O.; Jackowski, S.; Park, H.-W., The Structure of the Pantothenate Kinase-ADP-Pantothenate Ternary Complex Reveals the Relationship between the Binding Sites for Substrate, Allosteric Regulator, and Antimetabolites. *J. Biol. Chem.* **2004**, *279* (34), 35622-35629.
29. O'Toole, N.; Barbosa Joao, A. R. G.; Li, Y.; Hung, L.-W.; Matte, A.; Cygler, M., Crystal structure of a trimeric form of dephosphocoenzyme A kinase from *Escherichia coli*. *Protein Sci.* **2003**, *12* (2), 327-36.
30. Obmolova, G.; Teplyakov, A.; Bonander, N.; Eisenstein, E.; Howard, A. J.; Gilliland, G. L., Crystal structure of dephospho-coenzyme A kinase from *Haemophilus influenzae*. *J. Struct. Biol.* **2001**, *136*, 119-125.
31. Shulman, R. G.; Brown, T. R.; Ugurbil, K., Cellular applications of <sup>31</sup>P and <sup>13</sup>C nuclear magnetic resonance. *Science* **1979**, *205* (4402), 160-166.
32. Wang, M.; Herrmann, C. J.; Simonovic, M.; Szklarczyk, D.; von Mering, C., Version 4.0 of PaxDb: Protein abundance data, integrated across model organisms, tissues, and cell-lines. *PROTEOMICS* **2015**, *15* (18), 3163-3168.
33. Conradie, R.; Westerhoff, H.; Rohwer, J.; Hofmeyr, J.-H.; Snoep, J., Summation theorems for flux and concentration control coefficients of dynamic systems. *IEE P. SYST. BIOL.* **2006**, *153* (5), 314-317.
34. Conradie, R.; Bruggeman, F. J.; Ciliberto, A.; Csikász-Nagy, A.; Novák, B.; Westerhoff, H. V.; Snoep, J. L., Restriction point control of the mammalian cell cycle via the cyclin E/Cdk2: p27 complex. *FEBS J.* **2010**, *277* (2), 357-367.

# Chapter 5

## Conclusion

---

### 5.1 Overview of achievements

The biosynthesis of CoA presents a very important target for antimicrobial drug discovery studies. The essential nature of organisms' CoA requirements is not clearly defined because of the multifaceted functions of CoA. The relationship between CoA requirement and the regulation of CoA production is poorly understood. Current understanding of the regulation of CoA biosynthesis is that PanK is the rate limiting step and as such presents the best target for inhibition but PanK inhibitors have shown limited success as growth inhibitors. A lack of analytical tools to measure the intermediates of CoA biosynthesis has hampered investigations into regulation of the pathway and a holistic study has not been performed to elucidate the control profile. In this study we investigated the requirement for CoA as a redox buffer and developed a method for the simultaneous quantification of the CoA biosynthetic intermediates that was subsequently employed in the investigation of the regulation of the CoA salvage pathway.

The requirement for CoA as a redox buffer in the oxidative stress resistance observed in *S. aureus* USA 300 was investigated. Specifically, the regulation of CoA production as a response to oxidative stress resistance was evaluated. The role of bacillithiol (BSH) as a low molecular weight (LMW) thiol redox buffer was also assessed to determine the relative contribution of CoA and BSH in mediating the effects of oxidative stress. BSH was found to play a substantial role as redox buffer because cultures that do not produce BSH exhibited lower viability and required a longer time for recovery following induction of oxidative stress than wild type cultures that contain both CoA and BSH. Quantification of intracellular CoA levels, and that of its immediate precursors 3'-dephospho-CoA (DePCoA) and 4'-phosphopantetheine (PPanSH) following induction of oxidative stress revealed a significant increase in CoA levels. However, inhibition of increased CoA production under oxidative stress conditions by *N*-heptyl pantothenamide (N7-Pan) did not decrease viability of the cultures presumably due to compensation by BSH. Oxidative stress resistance and subsequent recovery was therefore attributed to both the presence of BSH and higher levels of CoA that is produced as a response to oxidative stress. An important conclusion from

these results is that the demand for CoA as a redox buffer increased the rate of CoA production. This demonstrates how just one of the many CoA-dependent processes that affects the regulation of its production. This highlights the need for a better understanding of the regulation of CoA production as it relates to the CoA-dependent processes required for survival.

In order to address the lack of information available on the regulation of the rate of CoA production a holistic study of the pathway was required. Previous studies investigating the pathway's regulation was hampered by the lack of a sensitive analytical method to measure all the intermediates of the CoA salvage pathway. A method was developed where all intermediates was visualized by derivatization with the fluorescent thiol probe CPM, and their subsequent analysis by HPLC for quantification. Validation of the method was performed and the method was found to be robust, sensitive and accurate. The method was successfully applied for the quantification of intermediates of the CoA salvage pathway in a simple cell-free matrix as well as in the complex matrix of bacterial extracts. This method paves the way for investigations of the regulation of CoA production by enabling analysis of the complete system of CoA production by the salvage pathway.

As mentioned above, studies performed to date have claimed that PanK stands central to the control of the rate of CoA production. This claim was therefore investigated by means of a systems analysis of the CoA salvage pathway. To this end, a kinetic model of the pathway was constructed from parameterized rate equations for each enzyme. The parameters were obtained from the literature but some parameters were also determined experimentally in this study where insufficient information was provided in the literature about the conditions under which reported values were determined. The newly developed analytical method for quantification of salvage pathway intermediates was used to trace the levels of the biosynthetic intermediate metabolites for time course analysis of the reconstituted pathway. Time courses were measured under various conditions of enzyme concentrations and ratios as well as differing initial substrate, intermediate and product concentrations for validation of the model. The time course analyses as well as predictions made by the validated model indicated that the rate of CoA production is controlled by dephospho-CoA kinase (DPCK) under most conditions tested and that the role of PanK in regulation is limited to very specific circumstances. These include conditions when the concentration of PanK is very low relative to phosphopantetheine adenylyltransferase (PPAT) and DPCK in addition to very high initial concentrations of CoA. The conditions required for PanK to make a meaningful contribution to the control of the pathway were deemed highly unlikely in a physiological setting. From

these results it was concluded that DPCK is the main regulator of the rate of CoA production under most of the conditions that were tested but especially physiological conditions. This implies that DPCK is the best target for antimicrobial drug discovery in the pathway because it is far more likely to be in control of the rate of CoA production under physiological conditions. The findings of this study provides an explanation for vulnerability studies that showed that *Mycobacterium tuberculosis* PanK activity had to be almost completely abolished to achieve inhibition of growth. As DPCK was shown to have the most control over the rate of production in our study it stands to reason that CoA production and cell growth would be more vulnerable to inhibition of DPCK.

## **5.2 Future work**

### **5.2.1 Regulation of CoA by a redox switch mechanism**

Increased production and accumulation of CoA in *S. aureus* under oxidative stress conditions indicates that production is up-regulated as a response to a redox signal. *S. aureus* PanK contains a cysteine that is predicted to undergo reversible oxidation under oxidative stress conditions. This is a possible mechanism for a redox switch in the pathway that could alter the regulation of CoA production. To investigate this premise, studies should be performed on isolated enzymes of the pathway to assess the effect such oxidations might have on their catalytic activity.

### **5.2.2. The relevance of CoA regulation in other metabolic pathways**

In this study it was demonstrated that the regulation of CoA production plays a role in the redox system of *S. aureus*. The relevance of CoA in metabolic pathways other than the redox system should also be investigated. Focused studies of the numerous CoA dependent processes should be performed in order to identify and validate specific pathways and enzymes that represent the life-sustaining requirement of CoA.

### **5.2.3 Extending time course analysis of the CoA salvage pathway to other species**

The newly developed analytical method can be applied for time course analysis of the CoA salvage pathway of any organism that harbours this pathway. Time course analysis should be performed of the pathway in *S. aureus* and *H. sapiens* to enable kinetic modelling and systems analysis of CoA production in these organisms to highlight any differences in the

regulation of CoA production. Such distinctions are important for future drug discovery studies aimed at the selective inhibition of CoA production. Time course analysis can also provide insight into the effect of variation in certain enzyme parameters on CoA production. For example, investigating what the effect will be on pathway control if the high  $K_M$  for DePCoA displayed by *E. coli* DPCK is lowered by substituting the *Corynebacterium ammoniagenes* DPCK. Pathway control could also be assessed under conditions where Pank does not experience feedback inhibition by substituting *S. aureus* Pank in the reconstituted pathway.

### 5.2.1 Optimization of the kinetic model of the CoA salvage pathway in *E. coli*

Although there is not a striking difference observed between the experimentally determined time course profiles of the CoA salvage pathway and predictions made by the model, a better fit is always possible. The kinetic model will be optimized by expanding the rate equation of PPAT to include parameters for inhibition by CoA.

## 5.3 Final remarks

The results presented in this thesis represent the first investigation of the regulation of CoA production based on a systems analysis approach. The development of a novel analytical method to measure pathway intermediates for time course analysis enabled the construction of a kinetic model of the pathway. This enabled the identification of DPCK as the main regulatory point in *E. coli* based on control distribution and not on the premise of a so-called single rate-limiting enzyme. This finding is significant to antimicrobial drug development efforts because it suggests that the focus should be shifted from Pank as target to DPCK. Therefore the findings of this study represent a major shift in our current understanding of the regulation of the rate of CoA production and also serve as a caveat to other drug development studies that plans to target the “rate-limiting” step of a pathway, especially in cases where no systems analysis has been performed.

# Appendix

## A. Derivation of the PanK rate equation

In the *EcPanK* reaction scheme five active complexes can be seen (Figure 4.1, complexes shown in green). With E representing the enzyme, these active complexes can be written as:



Assuming equilibrium binding, the concentrations of the active complexes can be expressed as follows:

$$\begin{aligned} \text{E-ATP.PanSH} & \frac{ATP}{K_{ATP}} \cdot \frac{PanSH}{K_{PanSH}} \\ \text{E-ATP.PanSH.ATP} & \frac{ATP}{K_{ATP}} \cdot \frac{PanSH}{K_{PanSH}} \cdot \alpha \cdot \frac{ATP}{K_{ATP}} \\ \text{E-ATP.PanSH.ATP.PanSH} & \frac{ATP}{K_{ATP}} \cdot \frac{PanSH}{K_{PanSH}} \cdot \alpha \cdot \frac{ATP}{K_{ATP}} \cdot \beta \cdot \frac{PanSH}{K_{PanSH}} \\ \text{E-ATP.PanSH.PanSH} & \frac{ATP}{K_{ATP}} \cdot \frac{PanSH}{K_{PanSH}} \cdot \frac{PanSh}{K_{iPanSH}} \\ \text{E-ATP.PanSH.CoA} & \frac{ATP}{K_{ATP}} \cdot \frac{PanSH}{K_{PanSH}} \cdot \frac{CoA}{K_{iCoA}} \end{aligned}$$

There are 15 complexes that can be formed in total, the concentrations of which can be expressed as follows:

$$\begin{aligned} & \alpha \cdot \left(\frac{ATP}{K_{ATP}}\right)^2 & 2 \alpha \cdot \left(\frac{ATP}{K_{ATP}}\right)^2 \cdot \frac{PanSH}{K_{PanSH}} & \alpha \cdot \left(\frac{ATP}{K_{ATP}}\right)^2 \cdot \beta \cdot \left(\frac{PanSH}{K_{PanSH}}\right)^2 \\ 1 \text{ (free enzyme)} & & \left(\frac{CoA}{K_{iCoA}}\right)^2 & \frac{CoA}{K_{iCoA}} \cdot \frac{PanSH}{K_{iPanSH}} \\ & 2 \cdot \frac{CoA}{K_{iCoA}} \cdot \frac{ATP}{K_{ATP}} & 2 \cdot \frac{CoA}{K_{iCoA}} \cdot \frac{ATP}{K_{ATP}} \cdot \frac{PanSH}{K_{PanSH}} & 2 \cdot \frac{CoA}{K_{iCoA}} \\ & 2 \cdot \frac{PanSH}{K_{iPanSH}} & 2 \cdot \frac{ATP}{K_A} & 2 \cdot \frac{A}{K_A} \cdot \frac{P}{K_P} \\ & \left(\frac{PanSH}{K_{iPanSH}}\right)^2 & 2 \cdot \frac{PanSH}{K_{iPanSH}} \cdot \frac{ATP}{K_{ATP}} & 2 \cdot \frac{PanSH}{K_{iPanSH}} \cdot \frac{ATP}{K_{ATP}} \cdot \frac{PanSH}{K_{PanSH}} \end{aligned}$$

The enzyme activity is then expressed as the fraction of the enzyme in the active form time the maximal rate ( $V_M$ ), times the enzyme concentrations [e]

$$v_{PanK} = \frac{e_{PanK} \cdot V_M \cdot \frac{ATP}{K_{ATP}} \cdot \frac{PanSH}{K_{PanSH}} \left(1 + \alpha \cdot \frac{ATP}{K_{ATP}} \left(1 + \beta \cdot \frac{PanSH}{K_{PanSH}}\right) + \frac{CoA}{K_{iCoA}} + \frac{PanSH}{K_{iPanSH}}\right)}{1 + 2 \cdot \frac{ATP}{K_{ATP}} \cdot \left(1 + \frac{PanSH}{K_{PanSH}}\right) + \alpha \cdot \left(\frac{ATP}{K_{ATP}}\right)^2 \left(1 + \frac{2 \cdot PanSH}{K_{PanSH}} + \beta \cdot \left(\frac{PanSH}{K_{PanSH}}\right)^2 + \left(\frac{CoA}{K_{iCoA}} + \frac{PanSH}{K_{iPanSH}}\right) \cdot \left(2 + \frac{CoA}{K_{iCoA}} + \frac{PanSH}{K_{iPanSH}} + \frac{2 \cdot ATP}{K_{ATP}} \cdot \left(1 + \frac{PanSH}{K_{PanSH}}\right)\right)\right)} \quad \text{Eq. 4.1}$$

When  $\beta$  is estimated as zero, the equation reduces to:

$$v_{PanK} = \frac{e_{PanK} \cdot V_M \cdot \frac{ATP}{K_{ATP}} \cdot \frac{PanSH}{K_{PanSH}} \left(1 + \alpha \cdot \frac{ATP}{K_{ATP}} + \frac{CoA}{K_{iCoA}} + \frac{PanSH}{K_{iPanSH}}\right)}{1 + 2 \cdot \frac{ATP}{K_{ATP}} \cdot \left(1 + \frac{PanSH}{K_{PanSH}}\right) + \alpha \cdot \left(\frac{ATP}{K_{ATP}}\right)^2 \left(1 + \frac{2 \cdot PanSH}{K_{PanSH}} + \left(\frac{CoA}{K_{iCoA}} + \frac{PanSH}{K_{iPanSH}}\right) \cdot \left(2 + \frac{CoA}{K_{iCoA}} + \frac{PanSH}{K_{iPanSH}} + \frac{2 \cdot ATP}{K_{ATP}} \cdot \left(1 + \frac{PanSH}{K_{PanSH}}\right)\right)\right)} \quad \text{Eq. 4.2}$$